Resource allocation in dense wireless communication networks

Cédric Abgrall

▶ **To cite this version:**

Cédric Abgrall. Resource allocation in dense wireless communication networks. Networking and Internet Architecture [cs.NI]. Télécom ParisTech, 2010. English. NNT : . pastel-00581776

HAL Id: pastel-00581776
https://pastel.hal.science/pastel-00581776

Submitted on 31 Mar 2011

HAL is a multi-disciplinary open access archive for the deposit and dissemination of scientific research documents, whether they are published or not. The documents may come from teaching and research institutions in France or abroad, or from public or private research centers.

L'archive ouverte pluridisciplinaire **HAL**, est destinée au dépôt et à la diffusion de documents scientifiques de niveau recherche, publiés ou non, émanant des établissements d'enseignement et de recherche français ou étrangers, des laboratoires publics ou privés.

École Doctorale
d'Informatique,
Télécommunications
et Électronique de Paris

Thèse

présentée pour obtenir le grade de Docteur de TELECOM ParisTech

Spécialité : Communications et Électronique

Cédric Abgrall

Allocation de ressoures dans les réseaux de communications sans fil denses

Version finale - 20/12/2010

Soutenue le 25 Octobre 2010 devant le jury composé de

Prof. Jean-Marc Brossier	Président
Prof. Josep Vidal	Rapporteurs
Prof. Jean-Marie Gorce	
Prof. Mérouane Debbah	Examinateur
Prof. Jean-Claude Belfiore	Directeurs de thèse
Dr. Emilio Calvanese Strinati	

TELECOM ParisTech THESIS

In Partial Fulfillment of the Requirements
for the Degree of Doctor of Philosophy
from TELECOM ParisTech

Specialization: Communications and Electronics

Cédric Abgrall

Resource Allocation in Dense Wireless Communication Networks

Final Version - December 20th, 2010

Defended on the 25^{th} of October 2010. The committee in charge is formed of:

President	Prof. Jean-Marc Brossier, GIPSA Lab (Grenoble, France)
Reviewers	Prof. Josep Vidal, UPC (Barcelona, Spain)
	Prof. Jean-Marie Gorce, INSA Lyon (Lyon, France)
Examiner	Prof. Mérouane Debbah, Supélec (Gif-sur-Yvette, France)
Thesis supervisors	Prof. Jean-Claude Belfiore, TELECOM ParisTech (Paris, France)
	Dr. Emilio Calvanese Strinati, CEA Grenoble (Grenoble, France)

Remerciements

Je souhaite adresser pour commencer ma plus vive gratitude à mes deux directeurs de thèse, Jean-Claude Belfiore, Professeur à TELECOM ParisTech, et Emilio Calvanese Strinati, Docteur au CEA Grenoble ; je les remercie très sincèrement pour leur encadrement et leur disponibilité tout au long de ces trois longues années de doctorat durant lesquelles ils ont su apporter des lumières pour éclairer mes plus obscures pensées scientifiques. Leur expérience, leur pédagogie et leur patience m'ont certes permis de mener à bien mes travaux de recherche, mais également de m'épanouir professionnellement.

Je souhaite également remercier chaleureusement Josep Vidal, Professeur à l'Université Polytechnique de Catalogne, et Jean-Marie Gorce, Professeur à l'INSA de Lyon, pour avoir accepté d'endosser le rôle de rapporteurs de ma thèse. Leurs conseils pertinents m'ont permis d'améliorer la qualité de mes travaux et de le présenter dans les meilleures conditions lors de la soutenance orale. Ma reconnaissance s'adresse également à Jean-Marc Brossier, Professeur à GIPSA-Lab à Grenoble, pour m'avoir fait l'honneur de présider mon jury de thèse. Enfin, mes remerciements vont à Mérouane Debbah, Professeur à Supélec à Paris pour avoir accepté le rôle d'examinateur et membre de mon jury.

Mes pensées vont ensuite à tous mes collègues au sein du laboratoire DSIS/LCS/CNA du CEA Grenoble qui ont su rendre plus facile mes trois années de labeur. Je les remercie pour leur aide, leur soutien et leur présence au quotidien, mais aussi pour l'atmosphère conviviale qu'ils ont su créer. Je remercie en outre tous les membres du laboratoire COMELEC de TELECOM ParisTech que j'ai eu le plaisir de côtoyer et qui ont su m'accueillir dans les meilleures conditions lors de mes visites épisodiques.

Enfin, ces remerciements ne sauraient être complets sans une mention spéciale à mes amis et ma famille pour leur soutien et leurs encouragements inconditionnels en dépit de mes changements d'humeur, de mon indisponibilité chronique et de mon comportement distant. A vous tous je dédie une partie de ma réussite.

Grenoble, le 20 décembre 2010
Cédric ABGRALL

Abstract

In this PhD thesis we look into interference aware Radio Resource Management (RRM) techniques for wireless cellular networks. Our goal is to limit the detrimental effects of in-band interference. We investigated two interference limited contexts of wireless communications.

First, we considered half-duplex two-hop cooperative communication systems, where spatial diversity, coverage and transmission reliability can be enhanced by judicious cooperative techniques. Aided-relay communications may be especially beneficial for cell-edge users, which experience important path-loss attenuation and suffer from strong inter-cell interference. On the contrary, from a viewpoint restricted to a source and its destination, the addition of relays is not always the best solution : noise is amplified with Amplify-and-Forward (AF) cooperative protocol, whereas erroneous decoding is possible with Decode-and-Forward (DF). Moreover, from the system viewpoint, cooperation introduces additional interfering sources in the system : relays overlap the same sets of resources as those of sources ever active. Cooperation in wireless networks is like a crowded cocktail party with a cacophony of conversations all around. There is hence a trade-off between the level of interference and beneficial effects of cooperation. The more people repeat the same information, the more likely you understand it. However, repeaters also introduce additional interference, which harms message understanding. The gains brought by cooperation of one relay should outperform the degradation that its activation may cause on neighbour cells.

With the work presented in this thesis we show how it is possible to effectively exploit the half-duplex hardware limitation of relays so as to coordinate in time and frequency the resource allocation of clusters of neighbour cells. We come out with a novel resource allocation strategy which efficiently adapts the activation of relays in cells as well as the pattern of resource allocation to time, frequency and space variations in the communication scenario.

Second, we address the case of non cooperative communications. We investigate how to classify the interference that a destination perceives on a given set of frequency bands. We come out with the proposal of a 'light' interference classifier that differentiates three regimes of interference *noisy*, *intermediate* and *very strong*. The merit of the proposed method is three-fold. First, the proposed three interference regimes are not overlapping. Therefore, a unique mapping between interfering signal and interference regime can be done. Second, once interference classification has been accomplished, resource allocation mechanisms can exploit such information to select the best set of parameters which meets a specific cost or utility function. Third, a specific technique for handling with in-band interference is associated with each interference regime.

This technique is proved to be effective when perceived INR is located between the

boundaries of the considered regime. Consequently, this classifier of in-band interference ensures an adaptive and effective processing of in-band interference which is adapted to time-varying nature of the channel. This adaptation precisely permits to achieve better interference mitigation than non-adaptive strategies. Contrary to previous contributions which involve till five regimes of interference, our classifier can be implemented in practical systems without complexity restrictions. Indeed, concurrent proposals usually focus on theoretical performance which cannot, up to now, be used conceivably in practice.

Then, we combined the proposed classifier with RRM and QoS satisfaction rate considerations. Two algorithmic approaches were considered for power allocation : a centralized algorithm (CPA) and a distributed algorithm (DPA). Both approaches aim at allocating the minimal transmit power vector, while ensuring the QoS satisfaction rate that each user targets, whatever the communication scenario may be. The centralized approach exploits the classifier to determine the suitable regime of interference, in line with the momentary communication context. Then, based on this classified regime, the minimal transmit power is computed for each active transmitter, such that reliable transmission is met at destination. Our simulations show how an adaptive handling of in-band interference may notably reduce the power budget for transmission without affecting transmission reliability.

Nevertheless, centralized approaches are not always feasible since they assume the presence of a coordinated and centralized network entity which monitors the allocation of resources (*i.e.,* powers). Consequently, control overhead and signalling are introduced. Moreover, all computation complexity is carried out at the network controller which becomes the bottleneck of the system. In order to achieve interference aware RRM in autonomous a non-centralized systems, we looked into distributed algorithmic solutions. The methodology is similar. However, constraints and assumptions are not. We indeed proposed to exploit the three-regime interference classifier like we did with the centralized solution. Consequently, our distributed proposal achieves theoretically the same performance as the ones of CPA.

Nevertheless, in autonomous systems, entities in charge of computing minimal transmit powers cannot estimate quality of link from sources to neighbour destinations. Therefore, they cannot predict transmit power of neighbour interferers and so they cannot predict if their transmit power will be optimal or not. Thus, an iterative process was considered : at each iteration, transmitters update their transmit power in turns so that their QoS satisfaction rate is ensured at reception, based on the momentary in-band interference power they sense. The algorithm stops when a balanced and optimal power vector is met.

Theoretical and numerical simulations prove that our distributed and autonomous proposal mostly allocate the same power vector than the centralized and optimal algorithm. However, in rare and specific communication scenarios, our iterative solution may never (or not quick enough) converge to the minimal power vector, because of restricted channel knowledge.

Keywords

Interference mitigation, resource allocation, power allocation, cooperative transmission, wireless communication network, interference-limited scenario, channel capacity, quality of service, transmission reliability.

Résumé long

Introduction

Dans le monde des communications radio, l'accès et l'utilisation des fréquences sont limités et réglementés afin d'assurer une bonne cohabitation entre les différents standards et systèmes de communication qui ne cessent de se multiplier et de se développer. La recherche actuelle dans ce domaine vise surtout à accroître la qualité des services offerts aux utilisateurs : augmentation du débit, accroissement de la fiabilité des transmissions, extension de la couverture pour les utilisateurs en bordure de cellule, hand-over à des vitesses de plus en plus rapides, etc. Toutes ces améliorations imposent de nouvelles exigences théoriques et pratiques qui resserrent davantage les contraintes sur les systèmes. Il devient de plus en plus difficile pour un système, voire impossible, de ne pas interférer avec son entourage. La limitation de la ressource fréquentielle et la coexistence de nombreux systèmes imposent par exemple le partage et la réutilisation de ces fréquences. Les transmissions ne sont par conséquent plus orthogonales les unes aux autres : de l'interférence intracellulaire (entre les utilisateurs d'une même cellule) et/ou intercellulaire (entre les utilisateurs de cellules différentes) est ainsi générée par l'utilisation simultanée d'une même ressource de communication pour transmettre des signaux entre plusieurs paires "émetteur-récepteur".

Cette interférence peut fortement dégrader les performances des transmissions et mérite d'être considérée avec le plus grand soin. Cette interférence est d'autant plus gênante que la destination est éloignée de sa source. Les utilisateurs en bordure de cellule perçoivent d'une part un signal utile plus faible que les utilisateurs proches de leur émetteur (*path loss* - atténuation due à la distance), et d'autre part subissent davantage l'interférence intercellulaire de par leur plus grande proximité des cellules voisines. Si l'interférence intracellulaire peut facilement être éliminée par l'emploi de systèmes OFDMA (allocation de canaux fréquentiels orthogonaux pour les différents utilisateurs d'une même cellule), l'interférence intercellulaire ne peut être gérée de la sorte (manque de canaux pour rendre orthogonales toutes les transmissions du système, ressources sous-exploitées, forte chute des performances). Des techniques connues sous le nom de *Interference Management* ou *Interference Mitigation* doivent ou peuvent alors être employées pour pallier ces problèmes. Plusieurs types de techniques se distinguent.

Une première façon de résoudre le problème est de rendre orthogonales ou partiellement orthogonales les transmissions (*Frequency Sharing*, *Time Sharing*). De telles techniques présentent des limites avec des réseaux denses et s'appliquent difficilement lorsque le nombre d'utilisateurs s'accroît fortement. Dans ces circonstances, le ratio entre le nombre de ressources disponibles et le nombre d'utilisateurs tend vers zéro et l'orthogonalité n'est plus envisageable. Pour accroître l'efficacité spectrale, une même ressource fréquentielle peut être utilisée simultanément pour plusieurs transmissions, si les émetteurs concernés sont

suffisamment distants les uns des autres (*Frequency Hopping*, *Frequency Reuse*) [1].

Une seconde approche du problème est de considérer un filtrage adapté au contexte de transmission. Si le filtrage est appliqué en émission, les techniques sont communément appelées *Interference Avoidance* et visent à éviter la génération d'interférence en réception en agissant sur les émetteurs. On trouve ainsi le *Dirty Paper Coding* qui suppose que l'interférence subie par le récepteur est connue de l'émetteur ; le message est alors envoyé avec l'interférence finale pré-soustraite, de telle sorte qu'en réception l'interférence pré-soustraite et l'interférence perçue se compensent [2].

Si le filtrage est appliqué en réception, on retrouve les techniques d'*Interference Cancellation* qui cherchent à s'affranchir de l'interférence subie en réception. Un exemple de telles techniques est le *Successive Interference Cancellation* qui décode le signal interférant le plus fort, considérant les autres signaux comme du bruit, puis le retranche et recommence itérativement avec le second signal le plus fort ; cela jusqu'à décoder le signal souhaité.

Une autre technique très en vogue actuellement dans la communauté de l'*Information Theory* et basée sur le *Beamforming* est l'*Interference Alignment*. Elle consiste à regrouper les signaux interférents dans un sous-espace propre du système (*i.e.,* une partie des degrés de liberté dont dispose le système) puis d'exclure ce sous-espace en réception pour ne se concentrer que sur les degrés de liberté restants, vierges d'interférence (ou presque).

Toutes ces techniques requièrent une certaine connaissance du système (coefficients des canaux) et un filtrage tant en émission (*pre-processing*) qu'en réception (*post-processing*) [3–5]. Enfin, des techniques d'optimisation peuvent s'appliquer pour résoudre ce problème d'interférence. Ces méthodes cherchent à optimiser une fonction d'utilité sous respect de contraintes imposées par les couches hautes et/ou par le système. Les concepts théoriques les plus puissants sont ceux de la théorie des jeux, de la coloration de graphes et de l'optimisation convexe [6]. Une application de tels concepts se retrouve dans le *Power Control* avec le célèbre *Water-Filling* (allouer plus de puissance pour les transmissions sur les canaux les plus favorables et limiter la puissance pour les transmissions sur les canaux les moins favorables) [7].

Deux approches ont été successivement étudiées durant ces trois années de thèse afin de mitiger l'interférence dans les réseaux cellulaires. Une première étude (Section 3) a été réalisée pour des réseaux cellulaires tri-sectorisés et coopératifs (*i.e.,* mettant en place des mécanismes de communications coopératives), dotés de relais *half-duplex* par bande de fréquence. Cette étude cherche à étudier dans quelle mesure les communications coopératives peuvent aider à combattre le problème d'interférence, sachant que l'introduction de communications coopératives rehausse habituellement le niveau d'interférence. En coordonnant efficacement les transmissions de chaque source, le niveau d'interférence perçu par les relais peut être minimisé ; il est ainsi possible d'accroître la fiabilité du lien "relais-destination" et obtenir d'importants gains en termes de performance. Une allocation adaptative des ressources, basée sur le contexte courant de transmission, a également été proposée.

Notre seconde étude (Sections 4–6) est ciblée sur un système de femto-cellules et de macro-cellules dans lequel chaque cellule a des contraintes différentes (débit cible, puissances minimale et maximale de transmission, priorité, etc.). De par la topologie hautement variable du système (utilisateurs mobiles) et la nature 'temps variable' des canaux de transmissions (*fading*, *shadowing*), le niveau d'interférence perçu diffère d'un utilisateur à l'autre. Différents régimes d'interférence sont définis avec pour chacun d'eux un traitement spécifique à appliquer pour gérer l'interférence. Nous nous intéressons ici à des algorithmes

d'allocation de puissance qui vérifient conjointement toutes les contraintes du système, tout en tenant compte de l'interférence que génère une cellule sur ses voisines.

Chapitre 1 - Bref aperçu de la thèse

Le premier chapitre du mémoire effectue une entrée en matière qui permet d'introduire le sujet de la thèse. Une présentation du contexte et de la problématique permettent de développer sommairement les motivations et les objectifs de ces travaux de thèse. Enfin, un bref descriptif des enjeux est proposé, chapitre par chapitre, avec pour chacun d'eux la dissémination scientifique correspondante.

Chapitre 2 - Connaissances pré-requises sur l'interférence dans les réseaux sans fil

Ce chapitre définit ou rappelle quelques notions essentielles concernant les réseaux sans fil, la théorie de l'information et l'interférence entre communications radio ; ces rappels sont destinés à faciliter la compréhension du mémoire et des travaux qui y sont présentés.

Dans un premier temps, un rappel de quelques pré-requis sur les communications sans fil est proposé. Certains modèles de système sont utilisés à l'identique tout au long du mémoire ; ils sont par conséquent introduits et définis une seule fois dans ce chapitre, accompagnés des notations correspondantes. Ainsi, sont détaillés le canal à diffusion (*Broadcast Channel*), le canal à accès multiple (*Multiple Access Channel*) ou encore le canal à interférence (*Interference Channel* - voir Figure 1 équivalente à l'équation 1). Il en va de même pour quelques concepts et définitions essentiels en théorie de l'information, tels la capacité d'un canal, les degrés de liberté, la diversité, la probabilité de coupure ou encore certaines métriques d'évaluation de la qualité du canal. Enfin, nous présentons les principales hypothèses adoptées pour ces travaux de thèse et nous détaillons les caractéristiques que nous avons retenues pour modéliser le canal de propagation radio.

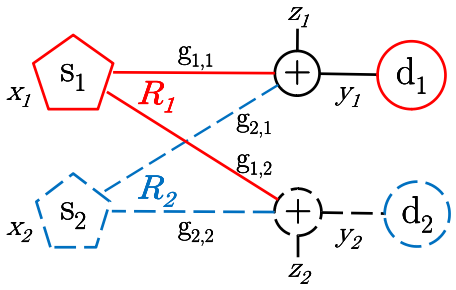

Figure 1 – Canal à interférence à deux utilisateurs : deux émetteurs s_1 et s_2 se partagent une même ressource de communication pour transmettre respectivement le message x_1 au récepteur d_1 et le message x_2 au récepteur d_2. La non-orthogonalité de ces deux transmissions dans un espace restreint occasionne de l'interférence co-canal ; le message reçu est perturbé par le bruit thermique et le message interférant.

$$\begin{cases} y_1 = g_{1,1} \cdot x_1 + g_{2,1} \cdot x_2 + z_1, \\ y_2 = g_{1,2} \cdot x_1 + g_{2,2} \cdot x_2 + z_2, \end{cases} \tag{1}$$

Dans un second temps, nous nous proposons de fournir une brève introduction aux systèmes de "femo-cellules" qui commencent à émerger dans le paysage des télécommunications et plus précisément dans les réseaux de communications sans fil domestiques et professionnels (voir Figure 2).

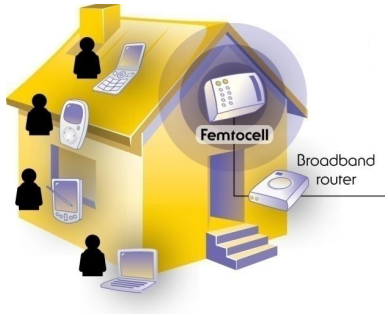

FIGURE 2 – Illustration d'un déploiement de femto-cellule pour une application domestique.

Pour conclure ce chapitre, nous dressons un état de l'art (non exhaustif) des principales techniques proposées dans la littérature et pertinentes avec notre problème d'interférence dans les réseaux sans fil. Cet état de l'art est détaillé selon les axes suivants : les techniques d'allocation orthogonale et non-orthogonale de ressources, les techniques de la théorie de l'information et du traitement du signal, ou encore les techniques de contrôle de puissance.

Chapitre 3 - Communications coopératives avec relais half-duplex

Une liste non exhaustive de techniques pour la réduction et le traitement de l'interférence a été établie en Section 2.4 mais dans ce chapitre nous proposons de traiter le problème d'interférence avec une approche peu conventionnelle, à savoir l'utilisation de communications coopératives. La coopération est basée sur l'utilisation d'une tierce entité, dite relais, qui va tenter d'aider un émetteur dans la transmission de son message vers son récepteur afin que ce dernier perçoive le message avec une qualité accrue. Pour ce faire, l'émetteur envoie son message en diffusion (*broadcast*) à destination de son récepteur et du relais. Le relais procède alors à quelques traitements sur le message reçu, puis le retransmet en direction du récepteur. Le récepteur final perçoit ainsi deux fois la même information. En plus de la redondance, un autre atout majeur est la diversité de route : les deux messages empruntent des routes différentes donc éprouvent des canaux radio différents ; si l'un des chemins est fortement interféré (fort évanouissement fréquentiel ou *fading*, obstacle à traverser, etc.), le second chemin peut alors devenir une alternative plus heureuse. La coopération offre également une extension de couverture en permettant éventuellement d'atteindre les utilisateurs les plus éloignés (par exemple ceux placés en bordure de cellule) Un système basique à un relais est représenté sur la Figure 3 avec le système d'équations équivalent :

$$\begin{cases} y_{d_i,1}^{(k)} = f_{i,i}^{(k)} \cdot x_{d_i}^{(k)} + n_{d_i} + I_{i,1}^{(k)} \\ y_{r_i}^{(k)} = h_{i,i}^{(k)} \cdot x_{d_i}^{(k)} + n_{r_i} + J_i^{(k)} \\ y_{d_i,2}^{(k)} = g_{i,i}^{(k)} \cdot x_{r_i}^{(k)} + n_{d_i} + I_{i,2}^{(k)} \\ y_i^{(k)} = y_{d_i,1}^{(k)} + y_{d_i,2}^{(k)} \\ x_{r_i}^{(k)} = \Phi(y_{r_i}^{(k)}). \end{cases} \tag{2}$$

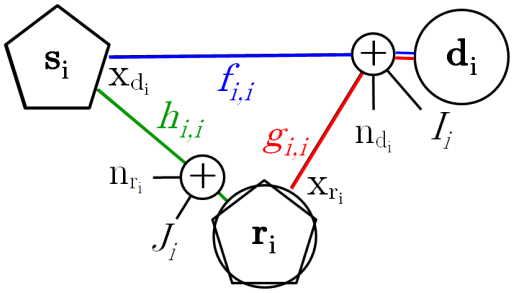

FIGURE 3 – Illustration du modèle de canal à relais à deux sauts avec lequel la destination finale d_i perçoit deux signaux issus de deux émetteurs différents mais qui renferment théoriquement la même information.

Les protocoles coopératifs ont toutefois leurs défauts. Avec le protocole *Amplify-and-Forward* (AF) le relais amplifie le signal qu'il perçoit avant de le retransmettre, c'est-à-dire qu'aussi bien le signal utile que le bruit additif et l'interférence sont amplifiés. Dans le cas du protocole *Decode-and-Forward* (DF), le relais décode le signal qu'il perçoit pour retransmettre ensuite une version ré-encodée du message utile : en cas d'erreur lors du décodage, l'erreur est transmise vers la destination ; en outre toute la fiabilité de la transmission entre l'émetteur et le relais est perdue lors du processus de décodage/codage. Des techniques hybrides sont étudiées afin de n'exploiter la coopération que lorsqu'elle améliore les performances au niveau du récepteur final [8].

La coopération n'est toutefois pas utilisée conventionnellement pour traiter le problème de réduction d'interférence. En effet, l'emploi de techniques coopératives peut paraître paradoxal : de nouvelles entités sont introduites dans le réseau (*i.e.,* les relais) ; ces entités utilisent les mêmes ressources de communication que les entités déjà présentes, ce qui accroît le niveau général d'interférence. Le problème sous-jacent traité dans ce chapitre est ainsi introduit ; il y a un compromis entre le surcoût d'interférence généré par l'activation des relais et les bienfaits de la coopération en termes d'accroissement des performances en réception. Le premier axe de cette thèse fut l'étude de ce compromis pour des transmissions en *Downlink (DL)*.

Ch.3-1 : Contexte

Le modèle adopté pour notre étude est celui d'un système cellulaire OFDMA trisectorisé coopératif, formé par trois secteurs adjacents dotés chacun d'une station de base, d'un relais et d'une destination (voir Figure 4). Ces trois secteurs se partagent deux bandes fréquentielles ; il est donc impossible d'orthogonaliser les communications des différents secteurs. Nous proposons l'emploi de relais dits *half-duplex par bande*. Un relais *half-duplex* ne peut, à un instant donné, soit qu'émettre, soit qu'écouter mais il ne peut réaliser ces deux actions simultanément. Avec un relais *half-duplex par bande*, la contrainte de non-simultanéité entre l'émission et la réception est restreinte à une bande fréquentielle et rendue indépendante d'une bande à l'autre : un tel relais peut donc simultanément émettre sur une bande et écouter sur une autre. L'emploi de relais *half-duplex* est communément admis, d'une part car l'utilisation de relais *full-duplex* requiert une duplication coûteuse et volumineuse du circuit RF (l'un pour la transmission et l'autre pour la réception) ; d'autre part car la tendance est à la réduction de la puissance consommée, ce qui va à l'encontre d'un double circuit RF. Dans le cadre de systèmes OFDMA avec une orthogonalisation des différentes bandes, notre hypothèse de relais *half-duplex par bande* se valide tout à fait. Nous supposons également des transmissions synchrones soumises à un bruit additif

Gaussien, à un *fading* de Rayleigh et à du *shadowing*. Le temps de cohérence des canaux est supposé supérieur à la durée de transmission d'une trame ainsi qu'à la période des *schedulers* pour l'allocation de ressources.

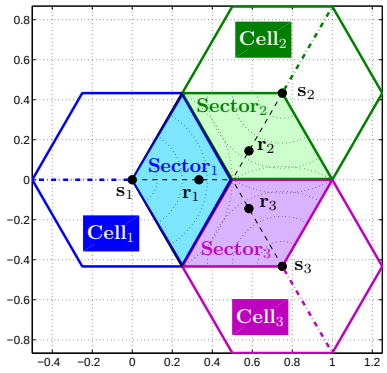

FIGURE 4 – Système de trois secteurs, dotés chacun d'une source ($\mathbf{s}_i$), d'un relais ($\mathbf{r}_i$) et d'une destination ($\mathbf{d}_i$). Dans cette étude le relais $\mathbf{r}_i$ est supposé fixe et est placé aux deux tiers de la distance maximale sur l'axe central du secteur. La destination $\mathbf{d}_i$ est mobile et peut se déplacée en tout point de son secteur.

Aucune technique avancée de contrôle de puissance n'est effectuée ; nous nous inspirons de l'allocation *'On-Off'* introduite dans [9]. Avec une telle technique, un émetteur (source ou relais) transmet soit à puissance maximale sur une bande (*'On'*), soit reste momentanément silencieux (*'Off'*) pour ne pas interférer avec ses voisins. Cette approche bien plus simple qu'une allocation optimale de puissance a le mérite d'être bien moins complexe.

Ch.3-2 : Patterns d'allocation de ressources

Pour gérer le compromis entre atouts et méfaits de la coopération, différents *patterns* ou modes d'allocation des ressources de communication ont été introduits et comparés. Ces différentes allocations mettent en jeu les "blocs-ressources" (la plus petite entité regroupant un *time slot* et une bande fréquentielle). L'idée est d'allouer efficacement ces blocs-ressources entre les émetteurs actifs du système, de coordonner judicieusement les émissions, afin de minimiser l'interférence subie, notamment au niveau du relais.

Les différents modes d'allocation se dérivent de la sorte : les trois stations de bases (appelées "sources" par la suite) émettent toujours à pleine puissance, sur une ou deux bandes fréquentielles ; les trois relais peuvent - indépendamment les uns des autres - être momentanément silencieux, ou actifs et transmettre à pleine puissance. L'état d'activation des trois relais définit le mode d'allocation : trois relais pouvant être indépendamment actifs ou inactifs dérivent $2^3 = 8$ modes différents. En guise de nomenclature pour faire référence à ces modes nous employons le formalisme suivant : un triplet de lettres décrit le mode, une lettre pour chaque secteur ; la lettre en position i est un 'C' (**C**oopération) si le relais du secteur S_i ($\mathbf{r}_i$) est activé, sinon cette i-ème lettre est un 'N' (**N**on coopération). Les Figures 7a, 7b et 7c illustrent les principaux modes proposés.

Les stratégies coopératives AF et DF habituelles s'exécutent sur deux *time slots* : dans un premier temps la source émet sur une bande, la destination et le relais écoutant sur cette bande ; dans un second temps le relais retransmet sur cette même bande et la destination écoute une nouvelle fois sur cette bande. De telles stratégies sont prises pour référence dans notre étude. Un relais *half-duplex par bande* écoute sur une bande le message émis par sa source au temps n alors qu'il retransmet simultanément sur une autre bande le

message émis par sa source au temps $(n-1)$. Les atouts d'une stratégie avec un tel relais sont multiples. Tout d'abord les ressources sont mieux exploitées et l'efficacité spectrale est accrue : la transmission d'une trame coopérative requiert asymptotiquement un seul *time slot* contre deux pour une stratégie coopérative classique. En effet avec un tel relais $n+1$ *time slots* sont requis pour l'envoi de n trames coopératives, contre $2n$ *time slots* avec une stratégie standard. La Figure 5 illustre ces propos.

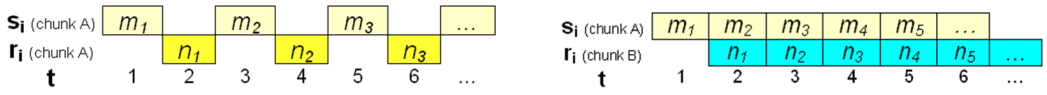

(a) Stratégies coopératives classiques

(b) Stratégie coopérative avec relais *half-duplex par bande*

FIGURE 5 – Comparaison de différentes stratégies coopératives au niveau de l'allocation des blocs-ressources.

En outre, il suffit de coordonner les transmissions dans chaque secteur pour aligner sur une même bande les transmissions d'un relais et celles de ces plus forts interféreurs. En opérant de la sorte, le relais ne perçoit pas l'interférence la plus contraignante : quand il émet sur une bande, il n'écoute pas sur cette bande et ne peut par conséquent pas être interféré. En revanche, l'accroissement de l'efficacité spectrale se fait au détriment de l'orthogonalité des transmissions : de l'interférence additionnelle est introduite par rapport aux protocoles classiques, mais c'est là que réside justement le compromis précédemment évoqué. La Figure 6 tente d'illustrer cette coordination entre sources et relais de secteurs (ou cellules) voisins en allouant des bandes orthogonales aux transmissions concurrentes. Mais cela n'exclut pas que les destinations puissent souffrir d'interférence intercellulaire.

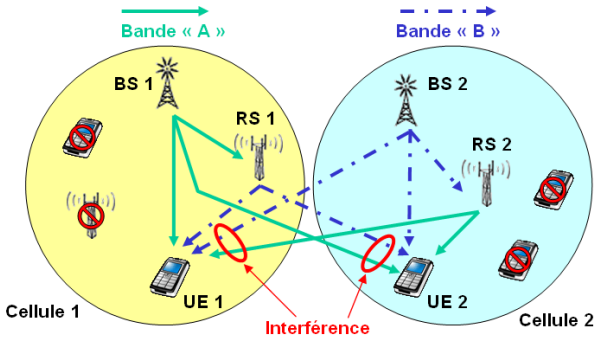

FIGURE 6 – Illustration d'une allocation de ressources entre émetteurs : deux bandes fréquentielles sont partagées entre deux stations de base et deux relais, les relais étant supposés *half-duplex par bande*. En coordonnant convenablement les transmissions des deux cellules, le relais **RS 1** écoute sur la bande A et transmet sur la bande B, alors que le relais **RS 2** écoute sur la bande B en transmettant sur la bande A. Ainsi, **RS 1** n'est pas perturbé par son plus fort interféreur (**BS 2**) mais cela n'empêche pas pour autant qu'il y ait de l'interférence entre relais ou du relais vers la destination voisine.

Avec le modèle que nous avons adopté nous avons deux bandes fréquentielles pour trois secteurs. A moins de séparer temporellement les transmissions (*Time-Sharing*), il est impossible de ne pas avoir d'interférence car la granularité des ressources est telle qu'il y

a plus de demandes en ressources de communication que d'offres. Il faut donc adopter une politique d'allocation de ressources entre secteurs. Deux règles, ou politiques d'allocation, sont ainsi distinguées :

- **R1** : Un des trois secteurs est avantagé par rapport aux deux autres ; il dispose ainsi d'une bande fréquentielle exclusive alors que les deux autres secteurs doivent se partager la seule bande restante.
- **R2** : Les trois secteurs utilisent et se partagent les deux bandes disponibles.

On comprend qu'avec la règle **R1** le secteur avantagé ne subira pas le même niveau d'interférence que les deux autres secteurs, alors qu'avec la règle **R2** le taux d'utilisation fréquentiel est maximal mais l'interférence est plus élevée. Pour la suite de l'étude, nous supposons que le secteur S_1 est le secteur privilégié, ce choix étant purement arbitraire : toute l'étude se transpose aisément avec un autre secteur prioritaire !

Nous proposons de décliner les huit modes (patterns) d'allocation de ressources introduits précédemment selon trois stratégies, en fonction de la stratégie coopérative adoptée et de la politique d'allocation entre secteurs. Ces trois stratégies sont dérivées de la façon suivante :

- Deux stratégies, dites *Classic 1* ($C1$) et *Classic 2* ($C2$), utilisent toutes les deux les stratégies coopératives usuelles (voir Figure 5a) mais diffèrent au niveau de la politique d'allocation entre secteurs : $C1$ suit la règle **R1** alors que $C2$ suit la règle **R2**.
- Une troisième stratégie, dite *Advanced* (A), exploite la nature *half-duplex par bande* des relais (voir Figure 5b).

Les patterns d'allocation sont donc référencés par le triplet d'activation des relais et par la stratégie employée. La métrique adoptée pour comparer les patterns d'allocation fut la quantité d'information mutuelle globale. Cette métrique est dérivée pour chaque pattern, aussi bien pour des protocoles coopératifs AF que pour des protocoles coopératifs DF. [10] apporte quelques éléments pour comprendre comment exprimer ces quantités d'information mutuelle. Les Figures 7a, 7b et 7c présentent quelques-uns des différents *patterns* proposés. Les patterns non représentés se déduisent aisément à partir de ceux illustrés.

Ch.3-3 : Processus d'allocation adaptative des ressources (ARAP)

Les performances de ces différents modes d'allocation ont été étudiées lors de simulations numériques. La métrique adoptée a été la quantité d'information mutuelle globale, c'est-à-dire la somme des quantités d'information mutuelle de chaque secteur. Cette dernière est notée *GMI* pour *Global Mutual Information* et est en lien avec la capacité du système. Toutefois, afin de prendre en considération la dépense énergétique imposée par chaque pattern, *GMI* est pondérée par le budget en puissance requis par chaque pattern. La nouvelle métrique ainsi obtenue est identifiée par $\widehat{GMI}$. Les patterns ne mettent en effet en jeu ni le même nombre, ni le même type d'émetteurs ; les puissances consommées diffèrent donc d'un pattern à l'autre. En guise d'illustration, considérons le mode 'NNN' où aucun secteur ne planifie de communication coopérative et le mode 'CCC' où chaque secteur met en place de la coopération. Dans le premier cas la puissance totale consommée est donnée par la somme des puissances de chacune des sources alors que dans le second cas il faut y ajouter la somme des puissances des relais. Nous avons supposé que les trois sources émettaient avec la même puissance P_s, de même pour les trois relais avec la puissance P_r. Le budget en puissance est résumé par pattern et par stratégie dans le Tableau 3.1.

Afin d'étudier le compromis entre les bienfaits et les méfaits de la coopération, nous pro-

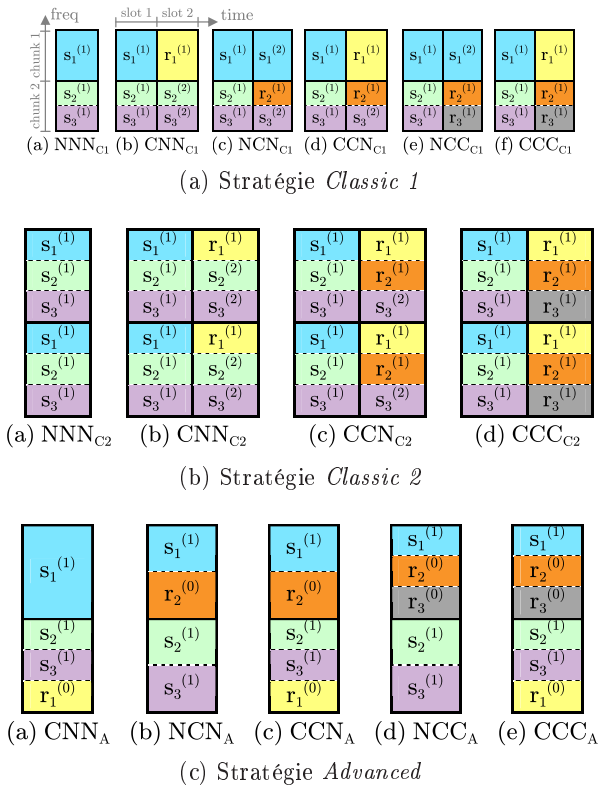

FIGURE 7 – Représentation des modes d'allocation pour les trois stratégies.

posons un processus adaptatif qui sélectionnera quel est le mode d'allocation des ressources qui maximise la métrique $\widehat{GMI}$ pour le contexte courant de communication. Plusieurs paramètres sont à considérer.

1. La puissance consommée. Les communications coopératives peuvent accroître la capacité d'un canal mais cette amélioration ne doit pas se faire au détriment d'un budget excessif en puissance ; c'est pour cela que nous considérons la métrique $\widehat{GMI}$ plutôt que GMI.
2. L'interférence générée. L'activation d'un relais peut certes apporter une amélioration des performances en termes d'information mutuelle pour la destination servie par le relais, mais l'activation de ce relais peut également causer de l'interférence intersecteur et ainsi affecter la qualité des communications dans les secteurs voisins. C'est pour cela que nous considérons une métrique globale (somme de l'information mutuelle de chaque secteur) plutôt qu'une métrique locale (information mutuelle d'un seul secteur). L'idée essentielle est que l'activation d'un relais doit apporter plus de bienfaits à sa destination que de méfaits qu'il cause sur son entourage et en particulier sur ses secteurs voisins.
3. Les canaux temps variable. Un mode d'allocation peut se trouver être optimal dans un contexte de communication donné mais se retrouver mauvais à l'instant d'après, par exemple en raison d'un fort évanouissement fréquentiel sur un lien. Le *fading* et le *shadowing* créent en effet un aléa temporel et fréquentiel qui impacte les performances entre deux contextes de transmission.
4. La mobilité des destinations. Tout comme le *fading* ou le *shadowing*, la mobilité des

entités joue aussi sur les performances. Dans notre étude, seules les destinations sont mobiles. Mais leur distance respective des différents émetteurs, à savoir les stations de base et les relais, impacte la qualité des canaux en raison du *path loss* (atténuation d'autant plus importante que la distance est grande).

Nous proposons d'étudier le compromis précédemment établi en tenant compte des différents paramètres énumérés ci-dessus. Pour ce faire, nous utilisons un processus d'allocation adaptative des ressources (ARAP - *Adaptive Resource Allocation Process*) qui calcule pour chaque contexte de communication (comprendre par contexte de communication un vecteur d'état de chaque canal avec *fading* et *shadowing* et un vecteur de position pour chaque destination) quel est le mode d'allocation de ressources qui maximise la métrique $\widehat{GMI}$.

Pour représenter d'une façon plus agréable les résultats, les performances sont moyennées sur un grand nombre de contextes de communication. Le critère retenu pour la représentation des résultats est la position de la destination $\mathbf{d}_1$ au sein de son secteur S_1. La métrique $\widehat{GMI}$ est ainsi indexée comme suivant $\widehat{GMI}_{d_1}$. Cette position devient donc le critère d'étude et tous les autres paramètres sont tirés aléatoirement puis les performances sont prises en moyenne. La Figure 8 illustre séquentiellement la façon dont sont obtenus les résultats ; ce processus se termine par la recherche du pattern optimal qui maximise la métrique.

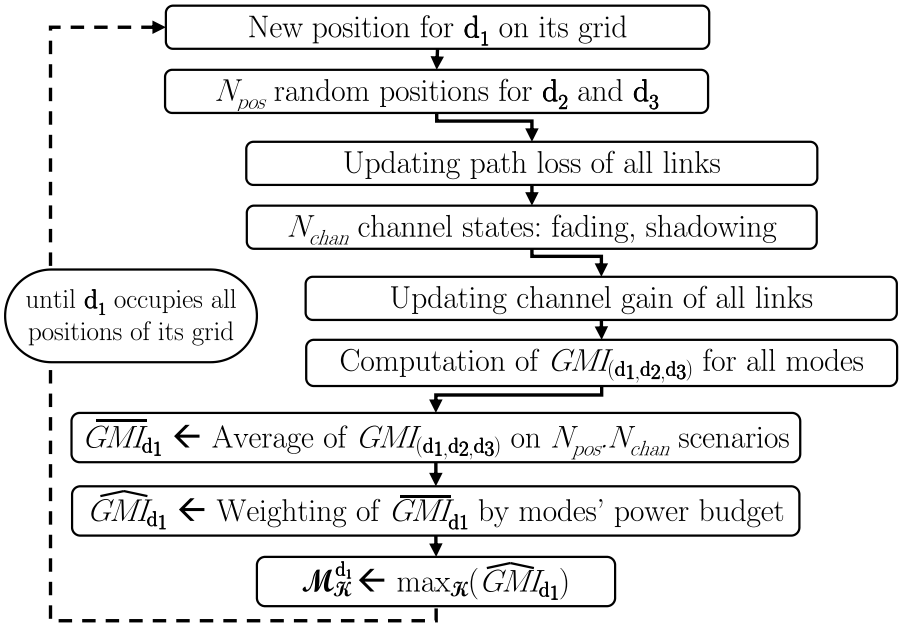

FIGURE 8 – Description du processus ARAP d'allocation adaptative des ressources de communication. Le paramètre d'entrée est la position de la destination $\mathbf{d}_1$ au sein de son secteur et compte tenu de cette position plusieurs contextes de simulation sont tirés de façon aléatoire et la métrique $\widehat{GMI}_{d_1}$ est calculée comme étant une moyenne de tous ces contextes. En fin de chaîne, le pattern d'allocation qui maximise la métrique est identifié ; il représente la façon la plus performante d'allouer les ressources avec pour seule connaissance la localisation de $\mathbf{d}_1$ dans son secteur.

Ch.3-4 : Résultats de simulation

Dans ce résumé les résultats ne seront que présentés de façon succincte ; pour une analyse plus détaillée le lecteur pourra se reporter au Chapitre 3 à partir de sa section 3.4.4. Les applications numériques des paramètres de simulation sont listées dans le Tableau 3.2.

Comme énoncé précédemment les résultats sont conditionnés par la position de la destination $\mathbf{d}_1$ dans son secteur et représentent une moyenne sur un grand nombre de contexte de communication. Plusieurs campagnes de simulation ont été réalisées, avec des protocoles coopératifs AF ou DF, avec des hautes puissances de transmission ou des puissances plus faibles. Nous ne parlerons dans ce résumé que des protocoles coopératifs de type *Decode-and-Forward* (DF) avec des émetteurs utilisant de hautes puissances en transmission. Nous supposons en outre que le relais décode sans erreur le message qu'il reçoit de sa source.

Les premiers résultats représentés par la Figure 9 permettent de comparer les performances de chaque pattern d'allocation de ressource lorsque la destination $\mathbf{d}_1$ se déplace le long de l'axe '$\mathbf{s}_1$-$\mathbf{r}_1$'. En abscisse nous retrouvons la distance entre la source $\mathbf{s}_1$ et sa destination $\mathbf{d}_1$ alors qu'en ordonnée figure la métrique $\widehat{GMI}_{d_1}$. Les courbes sont distinguées de la façon suivante : chaque type de pattern est représenté par des marqueurs et une couleur spécifique tandis que les stratégies coopératives sont indiquées par le type de trait (trait plein pour la stratégie *Advanced* (A) et trait discontinu pour la stratégie *Classic 1* (C1)). La position du relais $\mathbf{r}_1$ sur l'axe des abscisses est également précisée par une droite verticale rouge pointillée.

Comme nous pouvions le présager, la métrique $\widehat{GMI}_{d_1}$ diminue plus $\mathbf{d}_1$ s'éloigne de sa source, et ceci en raison du *path loss*. Toutefois $\widehat{GMI}_{d_1}$ croît au voisinage de $\mathbf{r}_1$ pour tous les patterns mettant en jeu la coopération avec $\mathbf{r}_1$. Ceci correspond à la zone de couverture du relais ; lorsque la destination $\mathbf{d}_1$ entre dans cette zone elle ressent les bienfaits de la coopération.

Une étude plus approfondie des résultats montre que la stratégie proposée (A) surpasse à tout niveau la stratégie coopérative de référence (C1). Les résultats obtenus avec la stratégie C2 ne sont pas représentés car ils sont toujours inférieurs à ceux obtenus avec la stratégie C1. En outre, on remarque que $\widehat{GMI}_{d_1}$ est d'autant plus grand que le nombre de secteurs usant de la coopération est faible, ceci pour la stratégie A. Cela indique que trop de coopération est plus préjudiciable au système que peu de coopération.

D'autres résultats ont été obtenus par l'exécution du processus ARAP décrit en Figure 8. Il s'agit de déplacer la destination $\mathbf{d}_1$ de telle sorte qu'elle occupe successivement toutes les positions de son secteur ; pour chacune de ses positions, la métrique $\widehat{GMI}_{d_1}$ est calculée et le pattern qui la maximise est identifié comme étant $\mathscr{M}_{\Omega_{all}}^{d_1}$, où Ω_{all} est l'ensemble de tous les patterns considérés. Le principe adopté pour représenter les résultats est le suivant :

- Chaque type de patterns d'allocation de ressources est identifié par une couleur particulière : par exemple rouge pour les patterns 'NNN', vert pour les patterns 'CNN', bleu pour les patterns 'NCN' ou blanc pour les patterns 'NNC'.
- Pour chaque position de $\mathbf{d}_1$ dans son secteur S_1 le processus ARAP identifie le pattern $\mathscr{M}_{\Omega_{all}}^{d_1}$.
- Pour une position donnée de $\mathbf{d}_1$ cette position est coloriée avec la couleur correspondant au type de pattern auquel appartient $\mathscr{M}_{\Omega_{all}}^{d_1}$.

Nous arrivons ainsi à créer des cartes d'optimalité telles que celle en Figure 10.

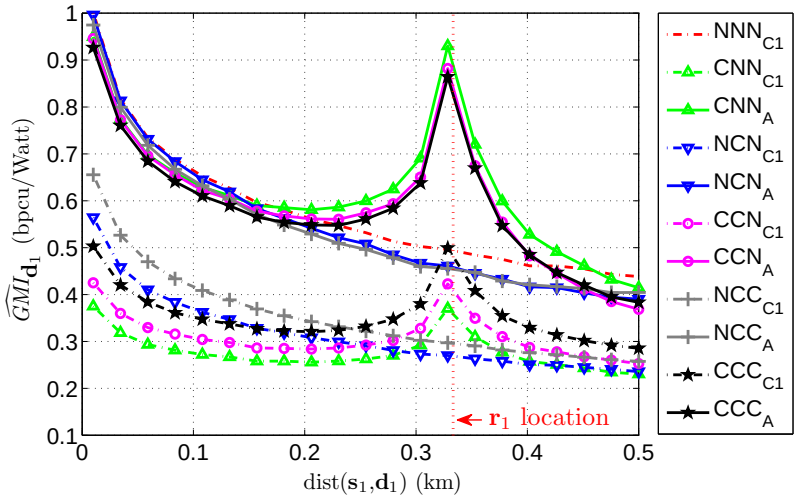

FIGURE 9 – Évolution de la métrique $\widehat{GMI}_{d_1}(M)$ lorsque la destination $\mathbf{d}_1$ se déplace le long de l'axe '$\mathbf{s}_1$-$\mathbf{r}_1$', M désignant un mode d'allocation de ressources. Ces performances sont obtenues avec un protocole coopératif de type DF et de hautes puissances en transmission pour les stations de base et les relais.

Avant toute chose, une étude plus approfondie révèle que pour chaque position de $\mathbf{d}_1$ le protocole optimal est toujours sélectionné parmi la stratégie *Advanced* (A). La recherche du pattern optimal peut donc se limiter à une recherche parmi tous les patterns de la stratégie 'A' plutôt qu'une recherche exhaustive entre tous les patterns Ω_{all}. Sur la Figure 10 nous voyons ainsi différentes zones de couleur. Autour du relais $\mathbf{r}_1$ il est optimal d'adopter un pattern 'CNN_A' alors qu'en s'éloignant un peu plus du relais, le pattern 'NNN_A' devient optimal. Ce changement de couleur traduit le fait que la destination $\mathbf{d}_1$ sort de la zone de bienfaisance de son relais et que l'activation de ce dernier cause plus de tort en termes d'interférence inter-secteur que d'accroissement en termes d'information mutuelle. La tendance s'inverse à nouveau dans les coins supérieur et inférieur du secteur où respectivement les patterns 'NNC_A' et 'NCN_A' deviennent optimaux. Pour la zone supérieure il faut comprendre que la destination $\mathbf{d}_1$ est si éloignée de son relais qu'il ne lui apporte aucune aide ; en revanche $\mathbf{d}_1$ est suffisamment éloignée du relais $\mathbf{r}_3$ pour que l'activation de ce dernier n'impacte pas $\mathbf{d}_1$ autant qu'il n'aide la destination $\mathbf{d}_3$. Il en est de même avec la zone inférieure et le relais $\mathbf{r}_2$ (reprendre la Figure 4 pour voir la localisation des secteurs).

Ch.3-5 : Conclusion de cette étude

Le travail réalisé dans le cadre de cette étude a fait l'objet de contributions pour le projet européen FP7-ICT ROCKET [11] et de deux publications en conférence. Une nouvelle approche est proposée pour mitiger l'interférence intercellulaire dans les réseaux coopératifs. Grâce à l'utilisation de relais *half-duplex par bande*, nous proposons plusieurs patterns d'allocation de ressources pour réduire l'interférence éprouvée au niveau du relais. Les transmissions coopératives peuvent ainsi fournir un gain qui surpasse les dégradations qu'elles occasionnent. Les performances des transmissions sont accrues au prix d'une consommation de puissance réduite. Un algorithme adaptatif permet de fournir une représentation géographique du compromis entre bienfaits et méfaits de la coopération.

Une généralisation de cette étude pour un nombre quelconque de bandes fréquentielles est également à l'étude ; une méthodologie est proposée pour réutiliser dans le cadre d'un

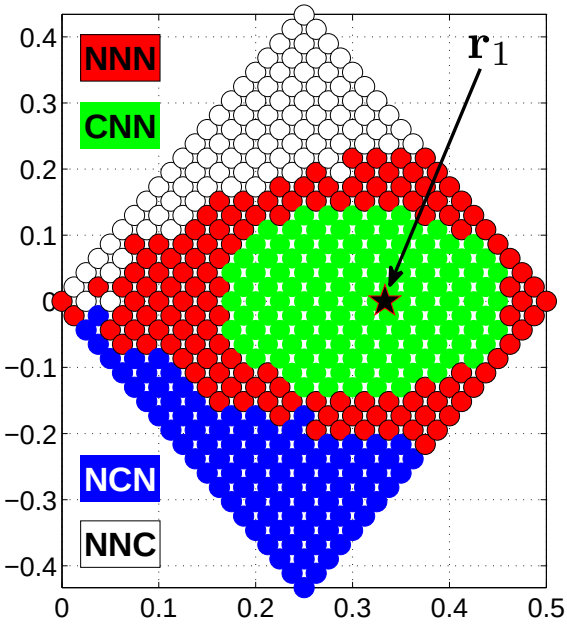

FIGURE 10 – Carte d'optimalité du secteur S_1 dans le cadre d'un protocole coopératif de type DF avec de hautes puissances de transmission pour les stations de base et les relais. Cette carte indique quel type de pattern d'allocation de ressources sied le mieux à chaque position de $\mathbf{d}_1$, c'est-à-dire quel est le protocole $\mathscr{M}_{\Omega_{all}}^{d_1}$ qui maximise la métrique $\widehat{GMI}_{d_1}$.

nombre quelconque de bandes fréquentielles l'étude menée pour deux bandes.

Chapitre 4 - Traitement adaptatif de l'interférence

Le second axe de recherche présenté dans ce mémoire s'intéresse toujours à la problématique de gestion de l'interférence. Toutefois le contexte choisi pour cadre applicatif est celui des réseaux de femto-cellules. De tels réseaux mettent en jeu d'une part des stations de base assurant une couverture étendue et transmettant à des puissances relativement importantes (macro-cellules), et d'autre part des stations de base plus petites destinées à offrir une couverture peu étendue, éventuellement temporaire et mobile, et transmettant à faible puissance (femto-cellule). Les femto-cellules ne doivent pas perturber les macro-cellules : l'idée est un peu celle de la radio cognitive où le système secondaire (femto-cellules) doit exploiter au mieux les ressources laissées disponibles sans perturber les transmissions du système primaire (macro-cellules).

Dans un tel réseau les exigences et contraintes de chaque cellule sont hautement hétérogènes. D'une part en raison de la mobilité des utilisateurs et de leur accès sporadique au réseau (topologie du réseau et densité d'utilisateurs variables) ; d'autre part car les contraintes en termes de qualité de service (QoS) varient d'une cellule à l'autre et éventuellement au cours de la journée : la charge du réseau peut être importante en pleine journée et réduite en soirée, des communications peuvent véhiculer du trafic voix alors que d'autres gèrent du trafic vidéo, etc. En outre, chaque canal de communication est soumis à l'interférence (intercellulaire) et aux dégradations temps variable du canal radio mobile (*fading*, *shadowing*, *path loss*).

Comme les macro-cellules transmettent à des puissances bien supérieures à celles des

femto-cellules, le rapport signal utile sur bruit et interférence (*Signal to Interference and Noise Ratio* - SINR) peut fortement varier d'une cellule à l'autre. Chaque paire "émetteur-récepteur" (E-R) va donc devoir s'adapter à son environnement et à la qualité du signal qu'il perçoit pour atteindre ses contraintes de QoS. Une technique statique et locale n'est toutefois pas envisageable : les interactions entre cellules (en matière d'interférence) et la dynamique du problème imposent l'emploi de techniques adaptatives et globales.

Nous proposons plusieurs méthodes adaptatives pour gérer l'interférence intercellulaire et ainsi permettre aux paires 'E-R' de vérifier conjointement leurs contraintes. La finalité de cette étude est de proposer un contrôle de puissance adapté au contexte de communication courant qui permet à chaque paire 'E-R' d'atteindre son degré de satisfaction (QoS) tout en tenant compte de l'interférence qu'elle génère sur ses paires voisines. Une version centralisée (Chapitre 5) ainsi qu'une version distribuée (Chapitre 6) ont été étudiées.

Lorsqu'une cellule détermine sa puissance de transmission, elle cherche certes à atteindre ses contraintes, mais doit également garder à l'esprit qu'elle impose alors un niveau d'interférence intercellulaire à ses voisines, et que cela pourrait leur empêcher de vérifier leurs contraintes. Avec notre approche, la problématique d'interférence est envisagée dans sa globalité et non pas cellule par cellule de façon égoïste.

Ch.4-1 : Régimes d'interférence

Mais avant de développer nos algorithmes d'allocation de puissance, nous présentons dans ce chapitre un nouveau classificateur de l'interférence intercellulaire. L'idée essentielle de ce chapitre est que le signal interférant n'est pas toujours une source de perturbation s'il est bien traité en réception. En effet, la théorie de l'information apporte quelques bases utiles en matière de gestion de l'interférence. Ainsi, différentes techniques pour réduire les effets néfastes de l'interférence sont possibles, selon l'intensité du signal interférant que le récepteur perçoit en comparaison de l'intensité de son signal utile.

Historiquement, plusieurs techniques et modèles de canaux ont été développés pour caractériser de la meilleure façon possible le canal à interférence (voir Chapitre 4). De ces études on retiendra principalement deux résultats. Le premier résultat des plus intéressants pour notre étude est connu sous le nom de *Superposition Coding* [12]. Un émetteur E cherche à transmettre un message m à son récepteur R via une ressource partagée. L'idée consiste à décomposer le message à émettre en deux : un premier sous-message 'public' destiné à être décodé par tous les récepteurs avoisinants et un second sous-message 'privé' que seul le récepteur R doit/peut décoder. Un tel concept est illustré sur la Figure 11.

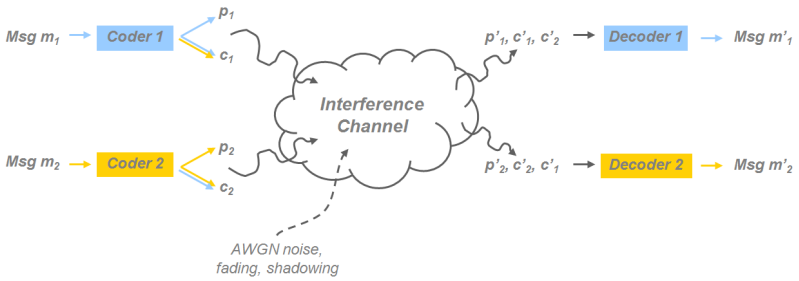

FIGURE 11 – *Superposition Coding* proposé par Han et Kobayashi : le message est décomposé en une information publique destinée à tous et une information privée uniquement destinée au récepteur visé.

Le second résultat est proposé dans [13] et met en avant une classification de l'interférence en cinq régimes basée sur le rapport entre le niveau d'interférence et le niveau du signal utile. Cette classification est issue d'une étude sur le nombre de degrés de liberté dans un canal à interférence à deux utilisateurs ; en fonction du niveau de l'interférence perçue, différentes hypothèses sont formulées pour maximiser la capacité du canal et se rapprocher ainsi au plus près des bornes théoriques. L'illustration des performances met en évidence une courbe en forme de 'W' comme l'atteste la Figure 12.

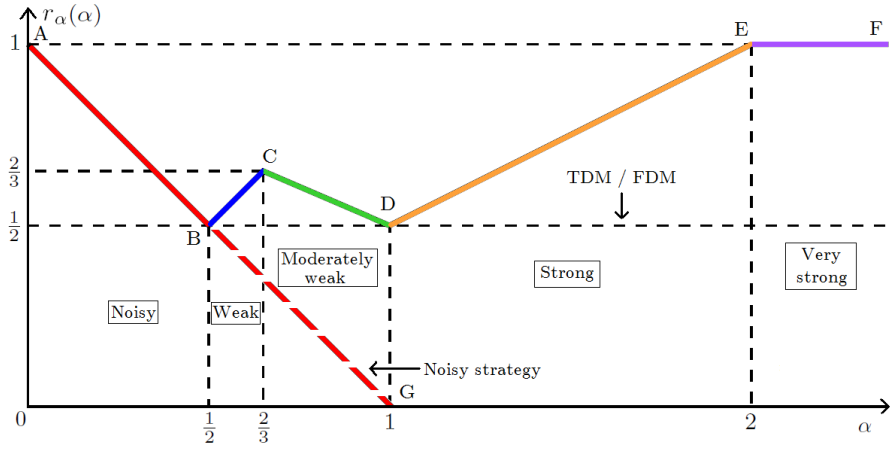

FIGURE 12 – Représentation de la courbe en 'W' décrivant le nombre de degrés de liberté en fonction du ratio entre log(INR) et log(SNR). En fonction des stratégies mises en place, une classification en cinq régimes de l'interférence est ainsi mise en évidence.

Ch.4-2 : Classification d'interférence proposée

Dans ce chapitre nous proposons un classificateur de l'interférence à trois régimes. Ce classificateur se veut moins complexe que celui à cinq régimes présentés précédemment, avec des hypothèses plus souples et une utilisation plus aisée dans un contexte pratique. Les trois régimes d'interférence que nous distinguons sont les suivants :

- Haut niveau d'interférence : l'intensité du signal d'interférence perçu par un récepteur est si élevée qu'il est préférable pour ce récepteur de commencer par décoder l'interférence en considérant le signal utile comme du bruit, puis de retrancher cette interférence du signal reçu ; subsiste alors le signal utile bruité. Les techniques utilisées pour ce régime sont basées sur le *Successive Interference Cancellation* (SIC).
- Faible niveau d'interférence : l'interférence perçue est à un niveau si faible qu'elle peut être assimilée au bruit et traitée comme tel, c'est-à-dire comme une source parasite que l'on ne cherche pas à décoder. L'avantage de ce régime est la faible complexité de son implémentation, puisqu'aucun traitement spécifique n'est appliqué.
- Niveau d'interférence intermédiaire : c'est le régime problématique de notre étude dans la mesure où aucune technique performante ne traite bien ce cas actuellement. Une solution est le *Time-Sharing*, en allouant successivement les ressources à chaque transmission pour les isoler les unes des autres et ainsi éviter qu'elles interfèrent. Cependant cela réduit fortement l'efficacité spectrale. Nous proposons un moyen plus efficace pour gérer ce régime : le *Joint Decoding*.

L'une des principales idées de notre étude est que l'interférence n'est pas nécessairement un obstacle si elle est bien traitée. Avec la connaissance du niveau d'interférence, et donc du

O_i	Scheme	Boundaries of applicability	Achievable SNR γ_i
1	Noisy	$\delta_i \leq A_j$	$\gamma_i \geq A_i(1+\delta_i)$
2	Joint decoding	$A_j \leq \delta_i \leq A_j(1+\gamma_i)$	$\gamma_i \geq A - \delta_i$
3	SIC-based	$\frac{\delta_i}{1+\gamma_i} \geq A_j$	$\gamma_i \geq A_i$

TABLE 1 – Récapitulatif des équations régissant ce classificateur d'interférence. On retrouve d'une part les équations délimitant les frontières de chaque régime, d'autre part les équations définissant la région du plan où les contraintes de QoS sont atteintes.

régime d'interférence, le couple 'E/R' peut déterminer dans quel régime il se trouve et alors mettre en place la technique de gestion de l'interférence adéquate. Ce chapitre présente avant tout un concept qui est par la suite exploité dans les Chapitres 5 et 6 pour mettre en place des algorithmes de contrôle de puissance. Les principaux résultats sont présentés dans le Tableau 1 et illustrés sur la Figure 13. Pour une explication plus détaillée de ces résultats ou des notations adoptées, nous invitions le lecteur à se référer au Chapitre 4.

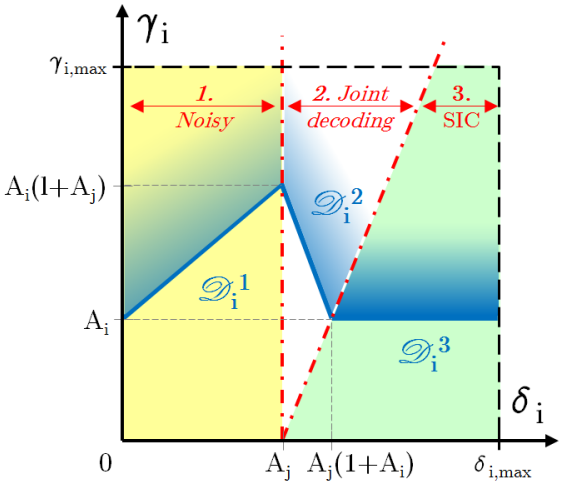

FIGURE 13 – Représentation du classificateur d'interférence dans le plan $(\delta_i; \gamma_i)$, c'est-à-dire le plan avec l'INR en abscisse et le SNR en ordonnée. Les droites rouges caractérisent les frontières entre chaque régime, représentés chacun par une couleur différente, tandis que les droites bleues délimitent la région où les contraintes de QoS sont atteintes (zone en dégradé bleu).

L'étude a été majoritairement menée dans le contexte d'un canal à interférence à deux utilisateurs. En fin de chapitre, nous étudions la possibilité d'exporter nos résultats à un modèle avec un nombre quelconque d'utilisateurs.

Chapitre 5 - Algorithme centralisé d'allocation de puissance

Ce chapitre exploite le classificateur d'interférence introduit dans le Chapitre 4 afin de mettre en place un algorithme centralisé de contrôle de puissance qui minimise les puissances de transmission sous respect de contraintes en débit de chaque paire 'E/R'. Un

premier modèle d'étude considère le cas simple de deux femto-cellules avec chacune une paire 'E/R' et une contrainte propre en débit.

Ch.5-1 : Algorithme CPA - Principe

Notre algorithme CPA (*Centralized Power Allocation*) fournit en amont de la transmission un ensemble de paramètres de transmission à adopter pour assurer que chaque cellule vérifie ses contraintes. Cet algorithme prend comme paramètres d'entrée les contraintes (débit, puissances minimale et maximale) ainsi que l'état du canal (variance de bruit, gains des différents canaux) et fournit en sortie le vecteur de puissance optimal ainsi que la façon de traiter efficacement l'interférence dans chaque cellule (information issue du classificateur d'interférence). A l'aide de ces deux sorties, les émetteurs savent qu'avec la puissance de transmission ainsi définie chaque récepteur pourra atteindre le débit souhaité. L'algorithme CPA est schématisé sur la Figure 14.

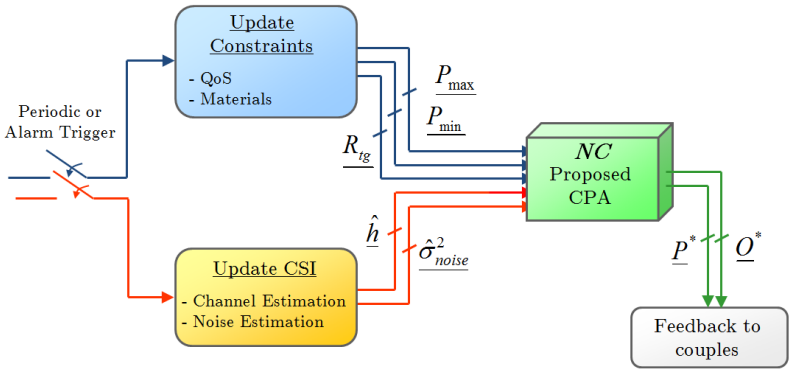

FIGURE 14 – Algorithme CPA de minimisation de la puissance de transmission sous contraintes en débit. La connaissance de paramètres sur les canaux et le système permet de déterminer en amont de la transmission le vecteur minimal de puissance et la stratégie adéquate de gestion de l'interférence dans chaque cellule.

Le principe général de notre algorithme CPA est d'exploiter les solutions du classificateur défini précédemment. Ce classificateur apporte une solution pour une paire 'E/R' ; il suffit donc de considérer l'intersection des solutions pour chaque paire 'E/R'. Moyennant un changement de repère, la Figure 13 se dérive aisément pour chaque paire 'E/R' du système et les résultats peuvent alors se superposer sur une même figure, comme représenté sur la Figure 15. Les droites rouges et vertes délimitent les frontières de chaque régime, respectivement pour la première et la seconde paire 'E/R'. Les droites bleues et violettes indiquent la fonction d'optimalité respectivement pour la première et la seconde paire 'E/R'.

L'intersection des droites bleues et violettes décrivent la solution optimale que l'on recherche. Les coordonnées de ce point définissent le vecteur de puissance optimal. La localisation de ce point définit quel est le couple de régimes d'interférence optimal qui permet de traiter convenablement l'interférence dans chaque cellule.

Une étude théorique montre qu'il existe dans le cas simple de deux femto-cellules toujours au moins une solution optimale, parfois trois. Il convient ensuite de vérifier la validité de cette solution avec les contraintes matérielles (puissances minimale et maximale de transmission). La convergence de l'algorithme est donc toujours assurée. Le vecteur de

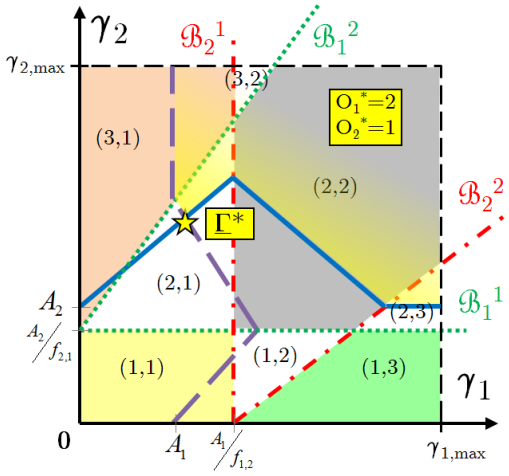

FIGURE 15 – Le processus de classification de l'interférence est exécuté pour chaque paire 'E/R' du système et le résultat est superposé sur une même figure. L'intersection des courbes d'optimalité définisse la solution optimale recherchée : le vecteur de puissance minimal qui permet d'atteindre conjointement les contraintes en débit de chaque paire 'E/R'. La solution Γ^* se trouve dans la région du plan référencée par le couple de régimes d'interférence $(2;3)$, c'est-à-dire que la première paire devrait mettre en place du *Joint Decding* alors que la seconde gèrerait son interférence avec une technique basée sur le SIC.

puissance ainsi défini est optimal, c'est-à-dire que toute puissance inférieure ne permettrait pas de respecter les contraintes. Des puissances supérieures permettraient éventuellement le respect des contraintes de débit, mais le critère de minimisation de la puissance de transmission ne serait alors plus respecté.

L'algorithme CPA est centralisé dans la mesure où tout le processus de classification est exécuté par une entité dotée de connaissances globales sur le système et non pas locales sur une cellule.

Ch.5-2 : Algorithme CPA - Résultats

Quelques résultats sont présentés ci-dessous. Le lecteur pourra en trouver bien plus avec la lecture des sections 5.4.5 et 6.4.6 où nous comparons nos deux algorithmes à d'autres approches couramment utilisées. La Figure 16 apporte une des façons les plus simples pour illustrer l'utilité d'adapter le traitement de l'interférence à l'intensité avec laquelle cette dernière est perçue. Avec l'algorithme CPA, la puissance est déterminée par la droite bleue continue par morceaux ; la droite $\mathscr{D}_i^1$ et son prolongement en pointillé caractérise la méthode NPA (interférence toujours traitée comme du bruit) ; la droite horizontale brune représente la méthode TSPA (*Time-Sharing* pour isoler les transmissions et éviter l'interférence) ; enfin la demi-droite horizontale bleue $\mathscr{D}_i^3$ illustre la méthode SIC où l'interférence est supprimée par décodage (cette dernière ne s'applique que dans le dernier régime d'interférence représenté par la région verte sur la figure).

Pour un niveau d'interférence donné, par exemple δ_i sur l'axe des abscisses, on dresse la verticale passant par ce point ; l'intersection de cette verticale avec les fonctions de chaque algorithme renseigne la puissance minimale déterminée par ces algorithmes. Sur la Figure 16 on voit ainsi que CPA permet d'allouer une puissance bien inférieure à celles définies par NPA ou TSPA ; en revanche pour cette valeur de δ_i aucune solution n'est

possible pour SIC.

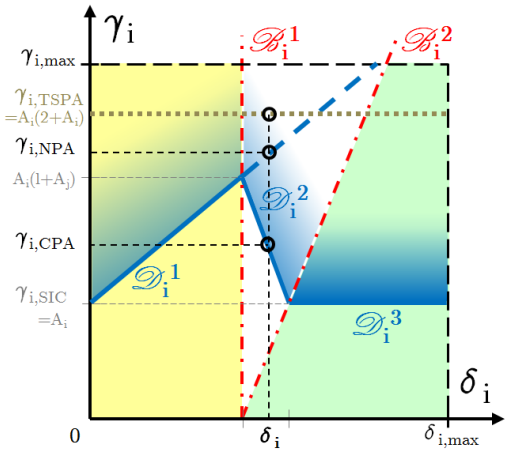

FIGURE 16 – Comparaison de notre algorithme CPA avec d'autres méthodes d'allocation de puissance. NPA détermine la puissance optimale en traitant l'interférence comme du bruit, quel que soit son intensité ; TSPA évite la génération d'interférence en orthogonalisant les transmissions concurrentes ; SIC supprime l'interférence en la décodant.

L'intérêt théorique d'adapter le traitement de l'interférence est peut-être établi, mais il convient de prouver son utilité en pratique ! Nous avons ainsi simulé un grand nombre de contextes de simulations où les deux paires 'E/R' sont mobiles et leur contraintes en débit varient, tout comme leurs canaux de communication. La fréquence selon laquelle chaque couple de régimes d'interférence est défini comme étant optimal est représentée sur la Figure 17. Si dans 60% des cas il sied de traiter l'interférence comme du bruit simultanément dans les deux cellules, on constate cependant que les 40% restants sont répartis sur les 8 autres couples de régimes. Des résultats plus précis montrent en outre que même si les contextes nécessitant l'emploi d'une méthode de type SIC (régime 3) sont rares, leur emploi permet de réduire considérablement la puissance en comparaison des autres méthodes d'allocation de puissance (comme l'atteste la Figure 16).

Ch.5-3 : Algorithme CPA - Conclusions

La version centralisée de notre algorithme s'effectue en une étape et assure de l'existence d'une solution théorique. Toutefois elle nécessite que les contraintes de chaque cellule et la totalité des coefficients des canaux soient disponibles au niveau d'un contrôleur centralisé qui appliquera l'algorithme et communiquera ensuite à chaque cellule les paramètres optimaux pour la transmission courante.

Une version distribuée de cet algorithme est proposée dans le Chapitre 6. En outre, une généralisation à un plus grand nombre de femto-cellules (n femto-cellules) avec présence de macro-cellules (p macro-cellules) est également envisagée.

Chapitre 6 - Algorithme distribué d'allocation de puissance

Dans ce chapitre nous étudions la possibilité de transposer l'algorithme CPA du chapitre précédent en une version distribuée et autonome. L'idée est de permettre à chaque paire

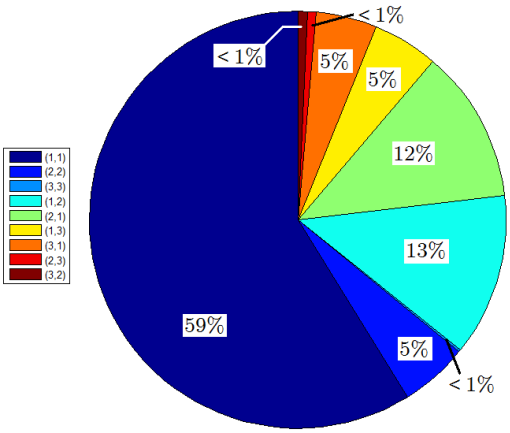

FIGURE 17 – Simulation de CPA sur de multiples contextes de transmission aléatoires : répartition des couples de régimes d'interférence optimaux définis par notre algorithme CPA (1 : Interférence traitée comme du bruit, 2 : *Joint decoding*, 3 : SIC).

'E/R' de prendre une décision en ne se basant que sur une connaissance locale de son environnement.

Ch.6-1 : Algorithme DPA - Principe

Nous proposons l'algorithme DPA (*Distributed Power Allocation*) avec lequel chaque paire 'E/R' ne requiert qu'une connaissance locale, typiquement les contraintes de cette paire ainsi que les gains des canaux mis en jeu dans cette paire. Chaque paire va sonder son environnement et mettre à jour sa puissance en se basant sur l'interférence qu'elle perçoit. Le fait pour une paire de modifier sa puissance de transmission fait qu'elle modifie l'intensité du signal interférant que ressent ses voisins ; ils réagiront à leur tour à cette modification du contexte d'interférence, et ainsi de suite jusqu'à trouver un état d'équilibre pour le système. Ce processus de "ping-pong" entre chaque paire 'E/R' est illustré sur la Figure 18 qui fait le lien avec la Figure 14 de l'algorithme CPA.

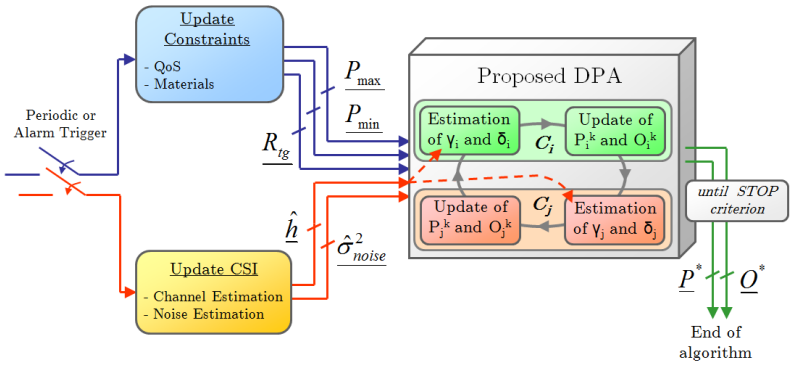

FIGURE 18 – Description de notre algorithme DPA via lequel le vecteur de puissance optimal ainsi que le couple optimal de régimes d'interférence sont établis au terme d'un processus itératif durant lequel chaque paire 'E/R' met tour à tour à jour sa puissance de transmission.

Toute la partie théorique de cet algorithme ne sera pas évoquée dans ce résumé. Mais pour faire bref, le Chapitre 6 détaille le formalisme mathématique (suite de fonctions itérées et théorème du point fixe pour des applications contractantes) qui permet d'étudier la convergence de cet algorithme itératif. Cette approche cherche à atteindre la même solution que l'algorithme CPA mais avec bien moins de connaissance sur le système. Par conséquent, la preuve de l'existence de la solution a déjà été établie dans le chapitre précédent. Il ne reste qu'à étudier la convergence du processus itératif, qui est une condition sine qua non pour atteindre la solution optimale à notre problème.

La Figure 19 illustre le déroulement du processus DPA au cours duquel à chaque itération le système se rapproche de la solution optimale. Le système doit toutefois bien se prêter à la convergence ; si ce n'est pas le cas, l'algorithme ne converge pas et il est nécessaire de savoir prédire ces situations problématiques pour éviter de gaspiller inutilement de la puissance et du temps. Le Chapitre 6 apporte quelques éléments de réponse pour caractériser la vitesse de convergence de l'algorithme : comment l'évaluer, quels sont les paramètres qui la régissent, comment se gère l'aspect 'multi-régimes', etc. Toutefois, à ce jour notre étude sur la convergence n'a pu être exploitée en pratique car une connaissance globale du système est requise, alors que nous cherchons justement à n'avoir recourt qu'à des informations locales pour notre algorithme distribué.

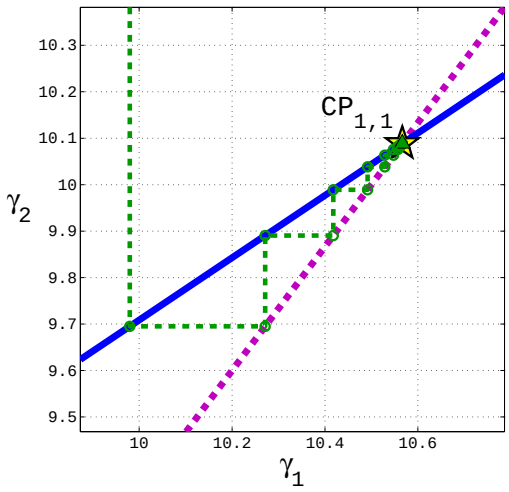

FIGURE 19 – Illustration du processus de 'ping-pong' mis en jeu par DPA. A tour de rôle les paires 'E/R' mettent à jour leur puissance (lignes horizontales : E/R-1 et lignes verticales : E/R-2), ce qui provoque une réaction de leur voisin. Un état d'équilibre est éventuellement atteint si le système s'y prête.

Ch.6-2 : Algorithme DPA - Résultats

Comme il l'a été précédemment évoqué, l'algorithme DPA vise à obtenir d'une manière distribuée les mêmes résultats que ceux obtenus par l'approche centralisée (CPA). Toutefois, DPA est sensible aux conditions initiales et au contexte de transmission courant qui peuvent rendre impossible la convergence du processus itératif. Dans de telles conditions, il est impossible pour DPA d'atteindre une solution stable et optimale ; l'allocation de puissance échoue alors.

Des campagnes de simulation ont été réalisées sur plusieurs contextes de communication tirés aléatoirement. Pour chacun d'eux les performances de différentes méthodes

d'allocation sont comparées. à celles de nos deux propositions (CPA et DPA). Les principaux résultats sont illustrés en Figure 20 : TSPA pour une méthode exploitant le *Time sharing* pour ne pas générer d'interférence, NPA pour une méthode où l'interférence est traitée comme du bruit, CPA et DPA pour nos deux propositions.

La Figure 20a détaille la fréquence et les causes d'échec des méthodes d'allocation de puissance. Pour NPA, il se peut que la solution au problème soit dans le domaine des puissances négatives ; une telle allocation provoque un échec dans 30% des scénarios. De la même façon pour DPA, nous avons vu que le processus itératif pouvait ne pas converger, ou bien trop lentement ; cela se produit pour 4% des scenarios.

Chaque méthode est confrontée à une seconde cause d'échec imposée par les limitations pratiques du système. En effet, des contraintes de puissances minimales et/ou maximales peuvent être imposées par le matériel, la norme ou le système ; le vecteur de puissance défini par les algorithmes est ainsi confronté à ces contraintes et des échecs sont possibles.

Nous proposons de traiter toutes les causes d'échec de la façon suivante : si les algorithmes NPA, CPA et DPA ne parviennent pas à assigner un vecteur de puissance convenable, alors l'algorithme TSPA est utilisé en remplacement. Cela permet de s'affranchir de tous les problèmes liés à l'interférence au prix d'une efficacité spectrale réduite. Toutefois, cela n'apporte pas toujours une fin heureuse à l'allocation de puissance, comme nous pouvons le constater sur la droite de la Figure 20a : certains contextes de communication problématique sont filtrés par ce recours à TSPA mais d'autres demeurent impossibles à satisfaire car la puissance requise par TSPA excède les limitations.

La Figure 20b permet de regarder comment se traduisent ces résultats en termes de puissance consommée. On y représente le budget moyen en puissance requis par chaque méthode d'allocation de puissance. Cette dernière figure est particulièrement importante car nous rappelons que nous visons ici à minimiser la puissance en transmission.

Pour bien lire ces résultats, il convient de les associer à ceux de la Figure 20a pour savoir quels sont les scénarios qui ont été comptabilisés pour effectuer la moyenne. Par exemple les performances sur la partie gauche de la Figure 20b semblent indiquer que CPA est bien moins performants que NPA ou encore DPA. Toutefois, si l'on regarde les histogrammes à gauche sur la Figure 20a, on constate qu'aucun des scénarios n'est exclu des comptes avec CPA, alors que jusqu'à 30% des scénarios le sont avec NPA. Les performances de gauche sur la Figure 20b sont donc un peu biaisées. En revanche les performances de droite montrent des gains allant jusqu'à 52% et 71% de réduction pour CPA par rapport à respectivement TSPA et NPA.

Ch.6-3 : Algorithme DPA - Conclusions

Ce chapitre apporte les outils mathématiques et théoriques nécessaires pour comprendre comment il est possible d'atteindre une allocation optimale de puissance avec juste une connaissance réduite du système. Cela est permis grâce au recours à un processus itératif en 'ping-pong' au cours duquel chaque paire 'E/R' vient tour à tour mettre à jour son vecteur de puissance en se basant sur son niveau d'interférence et de bruit courant Néanmoins, quelques contraintes de convergence peuvent empêcher l'algorithme d'atteindre sa solution. Une étude plus approfondie doit encore être menée pour filtrer les cas les plus problématiques qui viennent perturber la bonne convergence du processus itératif. De même, une extension de ces résultats à un système à plus de deux paires 'E/R' est également discutée.

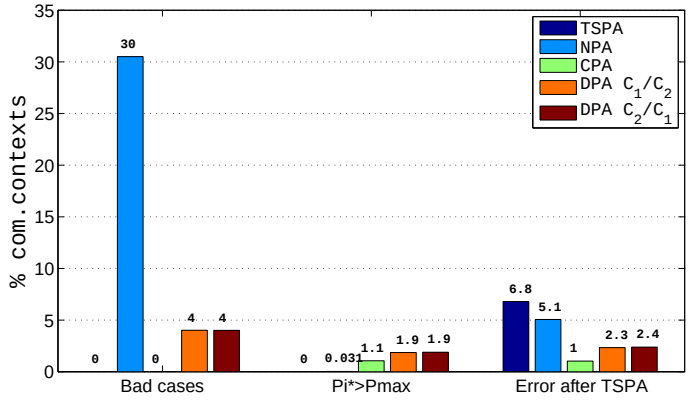

(a) Causes d'échec des méthodes d'allocation de puissance et fréquence d'apparition de ces échecs.

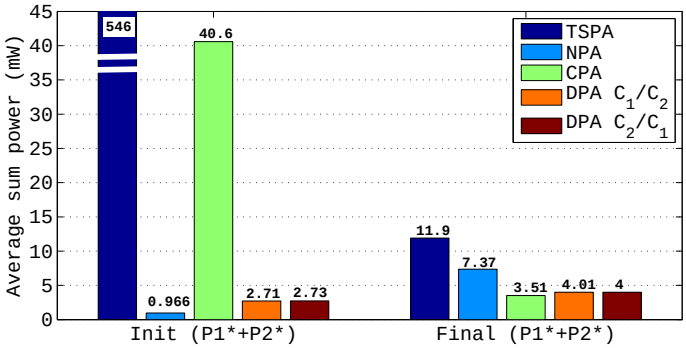

(b) Budget de puissance assigné par chaque méthode (somme des puissances des deux émetteurs) ; ce budget ne comptabilise que les contextes réalistes (pas de puissance négative, pas de contextes où la convergence n'est pas atteinte).

FIGURE 20 – Comparaison des performances en termes d'allocation de puissance pour les méthodes NPA, TSPA, CPA et DPA, cette dernière étant décomposée en deux, en fonction de la paire 'E/R' qui entame le processus itératif.

Chapitre 7 - Conclusions et perspectives

Dans le paysage actuel des télécommunications radio, l'apparition de nouveaux standards de communication avec des exigences toujours plus hautes en termes de qualité de service provoque une surexploitation du spectre fréquentiel. Le partage d'une même ressource de communication par au moins deux paires "émetteur-récepteur" dans un espace restreint provoque de l'interférence radio sur cette ressource, ce qui affecte la qualité des communications. Afin d'assurer que la qualité de service ciblée soit atteinte en réception, il est nécessaire, voire indispensable, de mettre en place des techniques performantes pour réduire les effets néfastes de l'interférence. Dans ce mémoire, ce problème d'interférence radio a été abordé de deux façons.

Dans un premier temps nous avons cherché à voir dans quelles mesures les communications coopératives peuvent permettre de gérer ce problème d'interférence. Cette étude est régie par un compromis : le recours aux communications coopératives provoque certes une amélioration locale de l'information mutuelle, mais également une hausse de l'interfé-

rence. Il est nécessaire que les bienfaits de la coopération outrepassent les méfaits qu'elle occasionne.

Dans un second temps nous avons étudié diverses techniques pour gérer l'interférence et sommes arrivés à la conclusion que l'interférence peut être un atout lorsqu'elle est bien exploitée. Nous en sommes venus à proposer un classificateur d'interférence qui sonde l'environnement courant et propose une technique adaptée pour traiter au mieux l'interférence. Ce classificateur a ensuite été repris pour proposer deux algorithmes d'allocation de puissance ; ces algorithmes minimisent la puissance de transmission du système sous contraintes de qualité de service minimale à assurer.

En guise de pistes pour des travaux futurs, voici une liste de chantiers ouverts :

- Généralisation de notre étude sur les communications coopératives à un cadre applicatif réel, avec un nombre quelconque de bandes fréquentielles et de paires "émetteur-récepteur".
- Dans le cadre de relais mobiles, étude approfondie sur la sélection et le positionnement des relais pour maximiser leurs bienfaits.
- Pour la partie sur le contrôle et l'allocation de puissance, il serait bon de caractériser davantage le contexte multiutilisateur avec notamment un nombre quelconque de paires "émetteur-récepteur". Il faudrait voir dans quelle mesure le classificateur peut s'adapter.
- Pour l'approche distribuée, il est nécessaire d'approfondir les résultats sur la vitesse de convergence afin de pouvoir prédire les convergences trop lentes ou les scénarios de non convergence.

Table des matières

Remerciements i

Abstract iii

Résumé long v

Contents xxxii

List of Figures xxxvii

List of Tables xxxix

Nomenclature xli

Abbreviations and Acronyms . . . xli
Thesis Specific Notations . . . xliii

1 Snapshot on the Thesis 1

1.1 Background and Motivations . . . 1
1.2 Thesis Objectives . . . 2
1.3 Thesis Outline . . . 3

2 Fundamentals of Interference in Wireless Networks 7

2.1 Introduction . . . 8
2.1.1 Technical Context . . . 8
2.1.2 Motivations . . . 8
2.1.3 Examples of Potential Industrial Applications . . . 9
2.2 Preliminary on Wireless Communications . . . 9
2.2.1 Classical System Models . . . 10
2.2.1.1 Broadcast Channel . . . 10
2.2.1.2 Multiple Access Channel . . . 10
2.2.1.3 Interference Channel . . . 11
2.2.1.4 X Channel and Z Channel . . . 12
2.2.2 Notions, Concepts and Definitions . . . 12
2.2.3 PhD Assumptions . . . 17
2.2.4 Characteristics of Radio Propagation Channels . . . 18
2.2.5 PhD Hints of Research . . . 20
2.3 Preliminary on Femtocells Networks . . . 20
2.4 Preliminary on Interference Mitigation Techniques . . . 21
2.4.1 Orthogonal Resource Allocation . . . 22

2.4.2 Non-Orthogonal Resource Allocation . . . 23
2.4.2.1 Frequency Reuse . . . 23
2.4.2.2 Divide and Conquer : Graph Colouring . . . 24
2.4.2.3 Cognitive Radio Approach . . . 24
2.4.3 Information Theory and Signal Processing Techniques . . . 25
2.4.3.1 Noisy Strategy . . . 25
2.4.3.2 Zero Forcing . . . 26
2.4.3.3 ML, MMSE Estimation, Sphere Decoder . . . 26
2.4.3.4 Dirty Paper Coding . . . 27
2.4.3.5 Successive Interference Cancellation . . . 27
2.4.3.6 Beamforming . . . 27
2.4.3.7 Interference Alignment . . . 28
2.4.4 Channel Aware Power Control . . . 29
2.4.4.1 Binary Power Allocation . . . 30
2.4.4.2 Water-Filling . . . 30
2.5 Conclusions . . . 31

3 Cooperative Communications with Half-Duplex Relays 33
3.1 Introduction . . . 34
3.1.1 Motivations . . . 34
3.1.2 Contributions . . . 35
3.1.3 Related Works . . . 35
3.2 System Model and Assumptions . . . 36
3.2.1 The Two-Hop Half-Duplex Relay Channel . . . 37
3.2.2 The Global System Model . . . 39
3.3 Preliminary on Cooperative Communications . . . 40
3.3.1 Cooperative Transmissions'Goals . . . 40
3.3.2 State of the Art on Cooperative Protocols . . . 41
3.3.2.1 Orthogonal, Non-Orthogonal and Slotted Protocols . . . 41
3.3.2.2 Amplify-and-Forward . . . 42
3.3.2.3 Decode-and-Forward . . . 43
3.3.2.4 Compress, Equalize and Hybrid Protocols . . . 44
3.3.3 Cooperative Trade-Off : Robustness vs. Interference . . . 44
3.3.4 Distributed Coding Techniques . . . 45
3.4 Radio Resource Management for Interference Mitigation . . . 45
3.4.1 Cooperative Communication Paradigm . . . 46
3.4.2 Description of Resource Allocation Patterns . . . 46
3.4.2.1 'Classic 1' Family of Allocation Patterns (C1) . . . 48
3.4.2.2 'Classic 2' Family of Allocation Patterns (C2) . . . 49
3.4.2.3 Proposed 'Advanced' Family of Allocation Patterns (A) . . . 50
3.4.2.4 Other Possible Allocation Patterns . . . 51
3.4.3 Adaptive Resource Allocation Process (ARAP) . . . 52
3.4.4 Simulation Results . . . 55
3.4.4.1 First Scenario : Unidirectional moving along 's1-r1 axis . . . 56
3.4.4.2 Second Scenario : Omnidirectional moving within sector . . . 59
3.5 Generalization to Multi-Chunks Allocations . . . 63
3.6 Conclusions . . . 67

4 Adaptive Interference Handling Techniques **69**
4.1 Introduction . . . 70
4.1.1 Motivations . . . 70
4.1.2 Contributions . . . 71
4.1.3 Related Works . . . 71
4.2 Preliminary on Adaptive Interference Handling . . . 73
4.2.1 Noisy Strategy : Treat Interference As Noise . . . 73
4.2.2 SIC-based Strategies . . . 74
4.2.3 Time/Frequency Sharing . . . 75
4.2.4 How Adaptation Can Be Achieved ? . . . 75
4.2.4.1 Han and Kobayashi Model : Superposition Coding . . . 76
4.2.4.2 Diversity Multiplexing Trade-Off and Interference Classifier 78
4.3 Proposed Slim Three-Regime Interference Classification . . . 82
4.3.1 The Noisy Regime . . . 83
4.3.2 The Joint Decoding Regime . . . 84
4.3.3 The Very Strong Regime . . . 85
4.3.4 Performance of Three-Regime Classifier . . . 85
4.3.5 Achievable SNR Region . . . 87
4.4 Three-Regime Classifier for n-user Interference Channel . . . 89
4.4.1 Generalization of the System Model . . . 89
4.4.2 Regimes Boundaries and SNR-Achievable Region . . . 90
4.4.3 Outage Probability Formulations . . . 93
4.4.4 Remarks . . . 94
4.5 Conclusions . . . 95

5 Centralized Power Allocation Algorithm **97**
5.1 Introduction . . . 98
5.1.1 Motivations . . . 98
5.1.2 Contributions . . . 99
5.1.3 Related Works . . . 99
5.2 System Model and Assumptions . . . 100
5.3 Preliminary on Centralized Algorithms . . . 102
5.3.1 Challenges and Assumptions . . . 102
5.3.2 Limitations of Centralized Algorithms . . . 103
5.3.3 Water-Filling Technique . . . 104
5.4 Proposed Centralized Power Allocation Algorithm . . . 105
5.4.1 Power Allocation and Interference Classification . . . 105
5.4.2 Optimal Power Allocation . . . 107
5.4.3 Proof of Existence . . . 109
5.4.4 Proof of Optimality . . . 110
5.4.5 Simulation Results and Remarks . . . 112
5.5 CPA Generalization to Multi-Source Multi-Destination Cases . . . 121
5.5.1 System Model and Notations . . . 121
5.5.2 Mathematical Formulation . . . 123
5.6 Conclusions . . . 127

6 Distributed Power Allocation Algorithm **129**
6.1 Introduction . . . 130
6.1.1 Motivations . . . 130
6.1.2 Contributions . . . 131
6.1.3 Related Works . . . 131
6.2 System Model and Assumptions . . . 131
6.3 Preliminary on Distributed Approaches . . . 132
6.3.1 Benefits of Distributed Allocation Algorithms . . . 133
6.3.2 Limitations of Distributed Allocation Algorithms . . . 133
6.3.3 A Step Towards Game Theory . . . 134
6.3.4 Distributed Norm and Convergence Criterion . . . 135
6.3.5 Centralized vs. Distributed Algorithms . . . 136
6.4 Proposed Distributed Power Allocation Algorithm . . . 137
6.4.1 Optimal Distributed Power Allocation . . . 137
6.4.2 The 'Ping-Pong' Iterative Process . . . 139
6.4.3 Proof of Convergence . . . 141
6.4.3.1 Fixed Point Theory . . . 141
6.4.3.2 Spectral Radius . . . 147
6.4.4 Rate of Convergence . . . 148
6.4.5 Additional Remarks . . . 151
6.4.6 Simulation Results . . . 156
6.5 DPA Generalization to Multi-Source Multi-Destination Cases . . . 159
6.6 Conclusions . . . 161

7 Conclusions and Future Work **163**
7.1 Conclusions . . . 163
7.2 Future Work and Hints for Future Research . . . 164

A Complements on Chapter 4: Outage Probability **167**
A.1 Preliminary on Outage Probability . . . 167
A.1.1 Probability Distributions . . . 167
A.1.2 Sum of Random Variables . . . 168
A.1.3 Outage Probability . . . 169
A.2 Interference Classification Based Outage Probability . . . 169
A.2.1 Noisy Strategy . . . 169
A.2.2 Joint Decoding Strategy . . . 170
A.2.3 SIC-Based Strategy . . . 170
A.2.4 Time-Sharing Strategy . . . 170
A.2.5 All-in-One Strategy . . . 170

Bibliography **184**

Table des figures

1 Canal à interférence à deux utilisateurs : deux émetteurs s_1 et s_2 se partagent une même ressource de communication pour transmettre respectivement le message x_1 au récepteur d_1 et le message x_2 au récepteur d_2. La non-orthogonalité de ces deux transmissions dans un espace restreint occasionne de l'interférence co-canal ; le message reçu est perturbé par le bruit thermique et le message interférant. vii

2 Illustration d'un déploiement de femto-cellule pour une application domestique. viii

3 Illustration du modèle de canal à relais à deux sauts avec lequel la destination finale d_i perçoit deux signaux issus de deux émetteurs différents mais qui renferment théoriquement la même information. ix

4 Système de trois secteurs, dotés chacun d'une source ($\mathbf{s}_i$), d'un relais ($\mathbf{r}_i$) et d'une destination ($\mathbf{d}_i$). Dans cette étude le relais $\mathbf{r}_i$ est supposé fixe et est placé aux deux tiers de la distance maximale sur l'axe central du secteur. La destination $\mathbf{d}_i$ est mobile et peut se déplacée en tout point de son secteur. x

5 Comparaison de différentes stratégies coopératives au niveau de l'allocation des blocs-ressources. xi

6 Illustration d'une allocation de ressources entre émetteurs : deux bandes fréquentielles sont partagées entre deux stations de base et deux relais, les relais étant supposés *half-duplex par bande*. En coordonnant convenablement les transmissions des deux cellules, le relais **RS 1** écoute sur la bande A et transmet sur la bande B, alors que le relais **RS 2** écoute sur la bande B en transmettant sur la bande A. Ainsi, **RS 1** n'est pas perturbé par son plus fort interféreur (**BS 2**) mais cela n'empêche pas pour autant qu'il y ait de l'interférence entre relais ou du relais vers la destination voisine. xi

7 Représentation des modes d'allocation pour les trois stratégies. xiii

8 Description du processus ARAP d'allocation adaptative des ressources de communication. Le paramètre d'entrée est la position de la destination $\mathbf{d}_1$ au sein de son secteur et compte tenu de cette position plusieurs contextes de simulation sont tirés de façon aléatoire et la métrique $\widehat{GMI}_{d_1}$ est calculée comme étant une moyenne de tous ces contextes. En fin de chaîne, le pattern d'allocation qui maximise la métrique est identifié ; il représente la façon la plus performante d'allouer les ressources avec pour seule connaissance la localisation de $\mathbf{d}_1$ dans son secteur. xiv

9 Évolution de la métrique $\widehat{GMI}_{d_1}(M)$ lorsque la destination $\mathbf{d}_1$ se déplace le long de l'axe '$\mathbf{s}_1$-$\mathbf{r}_1$', M désignant un mode d'allocation de ressources. Ces performances sont obtenues avec un protocole coopératif de type DF et de hautes puissances en transmission pour les stations de base et les relais. . . xvi

10 Carte d'optimalité du secteur S_1 dans le cadre d'un protocole coopératif de type DF avec de hautes puissances de transmission pour les stations de base et les relais. Cette carte indique quel type de pattern d'allocation de ressources sied le mieux à chaque position de $\mathbf{d}_1$, c'est-à-dire quel est le protocole $\mathscr{M}^{d_1}_{\Omega_{all}}$ qui maximise la métrique $\widehat{GMI}_{d_1}$. xvii

11 *Superposition Coding* proposé par Han et Kobayashi : le message est décomposé en une information publique destinée à tous et une information privée uniquement destinée au récepteur visé. xviii

12 Représentation de la courbe en 'W' décrivant le nombre de degrés de liberté en fonction du ratio entre log(INR) et log(SNR). En fonction des stratégies mises en place, une classification en cinq régimes de l'interférence est ainsi mise en évidence. xix

13 Représentation du classificateur d'interférence dans le plan $(\delta_i; \gamma_i)$, c'est-à-dire le plan avec l'INR en abscisse et le SNR en ordonnée. Les droites rouges caractérisent les frontières entre chaque régime, représentés chacun par une couleur différente, tandis que les droites bleues délimitent la région où les contraintes de QoS sont atteintes (zone en dégradé bleu). xx

14 Algorithme CPA de minimisation de la puissance de transmission sous contraintes en débit. La connaissance de paramètres sur les canaux et le système permet de déterminer en amont de la transmission le vecteur minimal de puissance et la stratégie adéquate de gestion de l'interférence dans chaque cellule. . . . xxi

15 Le processus de classification de l'interférence est exécuté pour chaque paire 'E/R' du système et le résultat est superposé sur une même figure. L'intersection des courbes d'optimalité définisse la solution optimale recherchée : le vecteur de puissance minimal qui permet d'atteindre conjointement les contraintes en débit de chaque paire 'E/R'. La solution Γ^* se trouve dans la région du plan référencée par le couple de régimes d'interférence $(2; 3)$, c'est-à-dire que la première paire devrait mettre en place du *Joint Decding* alors que la seconde gèrerait son interférence avec une technique basée sur le SIC. xxii

16 Comparaison de notre algorithme CPA avec d'autres méthodes d'allocation de puissance. NPA détermine la puissance optimale en traitant l'interférence comme du bruit, quel que soit son intensité ; TSPA évite la génération d'interférence en orthogonalisant les transmissions concurrentes ; SIC supprime l'interférence en la décodant. xxiii

17 Simulation de CPA sur de multiples contextes de transmission aléatoires : répartition des couples de régimes d'interférence optimaux définis par notre algorithme CPA (1 : Interférence traitée comme du bruit, 2 : *Joint decoding*, 3 : SIC). xxiv

18 Description de notre algorithme DPA via lequel le vecteur de puissance optimal ainsi que le couple optimal de régimes d'interférence sont établis au terme d'un processus itératif durant lequel chaque paire 'E/R' met tour à tour à jour sa puissance de transmission. xxiv

19 Illustration du processus de 'ping-pong' mis en jeu par DPA. A tour de rôle les paires 'E/R' mettent à jour leur puissance (lignes horizontales : E/R-1 et lignes verticales : E/R-2), ce qui provoque une réaction de leur voisin. Un état d'équilibre est éventuellement atteint si le système s'y prête. xxv

20 Comparaison des performances en termes d'allocation de puissance pour les méthodes NPA, TSPA, CPA et DPA, cette dernière étant décomposée en deux, en fonction de la paire 'E/R' qui entame le processus itératif. xxvii

1.1 History's first wireless signal interference. 6

2.1 Two-user Broadcast Channel versus two-user Multiple Access Channel. . . . 11
2.2 Two-user Interference Channel versus One-Sided Channel. 11
2.3 Classical representation of a wireless communication channel. 13
2.4 Frequency reuse technique with distinction for cell-centre and cell-edge users. 23
2.5 Beamforing and Power Control. 28
2.6 Two illustrations of Interference Alignment (IA) techniques : beamforming with orthogonal eigenspaces (left) and time separation by exploiting propagation delay (right). 29

3.1 Two-hop relay network with relays serving a source s and a destination d. . 38
3.2 System model with three adjacent sectors, each with a fixed relay r_i placed at two-thirds of r_{cell} from its base station s_i. 39
3.3 Frame structure and relaying procedure of (a) non-orthogonal and (b) slotted protocols, solid box for transmitted signal and dashed box for received signal. 42
3.4 Most representative resource allocation patterns for *Classic 1* family. 48
3.5 Most representative resource allocation patterns for *Classic 2* family. 49
3.6 Standard vs. HDPC frame structure for orthogonal cooperative protocols. . 50
3.7 Most representative resource allocation patterns for *Advanced* family. 51
3.8 Patterns of some CNN patterns initially considered but finally rejected. . . 52
3.9 Patterns of some NCC patterns initially considered but finally rejected. . . . 52
3.10 Patterns of some CCC patterns initially considered but finally rejected. . . . 53
3.11 Description of the algorithm for evaluating performance of ARAP. 55
3.12 AF protocol, High transmit powers - $\widehat{GMI}_{d_1}(M)$ variations along (s_1, r_1) axis. 57
3.13 DF protocol, High transmit powers - $\widehat{GMI}_{d_1}(M)$ variations along (s_1, r_1) axis. 57
3.14 AF protocol, Low transmit powers - $\widehat{GMI}_{d_1}(M)$ variations along (s_1, r_1) axis. 58
3.15 DF protocol, Low transmit powers - $\widehat{GMI}_{d_1}(M)$ variations along (s_1, r_1) axis. 59
3.16 Variations of $\widehat{GMI}_{d_1}(M)$ when d_1 moves everywhere in sector S_1. 60
3.17 High transmit powers - Adaptive selection of the optimal pattern $\mathscr{M}^{d_1}_{\Omega_{all}}$. . . 61
3.18 Low transmit powers - Adaptive selection of the optimal pattern $\mathscr{M}^{d_1}_{\Omega_{all}}$. . . 62
3.19 Generalization of ARAP to more than 2 chunks. 65
3.20 Illustration of a general adaptive RRM mechanism 66

4.1 Han and Kobayashi model for superposition coding : private and common information. 77
4.2 Superposition encoding example. The QPSK constellation of user 2 is superimposed on top of that of user 1. 77
4.3 Superposition decoding example. The transmitted constellation point of user 1 is decoded first, followed by decoding of the constellation point of user 2. 77

4.4 Illustration of channel diversity where the duration of deep fade events is minimized by fast changes. Here channel quality in ordinate axis may refer to CQI metric. . . . 79
4.5 Generalized degrees of freedom according to α-value. A 'W-shaped' curve exhibits a classification of in-band interference into five operating regimes. . 81
4.6 Generalized degrees of freedom according to α-value for our proposed three-regime classification of in-band interference. . . . 86
4.7 Achievable SNR region $\mathscr{R}_i^*$. . . . 88
4.8 Three-user Multiple Access and Interference Channels where pair '$s_i - d_i$' is QoS-constrained with a target rate $R_{tg,i}$. . . . 89
4.9 Achievable rate-region for the 3-user MAC. . . . 93
4.10 The region related to each pair of strategies is characterized by its boundaries and the lower-bound of its achievable SNR region $\mathscr{R}_i^*$. . . . 94

5.1 Two neighbour 'source-destination' pairs with a network controller. . . . 101
5.2 Decomposition of the whole two-user IC into two two-user MAC subsytems. 102
5.3 Water-filling power allocation over the N_{SC} sub-carriers. . . . 105
5.4 Superposition of both achievable SNR regions $\mathscr{R}_1^*$ and $\mathscr{R}_2^*$. A partition Ω of the region into nine (left) and eight (right) sectors is achieved. . . . 108
5.5 Principle of the continuous transformation of the map. The image of an intersection under a continuous function remains an intersection. . . . 110
5.6 Description of our CPA algorithm for minimizing transmission power in rate-constrained networks. Given some inputs, CPA outputs two vectors compliant with inputs : minimal power and advised strategies to efficiently handle in-band interference at each destination. . . . 112
5.7 Description of the successive computational steps of our CPA algorithm. . . 113
5.8 Behaviour of NPA algorithm for two different communication contexts. On the left there is a compliant allocation of power, while power allocation fails on the right. . . . 114
5.9 Comparison of CPA, NPA and TSPA for a given communication context. . 115
5.10 Numerical results for two given communication scenarios $\mathscr{P}_S$ . . . 116
5.11 Deployment of interfering femtocells. . . . 118
5.12 CPA Algorithm : Distribution of optimal sector O^* among all $\Omega_{k,l}$. . . . 120
5.13 CPA Algorithm : Selection of optimal sector (O_1^*, O_2^*) and percentage of excessive power assignment. . . . 121
5.14 Comparison of main results for CPA, NPA and TSPA. . . . 122
5.15 Which femtocell is responsible for failed power assignments ? . . . 122

6.1 A n-user MAC system for decentralized algorithms. . . . 132
6.2 Iterative process to achieve a balanced solution to power allocation problem. 134
6.3 Description of our DPA algorithm for power allocation. . . . 139
6.4 Illustration of the 'ping-pong' process for power allocation. . . . 140
6.5 $\mathscr{P}_S = \{1, 1, 2.5, 1.5\}$: optimal solution computed by CPA is shown on the left, while the iterative process of DPA is illustrated on the right. . . . 141
6.6 Investigation on convergence rate within sector $\Omega_{1,1}$: Impact of κ value . . 149
6.7 Investigation on convergence rate within sector $\Omega_{1,1}$: Zoom in on $\mathrm{CP}_{1,1}$ . . 149

6.8 $\mathscr{P}_S = \{2, 1, 1.29, 0.262\}$: DPA process does not converge to $\mathrm{CP}_{1,2}$ in spite of the relevance of sector $\Omega_{1,2}$. Mappings $\{\Phi_i^{(1,2)}\}_i$ have a Lipschitz constant $\kappa > 1$ and hence are not contracting. 152
6.9 $\mathscr{P}_S = \{2, 2, 1.75, 1.75\}$: Three attractors are simultaneously relevant. The final solution depends on the location of the starting point Γ^0. 153
6.10 $\mathscr{P}_S = \{2, 2, 1.75, 1.75\}$: The final solution depends first on the starting point Γ^0, second on the pair that launches the process. 154
6.11 DPA Algorithm : Selection of optimal sector $(O_1^*; O_2^*)$ and rate of convergence in each sector $\Omega_{k,l}$. 157
6.12 Comparison of causes of failure and power assignments for CPA, DPA $\mathscr{C}_1/\mathscr{C}_2$, DPA $\mathscr{C}_2/\mathscr{C}_1$, NPA and TSPA. 158
6.13 Which femtocell is responsible for failed power assignments ? 159

Liste des tableaux

1 Récapitulatif des équations régissant ce classificateur d'interférence. On retrouve d'une part les équations délimitant les frontières de chaque régime, d'autre part les équations définissant la région du plan où les contraintes de QoS sont atteintes. . . . xx

3.1 Power budget per family and per allocation pattern, when equal transmit powers P_s and P_r are assumed between sectors and chunks. . . . 53
3.2 System model and algorithm settings. . . . 56

4.1 Performance of our three-regime interference classifier with boundaries of regimes and achievable SNR within each regime. . . . 88
4.2 Formulation of applicability boundaries and achievable rates for each combination of strategies $(O_{j,i}; O_{k,i})$ when our three-regime interference classifier is employed in the three-user case. Results are derived in the region $(R_j; R_k; R_i)$. 91
4.3 Formulation of applicability boundaries and achievable rates for each combination of strategies $(O_{j,i}; O_{k,i})$ when our three-regime interference classifier is employed in the three-user case. Results are derived in the region $(\delta_{j,i}; \delta_{k,i}; \gamma_i)$. 92
4.4 Suite of power control optimization problems described with their objective function and their QoS constraints. . . . 95

5.1 Performance of our three-regime interference classifier applied to the MAC $\{s_i; s_j, d_i\}$: partition of the region $(\gamma_j; \gamma_i)$ and achievable SNR within each region. . . . 107
5.2 Coordinates of all possible intersection points $\{\mathscr{D}_1^k\}_k \cap \{\mathscr{D}_2^l\}_l$. . . . 111
5.3 System model settings. . . . 117
5.4 Comparison of assigned power vectors with CPA, NPA, TSPA and SIC-based strategy for the scenario $\mathscr{P}_S = \{R_{tg,1}, R_{tg,2}, f_{1,2}, f_{2,1}\}$. 'NF' means here 'not feasible'. . . . 117
5.5 Additional settings of system model. . . . 119
5.6 Description of CPA algorithm for any n. . . . 126

6.1 Divergences between centralized and distributed algorithms. . . . 136
6.2 Performance of our three-regime interference classifier applied to the MAC $\{s_i; s_j, d_i\}$: partition of the region $(\gamma_j; \gamma_i)$ and achievable SNR within each region. . . . 138
6.3 Updating mapping Φ_i and its attractor γ_i^+ . . . 144
6.4 How selection of (O_1^*, O_2^*) is affected by variations of channel coefficients ? . . . 155

Nomenclature

Abbreviations and Acronyms

3GPP	Third Generation Partnership Project
AF	Amplify-and-Forward
AMC	Adaptive Modulation and Coding
ARAP	Adaptive Resource Allocation Process
ARQ	Automatic Repeat reQuest
AWGN	Additive White Gaussian Noise
BC	Broadcast Channel
BS	Base Station
CAPEX	Capital Expenditure
CDMA	Code Division Multiple Access
CF	Compress-and-Forward
CPA	Centralized Power Allocation
CQI	Channel Quality Indicator
CSI	Channel State Information
CSIR	Channel State Information at Receiver
CSIT	Channel State Information at Transmitter
CV	Convergence
DVB	Digital Video Broadcasting
DF	Decode-and-Forward
DM	Decision-Maker
DMT	Diversity Multiplexing Trade-off
DOF	Degrees Of Freedom
DPA	Distributed Power Allocation
DPC	Dirty Paper Coding
DTC	Distributed Turbo Coding
EF	Equalize-and-Forward
EIRP	Equivalent Isotropically Radiated Power
FAP	Femto Access Point
FC	Femtocell
FDD	Frequency Division Duplex
FDM	Frequency Division Multiplexing
FDMA	Frequency Division Multiple Access
FRF	Frequency Reuse Factor
GMI	Global Mutual Information
GDFE	Generalized Decision-Feedback Equalizer

GMSK	Gaussian Minimum Shift Keying
H-BS	Home Base Station
HDPC	Half-Duplex Per Chunk
IEEE	Institute of Electrical and Electronics Engineers
IC	Interference Channel
INR	Interference to Noise Ratio
ISI	Inter-Symbol Interference
KKT	Karush-Kuhn-Tucker
LAN	Local Area Network
LLR	Log Likelihood ratio
LOS	Line Of Sight
LTE	Long Term Evolution
LTE-A	Long Term Evolution Advanced
MAC	Multiple Access Channel
M2M	Machine to Machine
MCS	Modulation and Coding Scheme
MIMO	Multiple Input Multiple Output
ML	Maximum Likelihood
MMSE	Minimum Mean Square Error
MRC	Maximum Ratio Combining
NC	Network Controller
NLOS	Non Line Of Sight
NPA	Noisy Power Allocation
OFDM	Orthogonal Frequency Division Multiplexing
OFDMA	Orthogonal Frequency Division Multiple Access
OPEX	Operational Expenditure
PA	Power Allocation
PSK	Phase Shift Keying
QoS	Quality of Service
RF	Radio Frequency
RRM	Radio Resource Mamanement
SDMA	Space Division Multiple Access
SIC	Successive Interference Cancellation
SINR	Signal to Interference and Noise Ratio
SNR	Signal to Noise Ratio
TDD	Time Division Duplex
TDM	Time Division Multiplexing
TDMA	Time Division Multiple Access
TSPA	Time-Sharing Power Allocation
TX	Transmitter
UE	User Equipment
VoIP	Voice over Internet Protocol
WiFi	'Wireless Fidelity'
WiMAX	Worldwide Interoperability for Microwave Access
WSN	Wireless Sensor Network
ZF	Zero Forcing

Thesis Specific Notations

The following list is not exhaustive and consists of the most relevant notations used in the dissertation. Vectors are denoted by underlined letters (e.g. $\underline{P}$) while matrices are denoted by bold underlined letters (e.g. $\underline{\mathbf{H}}$).

Other notational conventions are summarized as follows :

Notations applicable in all chapters

$\|x\|$	Modulus of variable x
$\|\|\underline{x}\|\|$	Norm of variable $\underline{x}$
C	Channel capacity
$\mathscr{C}_i$	Couple consisted of source s_i and destination d_i
d_i	Destination of the couple $\mathscr{C}_i$
$\delta_{j,i}$	INR between source s_j and destination d_i
$\mathbb{E}\{x\}$	Expectation of variable x
γ_i	SNR between source s_i and destination d_i
$H(X;Y)$	Entropy of variables X and Y
$\underline{\mathbf{H}}$	Channel matrix
$\mathscr{I}$	Mutual information
$\mathscr{I}(X;Y)$	Mutual information of variables X and Y
L_{dB}	Path loss attenuation [dB]
N_0	Noise variance
N_{SC}	Number of sub-carriers
P_{err}, P_{out}	Error and outage probability
$P_{s_i}^{(k)}$	Transmit power of source s_i on chunk k
$P_{\max}$	Maximal transmit power
$\mathbb{P}\{x\}$	Probability of the event x
R	Transmission rate
$\mathbb{R}^+$	Set of all positive real numbers
s_i	Source of the couple $\mathscr{C}_i$
$\sigma_{d_i}^2$	Noise variance at destination d_i

Notations specific to Chapter 3

$\mathscr{B}_P$	Overall power budget
$\overline{GMI}_{d_i}$	Sum-rate averaged on various communication contexts
$\widehat{GMI}_{d_i}$	$\overline{GMI}_{d_i}$ averaged by overall power budget $\mathscr{B}_P$
$\mathscr{K}$	A set of resource allocation modes
M	Resource allocation mode
$\mathscr{M}_{\mathscr{K}}^{d_i}$	Optimal mode chosen in set $\mathscr{K}$ given the location of d_i
Ω_{all}	Set of all resource allocation modes
Ω_{adv}	Set of all *Advanced* resource allocation modes
Ω_{clas}	Set of all *Classic* resource allocation modes
p_k	Pair of chunks
r_i	Relay in sector S_i
S_i	Sector i consisted of a base station s_i, a destination d_i and a relay r_i

Notations specific to Chapters 4–6

A_i	Variable related to target rate $R_{tg,i}$
α	Ratio between $\log \mathrm{INR}$ and $\log \mathrm{SNR}$
$\mathscr{B}_i^k$	Boundary between regime k and $k+1$ for MAC_i
$\mathrm{CP}_{k,l}$	Crossed point between $\mathscr{D}_1^k$ and $\mathscr{D}_2^k$
$\mathscr{D}_i^k$	Objective function in regime k for MAC_i
$\delta_{\max,j,i}$	Maximal INR for path between s_j and d_i in MAC_i
$\underline{\mathbf{F}}$	Interference matrix
$\gamma_{\max,i}$	Maximal SNR for MAC_i
$\underline{\Gamma}^*$	Optimal SNR vector
$\underline{\mathbf{I_n}}$	Identity matrix $n \times n$
$\underline{O}^*$	Vector of optimal classified interference regimes
$\Omega_{k,l}$	Sector defined by the superposition of regime $O_1 = k$ and $O_2 = l$
φ_i	Piecewise continuous objective function in MAC_i
$\underline{P}^*$	Optimal transmit power vector
$\mathscr{P}_S$	Set of parameters characterizing the momentary communication context
r_α	Multiplexing gain
$\mathscr{R}_i^*$	Achievable capacity region for MAC_i
R_{tg}	Target rate

Chapter 1

Snapshot on the Thesis

1.1 Background and Motivations

Radio propagation is affected by several sources of perturbations which can drastically limit performance of wireless communications networks. Commonly, a source seeks to send a message to a destination through the radio channel while a specific QoS is targeted. Nevertheless, their transmission encounters perturbations, and especially interference, which cause in some scenarios dramatic and often unpredictable momentary reduction of transmission performance and transmission reliability. The higher the perturbations, the harder it is to recover the initial message from the perceived signal. This issue is even more challenging nowadays, since services provided to customers by networks' operators are always more resource demanding, whereas resources are made meanwhile scarcer and scarcer. Indeed, the access to frequency band is regulated and limited, while the number of wireless communication based systems keeps increasing. Consequently, there are more transmitters competing for these scarce resources ; the global level of interference is so higher. It is fundamental to deal with interference so as to mitigate its effects on transmission robustness. Interference mitigation is precisely one of the main issues of this PhD thesis.

Interference is more than just a source of thermal noise. Interfering signals indeed convey also information which is just intended to some specific destinations. By exploiting the special structure of interfering signals with effective interference processing techniques, prejudicial effects of interference can be limited and hence important performance enhancements can be met in terms of transmission robustness and reliability. In the literature, several interference mitigation techniques have been proposed. Depending on the available knowledge of system and channel parameters at transmitter and receiver side, these techniques are performed either by the source, priori to transmission, or by the destination, after the reception.

Interference mitigation techniques are proved to be essential in interference-limited networks subject to QoS constraints. Interference management is for instance highly advised for femtocells networks, cognitive radio based systems with primary and secondary users, or heterogeneous networks where systems of different standard interoperate. With such networks, some nodes have to face unpredictable and very high interference, whereas

they seek to communicate reliably with their source. Such topics will be addressed from Chapter 3 to Chapter 6.

1.2 Thesis Objectives

The main objectives of this dissertation is to first identify, then investigate and finally propose effective techniques to cope with interference in wireless communication systems. We indeed aim at mitigating the reductive effects that interference may cause on wireless transmissions.

Several topics have been identified as candidates.

- **Resource allocation :** In-band interference is generated when at least two transmitters within a close area share simultaneously the same frequency band. Resource allocation techniques focus on how resources can be allocated to the different active users. Indeed, an efficient allocation of resources could assign disjoint frequency bands to users which strongly interfere each other. On the other hand, some frequency bands must be shared to avoid wasting spectrum with a low reuse of frequency bands.
- **Resource scheduling :** In wireless communication networks, the law of supply and demand does not profit to network operators since there are mostly more users to serve than available resources for transmission. On the one hand, the reuse of frequencies is sometimes not conceivable or not desired (it causes too much in-band interference). On the other hand, a given source cannot serve simultaneously numerous users. To deal with such limitations, a scheduler is in charge of defining periodically the set of active users for the next transmit period. Active users are elected based on their QoS requirements, their queue list, their priority, fairness, etc.
- **Cooperative communications :** By cooperative communications we mean two-hop relay-aided transmissions. It consists in a two-step protocol : first, a source transmits its message to a relay and possibly to its destination ; second, the relay forwards to the destination a copy of the signal it has just received. Cooperative communications are known to possibly help the destination in meeting more robust transmissions. Relays can be used as repeater to increase service coverage. We aim at planning cooperation in cellular networks first to help users in achieving higher transmission rates, and second to ensure border-cell users a more robust transmission.
- **Interference classification :** Interference classification techniques consist in exploiting the time-varying nature of wireless channel. The intensity of interference that a receiver perceives on a band depends on numerous parameters : the number and the location of the interferers, the transmit power of these interferers, the path loss attenuation gain occurring from the active transmitters to the receiver. Consequently, in-band interference is not a static and uniform variable. Nevertheless, weak interference does not affect a receiver as strong interference does ; interference should be handled in line with the momentary scenario of communication. Interference classification techniques are especially exploited to adapt the processing of interference to time, frequency, space and system variations of communication context. Such an adaptation may ensure that higher performance could be met, whatever the momentary scenario of communication may be.
- **Interference processing techniques :** Interference processing techniques focus on how interfering signals are handled by transmitters and/or receivers so as to mitigate their prejudicial effects. These techniques can address interference avoidance or interference cancellation topics. In other words, interference can be pre-processed

by transmitters prior any transmission, or post-processed by receivers once they have been sensed. Interference processing techniques are for instance adaptively selected by interference classification techniques, since each interference processing technique usually fits well to one interference regime.

– **Power allocation for interference mitigation :** Interference intensity perceived by a receiver is driven by the transmit power of its neighbour interferers. Power allocation in interference-limited wireless networks is a game theory problem : to success in achieving its own QoS requirements, a transmitter should set its power in line with the transmit power of its neighbours and momentary channel realizations. With most of optimal power allocation solutions, the transmitter needs to consider how much it affects neighbour receivers when it computes its transmit power ; a selfish strategy is not conceivable.

1.3 Thesis Outline

The general problem of interference is addressed in Chapter 2, where common solutions to tackle in-band interference are likewise introduced. An original study on cooperative communications is done in Chapter 3 to evaluate how the use of half-duplex per chunk relays can help facing in-band interference. In Chapter 4 an effective and adaptive interference classifier is proposed ; this interference classifier is then exploited for solving the minimal power allocation problem in rate-constrained networks ; a centralized and coordinated solution is proposed in Chapter 5 while an autonomous and distributed algorithm is derived in Chapter 6.

Chapter 2 - Fundamentals of Interference in Wireless Networks

Interference is a severe issue in modern wireless cellular networks, where a same spectrum is shared by many close network entities. Interference indeed severely reduces performance of transmissions from the source to the destination. In this chapter we first give preliminary knowledge about wireless communications to detail and discuss concepts and challenges of in-band interference. We finally propose a non-exhaustive list of techniques which let reduce the detrimental effects of interference.

This is a background chapter without any specific related work.

Chapter 3 - Cooperative Communications with Half-Duplex Relays

While two-hop cooperative transmissions may help destinations in achieving more robust and more reliable transmissions, they also generate at the same time additional in-band interference which make harder the decoding at destinations. Cooperative transmissions are so driven by a trade-off. The goal of this chapter is to deal with this trade-off by limiting inter-cell interference in two hops cooperative communication systems. We propose to exploit the standard half-duplex limitation of relays so as to coordinate in time and frequency the resource allocation of a cluster of neighbour cells. To this end, novel efficient inter-cell resource allocation patterns are proposed. Simulation results show how our proposed allocation patterns permit to outperform classical patterns in terms of cooperation effectiveness, power consumption and perceived QoS.

Moreover, we evaluate the performance of an ideal inter-sector resource allocation mechanism which adapts resource allocation to changes in the communication context. This

adaptive process targets to maximize the global channel capacity for the given instantaneous channel instance and location of users.

- "Inter-cell interference mitigation allocation for half-duplex relays based cooperation," *IFIP Wireless Days, WD'09* [15]
- "Multi-cell interference aware resource allocation for half-duplex relay based cooperation," *IEEE Vehicular Technology Conference, VTC'10 Spring* [16]
- "Méthode d'allocation de ressources de transmission dans un réseau cellulaire de type coopératif," Patent 2009 [17]

Chapter 4 - Interference Handling Techniques

In-band interference drastically limits performance of wireless communication systems where a same spectrum is shared by some network equipments in the same geographical area. While interference degrades differently the quality of communication, most of the time radio resource management algorithms do not exploit any information on the type of interference experienced at the receiver. The focus of this chapter is to define a methodology to classify the interference experienced at the receiver. After investigating previously proposed solutions on the domain [13], we come out with a novel three-regime in-band interference classifier. The advantage of the proposed interference classification is to be less complex than previously proposed solutions and, implementable in practical communications contexts.

Furthermore, the proposed interference classifier will be exploited as input information of two interference aware power allocation algorithms proposed in Chapters 5 and 6.

- "Classification d'interférences," Patent 2010 [18]

Chapter 5 - Centralized Power Allocation Algorithm

In this chapter we investigate a centralized power allocation algorithm that exploits the three-regime interference classification introduced in Chapter 4. This algorithm aims at improving performance in wireless interference-limited and rate-constrained networks where power budget is a matter of concern. Nowadays, network operators have to face a challenging trade-off. On the one hand the scarce spectrum is over-exploited by several concurrent and heterogeneous systems which target more demanding services and higher transmission rates. On the other hand the size of cells is shrunk to reduce their coverage and hence their transmit power, while ensuring the target QoS. Both issues are closely related to the allocated transmit power that directly affects the level of in-band interference sensed by neighbour receivers. Consequently, it seems challenging but necessary to consider jointly the allocation of power and the more suitable strategy to mitigate in-band interference. This is precisely our goal in this chapter.

To this end a centralized algorithm is performed by an omniscient (coordinated) network controller to minimize the power budget of transmission under constraints of target rate. The network controller exploits our three-regime interference classifier to determine how the momentary communication context affects each node in terms of in-band interference ; based on the current classification, the minimal transmit power that ensures to meet rate constraint is computed. Simulation results prove that important energy savings are reach by adapting the allocation of power to the momentary communication context.

– "Centralized power allocation for interference limited networks," *IEEE Vehicular Technology Conference, VTC'10 Fall* [19]
– "Allocation de puissance inter-cell centralisée," Patent 2010 [20]

Chapter 6 - Distributed Power Allocation Algorithm

In the previous chapter we investigated a centralized approach to solve a problem of power minimization under constraints of rate in wireless interference-limited networks. In this chapter, we address the identical problem of power minimization but we now aim at computing the optimal solutions on a non-centralized and fully autonomously way. Commonly centralized approaches require coordination between nodes to achieve a full knowledge of channel and system parameters. Nevertheless, such a coordination may not be feasible or desired in some networks; it besides suffers from three main drawbacks. First of all, full knowledge seems inconceivable and unachievable in dense networks with high mobility (wireless sensor networks, ad hoc networks), since signalling and control overhead would waste communication resources. Second, effectiveness of centralized approaches depends on the reliability of link quality estimation between each node. Third, all computation complexity is carried out at the network controller.

Therefore we target in this chapter to meet with a distributed and autonomous approach the same performance of those computed by CPA algorithm (see Chapter 5). To this end we derive an iterative process where each node updates in turns its transmit power to react to the power adjustment of its neighbour. The new power is computed based on the interference classifier of Chapter 4. Nevertheless, the convergence of this iterative process, as well as the optimality of the computed solution need to be proved. A rigorous reasoning is hence proposed to prove both optimality and convergence of our distributed power allocation (DPA) algorithm.

– "Distributed power allocation for interference limited networks," *IEEE International Symposium on Personal, Indoor and Mobile Radio Communications, PIMRC'10* [21]
– "Méthode distribuée pour l'allocation de puissance entre stations de base dans un réseau cellulaire," Patent 2010 [22]

Chapter 7 - Conclusions and Future Work

In this dissertation we have focused on the interference issue in wireless communication systems. It occurs when a same spectrum is shared by some concurrent network devices in a close geographical area. Interference may drastically limit transmission performance and make impossible for the destination to decode reliably the received signal. These limitations are even more pronounced when in-band interference is unpredictable. To address to in-band interference mitigation, various radio resource management (RRM) techniques have been proposed, investigated and evaluated. A two-fold gain results from this thesis. First, some of our goals have been met with besides interesting scientific improvements. Second, other issues have remained unsolved or have lead to identify new research hints for future work.

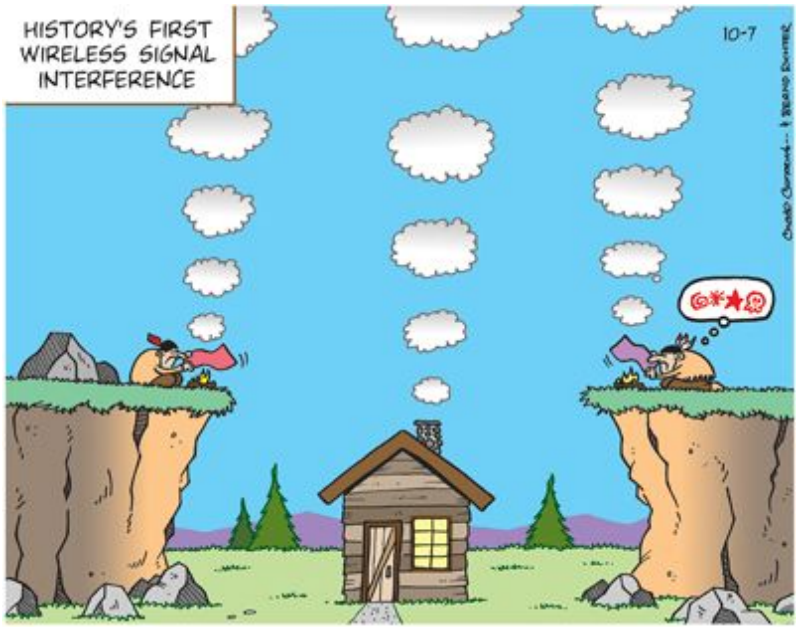

FIGURE 1.1 – History's first wireless signal interference.

Chapter 2

Fundamentals of Interference in Wireless Networks

In modern wireless cellular networks, many users compete for a scare shared resource : the spectrum. In this thesis we investigate how to limit the prejudicial effects of in-band interference. To this end, we detail and discuss in this chapter concepts and challenges of in-band interference.

The chapter is organized as follows. After introducing in Section 2.1 the technical context, our motivations and some possible application fields, Section 2.2 addresses some preliminary knowledge on wireless communications and presents successively the commonly adopted system models (2.2.1), some definitions (2.2.2) and assumptions (2.2.3), the characteristics of radio propagation (2.2.4), and finally examples of goals which can be targeted (2.2.5). Then, Section 2.3 provides some elements on femtocells networks. We lastly propose a brief state of the art on interference management techniques in Section 2.4 before to conclude the chapter with Section 2.5.

2.1 Introduction

2.1.1 Technical Context

Nowadays, operators of wireless networks target to improve transmission rates, increase coverage and limit waste of energy, while higher quality of service (QoS) requirements must be met. Since the number of user equipments (UE) to serve is keeping increasing, while applications and services are always more demanding, the global amount of resources is most of the time insufficient to achieve perfectly orthogonal resource allocation between concurrent transmissions in the network. Therefore, communication resources are shared, causing potential detrimental interference. Interference consists in a destination which perceives unintentionally a signal sent by a neighbour concurrent transmitter. In most cases, the reception of this not desired interfering signal reduces the reliability of the wished transmission, since the destination must face an unexpected source of perturbation which makes harder the decoding of the intended signal.

Interference can occur inside a given cell, in downlink mode, when a base station (BS) broadcasts a message which is not intended to all UEs ; this message is however perceived by all UEs and is referred by *intra-cell interference*. Likewise, a UE can be affected by the reception of a signal sent by a neighbour BS ; such a perturbation is known as *inter-cell interference*. Allocation of resources to active transmitters is made contingent on their QoS requirements : UEs with higher requirements need more resource blocks than UEs with low requirements. A same resource block can be assigned to more than one transmitter ; reliability of transmissions on this resource block is then limited by *in-band interference*, also called *co-channel interference*. However, even if disjoint resource blocks are assigned for two concurrent transmissions, imperfect RF filtering may cause these transmissions still interfere each other. Such an event is called *out-of-band interference*, also called *adjacent-channel interference* since it only occurs between contiguous sub-carriers.

In this context of interfered wireless communication networks, efficient approaches must be addressed to let mitigate detrimental effects of interference and thus meet higher QoS. Some elements are proposed in Tse and Viswanath [2], Berry and Yeh [23]. Throughout this dissertation, we will mainly focus on information theory metrics, such as channel capacity, to evaluate and compare performance of investigated techniques [7, 24, 25]

2.1.2 Motivations

Radio propagation is affected by several sources of perturbations which can drastically limit performance of wireless communications networks. Commonly, a source seeks to send a message to a destination through the radio channel while a specific QoS is targeted. Nevertheless, their transmission encounters perturbations, and especially interference, which cause in some scenarios dramatic and often unpredictable momentary reduction of transmission performance and transmission reliability. The higher the perturbations, the harder it is to recover the initial message from the perceived signal. This issue is even more challenging nowadays, since services provided to customers by networks' operators are always more resource demanding, whereas resources are made meanwhile scarcer and scarcer. Indeed, the access to frequency band is regulated and limited, while the number of wireless communication based systems keeps increasing. Consequently, there are more transmitters competing for these scarce resources ; the global level of interference is so higher. It is fundamental to deal with interference so as to mitigate its effects on transmission robustness. Interference mitigation is precisely one of the main issues of this PhD thesis.

Interference is more than just a source of thermal noise. Interfering signals indeed convey also information which is just intended to some specific destinations. By exploiting the special structure of interfering signals with effective interference processing techniques, prejudicial effects of interference can be limited and hence important performance enhancements can be met in terms of transmission robustness and reliability. In the literature, several interference mitigation techniques have been proposed. Depending on the available knowledge of system and channel parameters at transmitter and receiver side, these techniques are performed either by the source, priori to transmission, or by the destination, after the reception.

Interference mitigation techniques are proved to be essential in interference-limited networks subject to QoS constraints. Interference management is for instance highly advised for femtocells networks, cognitive radio based systems with primary and secondary users, or heterogeneous networks where systems of different standard interoperate. With such networks, some nodes have to face unpredictable and very high interference, whereas they seek to communicate reliably with their source. Such topics will be addressed from Chapter 3 to Chapter 6.

2.1.3 Examples of Potential Industrial Applications

Nowadays, interference management techniques are applied to quite all third generation cellular wireless mobile networks (3GPP, WiMAX, LTE, LTE-Advanced, etc.) as well as high data rate wireless LAN (WiFi). Industrial applications are mainly focused on interference limited scenarios in which several sources (from neighbour macro-cells, femtocells, sensors, clusters, etc.) transmit on the same frequency band. This is typically the application context of dense networks such as modern cellular and ad-hoc systems, where many UEs, BSs, femtocells, nodes share a common transmission resource, causing in-band interference. Such communication scenarios present an obvious problem : perceived interference increases as the number of coexisting devices (femtocells, BS, UE, sensors, etc.) sharing the same resources increases.

Examples of such industrial applications are for instance networks of femtocells where, both neighbour femtocells and macro-cells may transmit across the same geographical area and on the same frequency band, causing in-band interference [26, 27]. Another industrial application example is the interoperability and coexistence between multi-systems on the same frequency band such as with WiMAX and LTE, or Machine to Machine (M2M) communications based on LTE technology [28]. A last example of applications addresses the minimization of overall cluster cells transmission power with avoidance of inter-cell 'party effect' [14].

2.2 Preliminary on Wireless Communications

For acronyms and main notations, please refer to the dedicated chapter starting with page xli. Along this section, some preliminary knowledge on wireless communications will be developed. First, Section 2.2.1 presents the system models commonly adopted in the literature for dealing with wireless communications. Second, some fundamental definitions, notions and concepts are introduced in Section 2.2.2. Third, some usual assumptions dealing with wireless communications are proposed with Section 2.2.3. Then, Section 2.2.4 addresses characteristics of radio propagation. Finally, examples of goals which can be targeted by wireless communication based systems are derived in Section 2.2.5.

2.2.1 Classical System Models

Within this section we briefly introduce system models the most commonly adopted in the literature for describing wireless communications systems. The main purpose of these models is to state which are the active entities in presence and how they interact together. Conventionally, two sets are identified : the transmitters and the receivers. With the graph representation, transmitters and receivers are represented as vertices ; transmitters are plotted on the left while receivers are illustrated on the right. If a given transmitter communicates with a given receiver, deliberately or not, then an edge is represented between these two vertices. An edge thus refers either to an intended transmission or to an interfering transmission.

Throughout this PhD thesis, the word 'pair' will refer to a set of two entities constituted by a transmitter and its intended receiver. In other words, the two nodes of a pair want deliberately to communicate, whereas two nodes which do not belong to the same pair act as interferers together. Transmitters and receivers are called more generally 'sources' and 'destinations'. By 'pair' we hence describe a 'source-destination' set, also named $\mathscr{C}_i$ when we address the source s_i and the destination d_i. Commonly, the edge referring to the channel between a source s_i and a destination d_j is characterized by a channel coefficient $g_{i,j}$, where the first and second indexes are respectively related to the source and the destination.

Papers [29–31] are some of the first papers of information theory which address multi-access channels, in contrast with point-to-point channel. More recently, in [32, 33] the authors focus on multi-access fading channels and propose an interesting overview of the main concepts, challenges and results for these channels.

2.2.1.1 Broadcast Channel

The Broadcast Channel (BC) has been firstly addressed in [34–36]. It consists in a single source that communicates with several destinations. The transmitter broadcasts its message isotropically since this message is intended to all destinations located in its neighbourhood. The system model associated with the two-user BC is illustrated on Figure 2.1a. The single source s sends its message x towards destinations d_1 and d_2 at transmission rate R. Additive noise and channel state affect the perception of the message x. The perceived signal at destination d_i is

$$y_i = g_{1,i} \cdot x + z_i. \tag{2.1}$$

2.2.1.2 Multiple Access Channel

The Multiple Access Channel (MAC) is somehow the dual model of the broadcast channel. Here several transmitters send a message to a single destination which has to detect and decode the message of each transmitter. Some elements on the MAC are given in [37–40]. Figure 2.1b shows the classical representation of a two-user multiple access channel. Sources s_1 and s_2 respectively communicate their message x_1 and x_2 to the single destination d while the reception is affected by additional noise. Hence the perceived signal is given by

$$y = g_{1,1} \cdot x_1 + g_{2,1} \cdot x_2 + z. \tag{2.2}$$

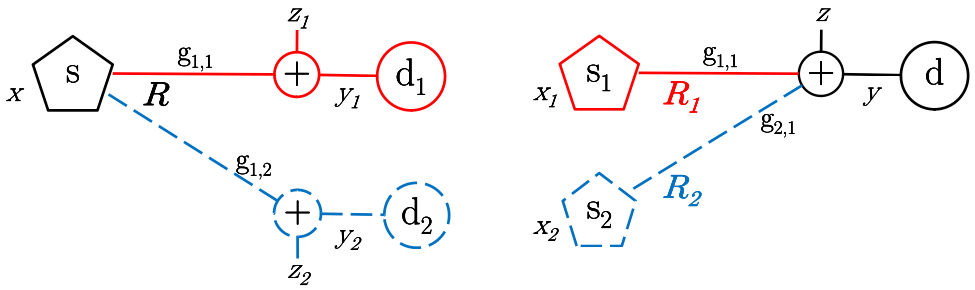

(a) Broadcast Channel (b) Multiple Access Channel

Figure 2.1 – Two-user Broadcast Channel versus two-user Multiple Access Channel.

2.2.1.3 Interference Channel

The Interference Channel (IC) is the most suitable model to deal with interference. It involves several concurrent pairs 'source-destination' which share a common frequency band. A source s_i sends a message x_i to its destination d_i, but this latter is affected by simultaneous transmissions of neighbour sources s_j $(j \neq i)$. The message x_i is only intended to the destination d_i. Consequently, all signals conveying messages x_j $(j \neq i)$ are actually in-band interference for destination d_i. Figure 2.2a illustrates a two-user interference channel with a pair $\mathscr{C}_1$ with red solid lines and a pair $\mathscr{C}_2$ with blue dashed lines. Each source s_i transmits with a rate R_i.

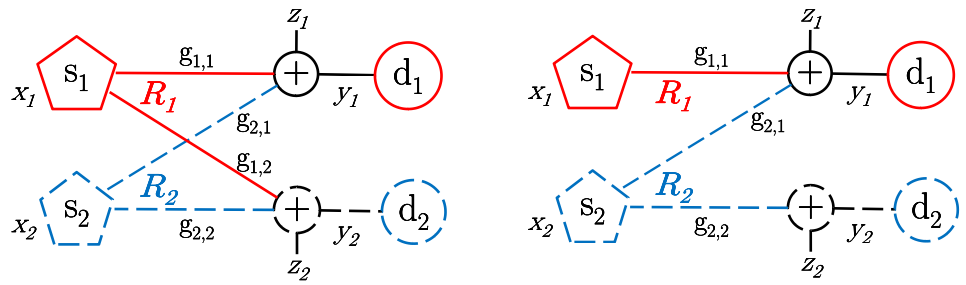

(a) Interference Channel (b) Z Channel

Figure 2.2 – Two-user Interference Channel versus One-Sided Channel.

Performance of interference channel in terms of reliable rates has been firstly addressed in [12, 41–44]. With this system model, two independent sources want to communicate reliably with their destination. Nevertheless, they cannot set their transmission parameters selfishly since each transmission affects the reception of other neighbour destinations. Commonly, information theory seeks to characterize and optimize the performance that all pairs can jointly achieve.

Interference channel can likewise be represented by the following system of equations

$$\begin{cases} y_1 = g_{1,1} \cdot x_1 + g_{2,1} \cdot x_2 + z_1, \\ y_2 = g_{1,2} \cdot x_1 + g_{2,2} \cdot x_2 + z_2, \end{cases} \tag{2.3}$$

where y_1 and y_2 represent respectively the signals perceived by d_1 and d_2. In such net-

works, the edge denoting by $g_i i, i$ is called the 'direct path' since it conveys the intended information, while the edges denoting by $g_{j,i}$ $(j \neq i)$ are called 'crossed paths'.

2.2.1.4 X Channel and Z Channel

Two other models are sometimes used in the literature. The first model is known as the X channel. Actually, the X channel and the interference channel seem to be very similar, since their representation can be identical (see Figure 2.2a). Nevertheless, there is a slightly difference between both models. Actually, as detailed in [45, 46], the X channel characterizes a more general system of m transmitters and n receivers, with possibly $m \neq n$. In such networks, each transmitter may have a message to transmit to each receiver. Consequently, 'crossed paths' do not necessarily convey interference.

Let us consider the two-user interference channel shown on Figure 2.2a as a X channel. It is then possible to divide this system model either into two independent broadcast channels, or into to independent multiple access channels (see for instance Figure 5.2 shown later in Chapter 5). Indeed, the two-user X channel involves two transmitters which communicate with two receivers. The systems $\{s_1, d_1, d_2\}$ and $\{s_2, d_1, d_2\}$ are actually two independent broadcast channels while systems $\{s_1, s_2, d_1\}$ and $\{s_1, s_2, d_2\}$ are two independent multiple access channels.

The second model is less common and known as the Z channel, also called one-sided channel. Some elements on this model are given in [13, 47, 48]. The Z channel is a special case of the interference channel, as shown on Figure 2.2b. Indeed, one of the two crossed paths is ignored. One destination is so not affected any more by interfering transmission of the neighbour source ; with the viewpoint of this destination, the transmission is identical to the one occurring over a point-to-point channel.

Several reasons can justify the absence of this interfering path. For sake of clarity, let us assume that the ignored path is the channel between the source s_i and destination d_j. First, the communication context between s_i and d_j can be so bad that they are out of reach of each other (too far apart, a building hides them, etc.). Consequently, the transmission of x_i is not perceived by d_j and hence does not affect it. Second, a kind of 'genie' can provide sufficient knowledge on the transmission of x_i for d_j so that the destination d_j is able to decode perfectly this interfering signal and then subtracting its contribution to make as if it has never existed.

2.2.2 Notions, Concepts and Definitions

In this section, some important conceptual or practical definitions are given in alphabetical order ; they will be used throughout the remainder of this document [2, 7, 49, 50].

Achievable Capacity Region : The achievable 'capacity' (see below) region of the two-user interference channel is the set of all pairs of rate $(R_1; R_2)$ that can be simultaneously met by both pairs 'transmitter-receiver' with arbitrarily small error probability. The classical representation of this region is given by a pentagon.

To define this region in case of more than two users, min-cut max-flow theorem must be used [51, 52]. The achievable capacity region is actually defined by an optimization problem which seeks to characterize the maximum achievable capacity in a flow network (here a flow is the transmission of a message through a path). The min-cut max-flow theorem states

that the maximum amount of flow passing from the source to the destination is equal to the minimum capacity that needs to be removed from the network so that no flow can pass from the source to the destination.

Channel Capacity : In information theory, channel capacity is the tightest upper bound on the amount of information that can be reliably transmitted over a communication channel (see Figure 2.3). By the noisy-channel coding theorem, the channel capacity of a given channel is the limiting information rate (in units of information per unit time) that can be achieved with arbitrarily small error probability.

Information theory, developed by Claude E. Shannon during World War II, defines the notion of channel capacity and provides a mathematical model by which one can compute it [29]. The key result states that the capacity of the channel, as defined above, is given by the maximum of the mutual information between the input and output of the channel, where the maximization is with respect to the input distribution.

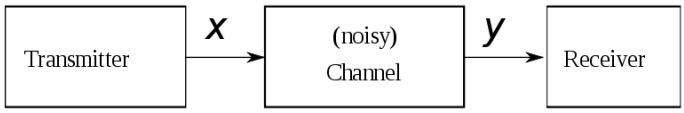

Figure 2.3 – Classical representation of a wireless communication channel.

The noisy-channel coding theorem states that for any $\epsilon > 0$ and for any rate R less than the channel capacity C, there is an encoding and decoding scheme that can be used to ensure that the probability of block error is less than ϵ for a sufficiently long code. Also, for any rate greater than the channel capacity, the probability of block error at the receiver goes to one as the block length goes to infinity.

Let X represent the space of signals that can be transmitted, and Y the space of signals received, during a block of time over the channel of Figure 2.3. Let $p_{Y|X}(y|x)$ be the conditional distribution function of Y given X. Treating the channel as a known statistic system, $p_{Y|X}(y|x)$ is an inherent fixed property of the communications channel (representing the nature of the noise in it). Then the joint distribution $p_{X,Y}(x,y)$ of X and Y is completely determined by the channel and by the choice of

$$p_X(x) = \int_x p_{X,Y}(x,y)dx \tag{2.4}$$

the marginal distribution of signals we choose to send over the channel. The joint distribution can be recovered by using the identity (Bayes theorem)

$$p_{X,Y}(x,y) = p_{Y|X}(y|x) \cdot p_X(x). \tag{2.5}$$

In information theory, entropy is a measure of the uncertainty associated with a random variable. The term by itself in this context usually refers to the Shannon entropy, which quantifies, in the sense of an expected value, the information contained in a message, usually in units such as bits. Therefore, the marginal entropy

$$\begin{array}{ll} H(X) & = \mathbb{E}\{-\log_2 p_X(x)\} \\ & = \int_x -\log_2(p_X(x)) \cdot p_X(x)dx \end{array} \tag{2.6}$$

quantifies the binary information contained in the variable X. Likewise, $H(Y|X)$ and $H(X,Y)$ are respectively the conditional entropy of Y given the knowledge of X and the joint entropy of X and Y.

The mutual information $\mathscr{I}(X;Y)$ of two random variables X and Y is a quantity that measures the amount of additional information on X brought by Y. The most common unit of measurement of mutual information is the bit, when logarithms to the base 2 are used. Mutual information can be equivalently expressed as

$$\begin{aligned}\mathscr{I}(X;Y) &= H(X) - H(X|Y)\\ &= H(Y) - H(Y|X)\\ &= H(X) + H(Y) - H(X,Y)\\ &= \int_y \int_x p_{X,Y}(x,y) \cdot \log_2 \frac{p_{X,Y}(x,y)}{p_X(x)\cdot p_Y(y)} dxdy.\end{aligned} \tag{2.7}$$

The maximum mutual information is called the channel capacity C and is given by

$$C = \sup_{p_X} \mathscr{I}(X;Y). \tag{2.8}$$

The capacity of the AWGN point-to-point channel is given in bits by $C = \log_2(1 + \text{SNR})$. Elements to calculate the capacity of frequency selective channels are given in [2, 7] while [53, 54] address the computation of mutual information for different modulations.

Channel gain : The propagation of a message x_i from a source s_i to a destination d_j occurs through a wireless channel. Some source of perturbation may affect the propagation (see Section 2.2.3). Commonly, there are the path loss attenuation which is inversely proportional to a power of the distance between the source and the destination, the shadowing, the fading and the antenna gain. The channel acts as a filter where the coefficient $g_{i,j}$ stands for the gain between the input x_i and the output y_j of the channel.

Channel Quality Indicator - SNR, INR, SINR : Channel Quality Indicator (CQI) is a metric aiming at describing the link quality of a given channel. Mostly, CQI is defined by the Signal-to-Noise Ratio (SNR), the Interference-to-Noise Ratio (INR) and/or the Signal-to-Interference-and-Noise Ratio (SINR). These ratios are respectively defined as

$$\begin{aligned}&\text{SNR}: \quad \gamma_i = \frac{|g_{i,i}|^2 \cdot P_{s_i}}{\sigma^2_{d_i}},\\ &\text{INR}: \quad \delta_{j,i} = \frac{|g_{j,i}|^2 \cdot P_{s_j}}{\sigma^2_{d_i}},\\ &\text{SINR}: \quad \text{SINR}_i = \frac{\gamma_i}{1+\sum_{j\neq i}\delta_{j,i}},\end{aligned} \tag{2.9}$$

where $\sigma^2_{d_i}$ is the variance of the background noise at destination d_i.

Channel State Information : In wireless communications, Channel State Information (CSI) refers to known channel properties of a communication link. This information describes how a signal propagates from the transmitter to the receiver and represents the combined effect of, for instance, scattering, fading, and power decay with distance. The CSI makes it possible to adapt transmissions to current channel conditions, which is crucial for achieving reliable communication with high data rates in multiantenna systems. CSI needs to be estimated at the receiver and usually quantized and fed back to the transmitter (although reverse-link estimation is possible in TDD systems). Therefore, the transmitter and receiver can have different CSI. The CSI at the transmitter and the CSI at the receiver are sometimes referred to as CSIT and CSIR, respectively.

Chunks : A chunk is a group of consecutive sub-carriers. For instance, in LTE-A, a chunk is defined as 12 sub-carriers on 15kHz each. Commonly, systems dispose of 50 chunks for a bandwidth of 9MHz. Actually, the bandwidth is equal to 10MHz because of extra band for overhead, guard interval and so forth.

Communication context : By communication context we refer to the momentary value of channel and system parameters, such as CQI of direct and crossed links, transmit powers, QoS requirements, noise variance, location of entities, and so forth. Such parameters entirely characterize the current scenario of communication, and so the performance that the system can meet. It is fundamental that the system adapts faster to changes in communication context than the period with which changes occur. The coherence time of the channel must hence be bigger than the delay requirement of the system. Such a condition ensures the system disposes of reliable information about the channel state and has enough time to adapt itself to the momentary communication context.

Degrees of freedom : In point-to-point links, the notion of degrees of freedom is a fundamental measure of channel resources. It tells us how many signal dimensions are available for communication [55, 56]. In the (scalar) AWGN channel, there is one degree of freedom per second per Hz. When multiple links share the communication medium, one can think of the mutual interference as reducing the available degrees of freedom for useful communication. The number of free degrees of freedom is related to the multiplexing gain (see page 80). In MIMO systems with M transmit and N receive antenna, the total numver of degrees of freedom is given by $\min M, N$.

Diversity : In telecommunications, a diversity scheme refers to a method for improving the reliability of a message signal by using two or more communication channels with different characteristics. Diversity plays an important role in combating fading and co-channel interference and avoiding error bursts. It is based on the fact that individual channels experience different levels of fading and interference. Multiple versions of the same signal may be transmitted and/or received and combined in the receiver. Alternatively, a redundant forward error correction code may be added and different parts of the message transmitted over different channels. Diversity techniques may exploit the multipath propagation, resulting in a diversity gain, often measured in decibels. Diversity can be met in time, frequency, space or with multi-user and cooperative (multi-antenna) schemes.

Interference-limited and noise-limited scenarios : Interference-limited and noise-limited scenarios define two kinds of communication contexts where the perceived power of respectively interference and background noise is so high that it dramatically affects the robustness and the reliability of the transmission. For instance, an interference-limited scenario is characterized by a relatively low SINR, while a noise-limited scenario is characterized by a low SNR (with INR < 1).

Modulation and Coding Scheme : Modulation and Coding Scheme (MCS) is a term used in latest communication standards to specify which of the nine different modulation and coding schemes is being applied. Several MCS have been defined ; they can be either GMSK (Gaussian Minimum Shift Keying) or 8-PSK (8-Phase Shift Keying). MCS is related to link adaptation techniques (Adaptive Modulation and Coding - AMC) which set several

transmission parameters according to the instantaneous conditions on the radio link. For instance, a transmission across a channel in deep fade cannot be reliable with a high order of modulation. Likewise, the encoding rate can be improved in case of good channel states, so as to increase the communication rate.

Since transmission context can quickly change in time, space and/or frequency domains, it seems fundamental to adapt transmission parameters to the instantaneous conditions on the radio link. Such adaptation guarantees to achieve the best performance the system can bear without being in 'outage' (see below). Transmission parameters can be updated at periodic time scales (millisecond, ten-second and hour) or as soon as channel conditions change. By matching the MCS to channel quality, minimal service with reliable and robust transmissions can be guaranteed. The higher MCS is, the better performance is but also the less robust transmissions are. There is then a trade-off between the performance (bit rate) and the robustness (bit error rate, outage probability).

Outage : In wireless communication networks, the channel capacity should be compared to the QoS requirements and more especially the target rate (or possibly throughput). The outage event defines a state where the channel capacity cannot satisfy rate requirements. Actually, as stated by the noisy-channel coding theorem (also called Shannon theorem [29], see above), the channel capacity C must be higher than the target rate R to ensure a reliable transmission.

The probability of outage is often used as a metric to characterize the performance of transmission :

$$P_{out} = \mathbb{P}\{C(\underline{\mathbf{H}}) \leq R\}, \tag{2.10}$$

where $\underline{\mathbf{H}}$ is the channel matrix and R[bit/s/Hz] is the rate. There is a fundamental difference between quasi-static channels and fast-fading (or ergodic) channels. With quasi-static channels, only one channel realization is used for the transmission of a message ; the channel capacity is easily computed as a function of the current value of the channel matrix $C(\underline{\mathbf{H}})$. On the other hand, several channel realizations occur during a single transmission with ergodic channels ; the channel capacity is an average of $C(\underline{\mathbf{H}})$. Let us recall that the concept of ergodicity says that the time average should converge to the same limit for almost all realizations of the fading process. We understand therefore better the concept of outage probability.

Quality of Service, Scheduling, Fairness : Quality of Service (QoS), scheduling and fairness are concepts addressed by upper-layers and are not investigated in this document. QoS refers to resource reservation control mechanisms ; it is the ability to provide different priority to different applications, users, or data flows, or to guarantee a certain level of performance to a data flow. For example, a required bit rate, delay and/or bit error rate may be guaranteed. QoS guarantees are important if the network capacity is insufficient, especially for real-time applications such as voice over IP. A best-effort network or service does not support QoS.

Scheduling refers to the way resources are assigned for transmissions to active users, contingent on their QoS requirements. Mostly there are less available resources than requested resources ; the scheduler has then to queue some users or to serve them partially. Different scheduling algorithms are responsible for the resource allocation. A fair scheduler aims at serving all users equally, in time average ; hence each user has the same chance to access to resources. Fairness is expected but it is not always an easy task.

Radio Resource Management : Radio resource management (RRM) is the system level control of in-band interference and other radio transmission characteristics in wireless communication systems. RRM involves strategies and algorithms for controlling parameters such as transmit power, channel allocation, handover criteria, modulation scheme, error coding scheme, etc. The objective is to exploit the scarce radio spectrum resources and radio network infrastructure as efficiently as possible.

Transmit power : The transmit power of the source s_i is defined as the average power of its message x_i :

$$P_{s_i} = \mathbb{E}(\| x_i \|^2). \tag{2.11}$$

Power can be expressed in Watt [W] or decibel [dB]. Sometimes, transmit power is substituted by Equivalent Isotropically Radiated Power (EIRP). EIRP is the amount of power that a theoretical isotropic antenna (which evenly distributes power in all directions) would emit to produce the peak power density observed in the direction of maximum antenna gain. EIRP can take into account the losses in transmission line and connectors (L_C) and includes the gain of the antenna (G_A) :

$$EIRP = P_{\mathrm{TX}} - L_C + G_A. \tag{2.12}$$

2.2.3 PhD Assumptions

Assumptions formulated in this section will be valid in the remainder of the document. First of all, we focus only on in-band interference. Therefore, we ignore out-of-band interference, which is due to imperfect filtering with leakage on undesired frequency bands. In the remainder, in-band interference, or shortly interference, will refer to interfering signals sent by all neighbour sources competing for the same frequency resources. Moreover, we assume OFDMA based communication systems. Consequently, resources are orthogonally assigned between active users inside a same cell to avoid intra-cell interference. In-band interference will then be caused only by inter-cell (or inter-cluster) transmissions on the same band.

Furthermore, we do not focus on coding schemes ; we assume that a **capacity achieving code** is used by physical layer. Consequently, performance of different approaches will be evaluated and compared by use of the amount of mutual information instead of common metrics such as bit error rate. As cited in [23], no matter what code lengths are used in practice, information theory provides an upper bound to all achievable rates. Furthermore, the gap between information-theoretic limits and the performance of practical codes with reasonable complexity has narrowed considerably in recent years, due to rapid advances in coding technology. Therefore, at the physical layer and at any time t, we assume that any set of powers and rates from the instantaneous multi-access information-theoretic capacity region can be allocated to the transmitters, as long as average and peak power constraints are satisfied.

Remainder assumptions are briefly enumerated :

- **Quasi-static channels** : we consider slow varying fading channels where the coherence time is longer than any delay requirements of the system (scheduling period, channel estimation period, etc.). Hence channel gains are constant during transmission of at least one message.

- **Perfect channel estimation** : CSI knowledge acquired by transmitter or receiver is assumed erroneous and coherent with the momentary communication context. Since channels are quasi-static, the reliability of channel estimation at any time t is not really a challenging issue.
- **Single antenna equipments** : devices are only equipped with a single antenna. Improvements would be reached with MIMO systems but such an issue is for future work.
- **Synchronisation between neighbour transmissions** : Even if sources are not coordinated via a backhaul network, we assume that their transmissions are synchronous and happen simultaneously. Besides, the delay between different paths is assumed negligible.
- **One active user per cell** : Since OFDMA techniques are performed, resources are orthogonally assigned inside a cell. Active users can hence be independently considered on each resource block.
- **Scheduling** : we do not focus on scheduling tasks, such as fairness, queue lists, priority order, latency and so forth. Scheduling is done by upper layers and we just assume the active user is the best eligible one at any time t, contingent on the momentary communication context and QoS requirements.
- **No inter-symbol interference** : ISI may be caused by multipath propagation ; Zero Forcing or guard interval between symbols can avoid ISI.

2.2.4 Characteristics of Radio Propagation Channels

The radio propagation of a message over a wireless channel is affected by several sources of perturbation. Channels are time and frequency varying. These variations are due to the nature of the medium of transmission (water, air, space, wood, brick, etc.) as well as the configuration of devices, their location in the environment and the specific properties of the environments (presence of walls, mobility of users, fading, shadowing, scattering, an so forth). We detail hereafter some causes of radio degradation we have considered in our numerical simulations.

Fading : it characterizes deviation of the attenuation that a carrier-modulated signal experiences over certain propagation media. A transmission can encounter slow fading, fast fading, block fading, flat fading, frequency-selective fading. We assume quasi-static channel and hence we rather consider slow varying fading. In the literature, two main models describe fading variations : the Rician fading for line of sight (LOS) transmissions and the Rayleigh fading for non line of sight (NLOS) transmissions. In our numerical simulations, we model fading events with a random Rayleigh variable, whose density probability function is given by

$$f(x,\sigma) = \frac{x}{\sigma^2}\exp(-\frac{x^2}{2\sigma^2}), \tag{2.13}$$

where σ is the parameter of the distribution whose mean is equal to $\sigma\sqrt{\frac{\pi}{2}}$.

Shadowing : it models the apparition of a large obstruction (building) that affects the path between the transmitter and the receiver. In our numerical simulations, shadowing is modelled as a log-normal distribution with a standard deviation [57].

Path loss attenuations : several models are given by communication standards to define how the transmission is affected on a given path. One of the most famous model is the Okumura-Hata model which calculates attenuation taking account of the percentage of buildings in the path, as well as natural terrain features. Commonly, log-distance path loss model is formally expressed as :

$$\begin{aligned} L_{\text{dB}} &= 10 \log_{10} \frac{P_{TX}}{P_{RX}}, \\ &= L_0 + 10\beta \log_{10} \frac{d}{d_0} + X_g, \end{aligned} \tag{2.14}$$

where L_{dB} is the total path loss in Decibel [dB], P_{TX} and P_{RX} are respectively the transmitted and received powers in Watt [W], L_0 is the path loss [dB] at distance d_0, d [m or km] is the length of the path, d_0 is the reference distance, β is the path loss distance exponent, specific to the propagation medium and X_g is a Gaussian random variable reflecting the shadowing. Shadowing can be treated outside this model so as to consider a simpler expression :

$$\begin{aligned} & L_{\text{dB}} = L_0 + 10\beta \log_{10} d \\ \Leftrightarrow \quad & L_{\text{linear}} = 10^{\frac{L_0}{10}} d^{\beta}. \end{aligned} \tag{2.15}$$

Values of parameters are defined according to the system [11, 14, 26, 28, 58].

Wall penetration loss : in line with the configuration of the system (indoor, outdoor propagations), a path may go through a wall. The sudden change of material of the propagation medium is not taken into account by the path loss model described above. It is useless to derive a specific model for the crossing of the signal through the wall ; it can be described by a single (negative) gain. The value of wall penetration loss depends on the thickness and nature of the crossed wall (exterior or interior wall). The global path loss should consider the number and nature of crossed walls. Moreover, different models should be defined for indoor and outdoor propagations, when the signal pass through an exterior wall.

Noise and In-band interference : additive white Gaussian noise (AWGN) is considered, with variance σ^2. Interference is of course one of the fundamental cause of perturbation that affects the transmission reliability, but we do not develop it here.

Effects of perturbation occurring during the radio propagation are many-fold. First, the 'near-far' problem, because of path loss attenuation, describes the difficulty of a receiver to detect a weak signal when a stronger signal is perceived. If two sources send their signal with the same power but are not located at the same distance of the destination, then one signal may be perceived with a power much higher than the other. Likewise, path loss attenuation lets to distinguish two classes of users : border-cell users which are hardly served reliably, regarding their QoS requirements, and cell-centre users which meet their satisfaction threshold.

If the overall loss of the channel is either not taken into account or under-evaluated when transmission parameters are set, then it will result in a signal perceived by the receiver which is worse than expected. Therefore, the channel capacity may not bear the transmission rate, causing an outage event. The message can thus not be recovered and must be transmitted again (Automatic Repeat reQuest - ARQ mechanism). Commonly, path loss attenuation can be easily foreseen, since sources are assumed disposing of perfect channel estimation ; they besides can estimate the location (or at least distance) of their

destination by use of pilot signals. However, in-band interference is not always predictable ; it may be difficult or impossible for the source to cope with interference : interference mitigation techniques must be performed at the destination.

2.2.5 PhD Hints of Research

As it was motivated in the introduction of this chapter, wireless communication networks target challenging issues which cannot be met without effective interference management techniques. For instance, latest communication standards such as WiMAX or LTE-A focus on higher data rates, demanding services for customers (higher QoS requirements), lower power budget, interoperability between heterogeneous systems. These goals must be achieved while paradoxically there are less resources, since networks are denser and numerous.

Under these conditions, great interest is given to cell-edge users since they often characterize the worst scenario of transmission. They indeed perceive the signal from their source with lower power than cell-center users, while they besides encounter a stronger level of interference. To succeed in serving cell-edge users with a sufficient QoS, different techniques can be performed :

- Resource allocation and scheduling,
- Cooperative communications,
- Power allocation,
- Interference cancellation, avoidance.

These different techniques will be investigated in the remainder chapters.

2.3 Preliminary on Femtocells Networks

The multiplicity of wireless communication systems increases the spectrum pollution due to interference. Networks operators aim hence at getting more reliable and robust wireless links between network access points and customers. An effective way for them to increase system capacity is by getting the transmitter and receiver closer to each other, which creates the dual benefits of higher-quality links and more spatial reuse. Indeed, close receivers are less affected by prejudicial events occurring during radio propagation. Besides, transmit power can be lowered, resulting in lower in-band interference. With nomadic users which sporadically access to the network, shorten distance inevitably involves deploying more infrastructure, typically in the form of microcells, hot spots, distributed antennas, or relays. In other words, numerous short-range low-power access points are deployed instead of wide-range high-power BSs. Recently, the concept of femtocells (FC) - also called home base stations (H-BS) or femto access point (FAP) - has been proposed and adopted as a less expensive alternative. Femtocells networks consist in equipping with FAPs local indoor or outdoor areas, such as home, office, mall, park, to get better coverage [27, 59, 60].

In practice, with the interoperability of standards and systems, femtocells networks can be shown as LANs, where H-BSs replace the common 'boxes' of network operators (Internet, VoIP, television DVB). Besides, H-BSs consist also in a gateway through the 3G/4G network. Advantages of such deployments are many-fold.

- H-BSs ensure local (short-range) coverage with reduced transmit power and so lower power budget.
- In-band interference between femtocells is such a way reduced.

- Moreover, the density of femto UEs (FUE) inside a femtocell is reduced since the area coverage is smaller.
- Therefore, the ratio between the number of resource-blocks and the number of active users is bigger and H-BSs are hence able to guarantee higher QoS to their FUEs. Typically, there are (much) more available resource blocks than active users to serve inside a femtocell.
- FUEs are provided with various heterogeneous services.

Benefits are likewise numerous for network operators, which are more interested in CAPEX-OPEX reductions. H-BSs are not complex devices and are hence not expensive to produce. Moreover, the deployment of low-cost H-BSs (less than 100€) is ensured by customers themselves who install H-BSs where they need them. This point is fundamental : on the one hand, network operators are not in charge of the deployment of H-BSs, on the other hand a ubiquitous coverage can be met since H-BSs may act as access points for nomadic users. Therefore, overlapping deployment of femtocells may occur.

Actually, femtocells networks are not really an alternative to cellular networks, but rather a complement, to achieve locally higher QoS. Consequently, it appears as the deployment of femtocells within a pre-established macro-cells network. In practice, UEs are attached either to a serving macro-BS or to a serving H-BS. Sometimes, macro-cells and femtocells are assigned disjoint frequency bands but mostly they share the same spectrum. Therefore, transmissions may be limited by macro to macro, macro to femto, femto to macro and femto to femto interference. Commonly, femtocells are considered as secondary systems whereas macro-cells form the primary system. Such as with cognitive radio approaches, femtocells have to opportunistically access to spectrum without affecting too much macro-UEs.

We conclude this section with brief remarks on users mobility in femtocells networks. Mobility is a challenging issue in wireless networks. H-BSs and macro-BSs are coordinated to possibly offer roaming and handover to nomadic users. However, femtocells define mostly private networks with restricted access : open, closed and hybrid accesses to H-BSs are proposed respectively to licensed, unlicensed and specific users. Mobile H-BSs are also addressed [26, 27] to provide ubiquitous coverage, even when users move on board a train or a bus. Power allocation and resource allocation techniques specifically designed for femtocells are proposed in [26, 61–65].

2.4 Preliminary on Interference Mitigation Techniques

In this section we present a selection of the most effective techniques to cope with the interference issue. The book of Tse and Viswanath [2] provides definitely useful basis to understand this issue. Each interference mitigation technique can be applied individually or combined with other techniques to achieve better performance. In most cases, a single technique cannot perfectly cancel interference alone. Furthermore, important tasks are done by upper layers, such as scheduling, which plays an important role in resource management to guarantee QoS and fairness between customers ; but such aspects are not addressed here.

Several approaches have been proposed in the literature to cope with in-band interference in dense communication systems. Interference aware techniques can be either static or dynamic. First, static techniques design a global and fixed solution to avoid catastrophic instances of in-band interference. On the other hand, dynamic techniques update periodically transmission parameters to take time, frequency, space variations of the communica-

tion context into account. The topology of the network (mobility of users with sporadic access to network) and customers requirements (possibly different between devices, varying with time of the day, location, etc.) are other fundamental system parameters.

With interference management, three axes can be distinguished. First, an easy way to deal with interference is to avoid creating it : **interference avoidance** or interference coordination techniques allocate and manage resources so that interference is not generated. Such techniques are performed prior to any transmission and assume commonly CSIT knowledge. Second, **interference cancellation** techniques are performed to suppress the perceived interference at destination. They mainly need CSIR knowledge. Finally, **interference randomization** techniques are less frequent but consist in spreading randomly users' transmissions over sets of sub-carriers so as to randomize the perceived interference and achieve frequency diversity gain [66]. However, another classification is adopted in the remainder to introduce interference mitigation techniques. We rather consider four topics, namely orthogonal resource allocation, resources sharing, information theory and signal processing, and lastly channel aware power control.

2.4.1 Orthogonal Resource Allocation

Frequency bandwidth is a common and scarce resource, whose access is regulated by governmental authorities. Spectrum must thus be shared efficiently between active network devices so as they meet their QoS requirements. However, since QoS constraints can differ between devices, the allocation of resources is not necessarily uniform and fair : a bigger fraction of bandwidth should be allocated to few devices.

The best way to deal wit interference is to avoid creating it. By allocating a disjoint and exclusive set of resource blocks to all active transmitters in the network, we prevent them from interfering each other. Concurrent transmissions are separated in time, frequency, space and/or code domains ; since two concurrent transmissions do not use the same resources, they cannot interfere (if perfect filtering is assumed, then there is no adjacent-channel interference). Transmission are then said 'orthogonalŠ. Several well-known resource allocation techniques have been proposed to achieve such orthogonalization :

- Time / Frequency Division Duplex techniques (TDD / FDD) where the downlink and the uplink phases are separated in time / frequency,
- Time / Frequency Division Multiple Access techniques (TDMA / FDMA) where several signals are multiplexed in time / frequency,
- Orthogonal Frequency Division Multiple Access (OFDMA) is the multi-user version of the popular Orthogonal Frequency Division Multiplexing (OFDM) scheme, used as a digital multi-carrier modulation method,
- Code Division Multiple Access (CDMA) and Space Division Multiple Access (SDMA) where transmission are respectively made orthogonal in code and space domains.

An easy way to achieve perfect orthogonality between concurrent transmissions in a cellular network is for instance to assign disjoint sets of chunks to cells so as to avoid inter-cell interference. Intra-cell interference can be dealt with a time-slotted fashion : each active user in a same cell accesses in turns to resources. However, such orthogonal resource allocations assume that the number of available resources is greater than the number of resources requested by active transmitters. Nevertheless, perfectly orthogonal resource allocations cannot be met in dense networks, since the set of available resources may be not enough to allocate exclusive resource blocks to all active transmitters with a sufficient degree of satisfaction. Moreover, such orthogonal allocation techniques result

in poor spectral efficiency and their performance is far from theoretic performance limits. Their main advantage is their easy implementation.

2.4.2 Non-Orthogonal Resource Allocation

In most networks, there are less available resources than required resources : resources need to be shared between neighbour concurrent active transmitters. We consider in this section systems where orthogonal allocations are not possible or not desired (bad spectral efficiency). Since at least two transmitters use simultaneously the same band, their transmission is limited by in-band interference. nevertheless, resources can be shared and reused in a smart fashion so as to mitigate in-band interference.

2.4.2.1 Frequency Reuse

The main idea here is that perceived in-band interference is not necessarily prejudicial : the more apart interfering 'source-destination' pairs are from each others, the less detrimental the perceived interference is. Since the sensed power decays with the increasing distance between a source and a destination, two pairs using the same resource block can be separated geographically and/or by power quantification. Indeed, if a resource block is reused in two remote spatial locations, or if the two pairs are quite narrow but their source transmits at low power level, in-band interference may not affect the transmission reliability.

Some frequency reuse techniques are proposed in [1, 67–70]. They mainly consist in allocating disjoint sets of sub-carriers to cell-edge devices of neighbour cells, while cell-centre devices use all the band, as illustrated on Figure 2.4. Actually, cell-edge devices use all the band but with power masks that differ between neighbour cells. Each cell disposes of a specific band for communicating with its cell-edge users at high power level, whereas the remainder of the spectrum is used with low power transmissions. Transmissions for cell-centre users are performed with an intermediate level of power.

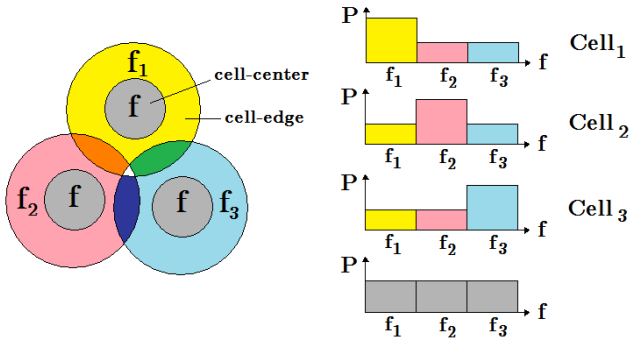

Figure 2.4 – Frequency reuse technique with distinction for cell-centre and cell-edge users.

Frequency reuse techniques commonly define a 'frequency reuse factor' (FRF) which states how a given band is reused. A unitary FRF means that the whole spectrum is used everywhere, while a FRF equal to 3, for instance, means that a given band is reused once every three cells. Frequency reused techniques can be classified as follows :

– The more basic technique is the Full Frequency Reuse technique where the whole frequency bandwidth is used by all cells (FRF=1).

- Hard Frequency Reuse techniques allocate the different chunks to cells according to a given frequency pattern.
- Soft Frequency Reuse techniques allocate in each cell some chunks to cell-edge devices while the remaining chunks are allocated to cell-centre devices. Such a process avoids the 'near-far' problem.
- Fractional Frequency Reuse techniques slightly differ from Soft Frequency Reuse techniques : some common chunks are allocated to all cell-centre devices, while remaining chunks are allocated according to a frequency reuse pattern to cell-edge devices in all cells.
- Hybrid techniques can change FRF or switch from one technique to another, according to reliability of transmission. The transmission starts with a low FRF : it causes more interference but it is more spectral efficient. If transmission is not reliable, a higher FRF is selected to reduce the reuse of frequency bands and so the level of interference (but also the spectral efficiency).

Frequency planning can be static in time (resources are allocated one for all at the beginning of the first transmission) or dynamic (resource are adaptively allocated according to instantaneous conditions).

2.4.2.2 Divide and Conquer : Graph Colouring

Graph colouring techniques consist in constituting clusters of devices and so in dividing the whole problem of interference into smaller ones. Each cluster is then treated independently. To make clusters independent, the idea is to assign a specific colour to each cluster and try to avoid contiguous clusters with same colour [71, 72]. A colour refers to a specific band : it is a kind of frequency reuse technique.

Clusters can be based on locations of devices, similar features, identical QoS requirements, etc. The simplest way to form clusters is to consider all devices belonging to a same neighbourhood. Two clusters can share a same band if these two clusters are sufficiently apart from each other so as to lower as much as possible the interference they cause each other. Inter-cluster interference is then avoided thanks to orthogonal allocation of resources. Intra-cluster interference has to be dealt with other techniques.

There is a trade-off between the size of the cluster (*i.e.,* the number of devices inside the cluster) and the performance of the transmissions of the cluster. First, a small cluster lets greatly reduce the perceived level of interference since most of interferers are located in a neighbour cluster and therefore transmit on an orthogonal frequency band. Nevertheless, the spectral efficiency is also reduced. On the other hand, a big cluster does not really mitigate interference since numerous interferers are gathered in the same cluster. They dispose however of more resource blocks and are thus more spectral efficient.

Accuracy of channel and system parameters is fundamental with graph colouring since these parameters lead how clusters are constituted.

2.4.2.3 Cognitive Radio Approach

Cognitive or opportunistic radio refers to systems where there are primary (or licensed) users with priority access to resources, and secondary (or unlicensed) users with low priority access to resources. Secondary users access opportunistically to resources : they should not disturb primary users. Secondary users sense the spectrum, looking for unoccupied bands : secondary users can access to blanks in spectrum.

The basis of opportunistic radio comes from the fact that spectrum is not uniformly used in time days and between channels. Secondary systems adapt their transmission and reception parameters to the momentary occupation of the spectrum. Consequently, secondary users avoid to cause in-band interference since they use orthogonal channels.

The concept used by cognitive radio is actually an adaptive frequency planning for frequency reuse. A secondary system can reuse a band if its transmission on this band does not affect the primary devices listening on this band. In practice, there is a threshold for the SINR of primary devices : the transmissions of secondary devices cannot lead to exceed this threshold.

2.4.3 Information Theory and Signal Processing Techniques

Interference is not just a source of perturbation, as is the noise. Interfering signals indeed convey information and have a structure which can be possibly exploited to mitigate their prejudicial effects. As cited in [73], interference between communication systems is harmful, not so much because of its intensity or power but, rather, because of the uncertainty (entropy) associated with the interfering signal. This uncertainty depends on the communication rate of the interfering system and may be increased by propagation effects such as random fading, etc. A clever receiver can diminish the reductive effects of interference if there is enough power and their entropy is not excessive. Of course, if the interference is quite unintelligible, it is preferred that it have low power.

In the literature, interference mitigation techniques belonging to information theory and signal processing tracks have been proposed to help in coping with detrimental effects of interference. With specific processing and filtering of signals, performed prior to any transmission and/or after any reception, in-band interference can be lowered by exploiting some knowledge of system and channel parameters.

Few years ago, interference was mostly treated as an additional source of thermal noise, *i.e.,* as a jamming signal whose structure was not exploited at all. Effective techniques propose for instance to decode interference so as to partially or fully cancel out its effect. Recently, interference alignment with its challenging results relaunches interest for interference mitigation processing. Nevertheless, signal processing techniques often present complex computational tasks and require mostly high level of CSI knowledge. In dense wireless networks with many neighbour interfering sources, these techniques seem to be just theoretical solutions to the interference issue, since they may be hardly applied in practice, or at most locally.

2.4.3.1 Noisy Strategy

Most papers dealing with interference mitigation strategies are more interested in designing schemes to avoid causing in-band interference rather than in dealing with in-band interference once it has already been perceived by a receiver. These schemes either orthogonalize concurrent transmissions by allocating them disjoint resource blocks, or perform a channel-aware filtering prior to transmissions such that concurrent in-band signals are cancelled out at destination. Nevertheless, if in-band interference is not entirely cancelled out, or if the destination perceives unpredictable in-band interference, then in-band interference will be mostly ignored. By ignoring in-band interference we refer to the strategy which consists in simply treating in-band interference as adding to the noise floor [13, 73]. We refer in the remainder to such processing of in-band interference as *noisy strategy* ; it is a non conventional but explicit denomination, since interference is treated as pure noise.

Noise is in most cases a white and Gaussian source of perturbation, which is decorrelated with the signal. Techniques used to cope with noise are signal detection (estimation of original signal based on perceived signal), link adaptation and AMC to make the transmission reliable and robust, power control to set SNR value above a given threshold.

The noisy strategy is underlined and corroborated with common CQI metrics that use SINR instead of SNR - see Equation (2.9) - to represent the power of the sensed signal. In multi-user dense wireless networks, performance is mostly limited by interference rather than by noise. At SINR denominator, the contribution of interference is hence greater than the contribution of noise (INR $>$ 1). With this strategy is does not matter to know if transmissions are noise-limited or interference-limited, since in both cases the virtual noise variance is the same.

To be effective, the noisy strategy intuitively requires a high SINR, or at least that SINR $>$ 1. The higher SINR, the more robust the transmission. If interfering signals are treated as noise, then perceived power of interference should not be too high, to be able to detect easily wished signal among background noise and interference, and then successfully recover the original message. Consequently, the noisy strategy fits well to communication contexts which are weakly affected by interference. Nevertheless, in-band interference can be treated as pure noise, whatever interference power may be ; transmission reliability will just be severely reduced in case of very low SINR (strongly interfered scenarios).

2.4.3.2 Zero Forcing

Zero Forcing (ZF) techniques were first introduced as an equalizer whose principle seems quite obvious. Assuming that the channel response is known by the receiver, the original signal can be restored by applying to the received signal the inverse of the channel response. Ideally, the combination of channel and equalizer gives a flat frequency response and linear phase. In practice, ZF equalization suffers from some prejudicial restrictions (infinitely long impulse response, zeros cannot be inverted, some frequencies have worse channel response and hence low SINR which is made even worse after inversion). ZF equalizer is mainly designed to cope with inter-symbol interference (ISI) ; an analogous technique has been derived for MIMO communications, known as interference nuller or decorrelator [2].

Likewise, ZF precoding has been designed as the dual approach of ZF equalization [74, 75]. The channel matrix is assumed known at the transmitter (CSIT) which can shape its messages to prepare them for the channel they will encounter. Nevertheless, ZF techniques cannot be ideal with noise-limited scenarios, since noise will be amplified. Moreover, these techniques are very sensitive to the accuracy of channel estimation. A more balanced linear processing is thus the Minimum Mean-Square Error (MMSE) which minimizes the noise and interference power component in the received signal rather than cancelling interfering signal.

2.4.3.3 ML, MMSE Estimation, Sphere Decoder

In this section we briefly introduce alternatives to ZF techniques which are proved to be more effective :

- Maximum Likelihood (ML) and Minimum Mean-Square Error (MMSE) estimation
- Matched-filter or Maximal Ratio Combining (MRC)
- Sphere decoders
- MMSE Generalized Decision-Feedback Equalizer (MMSE-GDFE)

Basically, they consist in detecting the wished signal among the received signal by trying to minimize a given metric [2, 76–78]. In [79] the authors propose a scheme to deal with multi-user detection when there are more variables than observations (more transmitters than receivers).

2.4.3.4 Dirty Paper Coding

Dirty Paper Coding (DPC), originally developed by Costa [80], is a coding technique which shapes the signal with embedding the pre-subtracted interference [81, 82]. DPC assumes that interference is known to the transmitter (CSIT). Consequently, the transmitter can encode its information message while pre-subtracting interference. Thus, at reception, the effects of interference will disappear since the pre-subtracting interference and the perceived interference will cancel out each other. However, the high complexity in implementing DPC motivates the investigation of more practical linear precoding schemes. Furthermore, noise and non pre-subtracted sources of interference must always be treated by destination.

2.4.3.5 Successive Interference Cancellation

Successive Interference Cancellation (SIC) technique tries to filter out interference perceived by the receiver to recover among all jamming interfering signals the one that conveys wished information. A fundamental assumption of SIC is the ability of the destination to decode all neighbour signals. Decode interference does not mean that the destination can access to information conveyed by its interfering signals ; it is just a way for subtracting the contribution of interference in the overall sensed signal. Actually, source encoding and channel encoding are performed prior to transmission. SIC techniques assume that the destination can perform the suitable channel decoding scheme for any of its interfering signals. Nevertheless, integrity and privacy of information are ensured since the requested source decoding scheme is unknown.

Basically, the destination first decodes the strongest sensed signal, while all other signals are treated as noise. Second, this strongest message is subtracted to the received signal. Then, SIC algorithm resumes with the second strongest sensed signal, and so forth until the wished signal is decoded [2, 73, 83–86]. Nevertheless, SIC techniques suffer from some limiting drawbacks. First, SIC process is very sensitive to the decoding success : in case of erroneous decoding at a step of the process, all remainder steps suffer from the error propagation. Second, CSIR knowledge is assumed to let the destination decode interfering signals. Finally, implementation of SIC algorithm needs high complex tasks, especially to perform well. For instance, error-free decoding may be met with infinitely long capacity achieving codes.

SIC technique intuitively suits well to highly interfered communication contexts. Indeed, in such scenarios interfering signals may be sensed with a power higher than the sensed power of intended signal. If possible, it seems natural to decode first strongest signals, even if they are not wished, because decoding and subtracting them lets to decode more easily intended signal.

2.4.3.6 Beamforming

(Antenna) beamforming proposes to mitigate interference with help of directional signals (beams) in transmission and/or reception. Commonly, antennas are omnidirectional

and isotropic [87, 88]. Consequently, transmit power is uniformly spread in all spatial directions, while sensitivity of receive antennas is lowered by the jamming of both information and interfering perceived signals.

Beamforming techniques propose first to restrict the transmission beam (radiation angle), and thus to concentrate transmit power in a selective direction ; second to reduce antenna sensitivity to certain directions of arrival so as to avoid jamming of hostile transmissions. Figure 2.5 illustrates how beamforming associated with power control can reduce interference by concentrating the transmission in the region of interest. Assuming a beamwidth of 10 degrees and r^4 propagation (and many other simplifying assumptions), the area of interference is reduced by a factor of 4 with only power control ($\frac{\pi r^2}{\pi (r/2)^2}$), a factor of 6 with only beamforming (energy is concentrated in a beamwidth $\frac{10}{360}$ smaller, which stands for radius increase of $(\frac{360}{10})^{1/4}$), and an amazing factor of 144 with both together ($\frac{10}{360} \cdot \pi (r/2)^2$ compared to πr^2).

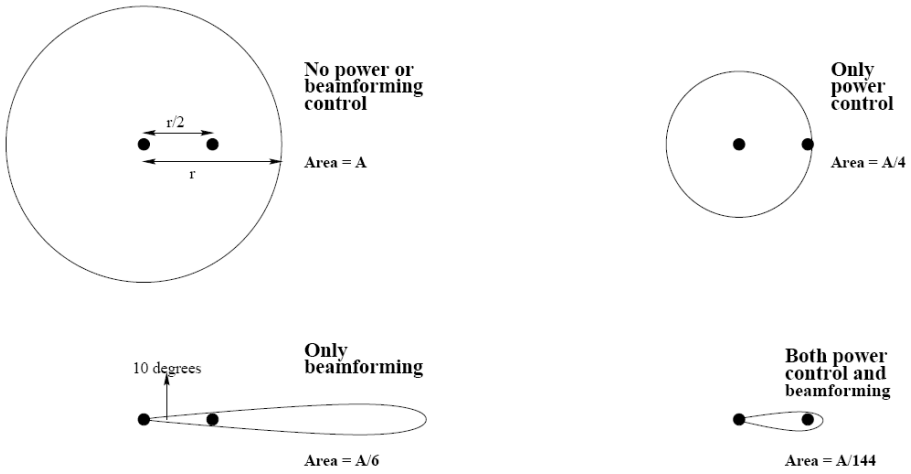

FIGURE 2.5 – Beamforing and Power Control.

Transmit and receive beamforming can define static or dynamic beams for antenna arrays. Based on communication conditions (mobility of devices, shadowing, reflection, diffraction, etc.), beams patterns can be adaptively aligned with the instantaneous direction of the expected signal so as to filter out interfering signals. Furthermore, different antenna beams can be defined on different chunks for increase diversify and selectivity of antenna arrays. More precisely, dynamic beamforming is performed by adaptive spatial signal processing (for instance matrix computation with eigenvectors) ; such performance is met without having to mechanically steer the array. Nevertheless, CSI and devices location knowledge is required to correctly direct and align transmit and receive beams.

2.4.3.7 Interference Alignment

Interference alignment is a kind of beamforming technique with specific signal filtering at transmitter and receiver. Each communication system has a limited amount of degrees of freedom (DOF). The basic idea of interference alignment is to separate at each destination the intended signal message from interfering signals by aligning them on two different eigenspaces which use each a part of DOF (half). Such signal alignment is achieved by channel-aware encoding and decoding filters. To achieve interference-free communications, the destination has then simply to restrict the decoding to the eigenspaces containing its

information message and 'sacrificeŠ the other eigenspace with interference [3, 4, 89, 90]. Nevertheless, interference alignment suffers from complex implementations and requires accurate CSI knowledge.

Separation of interference and information into two different spaces can be achieved in time, frequency, space and/or code domains. For instance, Figure 2.6a shows how interference alignment can make align on different directions the desired signal and all interfering signals. We show how channel matrix $\underline{\mathbf{H}}$ is exploited to meet such 'orthogonalization' : an orthogonal basis of beams has to be computed based on channel matrix. The intended signal is aligned on a given eigenspace while other concurrent neighbour signals are aligned on other eigenspaces On the other hand, Figure 2.6b illustrates a scenario where alignment is achieved in time domain by exploiting the propagation delay of each path : wished signal is on the even time slots and interference is on the odd time slots, the receiver has just to access channel each two slots.

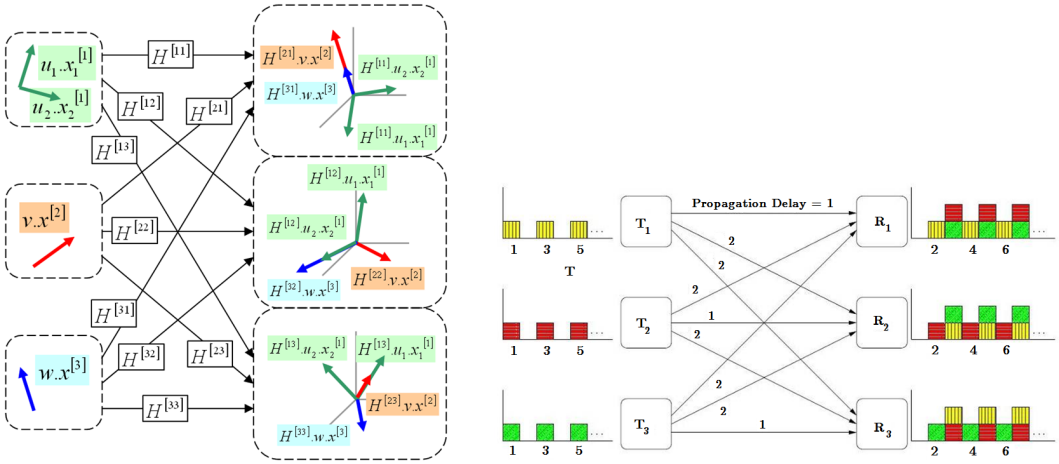

(a) Beamforming IA (b) Time IA

Figure 2.6 – Two illustrations of Interference Alignment (IA) techniques : beamforming with orthogonal eigenspaces (left) and time separation by exploiting propagation delay (right).

2.4.4 Channel Aware Power Control

Power control mechanisms are addressed in this section. In wireless communication networks subject to in-band interference, optimal transmit power allocation is a perfect illustration of the **game theory** concept. Game theory attempts to mathematically capture behaviour in strategic situations, or games, in which an individual's success in making choices depends on the choices of others. In our context, reliability is limited by in-band interference caused by neighbour concurrent transmitters. To enhance its reliability, a source tends to increase its transmit power such that it meets its QoS requirements, contingent on its momentary sensed communication context and interference state. The perceived level of interference is intrinsically related to the transmit power of interferers. Consequently, updating any transmit power changes the interference states perceived by all neighbour receivers.

Transmit power must be efficiently set, since power strongly impacts the overall sys-

tem. Basically, increasing transmit power lets the source extend its coverage and increase sensed signal power at the destination. Therefore, transmission between the source and its destination is made more reliable and robust to fading and shadowing events ; outage and dropped call probability are lowered, while a higher MCS can be set.

Nevertheless a higher transmit power cannot have just benefits. First, increasing power results in a higher power budget ; it is especially prejudicial to systems without power supply. Second, in-band interference is correspondingly enhanced. Consequently, performance is not necessarily better than with a lower transmit power. Actually, SINR should be considered instead of SNR.

To efficiently cope with in-band interference, selfish approaches where transmitters do not take into account of how much it affects its neighbours are not conceivable and sustainable. A joint and coordinated solution is highly advised to meet optimality. Moreover, the solution must rely on the momentary channel matrix $\underline{\mathbf{H}}$, system parameters and QoS constraints. Figure 2.5 can illustrate the main goal of optimal power allocation in interference-limited networks : there is no use serving users with extra QoS since it affects unnecessarily neighbour users.

Commonly, optimal power allocation is computed by solving (convex) optimization problems under constraints. Inputs of the objective function is the vector of transmit powers while constraints are characterized by QoS requirements. The objective function depends on the goals : for instance, minimizing power budget, maximizing the overall channel capacity, maximizing the transmission rate of the worse user, and so forth. We introduce below two examples of power allocation techniques.

2.4.4.1 Binary Power Allocation

Optimization of transmit power in all cells can become a hard and tedious task, especially in dense networks. An easy way to reduce computation time and complexity is to quantify transmit power with some accepted levels. The simplest quantification has a two-level granularity : source either remains silent (power is set to zero) or transmits at full-power. Such a binary power allocation has been introduced in [91, 92] and is denoted by 'On/Off power allocation'. Optimization problem is made relatively simple, even with numerous devices, since enumeration and check of all cases to find best solution is conceivable. Despite of its apparent lightness, [91, 92] prove binary power allocation achieves near optimal performance. This very simple technique can be easily improved with a finer quantification.

2.4.4.2 Water-Filling

The well-known water-filling principle will be developed later in Section 5.3.3. However, basis of this technique are detailed. Water-filling technique seeks to efficiently allocate a given power budget to all frequency bands without exceeding power limitation of each band. Water-filling power allocation can be explained with the following image : each band is represented as a hole, whose depth is inversely proportional to the CQI of the band. Then, power budget is represented as a water bowl which is poured out over holes. By free flowing between holes, water is spreading out on holes to reach a uniform level at surface of all holes. Such a way, the deeper a hole is, the most water the hole will contain. If the volume of water is not enough, shallow holes remain empty. This representation of power allocation issue is quite faithful. Indeed, each band has to be sensed to estimate its CQI :

more power will be allocated to better chunks. If quality of a chunk is too worse and does not exceed a given threshold, then this chunk will not be used for the current transmission.

2.5 Conclusions

Interference is a crucial issue in wireless communication networks, especially when the number of resource blocks available for transmission is much smaller than the number of concurrent active transmitters. This issue is even more complex in networks with demanding services where network operators must ensure their customers high QoS. Since the supply is smaller than demand, some resource blocks need to be shared by concurrent transmitters, which causes in-band interference.

Interference can severely reduces the robustness of a transmission. Indeed, transmission parameters, such as transmit power or MCS, are set in line with knowledge of the current channel instance, to ensure the target QoS requirements will be met in reception. Nevertheless, if the receiver must cope with unpredictable in-band interference, then the wished signal is perceived with a power lower than the one which was expected when transmission parameters were set. Consequently, the receiver might not be able to recover information from the received signal.

Different approaches can address the problem of interference so as to mitigate its prejudicial effects and so achieve the targeted QoS in reception. First, resource allocation techniques let define effective frequency planning. The main concept is to assign disjoint sets of sub-carriers to transmitters which strongly interferer each others, while a same sub-carrier can be shared by two transmitters which are sufficiently apart from each other so as not to affect mutually. Likewise, some destinations experience bad channel states and hardly succeed in achieving robust transmissions (*i.e.,* cell-edge users for instance because of remoteness with their sources). Some techniques propose to assign a small but exclusive set of sub-carriers to few users with worse CQI whereas other users are scheduled on the remainder sub-carriers. This way, different transmit powers can be set on each sub-carrier to meet a satisfaction rate for all users.

Second, information theory and signal processing propose challenging techniques, either to avoid or to cancel out interference. Assuming that the matrix of the channel is known by transmitter and/or receiver, specific filtering can be applied to signal. For instance, with CSIT, the transmitter can forecast the interference that the transmission will face ; so the transmitter can exploit this knowledge and shape its message to help the receiver in decoding the received signal more reliably. Other techniques propose to exploit the intrinsic nature of interference - interference is not like thermal noise since it carries information - to possibly decode it and then subtract its contribution from the perceived signal. Beamforming which sets specific antenna diagrams of radiation is another challenging solution.

Lastly, effective power control is undeniably promising since the perceived level of interference directly depends on the value of transmit powers. Power allocation for transmitters which share a common band is indeed an issue related to game theory. To lower interference as much as possible, power allocation must first be adapted to the momentary context of transmission and second, consider an objective function which quantifies how much a given transmit power value affects its neighbourhood (in terms of mutual information reductions).

Chapter 3

Cooperative Communications with Half-Duplex Relays

While two-hop cooperative transmissions may help destinations in achieving more robust and more reliable transmissions, they also generate at the same time additional in-band interference which make harder the decoding at destinations. Cooperative transmissions are so driven by a trade-off. The goal of this chapter is to deal with this trade-off by limiting inter-cell interference in two hops cooperative communication systems. We propose to exploit the standard half-duplex limitation of relays so as to coordinate in time and frequency the resource allocation of a cluster of neighbour cells. To this end, novel efficient inter-cell resource allocation patterns are proposed. Simulation results show how our proposed allocation patterns permit to outperform classical patterns in terms of cooperation effectiveness, power consumption and perceived QoS.

Moreover, we evaluate the performance of an ideal inter-sector resource allocation mechanism which adapts resource allocation to changes in the communication context. This adaptive process targets to maximize the global channel capacity for the given instantaneous channel instance and location of users.

The structure of the chapter is the following. First, we introduce our motivations, proposal and the work related to it. Then, we present in Section 3.2 the system model with its related assumptions which will be adopted along this chapter. Preliminary knowledge on cooperative communications is developed in Section 3.3. In Section 3.4, we successively detail the goals of our work, the resource allocation patterns we will evaluate in the remainder, our proposed adaptive resource allocation mechanism and simulation results. Finally, Section 3.5 proposes a generalization of our work to wider and more realistic systems, before to conclude with Section 3.6.

3.1 Introduction

The relay channel was introduced by van der Meulen in 1971 [93]. Nowadays, relay-aided cooperative transmissions are well-known in telecommunications systems [58, 94–96]. Relays in mobile radio concepts have been for a long time a niche product, mainly used as repeaters to fill coverage holes. Nevertheless, relays may serve other purposes, as shown hereafter.

3.1.1 Motivations

The mobile network operators' aim is to provide broadband services to its users in a cost efficient way. The nature of radio propagation gives a certain disadvantage to the cell-edge users in getting high data rate services. Increasing the density of base stations is one measure, but not the most cost efficient one. Relays are understood as a cost efficient measure to improve the individual user throughput at the cell-edge. The state of the art concepts consider a two-hop approach, where a base station communicates with a relay node, and the latter with the actual user terminal. The cell capacity is not increased in the current concepts, but the fairness between cell-edge and cell-centre users is clearly improved [58].

Benefits of cooperation are many-fold. First, higher redundancy and spatial diversity can be achieved at destination. Then, the transmission of a message from the source to the destination may be made more robust and reliable thanks to the relay. Besides, by combining signals coming from all paths, the probability of erroneous decoding can be lowered by the user terminal. Finally, since cooperative transmissions are multi-hop transmissions, the range of coverage is virtually extended by use of relay ; this profits especially to border-cell users which are commonly doubly penalized : they perceive a lower SNR from their source than cell-centre users but also a higher INR from neighbour sources.

In the literature, two-hop cooperative transmissions have been widely studied and several cooperative protocols have been proposed (Amplify-, Decode-, Compress-, Equalize-and-Forward, etc.). These protocols define how the relay processes the signals it just received before to forward them towards user terminals. However, performance of cooperative protocols may be limited by their design at relay. For instance, the well-known Amplify-and-Forward protocol consists in amplifying the power of the signal perceived by the relay and then in conveying this enhanced signal to the user terminal. By this way, the relay enhances the power of information as well as the power of noise and interference. To profit from benefits of each protocol without suffering from their drawbacks, hybrid protocols have been proposed.

Such hybrid protocols are even more interesting in interference-limited or noise-limited communications contexts. Indeed, interference mitigation becomes a more challenging issue because the addition of relays as active nodes of the network increases the global level of interference. Efficient interference mitigation must be adopted to prevent relays and destination from suffering from excessive and prejudicial interference.

Relays are commonly chosen to be half-duplex devices. A half-duplex device can either transmit or receive at a given time ; it cannot transmit and receive simultaneously. Consequently, transmission and reception phases are separated in time dimension with a half-duplex relay. This property suits well to our challenge of mitigating interference since the number of active transmitters is reduced when a relay is listening. By coordinating

efficiently neighbour transmissions between base stations and relay stations, effectiveness of cooperation could be increased. However, the main motivation for half-duplex device is other. A full-duplex device requests a duplication of RF circuits to be able to receive and transmit at the same time. This constraints enhances the complexity, the price, the power consumption but also the size of the device. Operators are not willing to adopt full-duplex relays for wide network deployments and propose instead cheaper half-duplex devices.

Consequently, the relay node can be an essential element of future mobile networks. Applying and combining interference mitigation techniques with the relay nodes will open up solutions for increased cell capacity combined with improved user throughput fairness.

3.1.2 Contributions

The novelty of this chapter is based on the patent [17] and two papers presented at the IFIP Wireless Days [15] and VTC2010-Spring [16] Conferences. This second paper was also invited in a workshop held in Darmstadt, Germany which dealt with interference management and cooperation strategies in communication networks. Lastly, the work introduced in this chapter has been done in the framework of the ICT project ROCKET [11]. The innovative contribution in this chapter is three-fold.

First, we propose and analyse novel resource allocation patterns exploiting two-hop cooperative transmissions with half-duplex relays. These patterns aim at dealing with the trade-off which states that destinations may on the one hand benefit from cooperative transmissions to enhance transmission robustness and reliability of good decoding, but on the other hand suffer from additional in-band interference, insofar as relays are additional transmitters which also share the scare transmission resource-blocks. Besides, performance of cooperative transmissions is constrained by some limitations due to the design of cooperative protocols. Consequently, we propose to reduce interference perceived by relays on the first hop of the relay path so as to improve effectiveness of cooperation and make cooperative transmission beneficial for destinations.

Second, by exploiting judiciously the half-duplex property of relays, resource-blocks are allocated to concurrent transmitters so as to meet higher spectral efficiency as well as lower power budget for transmission. Consequently, energy savings are achieved without affecting performance of transmissions in terms of channel capacity.

Third, an adaptive resource allocation mechanism is proposed to profit from time, frequency and space variations of the momentary communication context. This mechanism targets the maximization of the sum-rate for a cluster of neighbour cells which compete for the same resource blocks.

3.1.3 Related Works

Cooperative transmissions in wireless networks have been widely addressed in the literature for improving decoding reliability at receiver side, enhancing diversity, serving remote users or dealing with interference. Nevertheless, numerous techniques have been proposed under the pretence of 'cooperation', whereas they do not really target the same issue ; some distinctions should be made to differentiate cooperative techniques. Basically, the concept of 'cooperation' describes the idea that at least one node helps a 'transmitter-receiver' pair in improving some features of its transmission (reliability, rate, range of coverage, etc.). This additional node operates as an 'ally', either for the transmitter or for the receiver : we respectively speak about transmission cooperation and reception cooperation.

Some papers such as [97, 98] consider cooperation as a technique that exploits coordination between nodes. In cellular networks for instance, where bases stations are coordinated via a backhaul network, close base stations can share information intended to their users through this backhaul. Then, all base stations located within the vicinity of a given user transmit him its information data. Such a way base stations operate as a virtual MIMO system and hence may increase spatial diversity.

Nevertheless, cooperative techniques can also involve 'relay nodes' which are not coordinated with transmitters or receivers via a backhaul network. The relay operates in this case as a kind of repeater that forwards to the receiver a signal based on what it has just received from the transmitter. (We consider such cooperative communications.) Several cooperative protocols performed by the relay have been proposed and investigated in the literature. The most famous cooperative protocols are Amplify-and-Forwad (AF), Decode-and-Forward (DF), Compress-and-Forward (CF) and Equalize-and-Forward (EF) [99–106]. Furthermore, all these protocols can be derived into three families : orthogonal, non-orthogonal and slotted. There is thus a substantial number of cooperative protocols with each pros and contras. One of the most promising cooperative technique is to consider hybrid cooperation [8, 10, 50, 107] which consists in an adaptive selection of the protocol the best suited to the momentary communication context.

Cooperative communications can be of course addressed by the same issues as any other wireless communication. Thus, [108–110] propose for instance some power allocation strategies for optimizing an objective function under QoS constraints in cooperative networks. Interference management remains likewise a fundamental issue which is even more challenging in such networks. As stated by the authors in [111], there is a trade-off between the amount of cooperation and the amount of interference introduced into the network. In [112] for instance the authors investigate how cooperative communications can help in coping with inter-cell interference that drastically affects border-cell receivers. To this end they compare performance of cooperative communications to those obtained with a specific frequency reuse strategy. Interference mitigation issue is also addressed in [5] where the authors propose four interference avoidance strategies for cooperative networks, namely interference separation, interference alignment, interference suppression and interference neutralization.

Diversity-Multiplexing Trade-Off (DMT) is commonly used by Information Theory as a metric to determine which is the optimal performance that a scheme can achieve, either in terms of diversity or in terms of multiplexing gain. Since cooperative networks may be seen as virtual MIMO networks where both diversity and amount of degrees of freedom are enhanced, the known results on DMT should be extended to cooperative networks [82, 113–118].

3.2 System Model and Assumptions

This section describes the system model with some related assumptions adopted in the remainder of the chapter. We first introduce our two-hop half-duplex relay channel to define some notations. Then, we present the global system model associated with an OFDMA-based cellular cooperative network.

3.2.1 The Two-Hop Half-Duplex Relay Channel

A two-hop relay channel consists in a system with three nodes, namely a source s_i, a relay r_i and a destination d_i. The relay is here a node which aims at helping the source s_i in transmitting reliably its messages x_{d_i} to the destination d_i. The destination can receive the message x_{d_i} sent by the source s_i from two different paths : either the *direct path* from s_i directly to d_i, or the *relay path* from s_i to d_i passing by r_i. Such a system is named a 'two-hop relay channel' since the message x_{d_i} is conveyed by two channels along the relay path - first the channel from s_i to r_i an then the channel from r_i to d_i. The two-hop relay channel is the simplest derivation of the multi-hop relay channel where $n-1$ sequential (consecutive) relays are involved in the relay path which is hence characterized by n hops [117, 118]. Let us note that possibly no message may be conveyed through the direct path in such networks. Indeed, cooperative communications can be employed to reach remote or hidden users, as an alternative as direct transmissions with high transmit power (due to path loss attenuation, the bigger the distance between source and destination, the higher the transmit power). Consequently s_i and d_i may be out of communication range and then just the relay path can ensure the reliability of the transmission.

We express hereafter our assumptions which will be relevant in the remainder of this chapter. First, we assume that both direct and relay paths are effective ; cooperative communications are hence investigated as a way to 'boost' reliability and robustness of transmission. Second, relays are assumed to operate in *half-duplex per chunk mode*. As it was explained in the motivations section above, an half-duplex device cannot simultaneously transmit and receive. Nevertheless, with some specific RF adjustments, the half-duplex property can be made independent between chunks. In other words, if the spectral spacing between two consecutive chunks is high enough, then RF filters associated to each chunk do not overlap and we can restrict the half-duplex property to a given chunk. Hence a half-duplex per chunk relay cannot transmit and receive at the same time on the same chunk but it can transmit on a chunk while it is listening on another chunk. Third, we consider a network where all nodes are equipped with only one antenna (no MIMO techniques). The reader will understand that this assumption is consistent with the half-duplex assumption made for the relay since half-duplex devices do not require one transmit antenna and one receive antenna but use in turns their single antenna. Finally, we besides assume that the whole system disposes of a maximum of N_{SC} sub-carriers which are shared between all transmitters (sources and relays). Thus receivers (relays and destinations) can be possibly affected by in-band interference.

Adopted notations for the two-hop relay channel are specified below. We assume that transmitters could communicate over N_{SC} sub-carriers. Prior to any transmission, a scheduler is in charge to allocate to each transmitter a set of sub-carriers chosen among the N_{SC} available sub-carriers. Given its set of sub-carriers, a transmitter can choose to use either all or only a part of them. To refer to a specific sub-carrier with index k, we will precise for all system and channel parameters this index k in exponent between brackets. Source s_i and relay r_i transmit respectively with powers $P_{s_i}^{(k)}$ and $P_{r_i}^{(k)}$ on chunk k. Channels between s_i and d_j, r_i and d_j, s_i and r_j are respectively characterized by channel coefficients $f_{i,j}^{(k)}$, $g_{i,j}^{(k)}$ and $h_{i,j}^{(k)}$, on chunk k. These coefficients represent the channel gain, including fading, shadowing and path loss attenuation. They remain constant during at least one frame transmission (quasi-static channels). Fading follows a Rayleigh distribution with unitary expectation. Log-normal shadowing is generated using the method described in [57]. Path

loss model is the one of Okumura-Hata (see Section 2.2.2) with

$$L_{\mathrm{dB}} = L_0 + \beta \cdot \log_{10} d \tag{3.1}$$

in dB, where d [km] is the distance between the transmitter and the receiver. Transmitters are assumed to have perfect knowledge of all channel gains.

For sake of clarity, we assume in the remainder that the notations of sub-carriers and chunks coincide, *i.e.,* all system and channel parameters denoted with k refer to the chunk with index k. It does not mean that the channel is not frequency-selective within the range of a chunk ; we just want to avoid complicating expressions with summations.

A schematic illustration of the two-hop relay channel is given on Figure 3.1a. Receivers d_i and r_i are respectively affected by both AWGN noise with variance $\sigma^2_{d_i}$ and $\sigma^2_{r_i}$, and by in-band interference I_i and J_i.

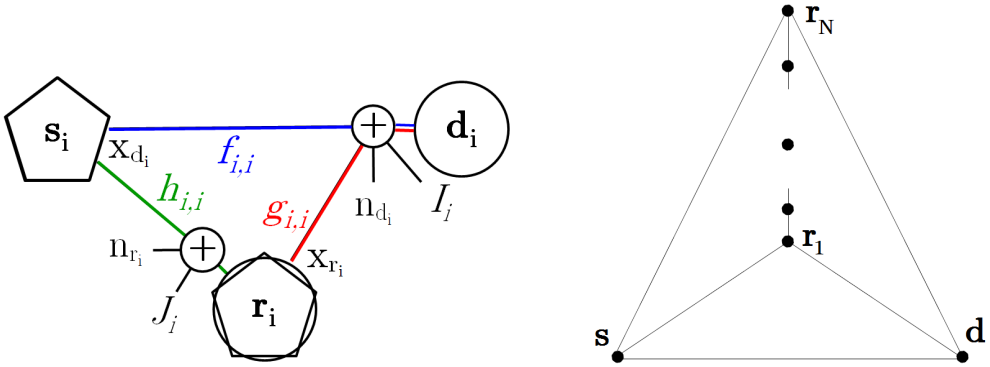

(a) The two-hop relay channel (b) Two-hop relay network

FIGURE 3.1 – Two-hop relay network with relays serving a source s and a destination d.

Basically, the two-hop relay channel is described as follows :

$$\begin{cases} y^{(k)}_{d_i,1} = f^{(k)}_{i,i} \cdot x^{(k)}_{d_i} + n_{d_i} + I^{(k)}_{i,1} \\ y^{(k)}_{r_i} = h^{(k)}_{i,i} \cdot x^{(k)}_{d_i} + n_{r_i} + J^{(k)}_i \\ y^{(k)}_{d_i,2} = g^{(k)}_{i,i} \cdot x^{(k)}_{r_i} + n_{d_i} + I^{(k)}_{i,2} \\ y^{(k)}_i = y^{(k)}_{d_i,1} + y^{(k)}_{d_i,2} \\ x^{(k)}_{r_i} = \Phi(y^{(k)}_{r_i}). \end{cases} \tag{3.2}$$

where $y^{(k)}_{d_i,1}$ and $y^{(k)}_{d_i,2}$ are the messages sensed at d_i which respectively pass through the direct path and through the relay path. The message $x^{(k)}_{r_i}$ sent by the relay r_i is based on the signal $y^{(k)}_{r_i}$ the relay r_i previously received ; the function Φ depends on the cooperative protocol performed by r_i (see Section 3.3). In our system relays perform either Amplify-and-Forward (AF) or Decode-and-Forward (DF) cooperative protocols, since these protocols are commonly adopted by almost all cooperative systems. A matrix form can be derived from (3.2) as

$$\underline{Y} = \mathbf{H} \cdot \underline{X} + \underline{n}, \tag{3.3}$$

where $\underline{Y}$, $\mathbf{H}$, $\underline{X}$ and $\underline{n}$ respectively refer to the vector with all signals received at destination, the matrix of the channel, the vector with all messages sent by the source and the vector with all perturbations. This is a general matrix form which will be clarified in Section 3.3.2.

3.2.2 The Global System Model

We focus on the downlink mode in an OFDMA-based cellular network aided by half-duplex per chunk relays. The considered system is shown on Figure 3.2 and accounts for tri-sectorized cells of radius r_{cell}. Three adjacent and neighbour sectors are represented with each a fixed base station and a fixed relay. We assume there is just one active and mobile user equipment per sector. This assumption is consistent in case of OFDMA techniques : there are enough chunks to achieve an orthogonal resource allocation between users of a given sector and hence avoid intra-cell interference. Consequently, all active users in a sector are made independent and can be considered separately. Furthermore, all relays have the same location relative to their sector : they are placed at $\frac{2}{3} \cdot r_{\text{cell}}$ from their base station, on the symmetry axis of the sector. In practice, a relay is not necessarily a fixed device exclusively devoted to the cause of its source and destination ; any entity of the system can play the role of the relay if it is located close to the source or to the destination. Commonly, a controller is in charge to select the optimal relay when cooperative communications are performed. This step does not concern us here since we consider fixed and devoted relay stations. Relay deployment has been investigated to determine the optimal location of relay according to the model of path loss attenuation. For sake of simplicity, we finally chose to place relays at two thirds of r_{cell} from their base station since it was intuitively a good trade-off.

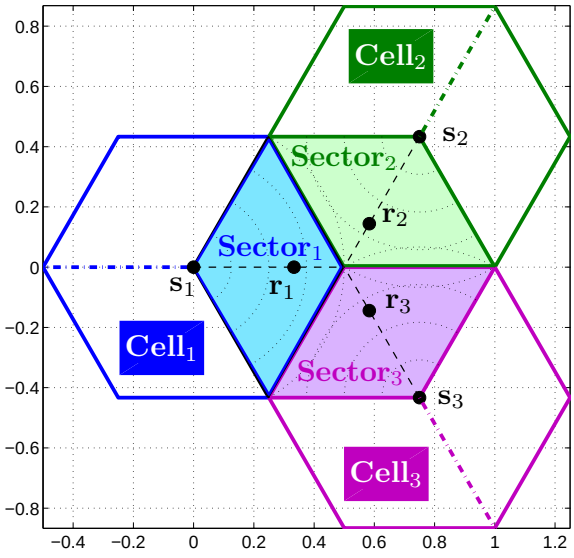

Figure 3.2 – System model with three adjacent sectors, each with a fixed relay r_i placed at two-thirds of r_{cell} from its base station s_i.

In relation with the previous section, s_i, r_i and d_i respectively refer to the base station, the relay station and the active user equipment of Sector i. The notation S_i refers to Sector i for shortness. In-band interference marked with I_i and J_i on Figure 3.1a actually stands for inter-sector interference. Destination d_i can be interfered by all simultaneous transmissions occurring on a same chunk. Hence I_i and J_i are caused by transmissions of neighbour sources and relays.

To conclude with this section, we introduce last assumptions. First, we assume that only two chunks are allocated to the three adjacent and neighbour sectors shown on Figure 3.2 which have then to share them. There is hence no way for sectors to achieve an

orthogonal resource allocation and destinations are necessarily affected by in-band inter-sector interference. But this is precisely the matter of our work, since we want to investigate the trade-off between the benefits brought by planning cooperation and the drawbacks in terms of interference caused by the activation of relays. Second, as it is commonly the case in cellular network, base stations are coordinated via a backhaul network that lets them share CSI knowledge of their sector, coordinate their resource allocation or synchronize the transmissions. Third, no coding is considering for transmissions in this chapter ; we assume that a capacity achieving code is used by physical layer. Consequently, performance of different approaches will be evaluated and compared by use of the amount of mutual information. We finally consider that each transmitter is constrained by a maximal transmit power it cannot exceed. This limit is imposed per chunk and per sector and is denoted respectively by $P_{s_i,\max}$ and $P_{r_i,\max}$ for the source s_i and the relay r_i.

3.3 Preliminary on Cooperative Communications

As it was previously cited in Section 3.1.3, two slightly different approaches are generally associated with the concept of cooperative communications in the literature. First, 'cooperation' can be a specific application of 'coordination'. Transmitters and/or receivers are coordinated via a secondary network (like a backhaul network) and share information to improve robustness and reliability of their transmissions. The system can be then thought of as a virtual MIMO system with cooperative coding between the delocalised transmit antennas and/or cooperative decoding between the delocalised receive antennas [97, 98]. Indeed transmit (respectively receive) antennas are not physically localised at a same place but due to cooperation between transmitters ((respectively receivers), they can be virtually seen as being localised at a single macro virtual transmitter (respectively receivers) which is then equipped with the sum of all transmit (respectively receive) antennas. We do not focus on this first consideration for cooperative communications.

Second, cooperative transmissions can involve a transmission-aiding node which is commonly named 'relay'. This relay helps the source in transmitting its message towards its destination by acting as a repeater. In a first step the source broadcasts its message aimed at the destination and the relay. In a second step the relay forwards to the destination a processing copy of the message it has just received during the first step. Commonly, the relay first listens to the source and then transmits towards the destination. The half-duplex property fits hence especially well to cooperative transmissions. We are interested in this viewpoint of cooperative transmissions and develop preliminary knowledge in the remainder of this section.

3.3.1 Cooperative Transmissions'Goals

Some elements of relay-aided cooperative transmissions have already been introduced in Sections 3.1.3 and 3.2.1, especially with the two-hop relay channel shown on Figure 3.1a. Goals targeted by relay-aided cooperative transmissions are three-fold. First, the receiver may enjoy higher spatial diversity as well as redundancy, since the same information is conveyed by different independent paths that encounter different communication contexts. More than one relay can help the source in transmitting its message to the source, as shown on Figure 3.1b. The receiver has then just to combine each contribution it just received by use of MRC techniques for instance. Second, coverage extension can be achieved since the relay acts as a hotspot or a repeater that forwards the message of the source to remote

destinations which may be out of reach of their source. As we said in Section 3.2.1, the direct path between the source and the destination is not necessarily effective. Source and destination may be either too far apart to communicate reliably, or hidden from each other by a building for instance ; a deep fade event could also make momentarily any communication unreliable. Multi-hop relay channel let to considerably extend coverage range of the source. Third, transmission robustness and decoding reliability are potentially enhanced since a higher SINR can be met at destination. On the one hand, the probability of erroneous decoding shrinks by efficiently combining all contributions of redundant messages ; on the other hand the information signal is perceived with a higher power if a relay station placed between the source and the destination acts as a repeater.

3.3.2 State of the Art on Cooperative Protocols

In this section we propose to draw up a state of the art dealing with the main cooperative protocols that relay stations can perform. A cooperative transmission consists in two steps (see Equation (3.2)). The first one is the listening step during which the relay listens to the signal x_{d_i} broadcasted by the source. The second one is the forwarding step during which the relay transmits towards the destination a message x_{r_i} based on the signal y_{r_i} it perceived from the source. This message x_{r_i} is defined in line with the cooperative protocol adopted by the relay. Four protocols are commonly proposed in the literature, namely Amplify-and-Forward (AF), Decode-and-Forward (DF), Compress-and-Forward (CF) and Equalize-and-Forward (EF). Hybrid protocols are also proposed ; they try to mix advantages of all protocols while avoiding their drawbacks. Finally, all these protocols may be derived in at least three families of protocols characterized by the way with which the listening step and the forwarding step follow on ; there are thus orthogonal protocols, non-orthogonal protocols and slotted protocols. Some elements concerning all these protocols are given hereafter. But we encourage the reader to refer to papers [8, 10, 50, 107, 113] for more details, especially to Yong et al. [10] for computation of mutual information amount.

3.3.2.1 Orthogonal, Non-Orthogonal and Slotted Protocols

A protocol is said 'orthogonal' when the listening step and the broadcasting step are separated, either in time domain or in frequency domain. Up to now and especially with Equation (3.2), we dealt with orthogonal protocols since we implicitly assumed that the source transmitted its message x_{d_i} during a first time slot, while both destination and relay listened to it, and then during a second time slot the source remained silent while the relay forwarded the message to the destination. Consequently the source transmits each two time slots.

However, the source could transmit a message at each time slot. With orthogonal protocols the relay would be hence unable to listen and then to forward all messages since two time slots are required per message from the source. To cope with such a limitation, the two-hop relay network illustrated on Figure 3.1b could be considered. Here N relays are involved instead of just one. Two other families of protocols, namely 'non-orthogonal' and 'slotted' protocols have been proposed ; they are characterized by their frame structure and their relaying procedure. Figures 3.3a and 3.3a respectively describe the frame structure for non-orthogonal and slotted protocols. In case of a single relay ($N = 1$), non-orthogonal and slotted protocols are equivalent. Further details can be found in [8, 10, 50, 107, 113].

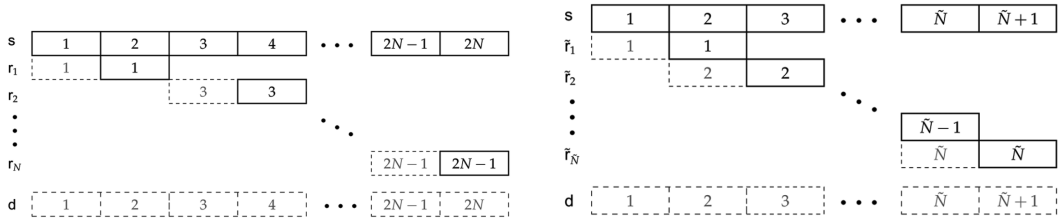

(a) Non-orthogonal protocol (b) Slotted protocol

FIGURE 3.3 – Frame structure and relaying procedure of (a) non-orthogonal and (b) slotted protocols, solid box for transmitted signal and dashed box for received signal.

3.3.2.2 Amplify-and-Forward

The Amplify-and-Forward cooperative protocol describes exactly what a repeater does, *i.e.,* the relay simply amplifies the signal y_{r_i} it listened by a amplification gain G_{AF} and then forwards it to the destination. In other words, we have the following condition :

$$x_{r_i} = G_{\mathrm{AF}} \cdot y_{r_i}. \tag{3.4}$$

Commonly, the amplification gain is defined so that the power of the signal sent by the relay does not exceed the power limitation :

$$\left\{ \begin{array}{ll} & \mathbb{E}\{|x_{r_i}|^2\} \leq P_{r_i,\max} \\ \Leftrightarrow & (G_{\mathrm{AF}})^2 \leq \frac{P_{r_i,\max}}{|h_{i,i}|^2 \cdot \mathbb{E}\{|x_{d_i}|^2\} + \sigma_{r_i}^2 + \mathbb{E}\{|J_i|^2\}}. \end{array} \right. \tag{3.5}$$

Advanced reasoning can be used to define the amplification gain. In [119] for instance the authors compute the optimal gain matrix for an AF MIMO relay which optimizes the instantaneous rate for a given uniform power allocation at the source.

The matrix form in (3.3) can be expressed for AF protocols as

$$\begin{pmatrix} y_{d_i,1} \\ y_{d_i,2} \end{pmatrix} = \begin{pmatrix} f_{i,i} \\ g_{i,i} G_{\mathrm{AF}} h_{i,i} \end{pmatrix} \cdot x_{d_i} + \begin{pmatrix} 1 & 0 & 0 \\ 0 & g_{i,i} G_{\mathrm{AF}} & 1 \end{pmatrix} \cdot \begin{pmatrix} n_{d_i} + I_{i,1} \\ n_{r_i} + J_i \\ n_{d_i} + I_{i,2} \end{pmatrix}. \tag{3.6}$$

This matrix form describes the Orthogonal-Amplify-and-Forward (OAF). In case of non-orthogonal (or slotted) protocol, the matrix form of NAF is

$$\begin{pmatrix} y_{d_i,1} \\ y_{d_i,2} \end{pmatrix} = \begin{pmatrix} f_{i,i} & 0 \\ g_{i,i} G_{\mathrm{AF}} h_{i,i} & f_{i,i} \end{pmatrix} \cdot \begin{pmatrix} x_{d_i,1} \\ x_{d_i,2} \end{pmatrix} + \begin{pmatrix} 1 & 0 & 0 \\ 0 & g_{i,i} G_{\mathrm{AF}} & 1 \end{pmatrix} \cdot \begin{pmatrix} n_{d_i} + I_{i,1} \\ n_{r_i} + J_i \\ n_{d_i} + I_{i,2} \end{pmatrix}. \tag{3.7}$$

The total amount of mutual information is given by

$$\mathscr{I} = \frac{1}{2} \log_2 \det(\underline{\mathbf{I_2}} + \underline{\mathbf{H}} \underline{\mathbf{Q}} \underline{\mathbf{H}}^\dagger), \tag{3.8}$$

where $\underline{\mathbf{H}}^\dagger$ is the conjugate transposition of $\underline{\mathbf{H}}$ and $\underline{\mathbf{Q}}$ is the covariance matrix of the signal $\underline{X}$. The factor $\frac{1}{2}$ comes from the half use of channel, since two time slots are required for

one relayed message. This expression can be expressed more precisely for OAF protocol by considering (3.5) with equality and by ignoring in-band interference I_i and J_i :

$$\mathscr{I}_{\text{OAF}} = \frac{1}{2}\log_2\left(1 + \text{SNR}_{\text{dp}} + \frac{\text{SNR}_{\text{rp1}}\text{SNR}_{\text{rp2}}}{1 + \text{SNR}_{\text{rp1}} + \text{SNR}_{\text{rp2}}}\right), \tag{3.9}$$

where $\text{SNR}_{\text{dp}} = |f_{i,i}|^2 \cdot \frac{P_{s_i}}{\sigma^2_{s_i}}$, $\text{SNR}_{\text{rp1}} = |h_{i,i}|^2 \cdot \frac{P_{s_i}}{\sigma^2_{r_i}}$ and $\text{SNR}_{\text{rp2}} = |g_{i,i}|^2 \cdot \frac{P_{r_i}}{\sigma^2_{s_i}}$ are respectively the SNR of the direct path, the first hop of the relay path and the second hop of the relay path.

Amplify-and-Forward protocol works quite well, expect when the relay encounters a bad communication context along the first hop of the relay path. One of its major drawbacks is clearly stated with (3.4) or (3.5) : noise and interference perceived by the relay are also amplified before being forwarded towards the destination. Intuitively, if the SINR sensed by the relay is low, then the message forwarded by the relay to the destination mostly conveys noise and interference instead of information.

3.3.2.3 Decode-and-Forward

With Decode-and-Forward cooperative protocol the processing performed by the relay is more complex than the one done in case of Amplify-and-Forward protocol. Here the relay first decodes the signal y_{r_i} it just received to recover the message x_{d_i} from the source. Then the relay re-encodes the message x_{d_i} and forwards it to the destination. We hence have

$$x_{r_i} = x_{d_i}. \tag{3.10}$$

The matrix form of Orthogonal-Decode-and-Forward (ODF) protocols is expressed as

$$\begin{pmatrix} y_{d_i,1} \\ y_{d_i,2} \end{pmatrix} = \begin{pmatrix} f_{i,i} \\ a \cdot g_{i,i} \end{pmatrix} \cdot x_{d_i} + \begin{pmatrix} n_{d_i} + I_{i,1} \\ n_{d_i} + I_{i,2} \end{pmatrix}, \quad \text{with } a = \sqrt{\frac{P_{r_i}}{P_{s_i}}}. \tag{3.11}$$

We note that the channel gain $h_{i,i}$ denoting the channel from s_i to r_i does not affect the received signal at destination since the relay decodes the message conveyed on the first hop of the relay channel.

The total amount of mutual information for ODF protocol, in absence of in-band interference I_i and J_i is given by

$$\mathscr{I}_{\text{ODF}} = \frac{1}{2}\min\left\{\log_2(1 + \text{SNR}_{\text{rp1}}), \log_2(1 + \text{SNR}_{\text{dp}} + \text{SNR}_{\text{rp2}})\right\}, \tag{3.12}$$

where SNR_{dp}, SNR_{rp1} and SNR_{rp2} have already been defined in Section 3.3.2.2. This expression seems surprising because only the second term of the min is expected, but the min form actually translates the fact that the first hop of the relay path can be limiting : if the relay does not manage to recover the message x_{d_i} of the source, then the relay cannot transmit a reliable message towards the destination.

Decode-and-Forward protocol is more complex than Amplify-and-Forward but cancels out noise and in-band interference perceived by the relay before forwarding the message to the destination. Nevertheless DF protocols suffer also from some drawbacks. First of all, the relay must know the codebook of the source to be able to recover x_{d_i} from its received signal y_{r_i}. Second, there is propagation of the error towards the source if the relay erroneously decodes the signal y_{r_i} and still forwards its message x_{r_i}. Third, soft information about reliability of transmission (Log-Likelihood Ratio - LLR) is lost. Such soft information is especially interesting in distributed turbo coding techniques (see Section 3.3.4).

3.3.2.4 Compress, Equalize and Hybrid Protocols

Compress-and-Forward and Equalize-and-Forward protocols are less used in the literature and we do not implement such protocols in our investigation. However we give some details on how they perform. The principle of Compress-and-Forward, as cited in [106], is that the relay quantizes the signal y_{r_i} it received from the source and encodes the samples into a new packet which is forwarded to the destination.

In case of Equalize-and-Forward, the relay performs linear MMSE equalization with a specific filter $\underline{\mathbf{G}}$ before forwarding its signal x_{r_i}. In [105] the filter $\underline{\mathbf{G}}$ is chosen to minimize the MSE between the source and the relay output. Thus, the goal of the equalizer at the relay is chosen will be to mitigate in-band interference introduced on the first hop of the relay path.

Hybrid cooperative protocols consist in an adaptive selection of the best suited protocol to the momentary communication context. In most papers only AF and DF protocols are considered. The basic idea is to conciliate advantages of cooperative communications without suffering from their drawbacks [8, 10, 50, 107]. In some communication contexts, transmissions over the first hop of relay path cannot support the target rate ; the channel is in outage. In such scenarios it is better not to plan cooperation since the relayed message will be not reliable and will not help the destination in decoding the original message x_{d_i}. On the other hand, in other communication contexts cooperative communications greatly increase the amount of mutual information in comparison to non-cooperative communications ; cooperation should then be planed to enhance decoding reliability at destination. Consequently, hybrid protocols switch between different protocols to always select the strategy which will maximize the amount of mutual information at the destination.

3.3.3 Cooperative Trade-Off : Robustness vs. Interference

Hybrid protocols state the trade-off leading performance of cooperative communications. On the one hand, the planning of cooperation may increase redundancy and spatial diversity at destination, which results in higher transmission robustness and hence higher decoding reliability at destination. It is precisely the scope of cooperative communications that aim at helping source in transmitting reliably its message to its destination. To this end cooperation lets create a 'relay zone' where the amount of mutual information is enhanced in the vicinity of the relay station. On the other hand, cooperative protocols performed by relay stations suffer from some drawbacks which should be carefully considered to avoid that the planning of cooperation affects more the destination than it helps in attempting to decode the message x_{d_i} from the source.

Let us now consider interference-limited or noise-limited communication contexts where cooperation is initially planed to achieve more robust transmissions towards the destination. Nevertheless, in such bad scenarios the drawbacks of cooperative communications are two-fold. First, from a selfish viewpoint restricted to the two-hop relay channel of Figure 3.1a, we have seen that the signal $y_{d_i,2}$ received by the destination from the relay could be not reliable because of the processing of AF and DF protocols. Indeed, AF protocol amplifies the information part of the signal y_{r_i} as well as its additional noise and interference, which are particularly prejudicial in interference-limited or noise-limited scenarios. Likewise, DF protocol may forward an erroneous message x_{r_i} if the relay does not success in recovering without error the original message x_{d_i}. Second, from a global viewpoint that takes all entities of the network into account (see for instance Figure 3.2), the issue

of in-band interference is emphasized and made even more difficult. Indeed sources and destinations devices have to share scarce communication resources, which causes in-band interference. By planning cooperation, new concurrent devices (*i.e.,* the relays) are added into the party while no additional resources are added ; hence it is even more challenging to allocate resources since the amount of in-band interference in the network increases.

There is consequently a trade-off between the amount of cooperation to plan in the network and the amount of interference caused by the recourse to cooperation. This trade-off was previously discussed in [111] where the authors try to design optimal relay zones in sensor networks to maximize the network sum-rate. As suggested by hybrid cooperative protocols that plan parsimoniously cooperation, we should wonder if the benefits brought by the planning of cooperation outperforms its detrimental effects in terms of additional in-band interference. We propose to investigate this trade-off in this chapter by comparing different patterns of resource allocation.

3.3.4 Distributed Coding Techniques

In this last preliminary section we quickly introduce the concept of distributed coding techniques. We do not consider such a technique in our work since no coding consideration were made ; we assume indeed capacity achieving coding and hence work with the amount of mutual information.. Nevertheless distributed coding techniques could be an interesting extension for further works.

The concept is to use cooperative transmissions jointly with coding techniques to improve robustness and meet higher reliability during the decoding process at destination. The most famous proposal is known as Distributed Turbo Codes (DTC) [120, 121]. Turbo-encoding is one of the most robust encoding for faded channels and consists in two convolutional coders and one interleaver at the input of one of the two convolutional encoders. Two convolutional codes are generated and then combined before to be transmitted.

The idea of DTC is to build a virtual turbo-coder with help of the relay. The source outputs one of the two convolutional codes. The relay receives this convolutional code and then interleaves it before to forward it ; the relay hence represents the second convolutional coder. These two convolutional codes are conveyed respectively by the direct and the relay paths. The destination combines these two codes and tries to decode them as if they were output by a turbo-coder. Such techniques are proved to be highly robust and to achieve a high order of diversity.

3.4 Radio Resource Management for Interference Mitigation

This section addresses the problem of inter-cell interference in cooperative communication systems and investigates the trade-off that links the benefits of cooperative communications to the additional interference they cause. First, we propose to exploit the standard half-duplex limitation to relays to coordinate in time and frequency domains the resource allocation of a cluster of adjacent neighbour sectors. Second, we propose to adapt the allocation of resources to variations in the communication context, so as to deal efficiently with the momentary interference state. Lastly, simulation results show how our proposed allocation patterns permit to outperform classical patterns in terms of cooperation effectiveness, power consumption and perceived QoS.

3.4.1 Cooperative Communication Paradigm

Cooperative communications are potentially highly beneficial for the destination in terms of both transmission robustness and decoding reliability, but cooperative transmission especially required a good communication context for the first hop of the relay path. Otherwise the planning of cooperation is not judicious since it could affect the destination more than it helps. If we manage to make this first hop more robust and less sensitive to changes of the communication context, it then will help in increasing the effectiveness of cooperation.

Meanwhile we assume half-duplex per chunk (HDPC) relays. With such devices the half-duplex property is made independent on each chunk : a relay can transmit on a band while it is listening on another. We recall that our system model described in Section 3.2.2 counts two chunks sharing by three adjacent and neighbour sectors. In each sector a fixed half-duplex relay can be activated or not, depending on how coordinated base stations decide to schedule and assign the resources. This half-duplex per chunk assumption seems greatly advantage the relay in comparison to a standard half-duplex relay which just transmit over one chunk. Intuitively, performance of HDPC relays in terms of mutual information amount will be of course outperforms those of a standard half-duplex relay which only disposes of one chunk. Nevertheless, additional in-band inter-sector interference is generated because of this HDPC assumptions in comparison to a standard half-duplex relay. Hence, despite appearances our HDPC assumption is not necessarily as good as it appears to be. Furthermore, to be fair in our comparison, we also investigate as baseline performance of a standard half-duplex relay which would dispose of both chunks to communicate.

To deal with the so called 'cooperative trade-off', we propose to exploit the HDPC property of relays in order to protect relays from being prejudicially affected by inter-sector interference. We aim at limiting interference perceived by relays to make the first hop of relay paths more reliable and hence enhance effectiveness of cooperative communications. To this end, we propose to coordinate between the three sectors the allocation of resources intended to each base station and each relay. We then introduce and evaluate different patterns of resource allocation which will let us deal with the cooperative trade-off.

3.4.2 Description of Resource Allocation Patterns

In preamble of this section we detail few elements concerning the way with which resources are allocated between sectors. First, no advanced power control technique is performed by sectors ; they do not attempt to optimize their transmit power. Sectors simply perform an 'On-Off' power allocation to define transmit power of sources and relays. Actually, sources and relays either do not transmit ('Off'), or transmit respectively with full power $P_{s_i,\max}$ and $P_{r_i,\max}$ ('On'). This principle is introduced in [9] and is shown to be near optimal. It was however not introduced for cooperative communications.

Second, each of the three relays can be independently active or remain silent for the current transmission instant. Since each relay has to possible states ('On' or 'Off'), $3^2 = 9$ different configurations are possible. We refer to the configuration of relays by 'cooperation planning' ; in other words a given plan of cooperation defines which sector has chosen to recourse to cooperative communications or not. For sake of clarity, we adopt the following notations. Each plan of cooperation is labelled with three letters. First, second and third letters respectively refer to the first sector S_1, the second sector S_2 and the third sector S_3. If sector S_i plans cooperation, then the i-th letter is equal to 'C' (cooperation), else

it is 'N' (no cooperation). For instance, the cooperation plan 'CNC' means that relays r_1 and r_3 are used for the current transmissions while r_2 has not been activated.

Third, resource allocation and cooperation planning is coordinated and lead by the three sectors. To this end we assumed that base stations are coordinated via a backhaul network. Base stations can then share their CQI knowledge to jointly decide how time and frequency resources will be allocated and relays activated. Such decisions are scheduled periodically by base stations. In the remainder of the chapter, a 'resource allocation pattern' will refer to a specific plan of cooperation and a specific allocation of time and frequency resources between the three sectors of the system.

Three families of resource allocation patterns are introduced, described and then compared by simulations result. Each of these three families is characterized by a specific policy for allocating time and frequency resources to the different transmitters of the system. An equal number of resource allocation patterns is gathered in each family ; there are as many resource allocation patterns as different cooperation plans, *i.e.,* nine resource allocation patterns per family. The three families are namely *Classic 1*, *Classic 2* and *Advanced* ; the respective abbreviations '*C1*', '*C2*' and '*A*' will be used sometimes for shortness. To refer to a particular allocation pattern within a given family, we combine with the three-letter notation previously introduced the short name of the family in index. The resource allocation pattern CNN_A, for instance, is the allocation pattern of the *Advanced* family where r_1 is the single active relay.

Each family has particular rules to assign resources. These rules are lead by a QoS policy that either advocates fairness between sectors, or favours one particular sector. We assume in the remainder that the first sector S_1 is the advantaged sector but by symmetry, any other combination is straightforward. Families *Classic 1* and *Classic 2* are both designed for classic half-duplex relays ; nevertheless *Classic 1* tends to advantage sector S_1 while *Classic 2* ensures fairness between sectors. Family *Advanced* exploits the HDPC property of relays and besides tends to advantage sector S_1. Since resource allocation and cooperation planning differs from one pattern to another, each pattern has a specific expression to compute the amount of mutual information.

Families *Classic 1*, *Classic 2* and *Advanced* are detailed in the following sections. Their most representative resource allocation patterns [1] are respectively illustrated on Figures 3.4, 3.5 and 3.7 by patterns describing the frame structure of the pattern, *i.e.,* resource allocation and cooperation planning. Patterns are represented as follows : rows and columns are respectively divided into time slots and frequency chunks that can be either assigned to one exclusive transmitter, or shared by two or more transmitters (see for instance pattern NNN_{C1} on Figure 3.4a : the second chunk is shared by s_2 and s_3). A cell of the pattern is a resource block, *i.e.,* the combination of one time slot and one chunk. The name of transmitters which are assigned to a given resource block is marked on this resource block. In exponent, between brackets, the index of the packet is also marked. For commodity, each transmitter has a distinct colour. If a resource block is exclusively assigned to one transmission, then this transmission is interference free. On the other hand, if a resource block is shared between several neighbour transmitters, then their communications will suffer from inter-sector interference. Resource blocks are delimited on patterns by solid thick lines, while dotted lines are used when a given resource block is shared by different

1. 'Mode' will be sometimes used instead of the word 'pattern' but in this dissertation their meaning is identical.

transmitters.

3.4.2.1 'Classic 1' Family of Allocation Patterns (C1)

With *Classic 1* family, when resources are scheduled, one chunk is granted exclusively one sector (S_1 for instance), while the other chunk is shared by the remainder two sectors (S_2 and S_3 for instance). Hence, one sector is advantaged in terms of inter-sector interference. Therefore, in our examples, S_1 is not affected by inter-sector interference, while destinations d_2 and d_3 are interfered by transmissions occurring respectively in sector S_3 and in sector S_2. Furthermore, relays are classic half-duplex devices : they do not perform the HDPC property. Most illustrative *Classic 1* allocation patterns are shown on Figure 3.4.

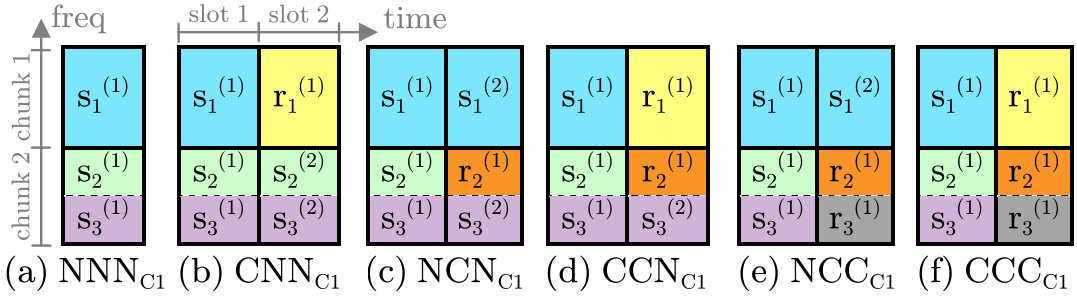

FIGURE 3.4 – Most representative resource allocation patterns for *Classic 1* family.

Expression of channel capacity can be specifically derived for each resource allocation pattern. When no sector plans cooperation (NNN$_{C1}$), the amount of mutual information is derived for sector S_1 as

$$\begin{aligned} \mathscr{I}^{1}_{\mathrm{NNN_{C1}}} &= \log_2\left(1+\frac{|f^{(1)}_{1,1}|^2\cdot P^{(1)}_{s_1}}{\sigma^2_{d_1}}\right) \\ &= \log_2\left(1+\mathrm{SNR}^{(1)}_{\mathrm{dp},1}\right) \end{aligned} \tag{3.13}$$

and for sectors S_2 and S_3 as

$$\begin{aligned} \mathscr{I}^{i}_{\mathrm{NNN_{C1}}} &= \log_2\left(1+\frac{|f^{(2)}_{i,i}|^2\cdot P^{(2)}_{s_i}}{\sigma^2_{d_i}+|f^{(2)}_{j,i}|^2\cdot P^{(2)}_{s_j}}\right) \\ &= \log 2\left(1+\frac{\mathrm{SNR}^{(2)}_{\mathrm{dp},i}}{1+\mathrm{INR}^{(2)}_{\mathrm{dp},j,i}}\right) \\ & i\neq j,\ \{i,j\}=\{2,3\}. \end{aligned} \tag{3.14}$$

The allocation pattern NCN$_{C1}$ characterizes a cooperation plan where only S_2 performs cooperative transmissions (see Figure 3.4c). Nevertheless, the chunk allocated to sector S_2 is already shared by sector S_3. In addition to AWGN noise, there is then inter-sector interference : destination d_3 is first interfered by transmissions from source s_2 and then by transmissions from relay r_2.

Equations (3.15) and (3.16) derive the amount of mutual information $\mathscr{I}^{2}_{\mathrm{NCN_{C1}}}$ in sector S_2 for pattern NCN$_{C1}$, when respectively OAF and ODF cooperative protocols are employed. For ODF protocol it was assumed that relay perfectly recovers its incoming

message ; consequently the message forwarded on the second hop does not depend on the channel quality of the first hop. Some materials on these expressions can be found in [10].

$$\begin{aligned}\mathscr{I}^2_{\mathrm{NCN_{C1},AF}} &= \tfrac{1}{2}\log_2\left(1+\frac{|f^{(2)}_{2,2}|^2\cdot P^{(2)}_{s_2}}{\sigma^2_{d_2}+|f^{(2)}_{3,2}|^2\cdot P^{(2)}_{s_3}}+X\right),\\ &= \tfrac{1}{2}\log_2\left(1+\frac{\mathrm{SNR}^{(2)}_{\mathrm{dp},2}}{1+\mathrm{INR}^{(2)}_{\mathrm{dp},3,2}}+Y\right),\end{aligned} \tag{3.15}$$

$$X=\frac{|h^{(2)}_{2,2}|^2\cdot P^{(2)}_{s_2}\cdot|g^{(2)}_{2,2}|^2\cdot P^{(2)}_{r_2}}{(\sigma^2_{d_2}+|f^{(2)}_{3,2}|^2\cdot P^{(2)}_{s_3})(\sigma^2_{r_2}+|h^{(2)}_{2,2}|^2\cdot P^{(2)}_{s_2}+|f^{(2)}_{3,2}|^2\cdot P^{(2)}_{s_3})+|g^{(2)}_{2,2}|^2\cdot P^{(2)}_{r_2}(\sigma^2_{r_2}+|f^{(2)}_{3,2}|^2\cdot P^{(2)}_{s_3})},$$

$$Y=\frac{\mathrm{SNR}^{(2)}_{\mathrm{rp1},2}\cdot\mathrm{SNR}^{(2)}_{\mathrm{rp2},2}}{(1+\mathrm{INR}^{(2)}_{\mathrm{dp},3,2})(1+\mathrm{SNR}^{(2)}_{\mathrm{rp1},2}+\mathrm{INR}^{(2)}_{\mathrm{dp},3,2})+\mathrm{SNR}^{(2)}_{\mathrm{rp2},2}\cdot(1+\mathrm{INR}^{(2)}_{\mathrm{dp},3,2})^{(2)}}.$$

where $\mathrm{SNR}^{(2)}_{\mathrm{dp},2}$, $\mathrm{SNR}^{(2)}_{\mathrm{rp1},2}$ and $\mathrm{SNR}^{(2)}_{\mathrm{rp2},2}$ are straightforward extensions of notations previously introduced in Section 3.3.2.2, while $\mathrm{INR}^{(2)}_{\mathrm{dp},3,2}$ is easily deduced from (3.15).

$$\begin{aligned}\mathscr{I}^2_{\mathrm{NCN_{C1},DF}} &= \tfrac{1}{2}\log_2\left(1+\frac{|f^{(2)}_{2,2}|^2\cdot P^{(2)}_{s_2}}{\sigma^2_{d_2}+|f^{(2)}_{3,2}|^2\cdot P^{(2)}_{s_3}}+\frac{|g^{(2)}_{2,2}|^2\cdot P^{(2)}_{r_2}}{\sigma^2_{r_2}+|f^{(2)}_{3,2}|^2\cdot P^{(2)}_{s_3}}\right),\\ &= \tfrac{1}{2}\log_2\left(1+\frac{\mathrm{SNR}^{(2)}_{\mathrm{dp},2}}{1+\mathrm{INR}^{(2)}_{\mathrm{dp},3,2}}+\frac{\mathrm{SNR}^{(2)}_{\mathrm{rp2},2}}{1+\mathrm{INR}^{(2)}_{\mathrm{dp},3,2}}\right).\end{aligned} \tag{3.16}$$

Neighbour transmissions are synchronized : momentary active transmitters in S_2 and S_3 (s_2, s_3, r_2 and/or r_3) simultaneously transmit on the second chunk. If cooperation is planned in S_2 for instance (see Figures 3.4c–f), listening phase of relay r_2 is interfered by transmissions of the neighbour source s_3. Relays have better not to cooperate if the signal they listen to is too interfered.

3.4.2.2 'Classic 2' Family of Allocation Patterns (C2)

With *Classic 2* family, when resources are scheduled, a fair policy allocates both chunks to the three sectors, no sector is 'boosted' contrary to *Classic 1* family. Therefore, each destination suffers, on both chunks, from interference caused by neighbour active transmitters (s_i or r_i). Furthermore, relays are classic half-duplex devices : they do not perform the HDPC property. Most illustrative *Classic 2* allocation patterns are shown on Figure 3.5.

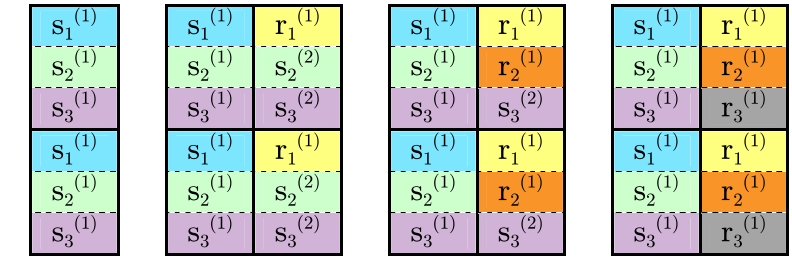

(a) $\mathrm{NNN_{C2}}$ (b) $\mathrm{CNN_{C2}}$ (c) $\mathrm{CCN_{C2}}$ (d) $\mathrm{CCC_{C2}}$

Figure 3.5 – Most representative resource allocation patterns for *Classic 2* family.

When cooperation is planned in a sector, listening phase of relay is interfered by transmissions of the two neighbour sources (see for instance pattern CNN_{C2} on Figure 3.5b). In comparison to *C1* allocation patterns, relays and destinations encounter more interference,

but sources and relays transmit in return on both chunks. There is hence a trade-off between an additional amount of mutual information and additional inter-sector interference.

Channel capacity $\mathscr{I}^{i}_{\mathrm{NNN_{C2}}}$ of sector S_i, $i \in \{1,2,3\}$, for pattern NNN_{C2} is derived as

$$\begin{aligned}\mathscr{I}^{i}_{\mathrm{NNN_{C2}}} &= \log_2\left(1+\frac{|f^{(1)}_{i,i}|^2\cdot P^{(1)}_{s_i}}{\sigma^2_{d_i}+|f^{(1)}_{j,i}|^2\cdot P^{(1)}_{s_j}+|f^{(1)}_{k,i}|^2\cdot P^{(1)}_{s_k}}\right)\\ &\quad+\log_2\left(1+\frac{|f^{(2)}_{i,i}|^2\cdot P^{(2)}_{s_i}}{\sigma^2_{d_i}+|f^{(2)}_{j,i}|^2\cdot P^{(2)}_{s_j}+|f^{(2)}_{k,i}|^2\cdot P^{(2)}_{s_k}}\right),\\ \mathscr{I}^{i}_{\mathrm{NNN_{C2}}} &= \log_2\left(1+\frac{\mathrm{SNR}^{(1)}_{\mathrm{dp},i}}{1+\mathrm{INR}^{(1)}_{\mathrm{dp},j,i}+\mathrm{INR}^{(1)}_{\mathrm{dp},k,i}}\right)\\ &\quad+\log_2\left(1+\frac{\mathrm{SNR}^{(2)}_{\mathrm{dp},i}}{1+\mathrm{INR}^{(2)}_{\mathrm{dp},j,i}+\mathrm{INR}^{(2)}_{\mathrm{dp},k,i}}\right),\\ i\neq j\neq k,&\quad \{i,j,k\}=\{1,2,3\}.\end{aligned} \tag{3.17}$$

3.4.2.3 Proposed 'Advanced' Family of Allocation Patterns (A)

This family of resource allocation patterns is designed for relays exploiting our HDPC property. Figure 3.6 compares the frame structure of a standard orthogonal cooperative protocol (performed in families *C1* and *C2*) to the orthogonal HDPC cooperative protocol of family *A*. For a classic protocol shown on Figure 3.6a, the cooperative transmission of one packet spreads over two time slots but exploits one chunk. First, source transmits while relay is listening; second, source remains silent while relay forwards a processed copy of what it previously listened. For more clarity, a specific colour differentiates both chunks. On Figure 3.6b for HDPC relay, source s_i transmits on chunk A the packet m_k, relay r_i listens to m_k on chunk A while transmits the packet n_{k-1} on chunk B (n_{k-1} is a processed copy of m_{k-1}). Transmission of one single packet always requires two time slots, but for n packets it needs $(n+1)$ time slots, which asymptotically tends to n. Hence the proposed cooperative protocol is more time efficient but needs two chunks instead.

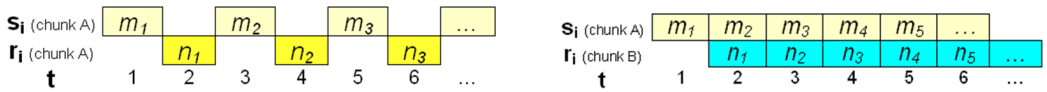

(a) Classical orthogonal cooperative protocol

(b) HDPC cooperative protocol

FIGURE 3.6 – Standard vs. HDPC frame structure for orthogonal cooperative protocols.

The resource allocation patterns illustrated on Figure 3.7 are thus reduced to one time slot, against two time slots with *C1* and *C2* families. When resource allocation is scheduled, an unfair policy is adopted : one chunk is exclusively granted one source (s_1 for instance), while remainder sources (s_2 and s_3 for instance) share the other chunk. Hence, one source is advantaged in terms of inter-sector interference. We assume in the remainder that s_1 is the advantaged source. Strictly speaking, we cannot say as with *C1* family, that the sector S_1 is advantaged insofar as it uses exclusively one chunk. Indeed with HDPC relays both chunks are exploited. Actually, we will see hereafter that s_1 and r_1 are still a little bit advantaged in comparison to their neighbour devices but their benefits are less obvious

than with *C1* family. The pattern NNN_A is not represented on Figure 3.7 because it exactly corresponds to the pattern NNN_{C1} shown on Figure 3.4a.

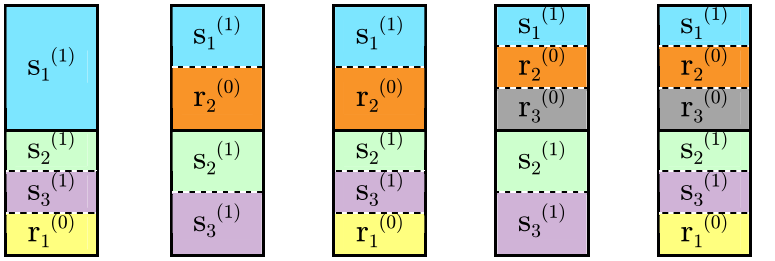

(a) CNN_A (b) NCN_A (c) CCN_A (d) NCC_A (e) CCC_A

Figure 3.7 – Most representative resource allocation patterns for *Advanced* family.

Let us consider successively inter-sector interference perceived by first destinations and second relays with patterns of this family. On the one hand, destination d_1 is interfered on the first chunk by neighbour relays r_2 and/or r_3, only if sectors S_2 and/or S_3 plan cooperation. Likewise, destinations d_2 and d_3 are interfered on the second chunk respectively by s_3 and s_2, but also by r_1 when sector S_1 plans cooperation. On the other hand, if S_1 plans cooperation, listening phase of r_1 on the first chunk is interfered by transmissions of neighbour relays, only if S_2 and/or S_3 plan cooperation too (see Figures 3.7a, 3.7c and 3.7e) ; meanwhile, d_1 is always interfered by s_2 and s_3 on the second chunk during the broadcasting phase of the relay. A similar reasoning can be done when S_2 and S_3 plan cooperation. If S_2 plans cooperation (likewise for S_3, by symmetry), r_2's listening phase on the second chunk is interfered by s_3, but also by r_1 if S_1 plans cooperation too ; d_2 is meanwhile always interfered on the first chunk by s_1, but also by r_3 if S_3 plans cooperation (see Figures 3.7b–e). We note that r_2 (respectively r_3) is indeed more affected by inter-sector interference than r_1.

$$\begin{aligned}\mathscr{I}^1_{\text{CNN}_\text{A},\text{AF}} &= \log_2\left(1+\frac{|f^{(1)}_{1,1}|^2\cdot P^{(1)}_{s_1}}{\sigma^2_{d_1}}\right)+\log_2\left(1+\frac{|h^{(1)}_{1,1}|^2\cdot P^{(1)}_{s_1}\cdot|g^{(2)}_{1,1}|^2\cdot P^{(2)}_{r_1}}{|g^{(2)}_{1,1}|^2\cdot P^{(2)}_{r_1}+X}\right),\\ &= \log_2\left(1+\text{SNR}^{(1)}_{\text{dp},1}\right)+\log_2\left(1+\frac{\text{SNR}^{(1)}_{\text{rp1},1}\cdot\text{SNR}^{(2)}_{\text{rp2},1}}{\text{SNR}^{(2)}_{\text{rp2},1}+Y}\right),\end{aligned} \tag{3.18}$$

$$X = (\sigma^2_{d_1}+|h^{(1)}_{1,1}|^2\cdot P^{(1)}_{s_1})\cdot(\sigma^2_{r_1}+|f^{(2)}_{2,1}|^2\cdot P^{(2)}_{s_2}+|f^{(2)}_{3,1}|^2\cdot P^{(2)}_{s_3}),$$
$$Y = (1+\text{SNR}^{(1)}_{\text{rp1},1})\cdot(1+\text{INR}^{(2)}_{\text{dp},2,1}+\text{INR}^{(2)}_{\text{dp},3,1}).$$

$$\begin{aligned}\mathscr{I}^1_{\text{CNN}_\text{A},\text{DF}} &= \log_2\left(1+\frac{|f^{(1)}_{1,1}|^2\cdot P^{(1)}_{s_1}}{\sigma^2_{d_1}}\right)+\log_2\left(1+\frac{|g^{(2)}_{1,1}|^2\cdot P^{(2)}_{r_1}}{\sigma^2_{r_1}+|f^{(2)}_{2,1}|^2\cdot P^{(2)}_{s_2}+|f^{(2)}_{3,1}|^2\cdot P^{(2)}_{s_3}}\right),\\ &= \log_2(1+\text{SNR}^{(1)}_{\text{dp},1})+\log_2\left(1+\frac{\text{SNR}^{(2)}_{\text{rp2},1}}{1+\text{INR}^{(2)}_{\text{dp},2,1}+\text{INR}^{(2)}_{\text{dp},3,1}}\right).\end{aligned} \tag{3.19}$$

The amount of mutual information $\mathscr{I}^i_{\text{NNN}_\text{C2}}$ in sector S_1 for CNN_A pattern is derived for AF and DF cooperative protocols respectively as (3.18) and (3.19) (see [10]).

3.4.2.4 Other Possible Allocation Patterns

Other possible resource allocation patterns that we have initially considered were not selected for our final investigation. We indeed proved them to be suboptimal. We nume-

rically evaluated their performance in terms of mutual information. Nevertheless, most representative patterns of such suboptimal patterns are illustrated on Figures 3.8, 3.9 and 3.10.

Figure 3.8 shows five patterns of resource allocation patterns designed for the CNN cooperation plan. These five patterns exploit the HDPC property of relay. The first pattern CNN_1 is an alternative to the pattern CNN_A : the first time slot of CNN_1 is equal to CNN_A and for the second time slot of CNN_1 the two chunks are simply permuted. On the other hand, the four other patterns CNN_2–CNN_5 are less spectral efficient since they need three time slots for two cooperative transmissions. However they cause less interference than CNN_1.

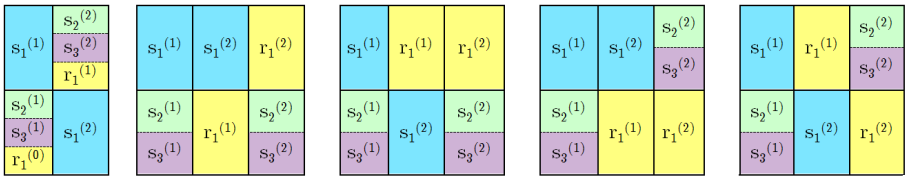

FIGURE 3.8 – Patterns of some CNN patterns initially considered but finally rejected.

Figure 3.9 illustrates the pattern of five patterns which are the straightforward extension of patterns shown on Figure 3.8 to the NCC cooperation plan. Instead of planning cooperation in sector S_1, the relay r_1 remains silent but relays r_2 and r_3 are used instead. The pattern NCC_1 is likewise an alternative to NCC_A. All these patterns are designed for HDPC relays.

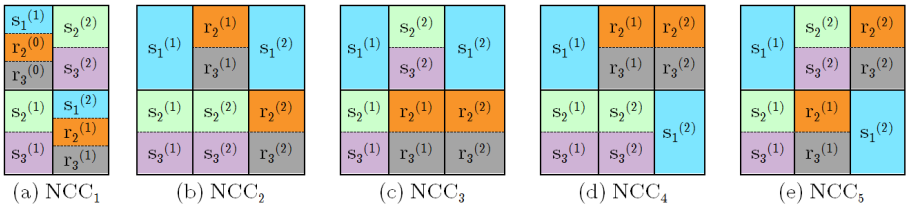

FIGURE 3.9 – Patterns of some NCC patterns initially considered but finally rejected.

Lastly, Figure 3.10 gives the pattern of three patterns designed for the CCC cooperation plan. All HDPC relays are used, but patterns are more or less spectral efficient. For instance the pattern CCC_2 is an alternative to CCC_A where chunks are simply permuted between the two time slots. All sources and relays transmit at each time slot. In the contrary, patterns CCC_1 and CCC_3 are less spectral efficient since relays transmit at each two time slots while sources transmit systematically at each time slot. Consequently, sources send twice more messages than relays. CCC_3 is an illustration of a non-orthogonal cooperative protocol : at the second time slot, both sources and relays transmit simultaneously on the same resource block.

3.4.3 Adaptive Resource Allocation Process (ARAP)

Relay-based transmissions in cooperative networks may extend coverage, improve channel capacity and so transmission robustness as well as decoding reliability. Nevertheless, cooperative communications also generate additional inter-sector interference. Such a

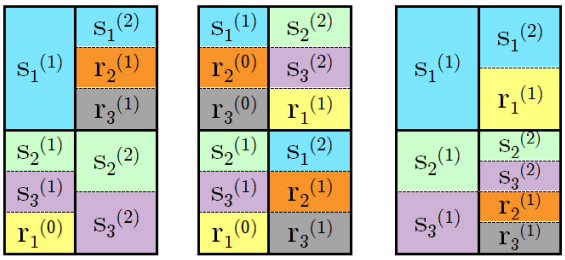

(a) CCC_1 (b) CCC_2 (c) CCC_3

Figure 3.10 – Patterns of some CCC patterns initially considered but finally rejected.

	NNN	CNN,NCN,NNC	CCN,CNC,NCC	CCC
C1	$3P_s$	$5P_s + P_r$	$2(2P_s + P_r)$	$3(P_s + P_r)$
C2	$6P_s$	$2(5P_s + P_r)$	$4(2P_s + P_r)$	$6(P_s + P_r)$
A	$3P_s$	$3P_s + P_r$	$3P_s + 2.P_r$	$3(P_s + P_r)$

Table 3.1 – Power budget per family and per allocation pattern, when equal transmit powers P_s and P_r are assumed between sectors and chunks.

trade-off should be carefully considered, especially in interference-limited communication contexts.

Since expressions for channel capacity differ from one resource allocation pattern to another, a pattern may perform well and be optimal in comparison to other patterns for a given communication context, whereas this same pattern becomes suboptimal for other contexts. Indeed, the perceived power of inter-sector interference is specific to each resource allocation pattern and also depends on the momentary scenario of communication. By changing position of nodes, fade events and transmit power, the perceived power of interference can be radically modified.

Moreover, power consumption is also considered. As cooperative communications add new network entities (namely the relays) and spread the transmission of one message over two time slots, the global power budget may be increased. However, channel capacity should not be improved at the expenses of an amazing increase of power budget. Our adaptive process also takes this aspect into account. Global transmit power required by resource allocation patterns depends on the number and nature of transmitters (sources and relays), as well as on the number of chunks used by each transmitter. Given the transmission pattern of a pattern M, its power budget $\mathscr{B}_P(M)$ is straightforwardly defined. To this end, Table 3.1 expresses power budgets for patterns families *C1*, *C2* and *A*, when equal transmit powers are considered between sectors and chunks.

Therefore, to profit from time, frequency and space variations of communication contexts, an *Adaptive inter-sector Resource Allocation Process* (ARAP) is proposed and evaluated. The goals of this adaptive mechanism are twofold. First, ARAP is designed to maximize the sum-rate, *i.e.,* the sum of the rates that are achieved in each sector. To this end, we consider for each resource allocation pattern M the sum

$$GMI(M) = \sum_{i=1}^{3} \mathscr{I}_M^i, \tag{3.20}$$

where GMI stands for 'Global Mutual Information' and refers to the sum of mutual information amount $\mathscr{I}_M^i$ met by pattern M in each sector S_i. Second, ARAP seeks to minimize the global power budget $\mathscr{B}_P(M)$ for transmissions according to the pattern M - let us think about non power-supplied devices and their battery life. Consequently, ARAP should grant patterns with low power budget while it should penalize patterns with high power budget.

To meet both these goals, we define a quality-metric based on channel capacity and power budget. This quality-metric is simply the ratio between $GMI(M)$ and $\mathscr{B}_P(M)$:

$$\varphi(M) = \frac{GMI(M)}{\mathscr{B}_P(M)}. \tag{3.21}$$

To maximize the sum-rate while minimizing the power budget, whatever the momentary communication context may be, our RRM adaptive mechanism has to optimize the following utility function :

$$\max_{M \in \mathscr{K}} \varphi(M), \tag{3.22}$$

where $\mathscr{K}$ is a set of resource allocation patterns. By solving this problem, ARAP hence selects in $\mathscr{K}$ the resource allocation pattern $\mathscr{M}_{\mathscr{K}}$ the best suited to the current scenario of communication.

The optimal pattern $\mathscr{M}_{\mathscr{K}}$ is of course computed jointly by the three coordinated sectors, since the quality-metric $\varphi(M)$ depends on the channel capacity and power budget of each sector. Nevertheless, we propose in the remainder of this chapter to evaluate performance of ARAP with the viewpoint of one sector. In other words, we will make as if the three sectors were independent and investigate the performance when we restrict our attention to only one sector. For instance, let us consider that the first sector S_1 is the sector of interest ; by an obvious symmetry of the system, results will be easily generalize to any other sector.

For any pattern M, the quality-metric $\varphi(M)$ depends on the momentary values of system and channel parameters (fading, shadowing, transmit power, etc.) but also on the position of nodes. Indeed, the value of the global channel gain (and so the value of $GMI(M)$) is related to the distance between transmitters and receivers, because of path loss attenuation (see Equation (3.1) for instance). In the downlink pattern, sources s_i are base stations, which are fixed. We besides assumed our relays r_i were also fixed. Therefore, for any pattern M, the variations in $\varphi(M)$ due to the mobility of nodes are strictly related to the mobility of destinations d_i within their sector S_i.

ARAP aims at profiting from time, frequency and space variations of communication contexts. We moreover decide to evaluate performance with the restricted viewpoint of sector S_1. However, there are a lot of causes that may affect the momentary value of $\varphi(M)$, whatever the pattern M may be : fading, shadowing, position of destinations, transmit power. We should concentrate only on a single cause of variations in order to better understand its effects. Consequently, our adaptive mechanism is evaluated in the framework of the algorithm illustrated on Figure 3.11. The location of destination d_1 within sector S_1 is kept under control, *i.e.,* the position of d_1 within S_1 is our input parameter which will let us discriminate how ARAP copes with space variations. The algorithm of Figure 3.11 is so performed for a specific position of d_1.

1. $N_{\text{pos}} \times N_{\text{chan}}$ communication contexts are randomly computed. N_{pos} random and independent positions are defined for destinations d_2 and d_3 within their sector. For

each random couple (d_2, d_3), N_{chan} random channel coefficients including fading and shadowing are computed for all links of the system.

2. For the current values of channel parameters and positions of destinations (d_1, d_2, d_3), $GMI_{(d_1,d_2,d_3)}(M)$ is computed for each pattern M.
3. $GMI_{(d_1,d_2,d_3)}(M)$ is averaged of all the $N_{\text{pos}} \times N_{\text{chan}}$ random communication contexts. The result is referred to by $\overline{GMI}_{d_1}(M)$ and does not depend any more on position of d_2 and d_3, since the average has been done on N_{pos} random positions. $\overline{GMI}_{d_1}(M)$ is just related to the current position of d_1.
4. $\overline{GMI}_{d_1}(M)$ is divided by the power budget $\mathscr{B}_P(M)$ of the pattern M. The ratio is an averaged value of $\varphi(M)$ and is referred to by $\widehat{GMI}_{d_1}(M)$.
5. ARAP selects among a set $\mathscr{K}$ of resource allocation patterns M the one that maximizes $\widehat{GMI}_{d_1}(M)$. This optimal pattern is identified by $\mathscr{M}_{\mathscr{K}}^{d_1}$.

The set $\mathscr{K}$ is chosen among $\{\Omega_{clas}, \Omega_{adv}, \Omega_{all}\}$, which are respectively the sets of all *Classical*, all *Advanced* and all investigated resource allocation patterns.

A $n_{step} \times n_{step}$ grid parcels out each sector. The destination d_1 is located on the grid of S_1, while d_2 and d_3 move randomly respectively on the grids of S_2 and S_3. $\widehat{GMI}_{d_1}(M)$ is computed for all positions of d_1 on its grid.

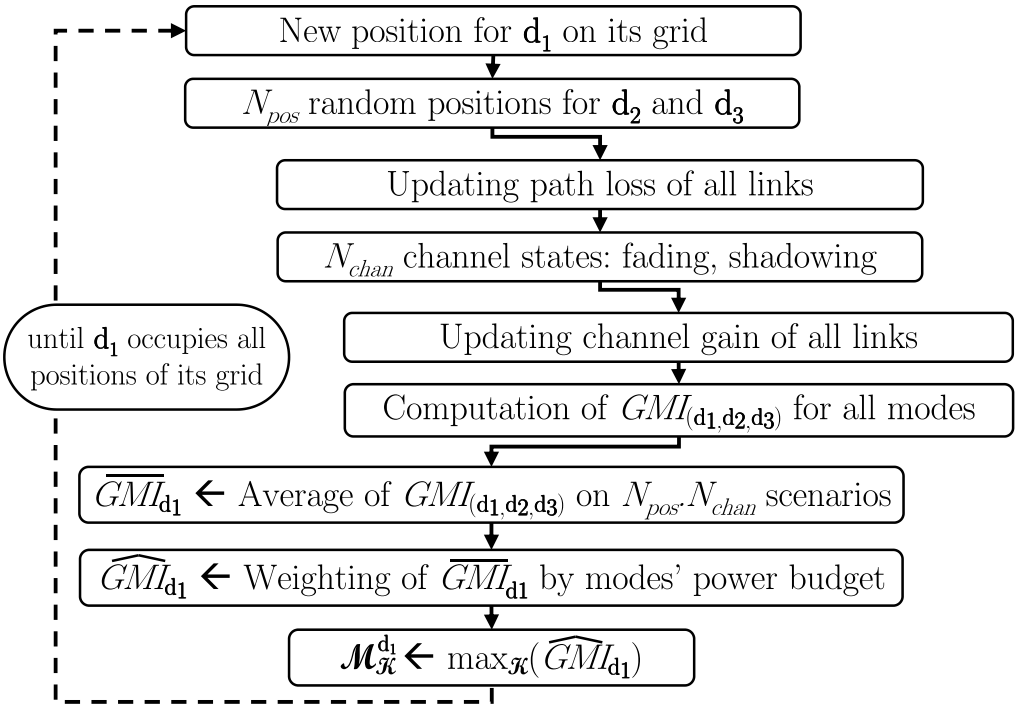

Figure 3.11 – Description of the algorithm for evaluating performance of ARAP.

3.4.4 Simulation Results

Previously introduced resource allocation patterns are evaluated by numerical simulations in this section. *Advanced* patterns are compared to *Classic 1* and *Classic 2* patterns. Two scenarios are considered. First, the mobility of d_1 within S_1 is constrained to the axis $(s_1 - r_1)$, while in sectors S_2 and S_3, destinations move randomly (Section 3.4.4.1).

System model			Algorithm
High TX power	Low TX power	$r_{\text{cell}} = 0.5\text{km}$	$N_{pos} = 1000$
$P_{s_i} = 10\text{W}$	$P_{s_i} = 10\text{mW}$	$\sigma^2_{d_i} = \sigma^2_{r_i} = -105\text{dBm}$	$N_{chan} = 500$
$P_{r_i} = 1\text{W}$	$P_{r_i} = 1\text{mW}$	$L_{\text{dB}} = 137.74 + 30.\log_{10}(d), d[\text{km}]$	$n_{\text{step}} = 20$

TABLE 3.2 – System model and algorithm settings.

Second, destination d_1 occupies alternately all positions of its grid, and for each position, destinations d_2 and d_3 are randomly mobile (Section 3.4.4.2).

Both scenarios are evaluated with two sets of transmit powers : high powers and low powers. These two sets are extreme cases but show that results highly depend on transmission powers. Moreover, both AF and DF cooperative protocols are evaluated. With AF protocol, the amplification gain is defined as stated in (3.5), where equality is considered instead of inequality. With DF protocol, relays are assumed to decode their signal without error (error-free transmission between sources and relays). System model and algorithm settings used for our numerical results are summarized in Table 3.2.

Let us not that whatever the pattern M may be, the mobility of d_1 within S_1 does not impact the amount of mutual information $\mathscr{I}^2_M$ and $\mathscr{I}^3_M$ of sectors S_2 and S_3. The mobility of one destination only affects performance of the related sector. Consequently, results presented hereafter illustrate how the sum-rate $\widehat{GMI}_{d_1}(M)$ behaves according to various positions of d_1 but actually only the fraction of $\widehat{GMI}_{d_1}(M)$ related to sector S_1 changes ; the fraction related to S_2 and S_3 is constant when d_1 moves.

3.4.4.1 First Scenario : Unidirectional moving along 's1-r1 axis

Figures 3.12–3.15 illustrate the evolution of $\widehat{GMI}_{d_1}$ with the increasing distance between s_1 and d_1. Dotted and solid curves represent respectively results for *Classic 1* and *Advanced* allocation patterns. Results for *Classic 2* patterns are not shown, since both *Classic 1* and *Advanced* families of patterns outperform the family *Classic 2* in all investigated scenarios. Each plan of cooperation uses a specific marker and a specific colour : NNN (red curve, no marker), CNN (green curve, upward-pointing triangle), NCN (blue curve, downward-pointing triangle), CCN (magenta curve, circle), NCC (gray curve, plus sign) and CCC (black curve, five-pointed star). Results for families NNC and CNC are identical respectively to those of families NCN and CCN (by design symmetry) and are thus not shown.

High Transmit Powers

The comparison between *C1* and *A* families of patterns for high transmit powers (see Table 3.2) is given on Figures 3.12 and 3.13, respectively for AF and DF cooperative protocols. As expected, due to path loss attenuation, the farer d_1 is from s_1, the lower is the channel capacity $\mathscr{I}^1$ of sector S_1, and so the lower is $\widehat{GMI}_{d_1}$. However, when S_1 plans cooperation (*i.e.,* CNN, CCN, CCC patterns for families *C1* and *A*), $\widehat{GMI}_{d_1}$ improves close to r_1. Indeed, a vertical red dotted line located at $dist(s_1, d_1) = 0.33\text{km}$ represents the position of the relay r_1 ; some patterns are enhanced in the vicinity of this red line.

The pattern CNN_A (green solid curve) shows the best results in this area ($\mathscr{M}^{d_1}_{\Omega_{all}} = \text{CNN}_A$). With our assumptions on cooperative protocols, the inter-sector interference perceived by the relays are cancelled out with DF protocols while this interference is amplified

with AF protocols. Enhancements of $\widehat{GMI}_{d_1}$ in the vicinity of r_1 are therefore bigger with DF protocols (Figure 3.13) than with AF protocols (Figure 3.12).

When d_1 is out of reach of r_1 ($dist(r_1, d_1) \gtrsim 0.11$km), NNN_{C1} allocation pattern (red dotted curve) - which is besides identical to NNN_A - outperforms all other patterns, for both AF and DF protocols ($\mathscr{M}^{d_1}_{\Omega_{all}} = \text{NNN}_A$). Consequently, our proposed *Advanced* allocation patterns outperform *Classic 1* patterns. Moreover, we can observe that with *Advanced* patterns, the smaller is the number of sectors in which cooperation is activated, the higher is $\widehat{GMI}_{d_1}$. This trend is opposite with *Classic 1* patterns.

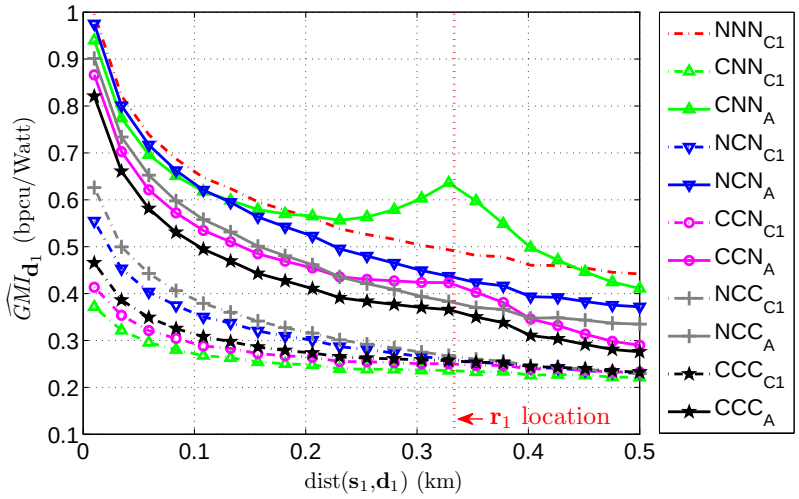

FIGURE 3.12 – AF protocol, High transmit powers - $\widehat{GMI}_{d_1}(M)$ variations along (s_1, r_1) axis.

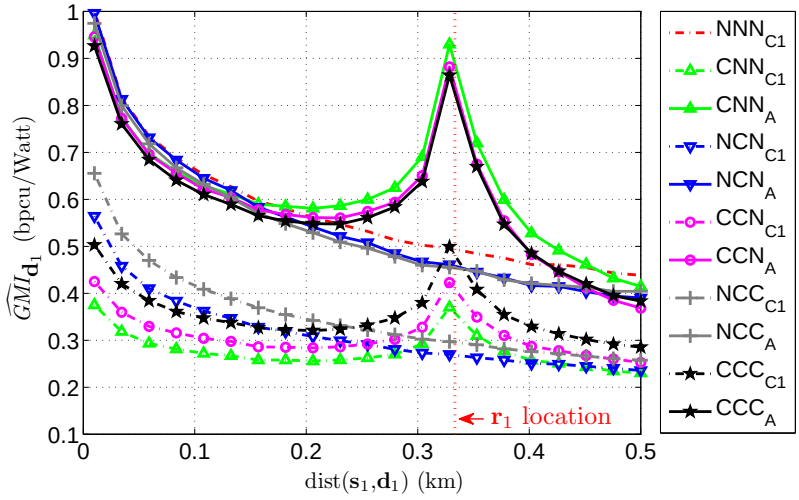

FIGURE 3.13 – DF protocol, High transmit powers - $\widehat{GMI}_{d_1}(M)$ variations along (s_1, r_1) axis.

Low Transmit Powers

The comparison between *C1* and *A* families of patterns for low transmit powers (see Table 3.2) is given on Figures 3.14 and 3.15, respectively for AF and DF cooperative

protocols. Like the results shown for high transmit powers, $\widehat{GMI}_{d_1}$ decreases with the increasing distance between source s_1 and destination d_1, while $\widehat{GMI}_{d_1}$ improves close to r_1 when S_1 plans cooperation (CNN, CCN, CCC cooperation plans for families *C1* and *A*).

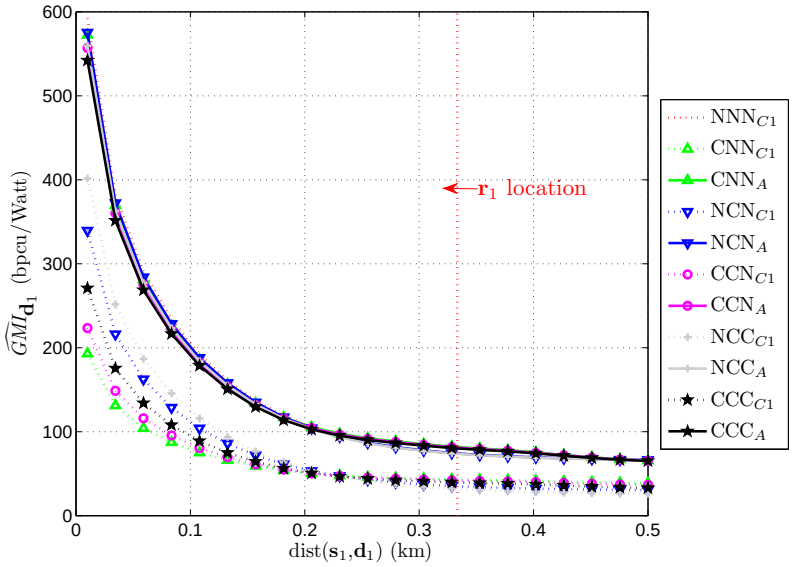

FIGURE 3.14 – AF protocol, Low transmit powers - $\widehat{GMI}_{d_1}(M)$ variations along (s_1, r_1) axis.

By observing Figure 3.14, this last remark does not seem true for AF protocols since the characteristic gain of cooperative patterns does not appear any more when d_1 is located around r_1. All patterns of a given family seem indeed nearly equivalent in terms of $\widehat{GMI}_{d_1}$ performance and it is difficult to determine which pattern performs best. However, Figure 3.18a (introduced hereafter in Section 3.4.4.2) shows that cooperative patterns are still better than non cooperative patterns in the surrounding of relay r_1. Indeed, CNN$_A$ achieves the highest $\widehat{GMI}_{d_1}$ close to r_1 ($\mathscr{M}^{d_1}_{\Omega_{all}} = \text{CNN}_A$), whereas NNN$_A$ is optimal when d_1 is out of reach of r_1 ($\mathscr{M}^{d_1}_{\Omega_{all}} = \text{NNN}_A$).

Our proposed *Advanced* family still outperforms *Classic 1* family for AF protocols in all investigated scenarios. Families *Classic 1* and *Classic 2* have nearly the same performance but results for *C2* patterns are not plotted for sake of readability.

Figure 3.15 gives results of DF protocols with low transmit powers. We observe there is a considerable improvement of $\widehat{GMI}_{d_1}$ when S_1 plans cooperation (CNN, CCN and CCC cooperation plans, for both families *C1* and *A*). The cooperative pattern CCC$_A$ presents the best performance for quite all position of d_1 along the (s_1, r_1) axis ($\mathscr{M}^{d_1}_{\Omega_{all}} = \text{CCC}_A$). Pattern NCC$_A$ is just slightly better than CCC$_A$ when d_1 is close to its source s_1 ($\mathscr{M}^{d_1}_{\Omega_{all}} = \text{NCC}_A$). In such a configuration, there is indeed no need for d_1 to be helped by r_1 since the signal perceived by d_1 along the direct path is quite good. The hidden *Classic 2* family is equivalent to *Classic 1* but both classical families are outperformed by *Advanced* family.

To conclude, let us sum up the main observations between both simulations scenarios and both cooperative protocols :

– **AF protocols** : Benefits of cooperative communications are reduced when transmit

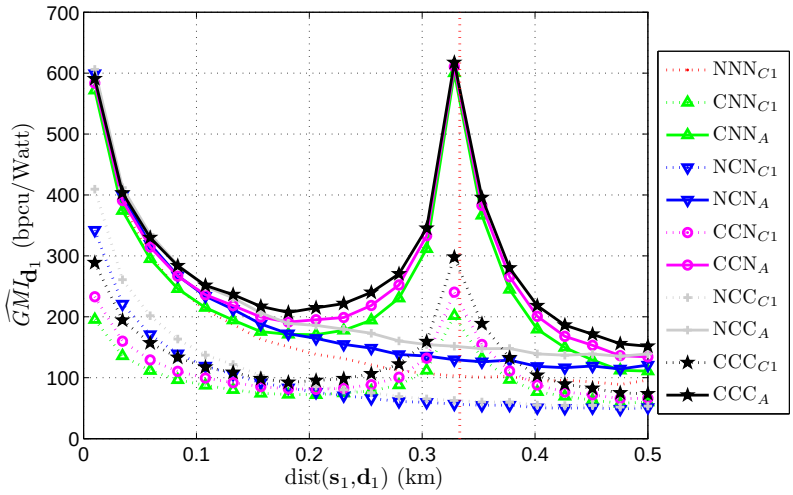

FIGURE 3.15 – DF protocol, Low transmit powers - $\widehat{GMI}_{d_1}(M)$ variations along (s_1, r_1) axis.

powers decrease. Indeed, the SINR perceived by relays decays and tends to 1 (or even less than 1) with decreasing transmit powers, even if inter-sector interference is together reduced. Consequently, it becomes harder at destination to detect and decode the wished signal among noise and inter-sector interference.

– **DF protocols, *Advanced* family** : With high transmit powers, the smaller is the number of sectors planning cooperation, the higher is $\widehat{GMI}_{d_1}$. With low transmit powers, the higher is the number of sectors planning cooperation, the higher is $\widehat{GMI}_{d_1}$. The effects of inter-sector interference are so reduced with lower transmit powers.

3.4.4.2 Second Scenario : Omnidirectional moving within sector

The most interesting results of ARAP are illustrated on Figures 3.17a–3.18b. We plot how evolves the adaptive selection of the optimal pattern $\mathscr{M}_{\mathscr{K}}^{d_1}$, when d_1 is alternately placed on all positions of its $n_{step} \times n_{step}$ grid. RRM adaptation is performed among all resource allocation patterns (families *C1*, *C2* and A : : $\mathscr{K} = \Omega_{all}$), for AF and DF cooperative protocols, with high and low transmit powers. A specific colour is assigned to each plan of cooperation : NNN (red with black edge), CNN (green), NCN (blue), NNC (white with black edge), CCN (magenta with black edge), CNC (yellow with black edge), NCC (cyan with black edge) and CCC (black). On results figures, each position of the grid is marked by a circle, filled with the colour assigned to the cooperation plan of the optimal pattern $\mathscr{M}_{\mathscr{K}}^{d_1}$.

High Transmit Powers

First of all, figures of Section 3.4.4.1 showed how $\widehat{GMI}_{d_1}$ evolved when d_1 was constrained to move along (s_1, r_1) axis. In this second scenario of simulation, Figures 3.16a–3.16b show how $\widehat{GMI}_{d_1}$ variates when d_1 occupies alternatively all positions on the $n_{\text{step}} \times n_{\text{step}}$ grid that parcels out sector S_1. For lack of space, we limit us to DF protocol and to the two resource allocation patterns which were optimal on Figure 3.13 : patterns NNN$_{C1}$ (*i.e.,* NNN$_A$) and CNN$_A$ whose results are respectively shown on Figures 3.16a and 3.16c. As a baseline, we also plot on Figure 3.16b the performance of CNN$_{C1}$ pattern. Arrows point

to the fixed location of source s_1 and relay r_1.

On Figure 3.16a, $\widehat{GMI}_{d_1}$ decreases isotropically with increasing distance between s_1 and d_1 (the inverse of the cubed distance, see Table 3.2). It is an expected behaviour since the source s_1 is the single transmitter in the sector when no cooperative transmissions are planned. On the other hand, decrease of $\widehat{GMI}_{d_1}$ is not isotropically any more on Figures 3.16c and 3.16b. In case of these two figures, the relay r_1 is activated and participates to the transmission. There is hence a gain in $\widehat{GMI}_{d_1}$ in the surrounding of r_1. As soon as d_1 is out of reach of either s_1 or r_1, $\widehat{GMI}_{d_1}$ rapidly falls off.

We further observe that cell-edge users do not particularly profit from cooperative transmissions. By comparing performance of CNN_A pattern to the baseline CNN_{C1}, we note that areas where cooperation ameliorates $\widehat{GMI}_{d_1}$ are enlarged (see more particularly the graduations of the colour bar on the right). Results obtained with AF protocols are quite similar ; the gain in $\widehat{GMI}_{d_1}$ is just lower in the vicinity of r_1.

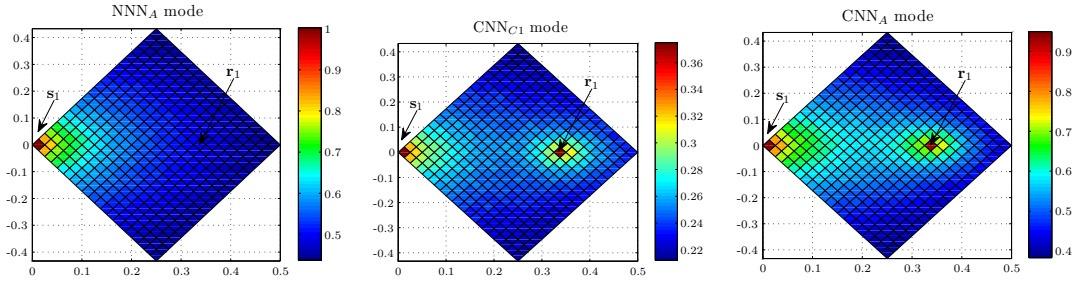

(a) NNN_A pattern (b) CNN_{C1} pattern (c) CNN_A pattern

FIGURE 3.16 – Variations of $\widehat{GMI}_{d_1}(M)$ when d_1 moves everywhere in sector S_1.

Now we analyse results of our adaptive mechanism (ARAP) and its selection of the optimal resource allocation pattern $\mathscr{M}^{d_1}_{\Omega_{all}}$. To this end, Figure 3.17 shows to which cooperation plan belongs $\mathscr{M}^{d_1}_{\Omega_{all}}$ when d_1 successively occupies all positions of the grid in sector S_1, respectively for AF and DF cooperative protocols. These two figures confirm our remarks about Figures 3.12 and 3.13 : the pattern with cooperation plan CNN (green) are optimal in the vicinity of r_1, while elsewhere the pattern NNN (red) is the best.

There are nevertheless two exceptions : the highest and the lowest areas of S_1, coloured respectively in white (NNC) and blue (NCN). When d_1 is placed on this white area for instance, d_1 is sufficiently remote from r_3, so that sector S_3 could plan cooperation (NNC) without interfering too much with d_1. Inter-sector interference caused by r_3 on d_1 is then lower than the gain in mutual information amount for sector S_3. By symmetry, NCN cooperation plan (blue area) is optimal when d_1 is sufficiently apart from r_2. Due to our assumptions on cooperative protocols, destination d_1 profits more from DF protocols than from AF protocols. Areas of relay activation are hence wider with DF protocols (Figure 3.17b) than with AF protocols (Figure 3.17a).

Consequently, ARAP suggests to plan cooperation in at most one sector simultaneously. Indeed, the four cooperation plans NNN, CNN, NCN and NNC cover all positions of the grid. For these four cooperation plans, at most one relay is activated at a given instant. When transmit powers are quite high, we can conclude that cooperative transmissions tend to cause prejudicial inter-sector interference and need to be planned with care. The cooperative trade-off between transmission robustness and inter-sector interference is cha-

racterized by Figure 3.17.

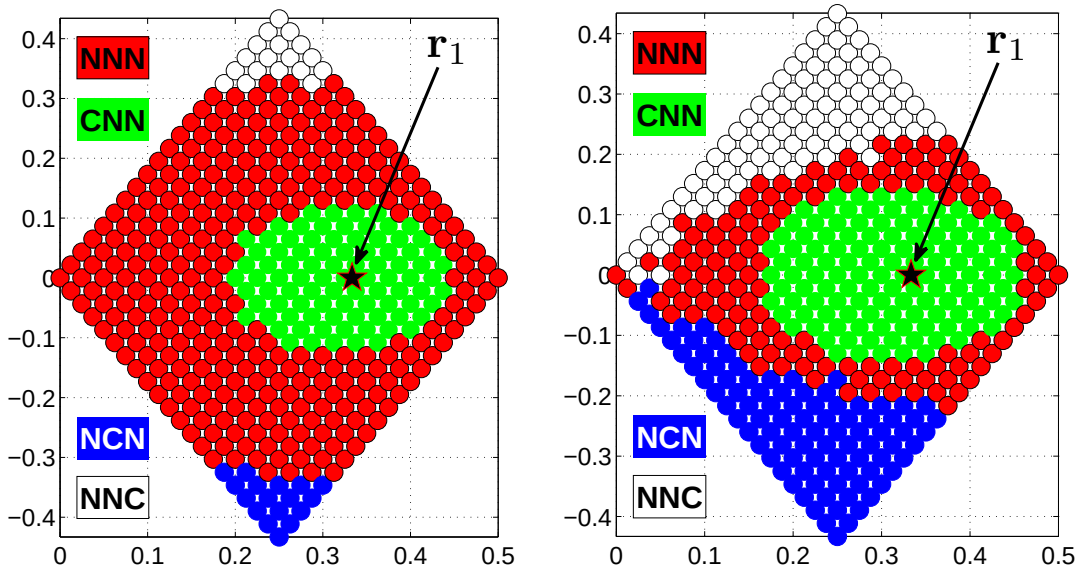

(a) AF protocol (b) DF protocol

Figure 3.17 – High transmit powers - Adaptive selection of the optimal pattern $\mathscr{M}_{\Omega_{all}}^{d_1}$.

Results presented above were obtained when selection of $\mathscr{M}_{\mathscr{K}}^{d_1}$ was performed among all patterns belonging to the set $\mathscr{K} = \Omega_{all}$. Results obtained with adaptation on Ω_{clas} (all *C1* and *C2* patterns) are not shown : NNN cooperation plan is everywhere optimal (all in red). There is a single exception with DF protocol : a unique black circle (CCC patterns) for the location of r_1.

On the other hand, if the RRM adaptation is restricted to Ω_{adv} (all *Advanced* patterns), then results are exactly the same as those on Figure 3.17 obtained for Ω_{all}. Consequently, *Advanced* patterns outperform everywhere classical patterns. Optimal adaptation can thus be restricted to Ω_{adv}, without degradation.

Simulation results indicate that cooperation is not used here for extending coverage and reaching cell-edge users, but rather for enhancing channel capacity. Moreover, patterns exploiting the HDPC property are proved to offer interesting gains in comparison to the standard cooperative protocol.

Low Transmit Powers

Results of ARAP are completely different with low transmit powers, as shown on Figure 3.18. Whereas ARAP tends to 'minimize' the number of sectors planning cooperation when transmit powers are high (at most one sector plans cooperation at a given time) so as to mitigate the inter-sector interference level, cooperation is more favourably planned simultaneously by several neighbour sectors when transmission powers are lower.

Figure 3.18a shows results for an adaptation among all patterns (Ω_{all}) for AF protocols. All cooperation plans are selected at least once to define the optimal pattern $\mathscr{M}_{\Omega_{all}}^{d_1}$, expect CCC (all sectors cooperate simultaneously).

– Around source s_1 NNN pattern (red) is optimal. Destination d_1 is sufficiently near from s_1 so as not to be helped by cooperation. Moreover, d_1 is too remote from r_1 :

cooperation of r_1 is more prejudicial to neighbour sectors than beneficial to sector S1. Cooperation in neighbour sectors would cause unjustified inter-sector interference.
- In the vicinity of r_1, CNN pattern (green) is optimal, as with high transmit powers.
- The optimal patterns in the highest and lowest areas of S_1 are respectively NNC (white) and NCN (blue), as with high transmit powers.
- When d_1 is in the extreme highest or lowest areas of S_1, both neighbour sectors can simultaneously plan cooperation : P_{r_2} and P_{r_3} are low enough so that transmissions of relays r_2 and r_3 do not interfere too much with sector S_1. On the other hand, activation of r_1 would cause excessive inter-sector interference on neighbour sectors S_2 and S_3 in regards to benefits for S_1. NCC pattern (cyan) is here optimal.
- There are transitional areas around r_1 between the green and white areas at the top and between the green and blue area at the bottom. CNC (yellow) and CCN (magenta) patterns are respectively optimal in these transitional areas.

Results of ARAP with adaptation on Ω_{clas} are not shown : NNN is everywhere optimal (all in red). ARAP restricted to Ω_{adv} shows exactly the same results as those of Figure 3.18a with Ω_{all}. Our *Advanced* patterns hence outperform everywhere standard cooperative protocols.

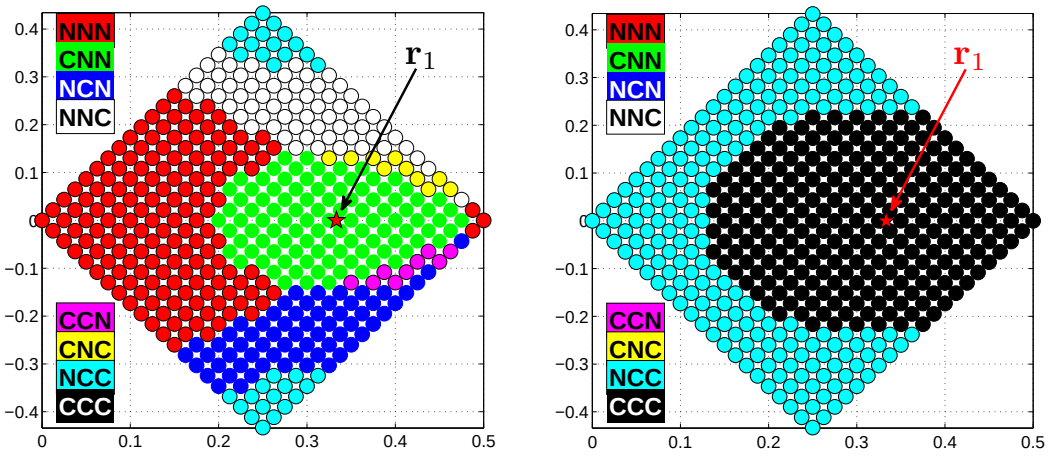

(a) AF protocol

(b) DF protocol

FIGURE 3.18 – Low transmit powers - Adaptive selection of the optimal pattern $\mathscr{M}^{d_1}_{\Omega_{all}}$.

Figure 3.18b shows results for an adaptation among all patterns (Ω_{all}) with DF protocols. This figure shows that cooperative transmissions are preferred to non-cooperative patterns when transmit powers are lower. Indeed NCC (cyan) and CCC (black) patterns cover single-handedly all positions of the grid.
- In the surroundings of relay r_1, all sectors should plan simultaneously cooperation (CCC : black circle).
- When d_1 moves away from r_1, S_1 has better not to plan cooperation so as not to cause too high inter-sector interference on S_2 and S_3. On the other hand, S_2 and S_3 can plan cooperation simultaneously (NCC : white circle). Cooperative transmissions in S_2 and S_3 do not affect especially d_1 in comparison to the gain met by d_2 and d_3.

Results of ARAP with adaptation on Ω_{clas} are not shown : NNN (red) is everywhere

optimal except in the vicinity of r_1 where CCC (black) is optimal. ARAP restricted to Ω_{adv} shows exactly the same results as those of Figure 3.18b with Ω_{all}. Our *Advanced* patterns hence outperform everywhere standard cooperative protocols.

Conclusion on ARAP results

With low or high transmit powers, the RRM adaptation can be reduced without loss of optimality to the set Ω_{adv}. The patterns exploiting the HDPC property let to meet interesting gains in terms of sum-rate with a power budget which is not especially high. Furthermore, these patterns tend to increase the sum-rate even if their design causes more inter-sector interference than standard cooperative patterns. We besides observe that if HDPC protocols do not help in extending sector coverage to meet border-cell users, the area where they improves performance is notably extended in comparison to standard cooperative protocols. The cooperative trade-off that links the transmission robustness and reliability to the inter-sector interference has thus been investigated and characterized.

Once the maps of Figures 3.17 and 3.18 are computed, they can be used at look-up tables to determine how resources should be optimally assigned between the three coordinated sectors. Let us recall that these figures illustrate performance of ARAP restricted to the viewpoint of single sector S_1 (see for instance Figure 3.11). Indeed, results are averaged in S_2 and S_3 on numerous communication contexts and the input parameter is just the momentary position of d_1.

These maps can therefore not serve S_2 and S_3. It is not at all a limitation : similar maps can be computed for the viewpoint of sectors S_2 and S_3. Consequently, there are look-up tables to determine $\mathscr{M}_{\mathscr{K}}^{d_1}$, $\mathscr{M}_{\mathscr{K}}^{d_2}$ and $\mathscr{M}_{\mathscr{K}}^{d_3}$, whatever the location of d_1, d_2 and d_3 may be within their sector. Since the three sectors are coordinated, the optimal pattern is chosen by considering among $\mathscr{M}_{\mathscr{K}}^{d_1}$, $\mathscr{M}_{\mathscr{K}}^{d_2}$ and $\mathscr{M}_{\mathscr{K}}^{d_3}$ the pattern that maximizes $\widehat{GMI}$:

$$\mathscr{M}_{\mathscr{K}} = \max\{\widehat{GMI}_{d_1}(\mathscr{M}_{\mathscr{K}}^{d_1}), \widehat{GMI}_{d_2}(\mathscr{M}_{\mathscr{K}}^{d_2}), \widehat{GMI}_{d_3}(\mathscr{M}_{\mathscr{K}}^{d_3})\}. \tag{3.23}$$

3.5 Generalization to Multi-Chunks Allocations

Up to now, resource allocation patterns and simulation results have been introduced for only two chunks. However, more than two chunks are available with current OFDMA networks compliant with standards such as LTE or WiMAX. For instance, with LTE or WiMAX standards, 50 chunks of 20MHz are commonly available for system transmissions. Along this section, we will propose a mechanism to extend all previous results to real systems disposing of more than two chunks. We will just explain how our previous work could be transposed to $N_{\text{chunks}} > 2$, without providing any simulation results. Likewise, no power control mechanism has been considered, except a simple 'On-Off' power allocation. Actually, any power control mechanism could be combined to our approach.

To generalize our previous work, the N_{chunks} available chunks could be assigned two per two to the three adjacent sectors, *i.e.,* independent pairs of chunks could be constituted and then allocated one after the other. Resource allocation patterns introduced in Section 3.4.2 could thus be re-used without any change.

Each sector S_i has to deal with its own QoS constraints and requirements (target rate, queue list, priority of transmission, etc.). The quality of channel links is time and

frequency varying but assumed constant during at least one frame transmission (quasi-static channels). Let us assume there are a *centralized scheduler* and a **RRM controller** provided with full CSI and system knowledge ; the scheduler is responsible for the allocation of N_{chunks} chunks between the three sectors, contingent to system constraints, while the controller is responsible for the optimal 'pairing' of chunks. We besides assume the period of scheduling is shorter than the period of coherence.

How does this centralized scheduler work is out of the topic of our work ; we just assume here that the assignment of chunks is done by a 'black box' upstream from our resource allocation patterns. This scheduler should however be compliant with LTE / WiMAX requirements ; it should perform and manage for instance channel estimation, link adaptation, priority of users, frequency planning, retransmission of erroneous packets, cooperation planning, etc. We propose on Figure 3.19 a schematic illustration of the mechanism that could let generalize our previous work to systems with more than two chunks.

1. In inputs of the centralized scheduler, there would be the available bandwidth BW with the N_{chunks} chunks as well as system requirements.
2. The scheduler would output an assignment of chunks between the three sectors that will comply with QoS requirements. For some chunks an orthogonal allocation between sector would be computed (no inter-sector interference), while other chunks would be shared by at least two sectors (inter-sector interference). Likewise, some chunks would be allocated for cooperative transmissions, while other chunks could not be used to plan cooperation.
3. Given the allocation of chunks performed by the centralized scheduler, the RRM controller would proceed to the optimal 'pairing of chunks' $\underline{p} = \{p_k\}$, where p_k is a pair of chunks. For each pair p_k, the RRM controller would select the optimal resource allocation pattern $\mathscr{M}_{\mathscr{K},p_k}$, as it was introduced with ARAP in Section 3.4.4.2. To this end, the RRM controller would need the look-up tables of Figures 3.17 and 3.18 and the location of all destinations.

Whereas our previous adaptive mechanism (ARAP) worked just with one pair of chunks, we generalize by this way the adaptive RRM process to several pairs p_k of chunks. To this end, a joint two-level optimization is required :

1. For each pair p_k of chunks, selection of the optimal resource allocation pattern $\mathscr{M}_{\mathscr{K}}(p_k)$ that leads to maximize $\widehat{GMI}_{\underline{d},p_k}$, where $\underline{d}$ refers to the location of the three destinations d_1, d_2 and d_3 within their sectors.
2. Pairing of chunks $\underline{p} = \{p_k\}$ that leads to maximize the overall $\widehat{GMI}_{\underline{d}}$ where

$$\widehat{GMI}_{\underline{d}} = \sum_{p_k} \widehat{GMI}_{\underline{d},p_k}. \tag{3.24}$$

For a given pair of chunks p_k, resources should be allocated so as to maximize a function

$$\varphi_{\underline{d},p_k}(\mathscr{I}^1_{p_k}(M), \mathscr{I}^2_{p_k}(M), \mathscr{I}^3_{p_k}(M)), \tag{3.25}$$

where $\mathscr{I}^i_{p_k}(M)$ is the channel capacity for sector S_i when the pattern $M \in \mathscr{K}$ is considered with the pair of chunks p_k. Thus, the first level of optimization introduced above would be derived as

$$\widehat{GMI}_{\underline{d},p_k} = \max_{M \in \mathscr{K}} \varphi_{\underline{d},p_k}(\mathscr{I}^1_{p_k}(M), \mathscr{I}^2_{p_k}(M), \mathscr{I}^3_{p_k}(M)). \tag{3.26}$$

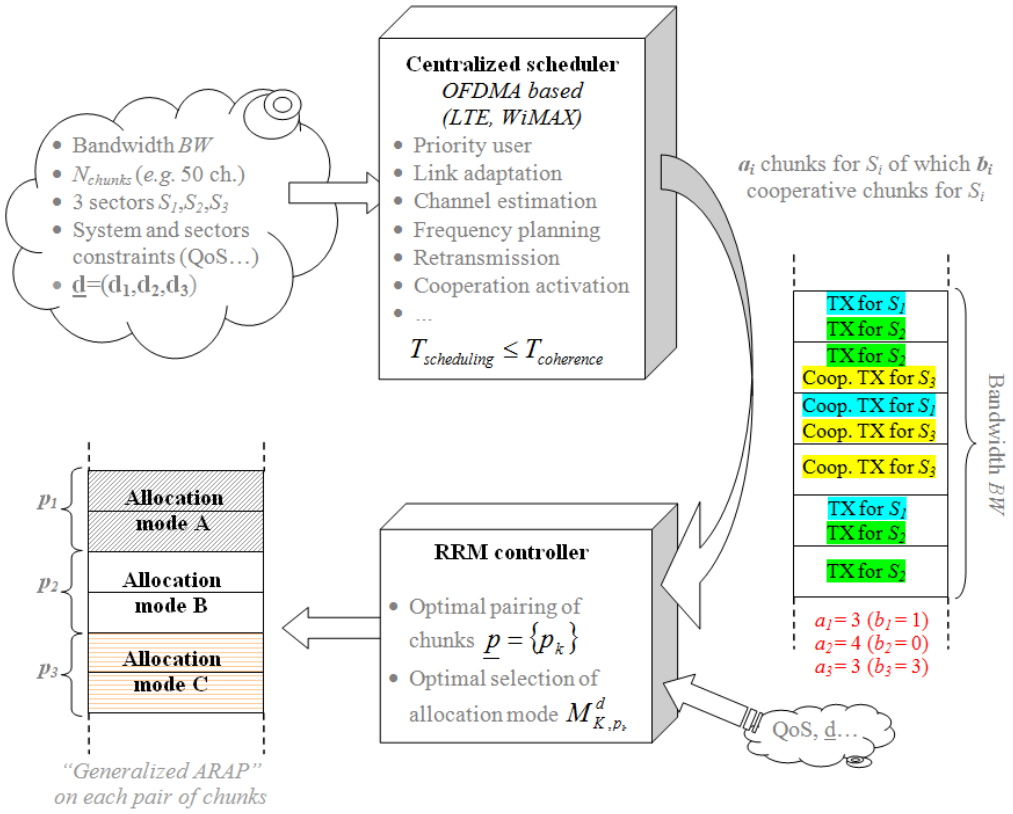

FIGURE 3.19 – Generalization of ARAP to more than 2 chunks.

The function $\varphi_{\underline{d},p_k}$ could compute a weighted-sum-rate instead of the sum-rate. The weight assigned to each partial channel capacity $\mathscr{I}^i_{p_k}(M)$ for a given pair p_k of chunks and pattern M would depend on weights assigned on other pairs of chunks $\{p_i\}_{i\neq k}$ and on QoS requirements. For instance, Equation (3.27) derives one possible expression for the weighted-sum-rate $\varphi_{\underline{d},p_k}$, where the weight $\alpha^{d_i}_{\underline{p},k}$ for sector S_i depends on the location of d_i, on the set $\underline{p}$ of all pairs $\{p_i\}$ and on the current index k of the pair p_k.

$$\varphi_{\underline{d},p_k}(\mathscr{I}^i_{p_k}(\mathscr{M}_{\mathscr{K}}(p_k))) = \max_{M\in\mathscr{K}} \sum_i \alpha^{d_i}_{\underline{p},k} \cdot \mathscr{I}^i_{p_k}(M). \tag{3.27}$$

The RRM controller should determine the pairing of chunks $\underline{p}$ according to an optimal mapping ϕ from the assignment of chunks done by the centralized scheduler :

$$\phi : \{BW\}_{\text{scheduler}} \mapsto \underline{p} = \{p_k\}. \tag{3.28}$$

ϕ is simply the permutation that optimally orders all chunks by pairs. The overall problem of optimization could be summed up as :

$$\widehat{GMI}_{\underline{d}} = \max_{\substack{\underline{p} \\ \text{QoS} \\ \text{CSI}}} \sum_{p_k} \widehat{GMI}_{\underline{d},p_k}, \tag{3.29}$$

$$\widehat{GMI}_{\underline{d}} = \max_{\substack{\underline{p} \\ \text{QoS} \\ \text{CSI}}} \max_{M \in \mathscr{K}} \varphi_{\underline{d},p_k}(\mathscr{I}^i_{p_k}(M)), \tag{3.30}$$

$$\widehat{GMI}_{\underline{d}} = \max_{\substack{\underline{p},\{\alpha^{d_i}_{\underline{p},k}\}_{k,i} \\ \text{QoS} \\ \text{CSI}}} \max_{M \in \mathscr{K}} \sum_i \alpha^{d_i}_{\underline{p},k} \cdot \mathscr{I}^i_{p_k}(M). \tag{3.31}$$

We assume that the centralized scheduler assigns chunks compliantly with QoS requirements and channel states. Nevertheless, extra constraints can be added at the inputs of the RRM controller. Consequently, we add in (3.29)–(3.31) 'QoS, CSI' as part of the maximization.

Two distinct pairs of chunks can suggest the use of two distinct resource allocation patterns. For instance, we assume on Figure 3.20 that we have six chunks. The adaptive mechanism computes three pairs of chunks (p_1, p_2, p_3) so that sector S_1 is advantaged with pair p_1, sector S_3 is advantaged with pair p_2 and resource are fairly assigned between the three sectors with pair p_3.

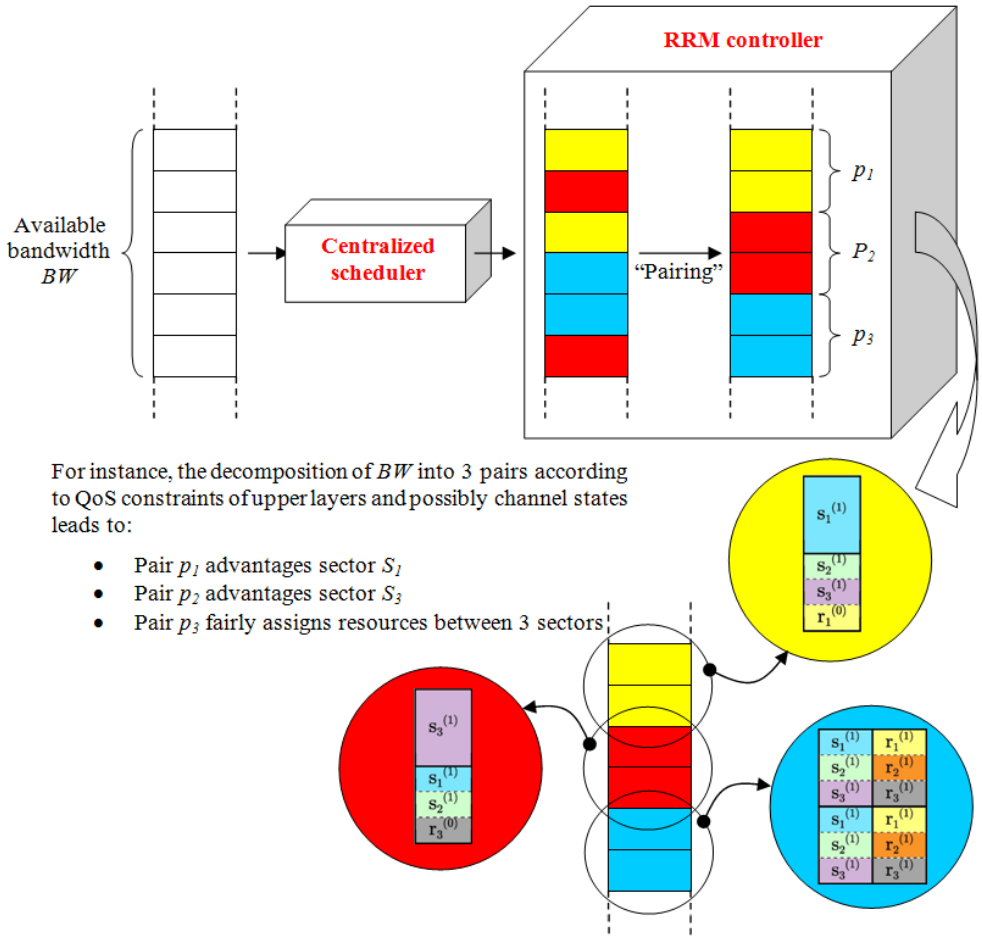

FIGURE 3.20 – Illustration of a general adaptive RRM mechanism

3.6 Conclusions

Novel and efficient RRM patterns were proposed in this chapter for downlink two-hop cooperative communication systems, where relays are half-duplex per chunk. We show by numerical evaluations that the advantages of the proposed solutions are twofold. First, overall power budget is lowered. Second, by protecting relays from inter-sector interference, effectiveness of cooperative transmissions is enhanced ; cooperation planning hence permits to notably increase the sum-rate in all investigated communication scenarios. These results are benchmarked by our simulation results.

We also evaluate the performance of an ideal and adaptive inter-sector resource allocation mechanism (ARAP) which selects the allocation pattern that maximizes the sum-rate for the given instantaneous channel instance and location of users. We observe that while cooperation is mostly not planned for border-cell users (cooperative transmissions do not help in extending sector coverage), the area of the cell in which cooperative transmissions improve performance is notably extended in comparison to standard cooperative RRM patterns. We success in enlarge the areas in cells where cooperation ameliorates performance, while limiting the interference caused to neighbour sites.

Further work could focus on the improvement of cooperation effectiveness for cell-edge users which suffer the most from inter-sector interference. The proposed generalization of the adaptive process for resource allocation could also be implemented and benchmarked for more realistic systems.

Chapter 4

Adaptive Interference Handling Techniques

In-band interference drastically limits performance of wireless communication systems where a same spectrum is shared by some network equipments in the same geographical area. While interference degrades differently the quality of communication, most of the time radio resource management algorithms do not exploit any information on the type of interference experienced at the receiver. The focus of this chapter is to define a methodology to classify the interference experienced at the receiver. After investigating previously proposed solutions on the domain [13], we come out with a novel three-regime in-band interference classifier. The advantage of the proposed interference classification is to be less complex than previously proposed solutions and, implementable in practical communications contexts.

Furthermore, the proposed interference classifier will be exploited as input information of two interference aware power allocation algorithms proposed in Chapters 5 and 6.

The chapter is organized as follows. After introducing our motivations, proposal and the work related to it, we recall in Section 4.2 some preliminary knowledge on interference processing techniques. Our proposed classifier is introduced in Section 4.3 where we focus on the two-user case. We first define in details each of the three proposed interference management strategies. Second, we evaluate the goodness of the proposed interference classifier in terms of achievable rate and SNR. We lastly extend this work to the n-user case in Section 4.4 before concluding with Section 4.5.

4.1 Introduction

Future wireless communication systems are targeting single-frequency deployment to further improve the system's capacity. Nevertheless, in modern communication systems a large variety of heterogeneous networks which consist in different cell scales - ranging from macro to micro, pico and even femtocells - may potentially share the same spectrum in the same geographical area. Although aggressive frequency reuse results in a significant potential increase of system capacity, it also generates additional in-band interference. Hence performance experienced by users may be drastically limited by interference. Efficient sharing of spectrum is not an easy task. Advanced interference management schemes are indeed crucial to efficiently solve the trade-off between band efficiency and communication robustness. Therefore, in this chapter we first present currently and commonly proposed interference management techniques, then we propose and analyse a novel interference classifier which will be adopted in Chapters 5 and 6 to perform a power allocation algorithm which minimizes the power budget under individual rate constraints.

4.1.1 Motivations

In interference-limited scenarios, transmitters and receivers must fight in-band interference to ensure to meet their QoS requirements. Communication robustness can be achieved by help of appropriated interference processing techniques (see Section 2.4). However, performance of these techniques is lead by a trade-off opposing spectrum sharing to communication robustness. More the spectrum is shared, more the nodes have transmission resources to achieve high data-rate communications but unfortunately higher is in-band interference. Nevertheless, interference is not just interference ! Interference actually carries information and has a structure that can be potentially exploited in mitigating its effect. Consequently, a strong interference scenario does not necessarily affect more transmission performance than a weak interference scenario. It depends first on the strategy employed by the receiver to deal with interference, and second on how efficient is this strategy contingent on the momentary communication context.

In fact, each interference mitigation technique implicitly assumes a specific scenario of interference to be applicable (*i.e.,* perceived power of interference at destination belongs to a specific range). Intuitively, the noisy technique cannot be applied to cope with in-band interference when the interfering source transmits with high power and is located very close to the destination. Indeed, destination would thus be highly interfered by the undesired neighbour source ; it would result in a low SINR at destination, which does not fit with the noisy strategy. Just the opposite, when the interfering source transmits with low power and is far away from the destination, the receiver perceives a high SINR : interference does not really affect the reliability of decoding information. The receiver can hence hardly adopt a SIC-based technique for decoding first the interfering signal.

These two simple but realistic scenarios illustrate that a single interference mitigation technique cannot perform well for all values of system and channel parameters. From this observation follows the idea of an adaptive solution that monitors the momentary scenario of interference. The focus of our work is so to adopt the interference mitigation technique the best suited to the momentary link quality experienced by each receiver. Several issues can be addressed by such an adaptive handling of in-band interference. More generally, a complex problem is made easier by adopting a scheme that is well suited to derive its

solution ; it is the concept of 'Divide-and-Conquer' theory. This adaptation of interference mitigation technique will be the object of Chapters 5 and 6.

At last, most of candidate techniques for handling in-band interference have been proposed by Information Theory. Admittedly some of them perform very well theoretically ; however they may suffer from infeasibility in practice because of excessive computational complexity or strict operating assumptions. Such limitations are imposed, for instance, by SIC-based techniques which can require infinitely long capacity-achieving codes, or by simultaneous superposition coding which is up to now too complex to be used in practice. In our work we suggest the use of techniques which can be implemented in practical systems without stringent limitations.

4.1.2 Contributions

The work presented in this chapter has been patented in [18]. In our proposal we design a novel three-regime in-band interference classifier which exploits momentary system QoS requirements and links quality between interferers to destination and source to destination. Three regimes of interference are introduced and investigated. These regimes realize a non-overlapping partition of the interference region. Each regime is related to a specific interference management technique, which is proved to process efficiently interference only within its regime.

Let us assume that there are n interfering 'source-destination' pairs. Therefore, a given receiver d_{i_0} perceives $n-1$ interfering signals. With our method, the receiver d_{i_0} classifies each of its $n-1$ interfering signals, for instance y_{j_1}, into one of the three proposed regimes of interference, according to a given communication context and a given set of QoS constraints. The selected regime states with which interference management technique the interfering signal y_{j_1} should be processed. Since such a regime is selected for each of the $n-1$ interfering signals that affect d_{i_0}, a $(n-1)\times 1$ vector of interference regimes is so computed for d_{i_0} (one regime of interference per interfering signal). This $(n-1)\times 1$ vector is likewise defined for each of the n receivers.

The proposed classifier permits hence to estimate the n vectors of interference regimes that comply with the momentary communication context and QoS constraints. Consequently, this classifier determines how receivers should process their interfering signals to ensure the QoS constraints will be met. The main contribution of this chapter is to adaptively cope with in-band interference by exploiting the momentary communication context.

4.1.3 Related Works

The idea presented in this chapter was motivated by some recent advancements in the domain of interference management with the derivation of an in-band interference classification into five regimes for the two-user interference channel [13]. Most of literature addresses the problem of the two-user interference channel. It is in fact the most simple, but however relevant, system model that lets to describe the scenario involving two neighbour pairs 'transmitter-receiver' sharing a common frequency band. The receiver d_i listens to information messages sent by its transmitter s_i, whose decoding is affected by in-band interference caused by simultaneous transmissions of s_j.

Performance of interference channel is conventionally characterized by its achievable rate region [31, 42–44, 122]. Since the boundaries of this region defines the best pair of rates

that can be simultaneously transmitted with arbitrarily small error probability, research in information theory field keeps trying to stretch this region and to adopt strategies that meet closer boundaries.

Carleial [73] in 1975 proposed one of the first valuable results for interference mitigation : the degradation caused by interference does not necessarily result from theoretical limitations but rather from the communication techniques employed. Thereby, the author shows that a strong scenario of interference does not always harm more than a scenario where interference is weak ; by decoding first interference and then subtracting it to the received signal, the receiver is able to decode its wished signal and achieved the same performance in terms of channel capacity than the one met without interference.

Few years later, based on the work presented in [31, 36, 41, 73], Han and Kobayashi [12] proposed an advanced model for the interference channel that extends previous achievable rate regions. With use of *simultaneous* superposition coding, the authors model each transmitter s_i as a 'virtual' pair of sources $s_i^{(p)}$ and $s_i^{(c)}$. The first and second sources respectively send *private* and *common* messages that both receivers listen to. Whereas common messages sent by $s_i^{(c)}$ must be decoded by both receivers d_i and d_j, private messages coming from $s_i^{(p)}$ are exclusively intended to d_i and are so ignored by d_j, *i.e.,* treated as an additional source of noise. Such a simultaneous superposition coding is proved to outperform other employed strategies, such as *sequential* coding used in [41].

Recently, Etkin et al. [13] extend the work of Han and Kobayashi [12] by investigating how close interference handling strategies can approach outer bounds of the channel capacity of the two-user Gaussian interference channel. The authors propose and investigate specific interference management schemes which are less complex than the superposition coding scheme proposed in [12]. They prove that for any pair (R_1, R_2) in the interference channel capacity region, their schemes achieve the rate pair $(R_1 - 1, R_2 - 1)$ for all values of the channel parameters, *i.e.,* their schemes achieve rates within 1 bits/s/Hz of the capacity of the interference channel. To prove this result, authors need to define some new outer bounds of the capacity region as well as five regimes of interference, according to the strength of INR in comparison to SNR. Indeed the qualitative behaviours of the capacity is highly sensitive to the channel parameters (noise-limited or interference-limited scenarios) and each interference regime should be investigated individually.

A generalization of the point-to-point concept of degrees of freedom (see Section 2.2.2) is furthermore derived for interference-limited scenarios and aims at evaluating how degrees of freedom are affected by in-band interference. Comparisons are also made with baseline strategies of time/frequency orthogonalization and treating interference as noise.

The notion of degrees of freedom, which is a key factor for evaluating performance of schemes, should be related to the Diversity Multiplexing Trade-off (DMT) [123]. This trade-off basically states the relation between the multiplexing gain (or degrees of freedom) and the diversity order. Both gains rather have an asymptotic meaning but basically the multiplexing gain states the amount of available resources for communications in the system while the diversity order indicates the ability of the system to cope with channel fading. These two gains evolve in an opposite way, *i.e.,* they cannot be simultaneously increased. Many papers propose to investigate DMT and degrees on freedom in interference-limited networks [55, 124, 125] and extend work of Etkin et al. [13].

4.2 Preliminary on Adaptive Interference Handling

This section addresses most famous strategies to handle in-band interference perceived at receivers in wireless communication networks. A special attention will be paid to their performance contingent on the communication context. At last it will be investigated how the processing of in-band interference can be adapted to the momentary communication context so as to optimize QoS-based metric (maximization of rates, minimization of power) for all values of the channel parameters. Consequently, the concept of generalized degrees of freedom introduced in [13] will be exploited to this end.

We furthermore assume OFDMA-based communication systems where no specific techniques of interference avoidance is performed between cells [1]. Two reasons can corroborate such an assumption. First, the system does not have enough transmission resources to assign exclusive resources to each cell so as to isolate them. Second, the system does not dispose of enough CSI-knowledge to perform an orthogonal inter-cell resource allocation because coordination between cells is impossible or not wished. Otherwise some other techniques could have been investigated by exploiting the presence of a backhaul or wire-line transmissions between transmitters and/or receivers (virtual MIMO, base-station cooperation [126]). However, the scope of our work is to investigate systems suffering from in-band inter-cell interference. Resources are then orthogonally allocated inside a cell ; in-band intra-cell interference is avoided and receivers have only to face in-band inter-cell interference. Consequently, we consider the presence of at most one pair 'transmitter-receiver' per cell and per unit of resources (sub-carrier, chunk).

4.2.1 Noisy Strategy : Treat Interference As Noise

The noisy strategy consists in ignoring perceived in-band interference and consequently processing it as an additional source of noise that enhances the level of background noise. Elements on this class of interference processing are given in Section 2.4.3.1. No specific processing is done to counteract prejudicial effects of in-band interference. Interfering signals are actually more than just noise since they carry information ; however this property is not exploited here. Intuitively, these noisy strategies work well in noise-limited communication context, *i.e.,* when INR is relatively low in comparison to SNR and INR is smaller than one. Indeed, with such scenarios in-band interference does not really affect the decoding reliability of the information message since in-band interference is lower than thermal noise. The variance of background noise is just slightly increased by addition of a new source of perturbation. Actually, a new noise variance can be defined as the sum of the true noise variance N_0 and the sensed power of in-band interference I : $N_0^{new} = N_0 + I$.

We investigate below how performance of these strategies evolve with variations of in-band interference level, in case of a symmetric channel. Let us define the ratio α between the logarithm of INR and the logarithm of SNR as firstly introduced in [13] :

$$\begin{aligned} & \alpha = \frac{\log_2 \mathrm{INR}}{\log_2 \mathrm{SNR}} \\ \Leftrightarrow \quad & \mathrm{INR} = \mathrm{SNR}^{\alpha}. \end{aligned} \tag{4.1}$$

This ratio is a good indicator to characterize the momentary communication context and state the impact of interference. Indeed, SNR or INR are not adequate on their own to

1. In case of non-cellular networks and clustered networks, 'cell' is also used in the remainder for referring to 'cluster' or group of devices within which coordination is performed

define how much a system is interfered. INR can be indeed very high, *i.e.,* much greater than the noise floor, but it does not harm if SNR is even greater.

In the noisy strategy in-band interference conveyed on the crossed-channel is treated as noise. The achievable rate $R^{\text{ach.}}$ of the pair 'transmitter-receiver' i disturbed by a neighbour transmitter j is expressed as :

$$\begin{aligned} R^{\text{ach.}} &= \log_2(1 + \tfrac{|g_{i,i}|^2 \cdot P_i}{N_0 + |g_{j,i}|^2 \cdot P_j}) \\ &= \log_2(1 + \tfrac{\text{SNR}}{1+\text{INR}}). \end{aligned} \tag{4.2}$$

The notion of generalized degrees of freedom is defined for large SNR and INR. Consequently $R^{\text{ach.}}$ can be approximated as :

$$\begin{aligned} R^{\text{ach.}} &\approx \log_2(1 + \tfrac{\text{SNR}}{\text{INR}}) \\ &\approx \log_2(1 + \text{SNR}^{(1-\alpha)}) \\ &\approx (1-\alpha) \cdot \log_2 \text{SNR} \\ \Rightarrow\ r_\alpha &= 1 - \alpha. \end{aligned} \tag{4.3}$$

For the AWGN channel, the number r_α of degrees of freedom (per second per Hz) cannot be greater than one. α is always positive within the considered range since SNR and INR are assumed large. The noisy strategy consequently meets the maximum of one degree of freedom per second per Hz when α is null (no interference) and is quite optimal for low values of α. Nevertheless this strategy collapses when in-band interference level enhances and α tends towards one per default since the amount of available degrees of freedom tends then towards zero. The behaviour of the noisy strategy is illustrated by the red straight line on Figure 4.5. When α is equal or greater than one, there is no point in trying to recover information while treating interfering signal as noise since the system is unable to detect information. With such scenarios, if the system wants to meet a reliable transmission (possibly at low rate) while conserving the noisy strategy, then power allocation or in-band interference avoidance techniques must be performed prior to transmission to modify the perceived power of signals : either enhancing SNR or lowering INR.

The noisy strategy is the most simple approach to deal with in-band interference. Its optimality is even proved for weakly interfered scenarios of communication where reliability of transmission is more subject to the noise floor than to the intensity of in-band interference (noise-limited scenarios). However, the noisy strategy is at fault when INR nearly equals SNR ($\alpha \approx 1$). In the literature, some papers propose some investigations on transmission contexts where in-band interference is very low in comparison to wished signal. For instance in [127] authors characterize the achievable rate region for more than two users in an interference network while in [128] the non-convexity of power control problems is addressed.

4.2.2 SIC-based Strategies

In opposition to the noisy strategy, SIC-based techniques (see Section 2.4.3.5) decode in-band interfering data rather than ignoring them. The general concept is to decode and cancel out first data of all sources of in-band interference in the aggregate received signal so as to obtain finally an interference-free signal that can be more easily decoded for recovering wished information. The order in which different signals are decoded is based on power with which each interfering flows are perceived. This concept was firstly introduce in Carleial [73] where the author shows that very strong in-band interference

does not reduce at all performance of transmission : since interference is so strong it can be perfectly subtracted from the received signal. Therefore the interference-limited system can meet same performance as the ones of the point to point AWGN channel which is not affected by in-band interference, just by noise.

SIC techniques seem well suited to highly interference-limited communication contexts where wished information signal is perceived with a power much lower than the received power of interfering signals. In terms of performance, SIC-based strategies permit to achieve one degree of freedom per second per Hz - as does the point to point channel. Nevertheless, this result is only ensured for highly interfered communication contexts. As mentioned in [13, 73, 129], it is assumed that the receiver is able to perfectly decode interfering data by handling information as noise. In other words, applicability requirements can be expressed as :

$$\begin{aligned} & \log_2(1+\tfrac{\mathrm{INR}}{1+\mathrm{SNR}}) \geq \log_2(1+\mathrm{SNR}) \\ \Leftrightarrow\ & \tfrac{\mathrm{INR}}{1+\mathrm{SNR}} \geq \mathrm{SNR} \\ \Leftrightarrow\ & \mathrm{INR} \geq \mathrm{SNR}^2 + \mathrm{SNR} \\ \Rightarrow\ & \log_2 \mathrm{INR} \geq \log_2 \mathrm{SNR}^2 \\ \Leftrightarrow\ & \alpha \geq 2. \end{aligned} \tag{4.4}$$

This result is illustrated by the purple line on Figure 4.5. For α greater than 2, the number r_α of degrees of freedom is equal to one ; this result is identical to the number of degrees of freedom achieved by the point to point channel which is not affected by interference ($\alpha = 0$).

In conclusion, SIC-based strategies guarantee theoretically to achieve the maximal number of degrees of freedom, whenever in-band interference predominates power of information signal. Nevertheless, some implementation limitations such as complexity or reliability of channel estimation should not be forgotten. Moreover, to ensure robustness of SIC-based techniques in scenarios where interference is moderately strong (α slightly lower than two), infinitely long capacity achieving codes should be employed.

4.2.3 Time/Frequency Sharing

This section gives some elements on performance of time-sharing and frequency-sharing techniques (TDM, FDM). Resources are here orthogonally shared between 'transmitter-receiver' pairs to avoid in-band interference. In case of an equal resource allocation between n pairs, each pair benefits from a $\frac{1}{n}$-fraction of the overall amount of degrees of freedom. Such a result is guaranteed for all communication contexts and does not depend on α-value since all transmission have been made orthogonal and consequently independent. Even for $n = 2$ pairs performance of time and/or frequency sharing is quite far from the one degree of freedom per second per Hz that noisy or SIC-based strategies can meet since orthogonal techniques just achieve an half degree of freedom per second per Hz. Nevertheless, this half-degree is not contingent on a specific range of α values and is furthermore constant for all value of channels. This result defines the lower-bound of achievable performance.

$$R_i^{\text{ach.}} = \frac{1}{n} \cdot \log_2(1+\mathrm{SNR}_i) \quad \forall i \in \{1,\ldots,n\}. \tag{4.5}$$

4.2.4 How Adaptation Can Be Achieved ?

The perceived power of information and interfering data closely depends on the experienced momentary communication context (location of neighbour transmitters, distance

between transmitter and receiver, fading and shadowing events, noise). In some contexts interfering sources are remote and insignificantly affect decoding of information data ; in some other highly interfered contexts information data is hardly detectable since information is 'swamped' by in-band interference. In previous subsections it was proved that that some strategies for handling with in-band interference work well in particular communication contexts but are bad in others. For instance we investigated two opposite strategies where interference is either entirely ignored or entirely decoded. Both strategies achieve one degree of freedom per second per Hz but not within the same α-ranges. The motivation of this subsection is twofold. First, in-band interference can be more efficiently fought and so reliability of decoding information data can be enhanced if the adopted in-band interference handling strategy is adapted to the momentary communication context [130, 131]. Adaptive interference processing lets select the strategy the best suited to the current communication scenario. Great improvements are obtained in comparison to fixed embedded interference strategies that collapse when they face an unexpected scenario of in-band interference. Second, some other strategies are considered as alternatives to noisy and SIC-based strategies. Ideally, each strategy works well within a α-range disjoint of the optimality range of other strategies. As a result all considered strategies complement each other and optimal results are met for all values of channel parameters.

Two approaches are introduced below to investigate how adaptation can be reached to efficiently cope with in-band interference. First [12] proposes superposition coding by dividing data flows of transmitters into two kinds of traffic : first a common data flow and second a private data flow. Second, some theoretical surveys try to characterize performance of interference channels and exhibit a five-level classification of perceived interference at destination [13, 125].

4.2.4.1 Han and Kobayashi Model : Superposition Coding

In 1981 Han and Kobayashi [12] derived a new model for the two-user Gaussian interference that lets extend the achievable capacity region in comparison to previous work [31, 36, 41, 73]. Let us recall that the capacity region of the two-user interference channel is the set of all pairs of rate $(R_1; R_2)$ that can be simultaneously met by both 'transmitter-receiver' pairs with arbitrarily small error probability. Authors proposed to output, at the coder, two types of data flows with different features. A first *private* data flow for an exclusive receiver and a second *common* data flow intended by all receivers. Each destination receives both flows output by both transmitters ; there are consequently four kinds of data listened to by receivers.

Private data, sent by the source $s_i^{(p)}$ at transmitter i, are only devoted to their intended destination d_i. Neighbour destinations d_j $(j \neq i)$ are unable to decode private data from $s_i^{(p)}$ and consequently process them as in-band interference. On the other hand, common data sent by the source $s_i^{(c)}$ at transmitter i are addressed to both destinations which are able to decode them. The ability of crossed destination d_j to decode common data sent by $s_i^{(c)}$ does not mean that these data convey useful information it (see Figure 4.1). Consequently we understand that either two different code books (a first private code book and a second shared code book), or two different kinds of encoding must be used by each coder. The technique which consists in aggregating such a way many data flows is known in literature as simultaneous superposition coding [2, 132, 133]. Basically, superposition coding scheme stands for the superimposition of constellations of different users that transmit simultaneously at the encoding step ; it results that the transmitted signal is the aggregation of

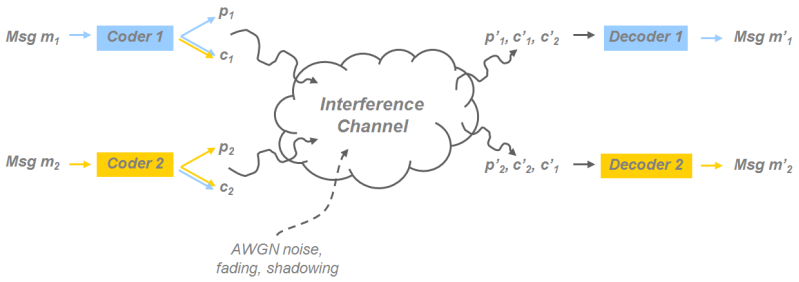

Figure 4.1 – Han and Kobayashi model for superposition coding : private and common information.

all individual signals (see Figure 4.2).

$$x[m] = x_1[m] + x_2[m] \tag{4.6}$$

where $x[m]$ is the transmitted signal at instant m and $x_i[m]$ is the signal intended for user i. The decoding step is a SIC-based strategy where the transmitted constellation point of one user is decoded first , followed by decoding of the second constellation point (see Figure 4.3).

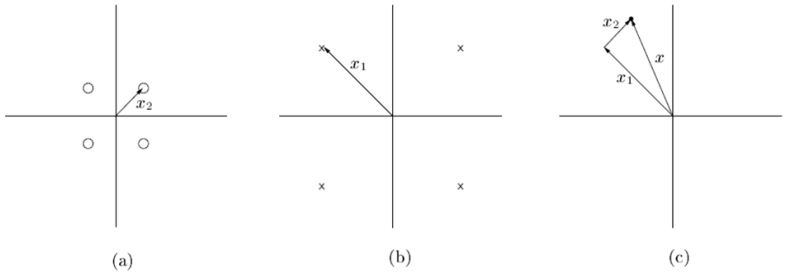

Figure 4.2 – Superposition encoding example. The QPSK constellation of user 2 is superimposed on top of that of user 1.

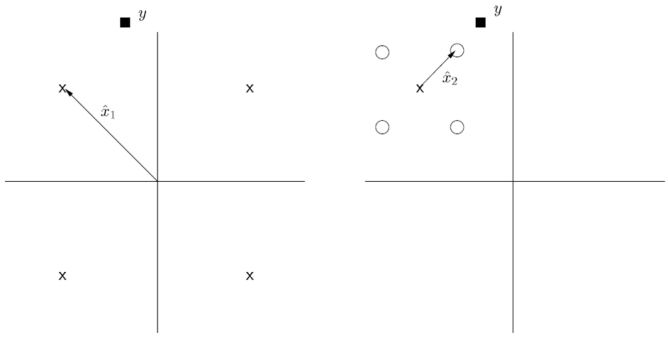

Figure 4.3 – Superposition decoding example. The transmitted constellation point of user 1 is decoded first, followed by decoding of the constellation point of user 2.

With the Hand and Kobayashi model, the combination of private and common data flows at the coder is so achieved by superposition coding. As mentioned in [13], while this model allows myriads of possibilities to split the transmitted signal into a private

and a common part, it is not well defined how to define the ratio between the amount of private data and the amount of common data. But we can easily assume that this ratio can be adapted to the encountered in-band interference at receiver so as to fit efficiently to the current communication context. This model is quite generic and lets derive a lot of strategies. For instance, both strategies introduced in the beginning of this section may be easily recovered by Han and Kobayashi model. The noisy strategy is nothing else than a full-private scheme : in-band interference is entirely considered as belonging to background noise, while SIC-based strategy is a full-common scheme where in-band interference is fully decodable by receivers.

Nevertheless such a simultaneous superposition coding scheme suffers from some restrictive limitations. First, this scheme hardly passes to an interference channel without coordination between transmitters or genie-aided transmitter. Superposition coding fits well to a one-to-many system (broadcast channel, downlink mode in a cellular network) where a single transmitter wants to superimpose each data flow of users. We are more interested in the many-to-one system (multiple access channel) where full-CSIT knowledge as well as interfering data are not provided for transmitters. Second, such myriads of configurations drastically increase the complexity of coders and decoders. Lastly, but not the least, superposition coding remains for the moment a theoretical concept that cannot be employed in practice. In fact, no capacity achieving code that lets superimpose two data flows is known.

4.2.4.2 Diversity Multiplexing Trade-Off and Interference Classifier

Two concepts are widely adopted in the literature to characterize features of a system with its space-time coding scheme. The first one is the notion of diversity gain whereas the second is the multiplexing gain, also called degrees of freedom. Both gains are closely related to systems and coding scheme parameters.

On the one hand the diversity gain describes the abilities of the system to counteract channel fading during transmissions. As mentioned in [123], the diversity gain intuitively corresponds to the number of independent faded paths that a symbol passes through ; in other words, the number of independent fading coefficients that can be averaged over to detect the symbol. A channel with more diversity has smaller probability to be in deep fades. Figure 4.4 illustrates how high diversity helps in reducing the probability to remain a long time in deep fade ; deep fade events correspond to peaks while the red straight line stands for the average behaviour. Diversity can be increased in space (spatial diversity) by adding antennas at transmitter (transmit diversity), at receiver (receive diversity) or both ; new antennas indeed add independent fading channels, what increases the diversity order. In a general system with m transmit and n receive antennas, there are in total $m \times n$ random fading coefficients to be averaged over ; hence the maximal (full) diversity gain provided by this channel is mn. The adopted space-time coding scheme can possibly lower this full diversity gain (see for instance Repetition coding, Alamouti, V-Blast with ML and V-Blast with nulling in Tse and Viswanath [2], Tse [134]). Diversity can also be increase in time and frequency domains. Since we assume wideband instead of narrowband channels, the transmission bandwidth W is greater than the coherent bandwidth W_c of the channel ; channels fading is then not flat but frequency-selective, which provides frequency diversity. Time diversity is achieved by averaging the fading of channel over time, *i.e.,* by interleaving codewords through (nearly) independent fading gains. An asymptotic approach to define the achievable diversity gain d uses the average error probability : $P_{\text{err}} \approx \text{SNR}^{-d}$ at high

SNR values.

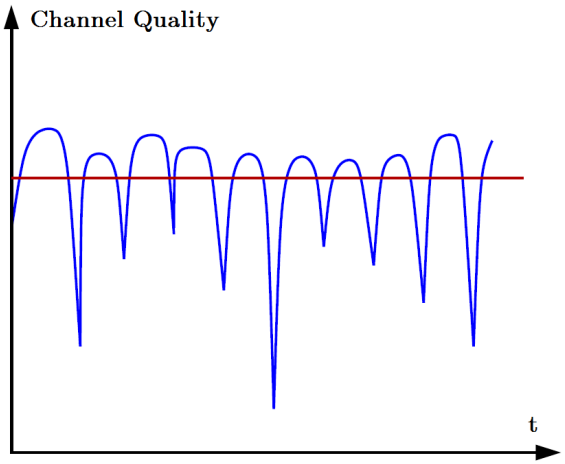

Figure 4.4 – Illustration of channel diversity where the duration of deep fade events is minimized by fast changes. Here channel quality in ordinate axis may refer to CQI metric.

On the other hand, if the path gains between individual transmit-receive antenna pairs fade independently, multiple parallel spatial channels are created. In case of multiple-antenna channel with m transmit and n receive antennas, the total number of parallel spatial channels is $\min m, n$. This amount of resources to communicate is the number of freedom degrees ; this characterizes the number of independent information symbols which can be transmitted in parallel through these spatial channels. A system whose signals are received across multiple directions benefits from multiple degrees of freedom for communication. The number of freedom degrees is also called spatial multiplexing gain which states for the information novelty (higher rate) in transmission whereas diversity states more for redundancy and reliability. The spatial multiplexing gain is in fact the 'pre-log' factor when communication rate R is expressed in logarithm form : $R = r \cdot \log \mathrm{SNR}$. The gain r defines how many dimensions are available for communicating. Note that amount of freedom degrees can also be increased via scattering, even when antennas are close together, since scattering environments modify directions of beams Poon et al. [135].

The multiplexing gain can be also thought as the margin in comparison to the AWGN capacity of the point to point channel which scales at high SNR as $C_{\mathrm{awgn}} \approx \log \mathrm{SNR}$. The notion of generalized degrees of freedom is introduced like this in [13] ; generalized degrees of freedom are thus a direct generalization of the measure of available channel resources for point to point channel to the interference-limited scenario. This aims to quantify how in-band interference affects and reduces the available resources for communication. Symmetric as well as asymmetric cases are considered for the two-user Gaussian interference channel with single-antenna devices. There is at most one degree of freedom per second per Hz but different schemes are investigated to counteract in-band interference reduction and maximizing the multiplexing gain. In [55, 125] authors generalized results to the MIMO and K-user interference channels.

Diversity gains and spatial multiplexing gain interact together though the DMT. This trade-off links the diversity order to the multiplexing gain and shows that these two values cannot be jointly enhanced, since they evolve in opposition. Diversity order characterizes

the ability of system to achieve reliable communications (lower outage probability) with redundancy through several paths, while multiplexing gain characterizes the number of different flows that the system can simultaneously convey. What this trade-off states is that a system with its coding scheme has a limited amount of resources and can achieve either redundancy or multiplexing, but not both simultaneously [2, 123, 134, 136, 137]. Intuitively, to achieve a maximum diversity gain, a transmitter needs to communicate at a fixed rate R, which becomes vanishingly small compared to the fast fading capacity at high SNR (which grows like $\min\{n, m\} \log \mathrm{SNR}$). Thus, the transmitter is actually sacrificing all the spatial multiplexing benefit of the MIMO channel to maximize the reliability. Likewise, to maximize its spatial multiplexing gain a transmitter has to exploit in parallel all independent spatial channels, which prevents him from meeting a high order of diversity (each symbol encounters less independent fading coefficients).

The diversity-multiplexing trade-off can thus be formulated with the definition given below. We think of a scheme $\{\mathscr{C}(\mathrm{SNR})\}$ as a family of codes, coding over one single coherence block, one at each SNR level. $R(\mathrm{SNR})$ refers their data rate (in bits per symbol period) and $P_{\mathrm{err}}(\mathrm{SNR})$ the ML probability of detection error.

Definition 1. *A scheme $\{\mathscr{C}(SNR)\}$ is said to achieve spatial multiplexing gain r and diversity gain d if the data rate*

$$\lim_{SNR\to\infty} \frac{R(SNR)}{\log SNR} \geq r, \tag{4.7}$$

and the average error probability

$$\lim_{SNR\to\infty} \frac{\log P_{err}(SNR)}{\log SNR} \leq -d. \tag{4.8}$$

For each r, define $d^*_{m,n}(r)$ to be the supremum of the diversity gain achieved over all schemes. Equivalently, for each d, define $r^*_{m,n}(d)$ to be the supremum of the multiplexing gain achieved over all schemes.

In case of slow fading, it is not possible to communicate reliability at a rate R since no averaging is possible over channel variations over time ; the ML probability of detection error $P_{\mathrm{err}}(\mathrm{SNR})$ is then replaced by the outage probability $P_{\mathrm{out}}(\mathrm{SNR})$ in the definition given above.

Some papers propose to investigate this DMT and extend results for the interference channel [13, 55, 124, 125, 138]. Their aim is more in maximizing the achievable rate of the interference channel ; that is why few interest is given to diversity order since achievable rate is maximized by minimizing the diversity order. Authors prove, as mentioned above, that achievable rate is sensitive to the scheme used to cope with in-band interference ; at the same time the efficiency of the employed scheme is contingent on the momentary communication context characterized by the value of α.

[13, 124] are the two most interesting reference handling with our purpose of adapting the processing of in-band interference to the current scenario of communication. In fact both papers derive five operating regimes of interference which are adjacent and non-overlapping, and whose bounds are α-dependent. The union of these five regimes covers

all possible values of α. This classification of in-band interference is derived as follows :

$$\begin{array}{lll} \text{Regime 1} & 0 \leq \alpha \leq \frac{1}{2} & \text{noisy interference} \\ \text{Regime 2} & \frac{1}{2} \leq \alpha \leq \frac{2}{3} & \text{weak interference} \\ \text{Regime 3} & \frac{2}{3} \leq \alpha \leq 1 & \text{moderately weak interference} \\ \text{Regime 4} & 1 \leq \alpha \leq 2 & \text{strong interference} \\ \text{Regime 5} & \alpha \geq 2 & \text{very strong interference.} \end{array} \tag{4.9}$$

The first and last regimes have already been introduced at the beginning of this section. Let us sum up the three other regimes. The strong regime is quite similar to the very strong regime, all data flows are common (Han and Kobayashi model) but the difference with the very strong regime lies in that here interference is not strong enough to be entirely decoded while considering its own signal as noise. Two last regimes are novelties derived from a genie-aided model that provide some knowledge on transmit signals at receiver side. More details about the definition and performance of these regimes are given in [13]. The graphic representation of the amount of generalized degrees of freedom subject to α value is a 'W-shaped' piecewise-continuous curve depicting performance over the five adjacent regimes of interference. This result is a special case of those derived in [124] where we restrict to the curve $d = 0$. The 'W-shaped' curve is illustrated on Figure 4.5 with the curve A-B-C-D-E-F. Different coloured straight lines illustrate behaviour of each scheme within their range of relevance : red, blue, green, yellow and purple respectively for the noisy, weak, moderately weak, strong and very strong regimes. The 'W-shaped' is indeed piecewise-continuous ; the dashed red line B-G stands for the α-range within which the noisy strategy is not optimal any more. Performance of TDM/FDM orthogonalization techniques is also illustrated and proved to be sub-optimal. However, treating interference as noise is optimal for all $\alpha \leq 2$ and time/frequency orthogonalization is also optimal for $\alpha \in \{\frac{1}{2}; 1\}$.

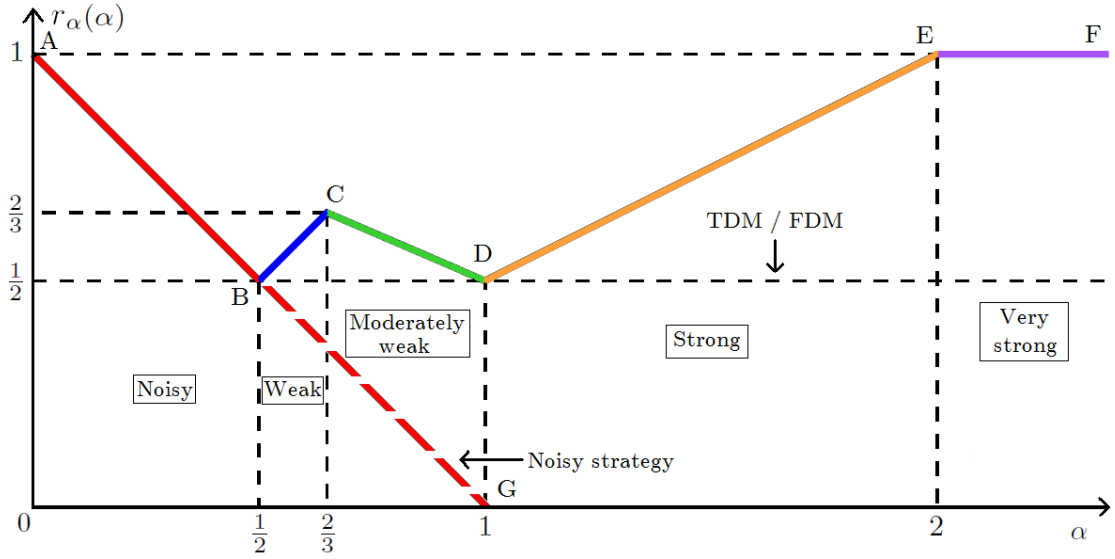

Figure 4.5 – Generalized degrees of freedom according to α-value. A 'W-shaped' curve exhibits a classification of in-band interference into five operating regimes.

In conclusion, α seems to be well-fitted to describe the momentary communication context and classify it in the relevant interference regime among the five previously defined.

The handling of in-band interference is specific to each regime and ensures to meet the best achievable performance for all values of channel parameters. Besides, the proportion of private and common information in the global transmit signal can be matched up with the five-level interference classification (full private, full common, or a ratio between private and common data that let to characterize the second and the third interference regimes). Nevertheless some results presented in this section need quite strict assumptions (genie-aided receiver, superposition coding for superimposing two kind of data flows) which cannot be ensured in practice. We are then motivated by deriving another classification for in-band interference which does not rely on theoretical notions which are not achievable in practice.

4.3 Proposed Slim Three-Regime Interference Classification

We propose hereafter a classifier of sensed in-band interference which can be easily implemented in an interference-limited system. In comparison to the five-regime in-band interference derived in [13], we develop in the remainder a classifier based on just three operating regimes of interference with each its specific strategies for handling in-band interference. Due to the reduction of the involved number or interference regimes, our proposal is of course suboptimal and less powerful than the classifier in [13]. Nevertheless, Etkin et al. were not motivated by providing a classification of in-band interference which can be easily employed in practice. They rather sought to characterize theoretically and closest the achievable rate region of the Gaussian two-user interference channel for all values of channel parameters ; this work necessitated to derive several interference regimes. They besides involved genie-aided models for dealing with the weak and moderately weak regimes. However, these genie-aided models are unrealistic in practice since they assume a knowledge of interfering signal is provided to receiver. Identically, results obtained with the superposition coding scheme of Han and Kobayashi [12] cannot be achieved for the moment in reasonable computation time since no capacity achieving encoding scheme is able to superimpose two different data flows.

Our work gets into this context of feasible implementation without rigid or unrealistic assumptions. We are motivated by providing an adaptive processing of in-band interference so as to more efficiently dealing with it, contingent on the momentary values of channel parameters and communication context. Such an adaptation is a major challenge in highly interference-limited networks since the sensed power of interference may greatly vary in time and thus its effects on decoding reliability at receiver. In case of QoS-constrained networks, operators must ensure in any communication context a sufficiently high QoS, even if their transmission with customers are drastically reduced by co-channel perturbations. In the remainder our three interference regimes will be introduced. They are based on relatively straightforward schemes which are known to perform well. One of the fundamental difference with the previously introduced work [12, 13] consists in encoding just one data flow at transmitter ; signals convey either private or common information but not both simultaneously.

For the sake of clarity, our classifier will be developed for two pairs 'transmitter-receiver' competing for a single time-frequency communication resource. The adopted model for our system is consequently the interference channel introduced in Section 2.2.1. We besides consider each pair is rate-constrained, *i.e.,* the pair i has to ensure the data rata $R_{tg,i}$ for its receiver ; constraints are besides known by both receivers. The work can easily be extended to more than two users or other QoS-constraints, as it will be shown in Section 4.4. Since we are interested in classifying the momentary in-band interference that the receiver

d_i encounters, the most fitted system model is then the multiple access channel formed by the receiver d_i and the two transmitters s_i and s_j. The source s_i wants to communicate with its destination d_i at the target rate $R_{tg,i}$ but their transmission is disturbed by a concurrent co-channel transmission initiates by the neighbour source s_j (which wants to transmit at rate $R_{tg,j}$ with its destination d_j). As detailed in Section 2.2.1 and shown on Figure 5.2, the original interference channel is so divided into two multiple access channels. In the remainder we will derive our classification for the viewpoint of destination d_i interfered by source s_j. The QoS-constraint of pairs is fundamental since this constraint will help to drive the classification of in-band interference, in line with the ability of receivers to decode or not received signals.

4.3.1 The Noisy Regime

Our first regime of interference is of course the noisy regime where in-band interference is not decoded by the receiver but rather ignored and treated as an additional source of noise. As we have already seen before, the noisy strategy can be thought as a full-private scheme (by considering the Han and Kobayashi model). Specific encoding and interleaving schemes may furthermore be employed to randomize the transmitted sequence of symbols so that it really appears as pseudo white noise for neighbour receivers.

Performance of this scheme in terms of generalized degrees of freedom has already been discussed above. Nevertheless, we derive below the main features of this regime. First of all, we have to define the range within which this noisy regime is optimal. Within our classification, this noisy regime is related to the incapacity of d_i to decode with arbitrarily small error probability the interfering message x_j conveyed by the crossed point-to-point channel. In other words, even in absence of interfering signal the crossed-path is in outage.

$$\begin{array}{rl} & R_j \geq \log_2(1+\delta_i) \\ \Leftrightarrow & \delta_i \leq 2^{R_j}-1 \end{array} \tag{4.10}$$

where $\delta_i = \frac{|g_{j,i}|^2 \cdot P_j}{N_0}$ is the INR perceived by d_i [2].

Then, under these conditions, the receiver d_i must decode its desired signal x_i in presence of background noise n_i and interfering signal x_j, while meeting its target rate :

$$\begin{array}{rl} & R_i \leq \log_2(1+\frac{\gamma_i}{1+\delta_i}) \\ \Leftrightarrow & \gamma_i \geq (2^{R_i}-1)\cdot(1+\gamma_i) \end{array} \tag{4.11}$$

where $\gamma_i = \frac{|g_{i,i}|^2 \cdot P_i}{N_0}$ is the SNR perceived by d_i.

By use of pilot messages and assuming slow-varying channels, d_i can sense the quality of the direct and crossed links in order to compute their CQI which are respectively SNR γ_i and INR δ_i. With knowledge of the value of δ_i, the receiver d_i is able to check if condition (4.10) is true or not ; in that event, the transmitter s_i can set its power based on (4.11) to meet its target rate $R_{tg,i}$.

At last, we investigate the asymptotic behaviour of this strategy (for large SNR and INR), by use of the α-metric. For more simplicity, we will restrict to the symmetric case. Our noisy regime is applicable if the crossed path is in outage while the direct path can

2. All inequalities will be expressed twice : first in terms of rates, then in terms of SNR and INR.

be decoded in presence of in-band interference.

$$\begin{array}{rl} & \frac{\mathrm{SNR}}{1+\mathrm{INR}} \geq \mathrm{INR} \\ \Leftrightarrow & \mathrm{SNR} \geq \mathrm{INR}^2 + \mathrm{INR} \\ \Rightarrow & \mathrm{SNR} \geq \mathrm{INR}^2 \\ \Leftrightarrow & \alpha \leq \frac{1}{2}. \end{array} \tag{4.12}$$

The derivation of the available generalized degrees of freedom r_α is useless since it has already been done in (4.3).

Likewise the classification in [13], our noisy regime is defined for $0 \leq \alpha \leq \frac{1}{2}$ but may also be used sub-optimally for greater values of α. Nevertheless, there is no point to adopt the noisy strategy beyond $\alpha = 1$ since rate would not linearly increase with SNR, even with infinite transmission power (the pre-log r_α is indeed null).

4.3.2 The Joint Decoding Regime

The second interference regime derived in our classification is named by *joint decoding* regime. Within this regime all information is common, *i.e.,* receiver d_i should decode both signals x_i and x_j to process optimally in-band interference, whereas in-band interference is not assumed strong enough to let d_i decode it while considering the wished signal x_i as noise. Consequently, both messages must be decoded together, *i.e.,* jointly. Nevertheless, such a problem of joint decoding seems quite hard insofar as there are two variables x_i and x_j to recover for just one single observation y_i ; the matrix that states this linear equation of decoding problem has so a rank deficiency. However, such rank deficiencies are quite usual ; consider for instance MIMO systems with more transmit antennas than receive antennas, MAC systems with single-antenna devices or the uplink mode in cellular networks without orthogonal resource allocation between users. Damen et al. [76, 79] proved there are powerful techniques to solve these rank deficiency equations. Authors used the concept of sphere decoding as well as lattice decoding with help of minimum mean square error generalized decision-feedback equalizer (MMSE-GDFE). The assumption of joint decoding has also been made in [13] for dealing with the strong regime.

Let us give a look at the applicability region of this second regime. In-band interference is too strong to be treated as noise, *i.e.,* the crossed path in absence of interference is not in outage any more. However in-band interference is not strong enough to employ a SIC-based technique. These two conditions translate as follows :

$$\begin{array}{rl} & \log_2(1 + \frac{\delta_i}{1+\gamma_i}) \geq R_j \geq \log_2(1+\delta_i) \\ \Leftrightarrow & \frac{\delta_i}{1+\gamma_i} \leq 2^{R_j} - 1 \leq \delta_i. \end{array} \tag{4.13}$$

As it was defined in Section 2.2.2, the region of achievable rate is characterized by the max-flow min-cut theorem in graph theory [51, 52]. Considering our multiple access channel and the assumptions stated in (4.13), the relevant cut is here the 'sum-rate' that precisely stands for the joint decoding strategy. The sum-rate in compliance with rate-constraints is defined by :

$$\begin{array}{rl} & R_i + R_j \leq \log_2(1 + \gamma_i + \delta_i) \\ \Leftrightarrow & \gamma_i \geq 2^{R_i+R_j} - 1 - \delta_i). \end{array} \tag{4.14}$$

The asymptotic behaviour of this joint decoding strategy is easily obtained. Indeed this strategy is jammed between the noisy strategy and the SIC-based strategy (see (4.13)).

Consequently, the α-range within which the joint decoding is optimal is lower bounded by (4.12) and upper bounded by (4.4). Thus it results :

$$\frac{1}{2} \leq \alpha \leq 2. \tag{4.15}$$

Lastly, assuming symmetric rate-constraints, the available amount of degrees r_α of freedom is easily derived :

$$\begin{array}{rl} & R^{\text{ach.}} + R^{\text{ach.}} \approx \log_2(1 + \text{SNR} + \text{INR}) \\ \Leftrightarrow & R^{\text{ach.}} \approx \frac{1}{2} \cdot \log_2(\text{SNR} + \text{SNR}^\alpha) \\ \Leftrightarrow & R^{\text{ach.}} \approx \frac{\max\{1,\alpha\}}{2} \cdot \log_2 \text{SNR} \\ \Rightarrow & r_\alpha = \frac{\max\{1,\alpha\}}{2}. \end{array} \tag{4.16}$$

4.3.3 The Very Strong Regime

The third regime has already been investigated above and involves the SIC-based strategy which consists in first decoding interfering signal x_j while treating desired signal x_i as noise, second subtracting the decoding signal x_j from the received signal y_i and finally decoding information signal x_i. This very strong interference regime is known to cause no transmission degradation and achieve the same performance as a point to point channel without in-band interference.

This regime is then relevant as soon as the crossed path is not in outage any more while information signal is handled as noise :

$$\begin{array}{rl} & R_j \geq \log_2(1 + \frac{\delta_i}{1+\gamma_i}) \\ \Leftrightarrow & \delta_i \geq (2^{R_j} - 1) \cdot (1 + \gamma_i). \end{array} \tag{4.17}$$

Since in-band interference has been decoded and subtracted from the received signal, the achievable rate is the same as the point to point channel :

$$\begin{array}{rl} & R_i \leq \log_2(1 + \gamma_i) \\ \Leftrightarrow & \gamma_i \geq 2^{R_i} - 1. \end{array} \tag{4.18}$$

It has already been proved that the SIC-based strategy is relevant for any α greater than 2 (see (4.4)). Furthermore, one degree of freedom per second per Hz is guaranteed :

$$r_\alpha = 1. \tag{4.19}$$

4.3.4 Performance of Three-Regime Classifier

Now that each regime has been individually investigated, the whole classifier can be considered and compared to the classification derived by Etkin et al. [13] and illustrated on Figure 4.5. The asymptotic behaviour of our three regimes is characterized by (4.3), (4.16) and (4.19) respectively for the noisy, joint decoding and very strong regimes of interference. The associated strategies for handling in-band interference in each regime are optimal within the α-range specified respectively by (4.12), (4.15) and (4.4). The amount of generalized degrees of freedom r_α available for transmission, depending on the momentary communication context characterized by α, is illustrated on Figure 4.6. The curve is also piecewise-continuous. The red and purple straight lines are identical to the former 'W-shaped' curve since these two regimes are the same. On the other hand, the weak,

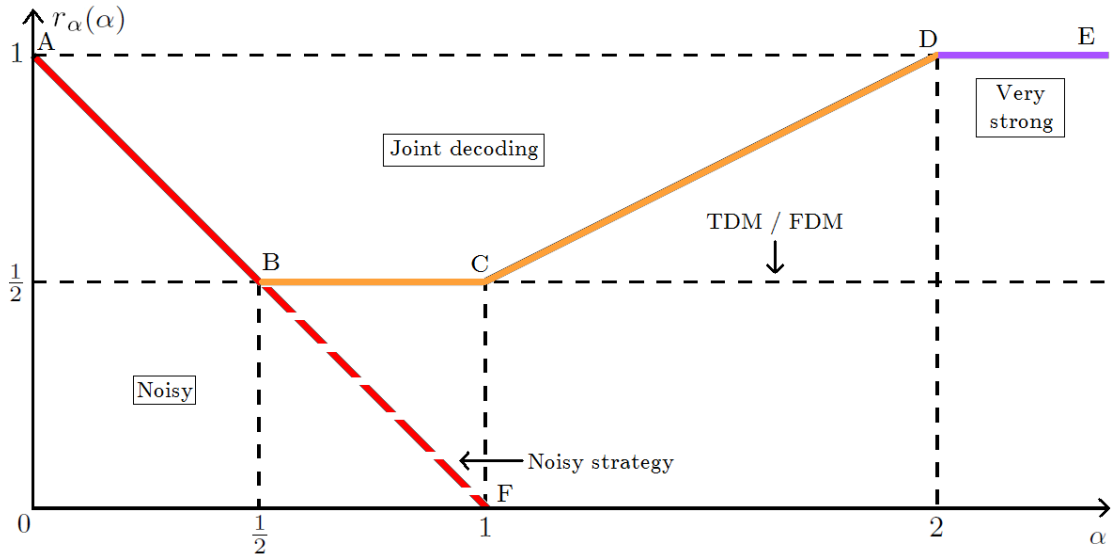

FIGURE 4.6 – Generalized degrees of freedom according to α-value for our proposed three-regime classification of in-band interference.

moderately weak and strong regimes in [13] have been substitute by our joint decoding regime, drawn by the yellow curve.

Figure 4.6 illustrates the amount $r_\alpha(\alpha)$ of generalized degrees of freedom that our classifier can achieve. Performance is described by the curve A-B-C-D-E. As expected, our classifier is proved to be outperformed by the former one (see Figure 4.5). We indeed achieve the same performance as [13], except for $\alpha \in \left[\frac{1}{2}; 1\right]$ where we meet the bound $r_\alpha = \frac{1}{2}$ of the suboptimal TDM/FDM techniques. However, such a bound is known to be achievable, whereas the two bounds derived in [13] for $\alpha \in \left[\frac{1}{2}; 1\right]$ are first of all theoretical and then cannot be met in practice (they need a genie providing knowledge of interfering message).

The comparison between Figures 4.5 and4.6 can get our results for quite reductive and not innovative, insofar as first we cannot do better than a scheme where resources are made orthogonal (for $\alpha \in \left[\frac{1}{2}; 1\right]$, line B-C) and second we do not extend previous results. Nevertheless, the innovation of our proposal does not reside in this asymptotic behaviour but more in the easy way to implement this classifier. In contradiction with the five-regime classifier where common and private data flows must be superimposed to deal with the weak and moderately weak regimes, our classifier does not impose such stringent restrictions.

Two cases can be considered :

- First, there is coordination between all devices (via a backhauling network for instance). In this case, the receiver d_i sensed quality of direct and crossed paths by measuring its SNR γ_i and INR δ_i via pilot messages. Then d_i notifies its neighbour transmitter s_j of its value of α. If $\alpha \leq \frac{1}{2}$, then s_j can encode its messages by outputting a private data flow that d_i cannot decode. For all other values of α, s_j must output a common data flow.
- The second configuration refers to a more general and simple case where if available, coordination is not exploited. Receiver d_i has not to notify its neighbour interferer s_j of its α value. Indeed both coders always output a common data flow (code books

are then known by each decoder) which is treated at the receiver either as a pseudo-private signal or a common signal, in line with the value of α. Consequently there is no need in exchanging information between receivers and transmitters for notifying them of the momentary communication context. The decision-maker is entirely the receiver which adapts itself to the current scenario.

In both cases, receivers have simply to evaluate their own sensed INR to check according to (4.10), (4.13) or (4.17) whether they have to face respectively a noisy, a joint decoding or a very strong regime. Once the momentary relevant regime has been identified, they can notify it to their transmitter which will compute the judicious transmission power to meet their constraint in rate. The process of identifying the relevant regime and adapting the process of in-band interference to it is elementary and does not request any additional feedback between devices.

Finally, let us note that the noisy strategy is optimal for α belonging to the range $\left[0; \frac{1}{2}\right]$ (red line A-B on Figure 4.6). However, the noisy strategy can also be used sub-optimally for α values beyond $\frac{1}{2}$ but performance will collapse from $\alpha = 1$ since no degree of freedom will be available (dashed red line B-F). The joint decoding strategy cannot be employed for any value of α smaller than $\frac{1}{2}$ since the crossed path is then in outage and cannot be decoded. For α between $\frac{1}{2}$ and 2, the joint decoding strategy is the only optimal scheme we propose (orange line B-C-D). This strategy could be used beyond $\alpha = 2$ but this would not result in any improvement since the maximal amount of degrees of freedom is already met. Lastly, from $\alpha = 2$, the SIC-based strategy can be employed and is proved to be optimal and less complex than the joint decoding strategy (purple line D-E).

4.3.5 Achievable SNR Region

In this last subsection our results are described with a non-conventional representation. Most of papers present their results with the region of achievable rates, in region $(R1; R_2)$; this achievable region is commonly a pentagon for the two-user MAC. This representation suits well to the problem of rate-maximization under power constraints. We propose to consider the region $(\delta_i; \gamma_i)$ for representing our results instead of the region $(R1; R_2)$. With an easy scalar transformation, the region $(\delta_i; \gamma_i)$ is equivalent to the region $(P_j; P_i)$ which is well adapted to the dual problem of power-minimization under rate constraints. We indeed quickly switch between regions $(\delta_i; \gamma_i)$ and $(P_j; P_i)$ with help of (4.20) and (4.21).

$$\gamma_i = \frac{|g_{i,i}|^2 \cdot P_i}{N_0} \quad \Leftrightarrow \quad P_i = \frac{N_0 \cdot \gamma_i}{|g_{i,i}|^2} \tag{4.20}$$

$$\delta_i = \frac{|g_{j,i}|^2 \cdot P_j}{N_0} \quad \Leftrightarrow \quad P_j = \frac{N_0 \cdot \delta_i}{|g_{j,i}|^2} \tag{4.21}$$

Our three regimes are respectively bounded by conditions (4.10), (4.13) and (4.17) while the strategy to perform within each regime achieves respectively the performance derived by (4.11), (4.14) and (4.18). For sake of clarity, three new variables are introduced :

$$A_i = 2^{R_{tg,i}} - 1, \quad A_j = 2^{R_{tg,j}} - 1 \quad \text{and} \quad A = 2^{R_{tg,i}+R_{tg,j}} - 1 = (A_i + 1)(A_j + 1) - 1. \tag{4.22}$$

Table 4.1 sums up the main results while Figure 4.7 illustrates them. In the region $(\delta_i; \gamma_i)$ our three regimes stand for three contiguous and non-overlapping areas ; the noisy, joint decoding and very strong regimes are respectively coloured in yellow, white and green. The applicability boundaries of regimes, recalled in Table 4.1, are drawn with dash-dot red

O_i	Scheme	Boundaries of applicability	Achievable SNR γ_i
1	Noisy	$\delta_i \leq A_j$	$\gamma_i \geq A_i(1+\delta_i)$
2	Joint decoding	$A_j \leq \delta_i \leq A_j(1+\gamma_i)$	$\gamma_i \geq A - \delta_i$
3	SIC-based	$\frac{\delta_i}{1+\gamma_i} \geq A_j$	$\gamma_i \geq A_i$

TABLE 4.1 – Performance of our three-regime interference classifier with boundaries of regimes and achievable SNR within each regime.

lines, while the blended shades of blue specify the SNR-achievable region $\mathscr{R}_i^*$. The SNR-achievable region is the set of all pairs (δ_i, γ_i) that ensure reliable transmissions at rate $R_{tg,i}$. $\mathscr{R}_i^*$ is lower-bounded by the solid blue lines $(\mathscr{D}_i^k)_{k=1..3}$. Assuming sources are constrained by maximal transmit power $P_{i,\max}$ and $P_{j,\max}$, it follows from (4.20) and (4.21) that γ_i and δ_i are respectively bounded by $\gamma_{i,\max}$ and $\delta_{i,\max}$.

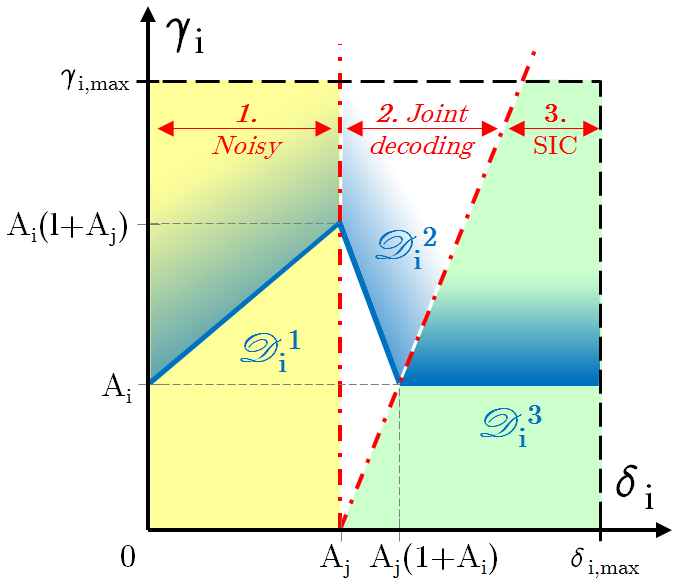

FIGURE 4.7 – Achievable SNR region $\mathscr{R}_i^*$.

Even if Figure 4.7 is not a conventional way to represent the problem of power minimization under rates constraints, its understanding is quite straightforward. The receiver d_i estimates its INR δ_i and transfers this value to the abscissa-axis. In line with this value of δ_i and depending on its SNR value γ_i (set by the transmit power of its source), d_i has just to check to which regime belongs the current point (δ_i, γ_i) to determine how interfering signal x_j should be handled. The regime within which (δ_i, γ_i) is located is referred to by $O_i \in \{1, 2, 3\}$.

On the other hand, for power allocation goals, the pair '$s_i - d_i$' can also use these results to set its transmit power P_i so as to ensure its target rate $R_{tg,i}$ will be met. P_i should be set such that the point whose abscissa is the current value of δ_i and whose ordinate is γ_i defined by (4.20) belongs to the blended shades of blue. Under these conditions, the target rate $R_{tg,i}$ is guaranteed.

4.4 Three-Regime Classifier for n-user Interference Channel

Up to now we have considered as model the two-user multiple access channel illustrated on Figure 2.1b. We started with the two-user interference channel from Figure 2.2a but we focused on the viewpoint of one of both receivers and considered instead the related two-user MAC. In this last section it will be investigated how the three-regime classification of in-band interference introduced in Section 4.3 can be extended to a wider system with n concurrent users sharing a single time-frequency resource.

4.4.1 Generalization of the System Model

For sake of clarity, generalization will be provide only for the 3-user case but the reader will understand that the work proposed in this section can be easily adopted for any value of K. The system model adopted in the remainder is shown on Figure 4.8a. Three transmitters named by s_i, s_j and s_k send respectively a signal x_i, x_j and x_k on the shared resource block ; the receiver d_i listens a linear combination y_i of these three signals and the additive noise z_i.

$$\begin{cases} y_i = g_{i,i} \cdot x_i + g_{j,i} \cdot x_j + g_{k,i} \cdot x_k + z_i \\ y_j = g_{i,j} \cdot x_i + g_{j,j} \cdot x_j + g_{k,j} \cdot x_k + z_j \\ y_k = g_{i,k} \cdot x_i + g_{j,k} \cdot x_j + g_{k,k} \cdot x_k + z_k \end{cases} \tag{4.23}$$

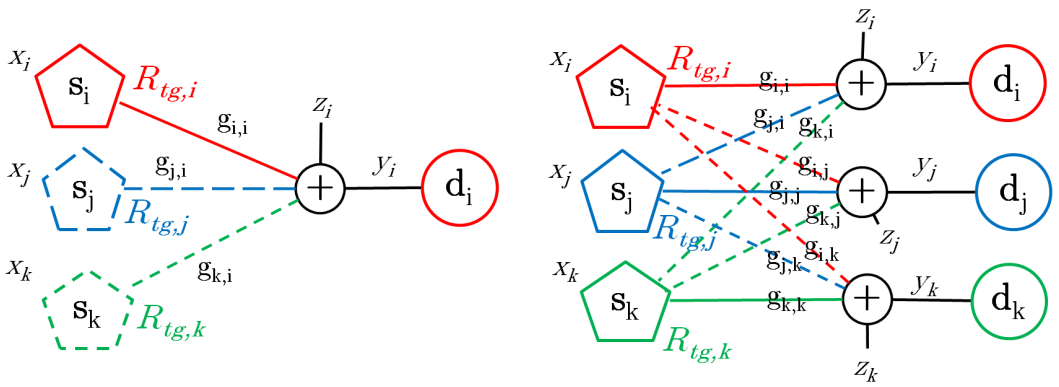

(a) 3-user MAC (b) 3-user IC

Figure 4.8 – Three-user Multiple Access and Interference Channels where pair '$s_i - d_i$' is QoS-constrained with a target rate $R_{tg,i}$.

Our system model is derived from the three-user interference channel shown on Figure 4.8b. Each pair 'source-destination' has a target rate it wants to meet. Direct and crossed paths are respectively drawn with straight and dashed lines.

For the pair '$s_i - d_i$' the following CQI metrics are defined :

$$\begin{cases} \gamma_i = \frac{|g_{i,i}|^2 \cdot P_i}{N_0} \\ \delta_{j,i} = \frac{|g_{j,i}|^2 \cdot P_j}{N_0} \\ \delta_{k,i} = \frac{|g_{k,i}|^2 \cdot P_k}{N_0}. \end{cases} \tag{4.24}$$

The receiver d_i can easily estimate these three metrics without requiring specific signalization ; pilots are commonly and frequently sent for channel monitoring and link adaptation,

pilots are exploited to compute these three metrics. New variables are besides defined $\forall\{m,n\} \in \{i,j,k\}$:

$$A_m = 2^{R_{tg,m}} - 1, \quad A_{mn} = 2^{R_{tg,m}+R_{tg,n}} - 1 \quad , A_{ijk} = 2^{R_{tg,i}+R_{tg,j}+R_{tg,k}} - 1. \tag{4.25}$$

4.4.2 Regimes Boundaries and SNR-Achievable Region

To generalize our results of the two-user case to the n-user case, we have to consider a multi-dimensional problem. For $n = 3$ for instance, the previous region of interest $(\delta_i; \gamma_i)$ becomes $(\delta_{j,i}; \delta_{k,i}; \gamma_i)$. In the multi-user case, our in-band interference classifier always counts three regimes of interference per crossed-paths. In other words, the receiver d_i must always choose among the three strategies (noisy, joint decoding or SIC-based) which is the relevant one for optimally processing the interfering signal x_j. However, the information signal x_i is recovered by the combination of all the strategies adopted to process the $(n-1)$ interfering messages $\{x_j\}_{j\in[1,\dots,n],j\neq i}$.

If $O_{j,i}$ refers to the strategy employed by d_i to process the interfering signal x_j, then $O_{j,i} \in \{1,2,3\}$ and there are $3^{(n-1)}$ possible combinations of strategies to recover the information signal x_i. Each combination is expressed as the vector $\underline{O_i} = (O_{j,i})_{j\in[1,\dots,n],j\neq i}$. To characterize the SNR-achievable region, we have to adopt the same approach as for the rate-achievable region ; that is to say, we have to consider the max-flow min-cut theorem. This theorem consists in investigating all possible cuts in the graph and keeping all those that maximize the sum of the rates. We can prove this is equivalent to investigate all the $3^{(n-1)}$ combinations of strategies $\underline{O_i}$. In the remainder of the section, we will set $n = 3$.

To recover x_i there are thus $3^{(3-1)} = 9$ possible combinations to investigate. Computation is not developed here since it is straightforward after the work done in Section 4.3. For each combination of strategies $\{O_{j,i}; O_{k,i}\}$, we derive the boundaries of its region of applicability as well as its region $\mathscr{R}_i^*$ of achievable SNR. Table 4.2 presents results in $(R_j; R_k; R_i)$ region whereas the results derived in region $(\delta_{j,i}; \delta_{k,i}; \gamma_i)$ are given in Table 4.3. We recall that the first, second and third strategies are respectively the noisy, the joint decoding and the SIC-based strategies.

The achievable rate-region for our 3-user MAC is illustrated on Figure 4.9, in case of equal channel quality for the three links. This region is a decahedron (polyhedron with 10 faces, 16 vertices and 24 edges) which has been drawn based on the nine combinations $\underline{O_i} = (O_{j,i}; O_{k,i})$ summarized in Table 4.2. To derive this region, we use the boundaries of each combination which are formulated in the third column of the table ; we besides add the rate positivity conditions to define the three hidden faces of the decahedron. Each face of the decahedron is differently coloured and stands for one specific combination $\underline{O_i}$. However, just seven faces are drawn on Figure 4.9a, while there are nine possible combinations $\underline{O_i}$ of strategies. The black and red faces are in fact divided each into two surfaces, as shown on Figure 4.9b. Text-arrows have been used to relate each face to its combination $\underline{O_i}$ of strategies. This decahedron is the generalization in the three-user case of the well-known pentagon defined for the two-user case.

To generalize the SNR achievable region $\mathscr{R}_i^*$ depicted on Figure 4.7 to the three-user case, results of Table 4.3 are plotted in region $(\delta_{j,i}; \delta_{k,i}; \gamma_i)$. Let us recall that in 3-dimensions straight lines and planes are respectively characterized by two and one single equations. With the 2-dimensional representation, a straight line is only defined by a single equation. More generally, in n-dimensions, $(n-1)$ equations define a line, $(n-2)$ a plane and so forth

$O_{j,i}$	$O_{k,i}$	Boundaries of Applicability	Achievable rate R_i
1	1	$R_j \geq \log_2(1+\frac{\delta_{j,i}}{1+\delta_{k,i}})$ $R_k \geq \log_2(1+\frac{\delta_{k,i}}{1+\delta_{j,i}})$ $R_j + R_k \geq \log_2(1+\delta_{j,i}+\delta_{k,i})$	$R_i \leq \log_2(1+\frac{\gamma_i}{1+\delta_{j,i}+\delta_{k,i}})$
1	2	$R_j \geq \log_2(1+\delta_{j,i})$ $\log_2(1+\frac{\delta_{k,i}}{1+\gamma_i+\delta_{j,i}}) \leq R_k \leq \log_2(1+\frac{\delta_{k,i}}{1+\delta_{j,i}})$	$R_i + R_k \leq \log_2(1+\frac{\gamma_i+\delta_{k,i}}{1+\delta_{j,i}})$
1	3	$R_j \geq \log_2(1+\delta_{j,i})$ $R_k \geq \log_2(1+\frac{\delta_{k,i}}{1+\gamma_i+\delta_{j,i}})$	$R_i \leq \log_2(1+\frac{\gamma_i}{1+\delta_{j,i}})$
2	1	$R_k \geq \log_2(1+\delta_{k,i})$ $\log_2(1+\frac{\delta_{j,i}}{1+\gamma_i+\delta_{k,i}}) \leq R_j \leq \log_2(1+\frac{\delta_{j,i}}{1+\delta_{k,i}})$	$R_i + R_j \leq \log_2(1+\frac{\gamma_i+\delta_{j,i}}{1+\delta_{k,i}})$
2	2	$R_j \leq \log_2(1+\delta_{j,i})$ $R_k \leq \log_2(1+\delta_{k,i})$ $R_j \geq \log_2(1+\frac{\delta_{j,i}}{1+\gamma_i+\delta_{k,i}})$ $R_k \geq \log_2(1+\frac{\delta_{k,i}}{1+\gamma_i+\delta_{j,i}})$ $R_j + R_k \leq \log_2(1+\delta_{j,i}+\delta_{k,i})$ $R_j + R_k \geq \log_2(1+\frac{\delta_{j,i}+\delta_{k,i}}{1+\gamma_i})$	$R_i + R_j + R_k \leq \log_2(1+\gamma_i+\delta_{j,i}+\delta_{k,i})$
2	3	$R_k \leq \log_2(1+\frac{\delta_{k,i}}{1+\gamma_i+\delta_{j,i}})$ $\log_2(1+\frac{\delta_{j,i}}{1+\gamma_i}) \leq R_j \leq \log_2(1+\delta_{j,i})$	$R_i + R_j \leq \log_2(1+\gamma_i+\delta_{j,i})$
3	1	$R_j \leq \log_2(1+\frac{\delta_{j,i}}{1+\gamma_i+\delta_{k,i}})$ $R_k \geq \log_2(1+\delta_{k,i})$	$R_i \leq \log_2(1+\frac{\gamma_i}{1+\delta_{k,i}})$
3	2	$R_j \leq \log_2(1+\frac{\delta_{j,i}}{1+\gamma_i+\delta_{k,i}})$ $\log_2(1+\frac{\delta_{k,i}}{1+\gamma_i}) \leq R_k \leq \log_2(1+\delta_{k,i})$	$R_i + R_k \leq \log_2(1+\gamma_i+\delta_{k,i})$
3	3	$R_j \leq \log_2(1+\frac{\delta_{j,i}}{1+\gamma_i})$ $R_k \leq \log_2(1+\frac{\delta_{k,i}}{1+\gamma_i})$ $R_j + R_k \leq \log_2(1+\frac{\delta_{j,i}+\delta_{k,i}}{1+\gamma_i})$	$R_i \leq \log_2(1+\gamma_i)$

Table 4.2 – Formulation of applicability boundaries and achievable rates for each combination of strategies $(O_{j,i}; O_{k,i})$ when our three-regime interference classifier is employed in the three-user case. Results are derived in the region $(R_j; R_k; R_i)$.

$O_{j,i}$	$O_{k,i}$	Boundaries of Applicability	Achievable SNR γ_i
1	1	$\delta_{j,i} \leq A_j(1+\delta_{k,i})$ $\delta_{k,i} \leq A_k(1+\delta_{j,i})$ $\delta_{j,i}+\delta_{k,i} \leq A_{jk}$	$\gamma_i \geq A_i(1+\delta_{j,i}+\delta_{k,i})$
1	2	$\delta_{j,i} \leq A_j$ $\frac{\delta_{k,i}}{1+\gamma_i+\delta_{j,i}} \leq A_k \leq \frac{\delta_{k,i}}{1+\delta_{j,i}}$	$\gamma_i \geq A_{ik}(1+\delta_{j,i})-\delta_{k,i}$
1	3	$\delta_{j,i} \leq A_j$ $\delta_{k,i} \geq A_k(1+\gamma_i+\delta_{j,i})$	$\gamma_i \geq A_i(1+\delta_{j,i})$
2	1	$\delta_{k,i} \leq A_k$ $\frac{\delta_{j,i}}{1+\gamma_i+\delta_{k,i}} \leq A_j \leq \frac{\delta_{j,i}}{1+\delta_{k,i}}$	$\gamma_i \geq A_{ij}(1+\delta_{k,i})-\delta_{j,i}$
2	2	$\delta_{j,i} \geq A_j$ $\delta_{k,i} \geq A_k$ $\delta_{j,i} \leq A_j(1+\gamma_i+\delta_{k,i})$ $\delta_{k,i} \leq A_k(1+\gamma_i+\delta_{j,i})$ $\delta_{j,i}+\delta_{k,i} \geq A_{jk}$ $\delta_{j,i}+\delta_{k,i} \leq A_{jk}(1+\gamma_i)$	$\gamma_i \geq A_{ijk}-\delta_{j,i}-\delta_{k,i}$
2	3	$\delta_{k,i} \geq A_k(1+\gamma_i+\delta_{j,i})$ $\frac{\delta_{j,i}}{1+\gamma_i} \leq A_j \leq \delta_{j,i}$	$\gamma_i \geq A_{ij}-\delta_{j,i}$
3	1	$\delta_{j,i} \geq A_j(1+\gamma_i+\delta_{k,i})$ $\delta_{k,i} \leq A_k$	$\gamma_i \geq A_i(1+\delta_{k,i})$
3	2	$\delta_{j,i} \geq A_j(1+\gamma_i+\delta_{k,i})$ $\frac{\delta_{k,i}}{1+\gamma_i} \leq A_k \leq \delta_{k,i}$	$\gamma_i \geq A_{ik}-\delta_{k,i}$
3	3	$\delta_{j,i} \geq A_j(1+\gamma_i)$ $\delta_{k,i} \geq A_k(1+\gamma_i)$ $\delta_{j,i}+\delta_{k,i} \geq A_{jk}(1+\gamma_i)$	$\gamma_i \geq A_i$

TABLE 4.3 – Formulation of applicability boundaries and achievable rates for each combination of strategies $(O_{j,i}; O_{k,i})$ when our three-regime interference classifier is employed in the three-user case. Results are derived in the region $(\delta_{j,i}; \delta_{k,i}; \gamma_i)$.

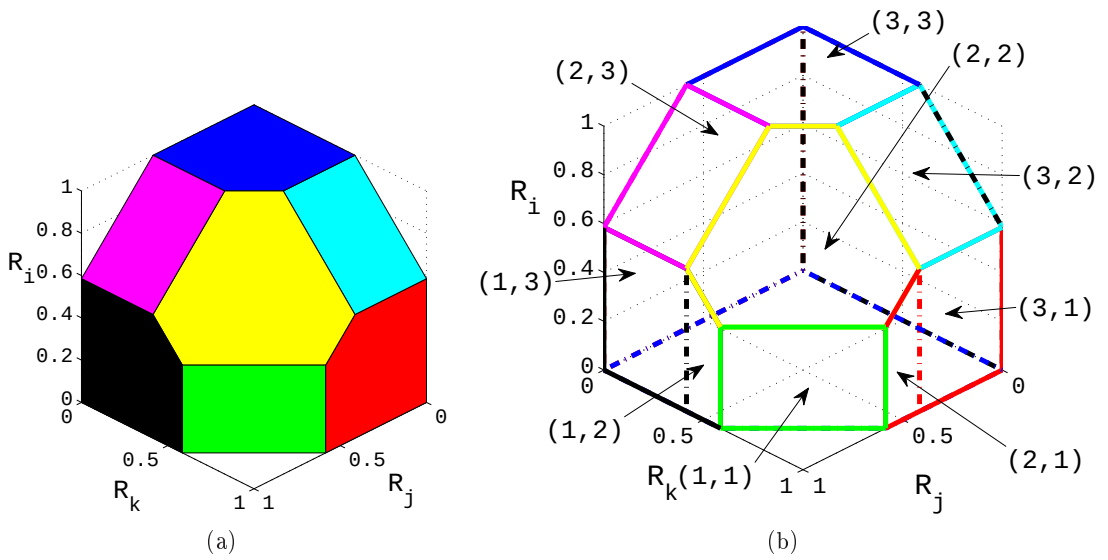

Figure 4.9 – Achievable rate-region for the 3-user MAC.

until the hyperplane defined by a single equation. Consequently, each boundary equation is represented by a plane. All these planes are plotted on Figure 4.10a with different colours. The figure is a little bit complex but nine contiguous regions are indeed defined. To prove that, let us consider Figure 4.10b. For each combination of strategies $O_{j,i}$ with $(j,k) \in [1,\ldots,n], (j,k) \neq i$, the surface describing the lower-bound of the achievable SNR region $\mathscr{R}_i^*$ is plotted in brown. Since surfaces are plotted with transparency, hidden surfaces can be guessed; nine surfaces are represented.

In the same way as the two-user case, two last figures can be used to check how interfering messages x_j and x_k should be processed, contingent on the momentary interference context $(\delta_{j,i}; \delta_{k,i})$. According to the region to which the current point $(\delta_{j,i}; \delta_{k,i}; \gamma_i)$ belongs, the optimal combination of strategy O_i^* can be identified. Besides, SNR achievable surfaces $\mathscr{R}_i^*$ may also be used to set transmit power P_i to ensure target rate $R_{tg,i}$ will be met.

4.4.3 Outage Probability Formulations

Throughout this section we consider QoS-constrained systems and more especially constraints in rate. Each pair 'transmitter-receiver' i has to ensure a minimal transmission rate $R_{tg,i}$. In case of bad communication contexts, the channel capacity may be not high enough to guarantee a reliable transmission at rate $R_{tg,i}$; the channel is said to be in 'outage'.

In case of slow fading channel, coherence time spreads over several transmission delays. For a given transmission, the channel is said 'quasi-static'. With fast fading channels, the coherence time of channel is much shorter than requirement delays of transmission; several fade events occur during the transmission of a packet. System cannot monitor channel quality at any time and any change of fade, because channel estimation is resource consuming; channel estimation has to be made periodically. Consequently, instantaneous channel quality can be hardly tracked; channel estimation is most of time not reliable. To cope with such limitations, statistics of channel must be exploited; average channel

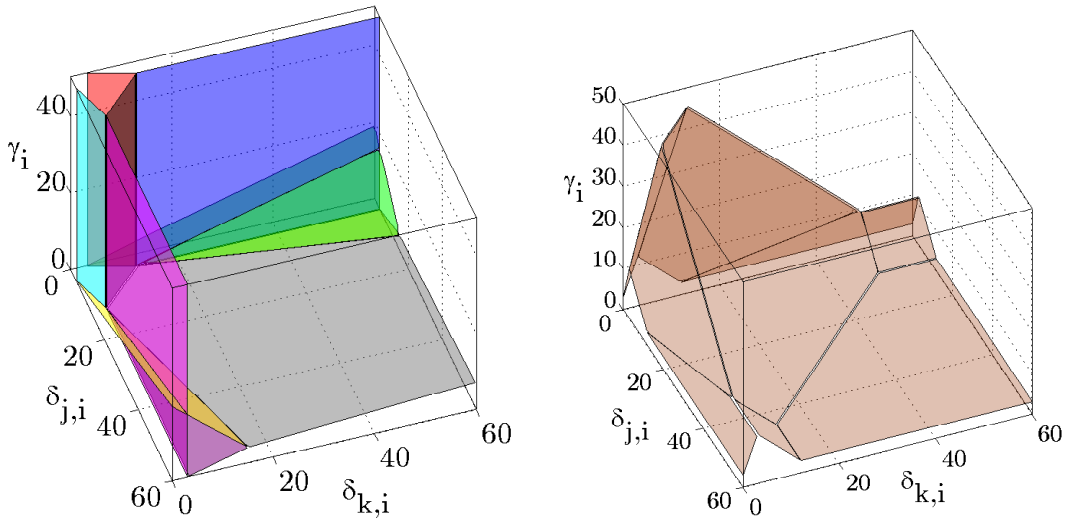

(a) Applicability bounds (b) Achievable SNR region $\mathscr{R}_i^*$

FIGURE 4.10 – The region related to each pair of strategies is characterized by its boundaries and the lower-bound of its achievable SNR region $\mathscr{R}_i^*$.

quality is used rather than instantaneous channel quality. Performance is computed with expectation on numerous channel sates.

Outage probability is proved to be a powerful metric to estimate reliability of transmission, in line with QoS requirements. It indeed indicates how system can support these requirements. We thus derive the probability of outage for the general n-user case when our interference classification is employed. In other words, the outage probability is computed for a given pair 'source-destination' interfered by $(n-1)$ neighbour sources which are each classified among one of our three interference regimes. There are typically P sources handled by the noisy strategy, Q sources which are jointly decoded and remainder $n-1-P-Q$ source processed by a SIC-based strategy. Results are given in Appendix A.

4.4.4 Remarks

Our interference classifier has now been extended from the two-user to the three-user case. Identical computation can be done for any value of n. Representation of results for any n greater than 3 becomes nevertheless tedious.

There is a fundamental assumption with our interference classifier on which we want to insist again : the relevance of our classification to the momentary communication context. As introduced in previous sections, especially with the summary in Tables 4.1, 4.2 and 4.3, boundaries of each regime and performance of strategies within these boundaries intrinsically depend on values of channel and system parameters. As soon as one of these values changes, most of the equations are modified ; a strategy which could be optimal before the modification is not necessarily optimal with the new scenario. For instance, if a neighbour interferer s_j enhances its transmission power assuming all other parameters are kept identical, then the corresponding INR $\delta_{j,i}$ will also increase. If the interfering signal x_j was previously treated as an additional source of noise, then the increase in transmission power P_j may result in another optimal processing for x_j, such as decoding x_j before x_i (SIC-based). Reliability of channel estimation is then of fundamental matter.

Objective Function	Constraints
Maximize R_{i_0} (a specific user)	$R_i \geq R_{i,\min}$ (rate const.)
Maximize $\min_i R_i$ (worst-case user)	$\lvert g_{i_1}\rvert^2 \cdot P_{i_1} = \lvert g_{i_2}\rvert^2 \cdot P_{i_2}$ (near-far const.)
Maximize $\sum_i R_i$ (total throughput)	$\sum_i R_i \geq R_{\text{system,min}}$ (total throughput const.)
Maximize $\sum_i w_i R_i$ (weighted rate sum)	$P_{\text{out},i} \leq P_{\text{out},i,\max}$ (outage proba. const.)
Minimize $\sum_i P_i$ (total power)	$0 \leq P_i \leq P_{i,\max}$ (power const.)

Table 4.4 – Suite of power control optimization problems described with their objective function and their QoS constraints.

We furthermore announced in the beginning of Section 4.3 that we consider a problem of power minimization under constraints of rates. Nevertheless the proposed classifier suits without any modification to the problem of rate maximization under constraints of power. All our bounds were indeed derived for both dual problems. However with slight adaptation this classifier can pass to other optimization under QoS constraints. A utility function conditioned by the momentary communication context should be defined. This utility function will be optimized contingent on values of channel and system parameters. What matters is that the handling of in-band interference is adapted in order to benefit from best achievable performance for any scenario.

- In a dense network with many users competing for few resources, access to communication resource blocks can be driven by a scheduler that allocates, periodically or on a factual way, resources to some elected users while others must wait for. Selection of users is typically based on the CQI of users and on their priority order. Type of traffic, requested amount of resource blocks or fairness between users may also be considered. A latency based utility function may then be minimized, assuming latency inversely evolves with CQI of crossed paths $(\delta_{j,i})_{j\neq i}$.
- The coverage of each transmitter can be another utility function. Assuming possibly coordination between each transmitter, the range of coverage can be optimized such that each destination is most efficiently served by a source. The challenge here consists in the fact that coverage is lead by transmission power which also leads in-band interference perceived by neighbour cells.
- Sum-rate or weighted sum-rate maximization problem can also be investigated.

In [139] authors list some other power control optimization problems which could employ our interference classifier. Objective functions linked to their QoS constraints are summarized in Table 4.4.

4.5 Conclusions

This chapter addresses a three-regime classifier of the in-band interference perceived by the destination. The proposed classifier aims at estimating how much the destination is affected by each interfering signal so that the destination can cope with each interfering signal by applying the most effective interference processing technique. Motivations of this work are two-fold. First, interfering signals are not just interference. Of course these signals are not desired by the destination which perceives them. However, they also carry information and their specific structure can therefore be possibly exploited to mitigate their

detrimental effects. A naive solution would consist in ignoring this particular structure of interference and simply treating interference as added to the background noise level.

Second, the sensed intensity of interference is not constant in time, frequency and space domain. Indeed, the level of interference is lead by numerous system and channel parameters which change in time, frequency and space. For example, each transmitter sets its own transmit power, which results in space variations, according to the location of the source and destination. Likewise, each path between a source and a destination encounters a more or less severe path loss attenuation ; this attenuation depends on the distance from the source to the destination as well as on the momentary shadowing and frequency fading. Hence, a uniform and static interference processing technique cannot perform well for all communications contexts.

In this chapter, we first evaluate how some interference mitigation techniques face interference according to its sensed intensity at destination. Then, we consider previous work belonging to information theory to find how interference can be dealt efficiently, whatever the communication context may be. Nevertheless, even if some proposals are very effective theoretically, they unfortunately cannot be performed decently in practice because of their drastic assumptions. Consequently, we design our interference classifier by using less complex interference processing techniques ; these techniques are may be a little bit less effective but they are proved to perform quite well in practice. The adopted techniques are a noisy strategy, the joint decoding technique and a SIC-based technique ; each of them is applied in one of the three regimes of interference.

Finally, the region of applicability of each regime is characterized in both rate region and SNR region. The three regimes are proved to form a non-overlapping partition of the region, which corroborates the interest of such a classifier. Considering a particular QoS requirements such as a target rate, performance of our three-regime classifier is derived by its achievable SNR regions.

With this classifier of interference we aim at meeting an adaptive processing of in-band interference which is lead by the momentary channel realization and system parameters. Such goals are addressed by Chapters 5 and 6 which focus on minimal power allocation subject to rate constraints.

Chapter 5

Centralized Power Allocation Algorithm

In this chapter we investigate a centralized power allocation algorithm that exploits the three-regime interference classification introduced in Chapter 4. This algorithm aims at improving performance in wireless interference-limited and rate-constrained networks where power budget is a matter of concern. Nowadays, network operators have to face a challenging trade-off. On the one hand the scarce spectrum is over-exploited by several concurrent and heterogeneous systems which target more demanding services and higher transmission rates. On the other hand the size of cells is shrunk to reduce their coverage and hence their transmit power, while ensuring the target QoS. Both issues are closely related to the allocated transmit power that directly affects the level of in-band interference sensed by neighbour receivers. Consequently, it seems challenging but necessary to consider jointly the allocation of power and the more suitable strategy to mitigate in-band interference. This is precisely our goal in this chapter.

To this end a centralized algorithm is performed by an omniscient (coordinated) network controller to minimize the power budget of transmission under constraints of target rate. The network controller exploits our three-regime interference classifier to determine how the momentary communication context affects each node in terms of in-band interference ; based on the current classification, the minimal transmit power that ensures to meet rate constraint is computed. Simulation results prove that important energy savings are reach by adapting the allocation of power to the momentary communication context.

The chapter is structured as follows. After introducing our motivations, proposal and the work related to it, we describe in Section 5.2 the system model and assumptions adopted within this chapter. Then, some preliminary knowledge on centralized algorithms are given in Section 5.3. In Section 5.4 our centralized power allocation (CPA) algorithm is introduced for the two-user case. CPA is first developed, then investigated and finally validated by theoretical and numerical results. We discuss in Section 5.5 some possible solutions to extend CPA to the n-user case. Finally, conclusions are drawn on Section 5.6.

5.1 Introduction

Power management is a fundamental issue : power management techniques aim at reducing overall energy consumption, prolonging battery life for nomad and embedded systems, reducing cooling requirements and reducing operating costs for energy and cooling. Lower power consumption also means lower heat dissipation, which increases system stability, and less energy use, which saves money and reduces the impact on the environment. A new trend emerges since few years in the landscape of wireless communications that focuses on the design of 'green communication' systems. Such systems have to achieve higher performance while reducing their power budget. Efficient power management techniques are more than ever welcome.

Broadly speaking, transmission power is a resource of communication which should be judiciously assigned. Power allocation algorithms mostly come with resource blocks allocation techniques. Assignment of power, time resource and frequency resource, as well as spatial resource in case of multi-antenna devices, should be jointly considered.

5.1.1 Motivations

With the scarcity of frequency spectrum and the proliferation of wireless networks that target high capacity transmissions, interference becomes more than ever a detrimental and QoS-limiting bottleneck of the system. Network operators must therefore efficiently face interference issue to be able to guarantee satisfactory QoS to their customers. Indeed, in some cases services provided by operators are constrained by a quality target, as opposed to 'best effort' services without any warranty of satisfaction for customers. We saw previously that the quality level of the signal perceived by the receiver is directly related to the power level used by the transmitter.

Nevertheless, the high spectrum reuse by close concurrent transmitters as well as the game theory nature of power allocation prevent these transmitters from acting selfishly by setting their power irrespective of how they impact their vicinity. Transmission power should rather be allocated by a process that takes into account both in-band interference and QoS requirements of customers.

Furthermore, as previously stated in Chapter 4, in-band interference ought to be handled in line with the momentary communication context. In networks where cells are coordinated, a centralized and coordinated algorithm fits well since an optimal solution can be quickly computed. Sometimes a specific and common device, named 'network controller' (NC), is responsible for the computation of the whole process ; in this case all requested information and knowledge must be gathered at NC.

Meanwhile network operators focus on lowering transmission power ; this trend is threefold. First, lower power lets reduce spectral pollution in this context of dense and interference limited wireless networks. Second, battery life can thus be extended for devices which are autonomously power supplied. Third, money is saved by reducing both power budget and expenditure for manufacturing circuities with reduced transmission capacity.

Therefore we propose and investigate in this chapter a novel centralized inter-cell power allocation algorithm for rate-constrained networks. Based on the classification of the perceived in-band inter-cell interference proposed in Section 4.3, we manage to reduce the power budget required in each cell while meeting rate requirements of customers.

5.1.2 Contributions

The novelty of this chapter is based on the classification of in-band interference, presented in Chapter 4, which has been extended to power allocation purposes. This work has been presented at the 2010 IEEE 71st Vehicular Technology Conference [19] and has also been patented by CEA [20]. It has furthermore been performed in the framework of the ICT project BeFEMTO, which is partly funded by the European Union [26]. A journal paper in preparation for IEEE Transactions on Wireless Communications also relies on some aspects of this chapter [140]. The innovative contribution in this chapter is three-fold.

First, rates that customers target are in most cases met ; this is ensured in spite of in-band interference which may be potentially very strong. Second, the computed power budget for transmission is minimized ; energy waste is then reduced. Third, in-band interference is handled by effective strategies ; these strategies are selected according to the momentary communication context. Such an adaptive processing of in-band interference lets efficiently cope with the perceived interference. This furthermore results in notable reduction of power and user rejection, in comparison to non-adaptive power allocation techniques.

5.1.3 Related Works

The problem of maximizing a rate-based objective function, such as sum-rate or min-rate, under various QoS constraints has been widely investigated in the literature. Its dual optimization problem of minimizing transmission power under specific QoS constraints has also been addressed by numbers of power allocation algorithms. Nearly all papers dealing with optimization issues refer to the theory of convex optimization, for which the book of Boyd and Vandenberghe [6] is certainly one of the most cited and complete reference. In case of non-convexity, some papers either investigate how problem can be assumed convex, or propose specific algorithms to deal with these non-convex scenarios. In the general case, solution is attained by computing the Lagrangian associated with the optimization problem. Lagrangian links the objective function to equality and inequality constraints functions by using Lagrange multipliers. Karush-Kuhn-Tucker (KKT) conditions are used to derive an optimal solution to the problem. Kandukuri and Boyd [141] for instance address the minimization of transmitter power subject to constraints on outage probability and minimization of outage probability subject to power constraints. On the other hand, the power allocation problem of maximizing the ergodic capacity of the broadcast channel subject to minimum rate constraints is addressed in [142].

The most famous power allocation algorithm in wireless communication networks is surely water-filling. The technique of water-filling directly follows from Lagrangian and KKT conditions. This technique seeks to efficiently allocate a given power budget to all frequency bands without exceeding power limitation of each band. The general concept comes from its own name and can be described as follows : each frequency band is represented as a hole, whose depth is inversely proportional to its CQI. Power budget is represented as a water bowl that is poured out over holes. By free flowing between holes, water is spreading out on holes to reach a uniform level at surface of all holes. Such a way the deeper a hole is the more water the hole will contain. If the volume of water is not enough, shallow holes remain empty. Basis of water-filling are for instance recalled in [2, 7, 143].

But water-filling is not the only powerful power control algorithm. In Chapter 3 we adopted another simple but efficient technique to perform power allocation, known as 'On-Off' power allocation [91, 92]. Transmission power is simply set either to the maximal power or to the minimal (null) power.

In wireless communication networks, power control techniques aiming at rate maximization or power minimization are commonly dealt with a combination of two steps. First step consists in resource block assignment where each active user is allocated a certain amount of sub-carriers. Various criteria can define how sub-carriers are assigned to users : the best channel may be assigned to the user with the highest CQI for this channel, to the user farthest from its QoS constraint or why not randomly assuming fairness in time average. Second, independent power control processes are performed over each sub-carrier. Channel are indeed orthogonal, out-of-band interference is then neglected. Consequently, power allocation techniques only involve users that share a same sub-carrier. Such a separation in two steps fits well to interference-limited situations, especially to OFDM/OFDMA based systems. By efficiently allocating sub-carriers, interference avoidance may be achieved. [71, 144–148] are possible references to illustrate this idea.

Nevertheless, no paper addresses the management of in-band interference on an adaptive manner. In-band interference is commonly handled on a single and fixed way during the whole process of power allocation. We proved in Chapter 4 that such fixed strategies are not effective to cope with in-band interference in highly variable interference-limited scenarios where in-band interference may be quite low or very strong.

5.2 System Model and Assumptions

In this chapter we develop a centralized power allocation algorithm designed to adaptively face in-band interference sensed at receivers in rate-constrained interference-limited networks. For the sake of clarity, algorithm principle will be introduced for two 'source-destination' pairs that compete for the same frequency band while they both target a specific transmission rate. We will derive at the end of the chapter a generalization to any number of sources, destinations and frequency bands. We first consider the smallest interfered subsystem in which a whole system can be subdivided into. It could of course be possible to assign one specific band to each pair so as to perfectly avoid in-band interference but it is not the focus of our work.

The adopted system model was firstly introduced in Section 2.2.1 but it will be recalled hereafter with some additional elements. Figure 5.1 illustrates our updated system model which is described by the following system of equations :

$$\begin{cases} y_i = g_{i,i} \cdot x_i + g_{j,i} \cdot x_j + z_i \\ y_j = g_{i,j} \cdot x_i + g_{j,j} \cdot x_j + z_j. \end{cases} \tag{5.1}$$

This model consists in four single-antenna devices, two sources s_i and s_j as transmitters and two destinations d_i and d_j as receivers that all share the same frequency band. The source s_i intends to send the message x_i to its destination d_i while targeting the transmission rate $R_{tg,i}$. However this transmission is affected by AWGN noise z_i with variance N_0 and by the interfering message x_j sent by the neighbour source s_j. Message x_j is not intended to d_i but we assume d_i is able to decode it if necessary. The global gain of the

channel between a source s_k and a destination d_l is named by $g_{k,l}$. This gain includes all wireless perturbations encountered during transmission (fading, shadowing, path loss attenuation, diversity gain) and is assumed to be perfectly estimated thanks to pilot messages for instance. Source s_i is also constrained in power by the system limitation $P_{i,\max}$.

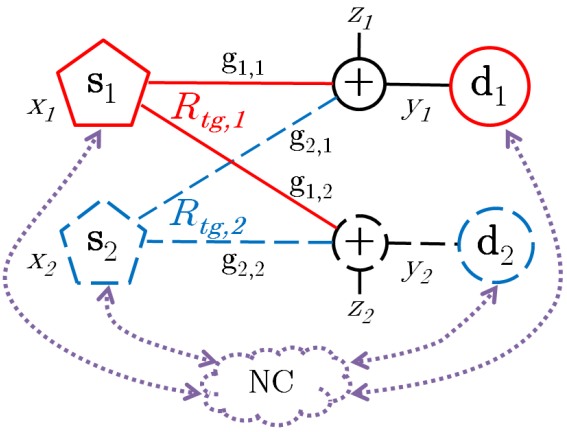

Figure 5.1 – Two neighbour 'source-destination' pairs with a network controller.

We furthermore introduce a fifth device, named 'network controller' or shorter 'NC'. NC is a centralized and common device which is coordinated with all other four devices. NC can be seen as an omniscient genie with full-knowledge of system and channel parameters (constraints in rate $R_{tg,i}$, limitations in power $P_{i,\max}$, channel gains $g_{i,j}$). This entity is responsible for the computation of the optimal power vector. To this end, NC needs to know all system and channel parameters : these parameters are so broadcasted by sources and destinations. All devices are consequently able to send data to NC. Once the computation of power vector is done, NC has to notify sources of their optimal transmission power. NC is then able to send data to sources, but also to destinations since our algorithm outputs as well how in-band interference should be handled efficiently by destinations. All links to NC are then bidirectional.

We do not need any other elements for the general framework of our algorithm. However, the manner with which devices communicate with NC should be developed for practical implementations. NC is not necessarily a real and devoted device. Indeed, by use of transmit and receive cooperation as well as a backhaul network, all requested information can be sent between devices which do not need to gather it in a single location (NC) ; sources and/or destinations can then compute themselves their optimal power vector. Nevertheless, we will assume hereafter the presence of NC. Furthermore, we will assume error-free transmissions between NC and all other devices. Such transmissions can be ensured by a specific communication network with low data rate, exclusively devoted to exchange of system and channel parameters. A wire-line network can also be employed, if possible ; no line of sight transmissions between NC and devices are then solved.

As it was previously presented in Chapter 4, we propose an adaptive classifier for in-band interferenec perceived by receivers. Our adopted system model is the one of Figure 5.1 but with the viewpoint of a specific destination, the model can be subdivided into two two-user multiple access channels, as shown on Figure 5.2. Such a representation is validated by (5.1). One goal of our algorithm is that NC notifies d_i of the strategy it should employ to optimally handled the in-band interfering message x_j. To this end, the model of a MAC

is then sufficient. We recall useful notations below :

$$\gamma_i = \frac{|g_{i,i}|^2 \cdot P_i}{N_0} \quad \text{and} \quad \delta_i = \frac{|g_{j,i}|^2 \cdot P_j}{N_0} \tag{5.2}$$

$$A_i = 2^{R_{tg,i}} - 1, \quad A_j = 2^{R_{tg,j}} - 1 \quad , A = 2^{R_{tg,i}+R_{tg,j}} - 1 = (A_i + 1)(A_j + 1) - 1. \tag{5.3}$$

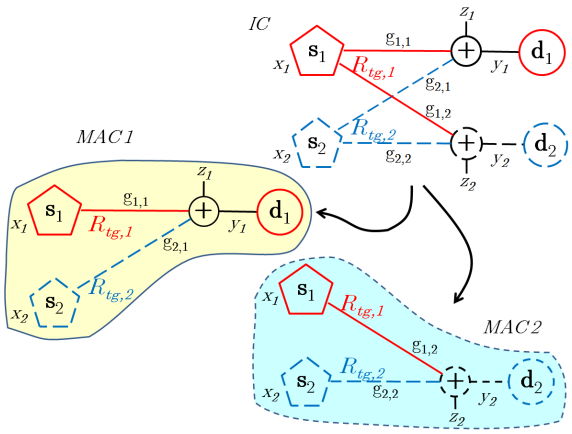

FIGURE 5.2 – Decomposition of the whole two-user IC into two two-user MAC subsytems.

5.3 Preliminary on Centralized Algorithms

This section aims at recalling some main concepts and fundamentals assumptions of centralized and coordinated algorithms in wireless communication networks. Intrinsic differences between centralized and non-centralized (called distributed) approaches will not be addressed in this chapter but rather in Chapter 6. Challenges and application assumptions of centralized approaches are given in the first subsection, while the second one focuses on their limitations. Finally, synoptic principle of the famous water-filling technique of power control will be discussed.

5.3.1 Challenges and Assumptions

The main and fundamental assumption of centralized algorithms in wireless communication networks is the presence of an entity (NC) which is devoted to carry out algorithm tasks. Commonly NC is a device exclusively devoted to the process of algorithms. Since the running of algorithms can be resource demanding due to computational burden and possible complexity of algorithms, NC is usually power supplied. Its computational capabilities should be set in accordance with complexity of algorithms so that NC does not act as the bottleneck of the network.

Furthermore NC aims at computing an optimal solution to a problem. Such a goal implies that all information required to meet optimality is supplied to NC. Typically, devices first inform NC about the quality of their channels as well as their system limitations and QoS requirements [149]. NC then becomes an omniscient genie with full-CSI knowledge. Once the optimal solution has been computed, NC must notify devices of the algorithm outputs. The whole system is then represented as shown on Figure 5.1.

Such assumptions are not really restrictive, especially in cellular networks where base stations are coordinated by a backhaul network. NC can be assumed to be linked to this backhaul and then links between NC and base stations are error-free. To communicate with user entities, NC may pass through BSs by exploiting signalling messages. In this case, no additional signalling is needed between BSs and their assigned UEs. Base stations indeed periodically refresh their CSI estimations on locally active UEs to perform link adaptation techniques (AMC, power control, channel aware scheduling, etc.). BSs besides exchange information with their active UEs to set QoS requirements and define system limitations. BSs are then omniscient of their local vicinity. Through backhaul coordinated all BSs, NC can achieve its requested full knowledge.

Once system knowledge has been gathered at NC, an optimal solution can be quickly computed. In case of optimization problems, NC is fully able to eliminate all suboptimal solutions, referring for instance to local extrema solutions. Such a centralized device is well fitted to adapt its behaviour to momentary communication contexts to pass to channel and system variations. There is consequently no limitation for NC to perform our interference classifier proposed in Section 4.3. Let us note that in case of non cellular networks which are not supplied with a backaul network that coordinates all nodes, we recall that in case of centralized deployments there is commonly a centralized scheduler responsible for traffic monitoring, channel estimation, sub-carriers allocation and many other supervising tasks. The role of NC can be played by such a scheduler.

5.3.2 Limitations of Centralized Algorithms

However, centralized approaches may suffer from some theoretical and practical limitations. We talked in Section 5.2 about the ability of system to perform centralized algorithm without requiring a NC. Indeed cooperation or coordination between nodes may be exploited to acquire full system knowledge. Computational tasks may then be performed by the nodes with the highest capabilities, possibly dispatched between several nodes. The algorithm is not necessarily carried out is only one location but the processing is however always centralized since all nodes involved in the process are coordinated and knowledge of the whole system is required to guarantee quick and optimal solution.

Nevertheless, in some wireless communication systems centralized solutions cannot be applied to all communication scenarios. On one hand coordination or cooperation between nodes may be not possible or not desired because it would cause prohibitive amount of signalling and energy waste to exchange so many data and compute such algorithms. On the other hand, while a NC is required, it may be simply infeasible to use such a centralized and omniscient entity in the network. Such limitations are for instance encountered with wireless sensor networks (WSN) or ad-hoc networks. These networks are indeed unable to reach a full and perfect knowledge of their topology, even at the cost of fastidious mechanisms. WSNs and ad-hoc networks characterize highly mobile and possibly dense nodes architecture within which each node has only a local and limited knowledge of its vicinity. Even if some privileged nodes are able to monitor traffic and routing, they have not enough skill to shoulder the role of NC. Furthermore, such networks are designed to be sustainable and operating at low cost to preserve battery life of nodes. It is strictly inconceivable for nodes to compute additional and possibly demanding tasks without supplying them with power. It is thus an open problem to consider distributed approaches (see Chapter 6) !

We lastly address some other limitations encountered by the presence of NC. Firstly, the main drawback of any centralized approach consists in its effectiveness to achieve accurate and reliable estimations of channel and system parameters. It is even more difficult in network with remote or hidden nodes. Second, in some networks with low traffic, the presence of NC generates a prohibitive additional traffic due to signalling (for channel estimation) and control overhead (notification for nodes). Finally, all computation complexity is carried out at NC which may be the bottleneck of network and may suffer from excessive computation burden if it is not well sized.

5.3.3 Water-Filling Technique

An introduction to power allocation techniques could not be complete without a brief overview of water-filling principle. Let us note that water-filling is presented here in a chapter dealing with centralized algorithms, whereas it is quite possible to perform water-filling on a distributed manner [150, 151]. It just depends on what the optimization problem consists in and which CSI knowledge is available at the executive entity. Water-filling based power allocation techniques have been widely presented [2, 6, 7, 143] and investigated [144, 146, 152–154] in the literature.

For the sake of clarity, we will derive the easiest case of water-filling. We assume an OFDMA system where each user is allocated a set of exclusive sub-carriers. There is consequently no in-band interference ; transmission rate is then just limited by AWGN noise sensed at receiver. The optimization problem considered hereafter is the maximization of the reliable rate of communication that a transmitter can achieve over N_{SC} independent sub-carriers. We do not know precisely if these N_{SC} sub-carriers form the set of resources assigned to a specific user or if they form the set of all resources assigned to active users served by this transmitter. In the first case the problem addresses the maximization of a specific rate while the second targets the sum-rate. The transmitter uses power P_k for sub-carrier k ; the sum of powers assigned to each sub-carrier cannot exceed the technical limitations $N_{\mathrm{SC}} \cdot P$. The global problem is expressed as follows [2] :

$$\begin{aligned} &\max_{\{P_1,\ldots,P_{N_{\mathrm{SC}}}\}} \sum_{k=1}^{N_{\mathrm{SC}}} \log_2\left(1+\tfrac{|g_k|^2 \cdot P_k}{N_0}\right), \\ &\text{subject to} \quad \sum_{k=1}^{N_{\mathrm{SC}}} P_k \leq N_{\mathrm{SC}} \cdot P, \\ &\qquad\qquad\quad P_k \geq 0, \quad \forall k \in \{1,\ldots,N_{\mathrm{SC}}\}, \end{aligned} \tag{5.4}$$

where g_k refers to channel gain between source and destination on sub-carrier k ; there is here no need to specify the source and the destination.

The optimal power allocation vector of (5.4) can be explicitly found. Since the objective function is jointly concave in the powers, (5.4) can be solved by Lagrangian methods. Consider the Lagrangian :

$$\mathscr{L}(\lambda, P_1, \ldots, P_{N_{\mathrm{SC}}}) = \sum_{k=1}^{N_{\mathrm{SC}}} \log_2\left(1+\frac{|g_k|^2 \cdot P_k}{N_0}\right) - \lambda \sum_{k=1}^{N_{\mathrm{SC}}} P_k, \tag{5.5}$$

where λ is the Lagrange multiplier. KKT conditions are summarized as follows :

$$\frac{\partial \mathscr{L}}{\partial P_k} \begin{cases} = 0 & \text{if} \quad P_k > 0 \\ \leq 0 & \text{if} \quad P_k = 0. \end{cases} \tag{5.6}$$

The optimal solution can be derived from (5.6) :

$$\begin{array}{lll} & \frac{\partial \mathscr{L}}{\partial P_k} = 0 & \text{if} \quad P_k > 0 \\ \Leftrightarrow & \frac{|g_k|^2}{N_0+|g_k|^2 \cdot P_k} - \lambda = 0 & \text{if} \quad P_k > 0 \\ \Leftrightarrow & P_k = \frac{1}{\lambda} - \frac{N_0}{|g_k|^2} & \text{if} \quad P_k > 0 \\ \Rightarrow & P_k^* = (\frac{1}{\lambda} - \frac{N_0}{|g_k|^2})^+, & \end{array} \tag{5.7}$$

where $x^+ = \max(x, 0)$. The Lagrange multiplier λ is chosen to met the power constraint :

$$\frac{1}{N_{\text{SC}}} \sum_{k=1}^{N_{\text{SC}}} (\frac{1}{\lambda} - \frac{N_0}{|g_k|^2})^+ \leq P. \tag{5.8}$$

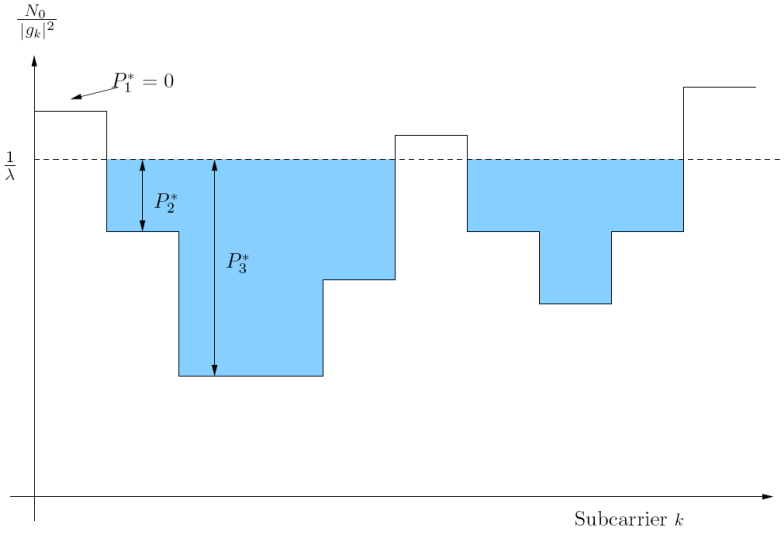

Figure 5.3 – Water-filling power allocation over the N_{SC} sub-carriers.

An illustration of water-filling principle is given on Figure 5.3 where the baseline is illustrated by the dashed line at $\frac{1}{\lambda}$. All sub-carriers holes whose bottom is above this baseline cannot be filled by water and remain empty, *i.e.*, $P_k^* = 0$, whereas all other holes are filled by a level of water corresponding to the difference between their bottom and the baseline $\frac{1}{\lambda}$.

5.4 Proposed Centralized Power Allocation Algorithm

As it has been said in Section 5.2, we first consider a scenario with just two 'source-destination' pairs (see Figure 5.1). The pair '$s_i - d_i$' targets a transmission rate $R_{tg,i}$ and is limited in power by $P_{i,\max}$. The receiver d_i is furthermore able to decode interfering signals coming from the neighbour source s_j. We will sometimes refer to our centralized power allocation algorithm as CPA algorithm in the remainder.

5.4.1 Power Allocation and Interference Classification

We introduced in Section 4.3 a process for dealing with in-band interference. We aim at first evaluating in-band interference that a receiver perceives, then classifying it into the

suitable regime of interference, and finally recommending the receiver the best strategy to employ for efficiently handling in-band interference. Our three-regime interference classification is exploited hereafter to perform minimal power allocation in rate-constrained networks. This algorithm is more a heuristic than a pure problem of optimization under constraints. Nevertheless, the problem that we seek to solve can be expressed as follows (in this section with $n = 2$) :

$$\begin{aligned} &\min_{\{\underline{O_1},\dots,\underline{O_n}\}} f(P_1^{(\underline{O_1})},\dots,P_n^{(\underline{O_n})}) = f(\underline{P}), \\ &\text{subject to} \quad R_k^{(\underline{O_k})}(\underline{P}) \geq R_{tg,k}, \quad \forall k \in \{1,\dots,n\}, \\ &\qquad\qquad 0 \leq P_k^{(\underline{O_k})} \leq P_{k,\max}, \quad \forall k \in \{1,\dots,n\}, \end{aligned} \tag{5.9}$$

where $\underline{O_k} = (O_{l,k})_{l\in[1,\dots,n],l\neq k}$ has been defined in Section 4.4.2 as the vector that states with which strategy each interfering message x_l perceived at receiver d_k should be handled. $P_k^{(\underline{O_k})}$ and $R_k^{(\underline{O_k})}$ are respectively the transmission power of source s_k and its transmission rate, which are both computed contingent on $\underline{O_k}$. Indeed, each strategy implies specific objective and constraint functions.

We do not specify the function f at this step. Mostly, we consider the identity function on $\mathbb{R}^n$,*i.e.,* $f = id_{\mathbb{R}^n}$. In other words, we want to minimize individually each component of the power vector $\underline{P}$. Nevertheless, other functions f may sometimes be adopted, such as the sum-power : $f(\underline{P}) = \sum_{k=1}^{n} P_k^{(\underline{O_k})}$.

The novelty of our algorithm comes from handling of in-band interference which is adapted to the momentary context of communication. Three strategies are proposed ; each of them is optimal within a specific range of scenarios.

Non-adaptive handling interference strategies are not efficient for all values of channel and system parameters (see Section 4.2). When these fixed strategies are employed in order to optimally allocate power, they may lead to set huge transmission powers for handling scenarios where their performance collapse (see later Figure 5.9). Furthermore, they cannot ensure that rate $R_{tg,k}$ will be met in such bad scenarios. In comparison to these fixed strategies, our adaptive classifier lets to allocate low power budget for the whole range of scenarios, while meeting all rate constraints $(R_{tg,k})_k$.

Main equations leading to our classifier (for $n = 2$) have been summarized in Table 4.1 and illustrated with Figure 4.7. Two major challenges are addressed and solved. First, in-band interference is classified into the suitable regime in line with the current vector (δ_i, γ_i). This regime is specified by O_i and suggests an efficient strategy to handle in-band interference encountered due to signal x_j. Second, the region of all points (δ_i, γ_i) that lets meet rate constraint $R_{tg,i}$ is characterized as the SNR achievable region $\mathscr{R}_i^*$. The translation between power and SNR is straightforward with (4.20), especially when full-CSI knowledge is assumed. These results fit well to solve the power allocation problem (5.9), as developed hereafter.

Our classification of interference is designed to be employed at the receiver side. The system model associated with this classifier then looks like a MAC channel, since a single destination listens to several sources. Our initial two-user interference channel is consequently divided into two subsystems (see Figure 5.2) ; interference classification is adopted independently for both of them. Nevertheless, there is a fundamental difference between

O_i	Scheme	Partition $\omega_i^{O_i}$	Achievable SNR γ_i
1	Noisy	$\omega_i^1 = \{(\gamma_j, \gamma_i) \vert 0 \leq \gamma_j \leq \frac{A_j}{f_{j,i}}\}$	$\gamma_i \geq A_i(1 + f_{j,i} \cdot \gamma_j)$
2	Joint decoding	$\omega_i^2 = \{(\gamma_j, \gamma_i) \vert \frac{A_j}{f_{j,i}} \leq \gamma_j \leq \frac{A_j}{f_{j,i}}(1 + \gamma_i)\}$	$\gamma_i \geq A - f_{j,i} \cdot \gamma_j$
3	SIC-based	$\omega_i^3 = \{(\gamma_j, \gamma_i) \vert \gamma_j \geq \frac{A_j}{f_{j,i}}(1 + \gamma_i)\}$	$\gamma_i \geq A_i$

Table 5.1 – Performance of our three-regime interference classifier applied to the MAC $\{s_i; s_j, d_i\}$: partition of the region $(\gamma_j; \gamma_i)$ and achievable SNR within each region.

our MAC-based model and the classic model of a MAC. On the one hand, all sources of a true MAC system send intentionally information to the common destination. On the other hand, with our MAC-based model, all crossed-links are not desired but destination has to face them to recover its intended signal. Power allocation is a game theory problem ; local and selfish optimization is inconceivable since a given transmission affects all destinations located in its surrounding. A global approach must be performed to reach a balanced and optimal solution to (5.9).

5.4.2 Optimal Power Allocation

Results presented in Section 4.3, and especially the achievable SNR region, have been derived for one of the two MAC-based subsystems of Figure 5.2. However, both subsystems are closely related together :

$$\gamma_i = \left|\frac{g_{i,j}}{g_{i,j}}\right|^2 \cdot \frac{|g_{i,i}|^2 \cdot P_i}{N_0} = \left|\frac{g_{i,i}}{g_{i,j}}\right|^2 \cdot \frac{|g_{i,j}|^2 \cdot P_i}{N_0} = \left|\frac{g_{i,i}}{g_{i,j}}\right|^2 \cdot \delta_j. \tag{5.10}$$

SNR in one subsystem is actually proportional to INR in the other subsystem. It seems then natural to consider region $(\gamma_1; \gamma_2)$ instead of independent regions $(\delta_i; \gamma_i)$ for $i = 1, 2$. Results are straightforward in the new region by being careful about scaling both axis correctly. To this end, we introduce two new variables to switch more easily between regions $(\delta_i; \gamma_i)$ and $(\gamma_j; \gamma_i)$:

$$f_{i,j} = \left|\frac{g_{i,j}}{g_{i,i}}\right|^2 \quad \Rightarrow \quad \delta_j = f_{i,j} \cdot \gamma_i \qquad i \neq j = 1, 2. \tag{5.11}$$

With use of variables $\{f_{i,j}\}_{i,j}$, new equations are summarized in Table 5.1. The interference classifier determines a non-overlapping partition $(\omega_i^1, \omega_i^2, \omega_i^3)$ of the region $(\gamma_j; \gamma_i)$. Each region of the partition stands for a strategy O_i of interference where the line $\mathscr{D}_i^{O_i}$ is the lower bound of the achievable SNR $\mathscr{R}_i^*$ within this partition.

A graphical illustration of these new results is easily obtained by superimposing on the same figure both achievable regions $\mathscr{R}_1^*$ and $\mathscr{R}_2^*$, as shown on Figure 5.4. Lower bounds $(\mathscr{D}_1^k)_k$ of $\mathscr{R}_1^*$ and $(\mathscr{D}_2^k)_k$ of $\mathscr{R}_2^*$ are illustrated respectively by purple dashed lines and blue solid lines. The partition $(\omega_1^k)_k$ is delimited by dotted green lines, while partition $(\omega_2^l)_l$ is bounded by dash-dot red lines. The superposition of both SNR achievable region $\mathscr{R}^* = \mathscr{R}_1^* \cap \mathscr{R}_1^*$ is illustrated by blended shades of yellow

Each destination perceives an own and independent level of in-band interference. There are consequently three possible regimes for classifying interference perceived by d_1 and

three others for d_2. By superimposing on the same figure all possibilities for d_1 and d_2, at most nine pairs of regimes (O_1, O_2) are created. They are captioned between brackets on Figure 5.4. This superposition is equivalent to $\underline{\Omega} = \{\omega_1^1, \omega_1^2, \omega_1^3\} \cap \{\omega_2^1, \omega_2^2, \omega_2^3\}$. The region $(\gamma_1; \gamma_2)$ is thus divided into nine regions $\Omega_{k,l} = \omega_1^k \cap \omega_2^l$, called 'sectors' in the remainder. Each sector has been differently coloured on Figure 5.4.

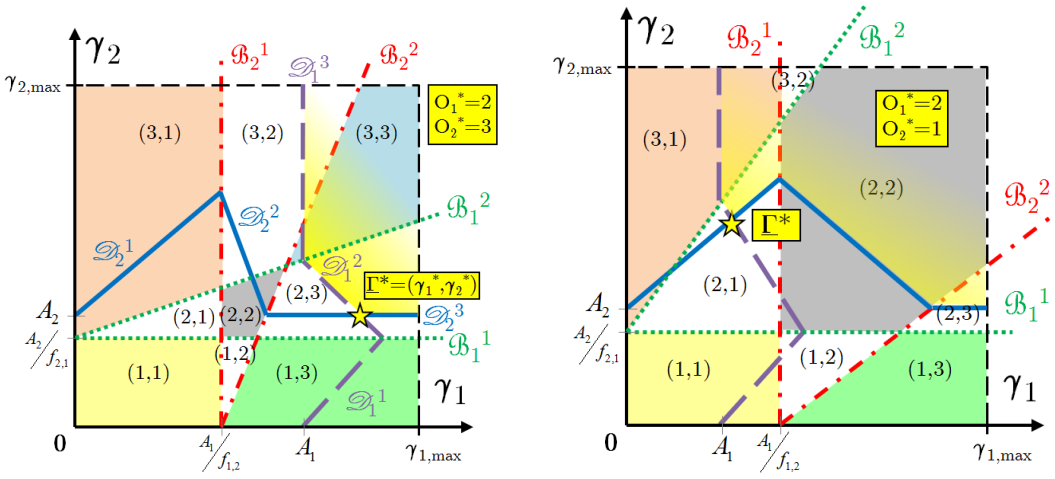

(a) Region $(\gamma_1; \gamma_2)$ divided into 9 sectors

(b) Region $(\gamma_1; \gamma_2)$ divided into 8 sectors

FIGURE 5.4 – Superposition of both achievable SNR regions $\mathscr{R}_1^*$ and $\mathscr{R}_2^*$. A partition Ω of the region into nine (left) and eight (right) sectors is achieved.

There is indeed at most $3^2 = 9$ sectors. Each partition $(\omega_i^k)_k$ is characterized by a pair $(\mathscr{B}_i^1, \mathscr{B}_i^2)$ of boundaries which are affine functions (see dotted green and dash-dot red straight lines on Figure 5.4). Since boundaries between regimes are straight lines, their intersection is easily investigated. It is straightforward that the vertical boundary $\mathscr{B}_1^1$ always intersects with $\mathscr{B}_2^1$ and $\mathscr{B}_2^2$. Likewise, the diagonal $\mathscr{B}_1^2$ always intersects with the horizontal $\mathscr{B}_2^1$. However, the two diagonal boundaries may never intersect in the positive region. This is contingent on their slopes ; intersection is ensured iff $A_i A_j > f_{i,j} f_{j,i}$ holds. If this condition holds, there are nine sectors, else eight sectors. We plot on Figure 5.4b an illustration of a scenario where the previous condition does not hold. Furthermore, we recall that results are relevant for the momentary communication context ; as soon as the value of one parameter changes, all results change. Finally, this partition into sectors is also monitored by power limitations $P_{1,\max}$ and $P_{2,\max}$ which directly translate into $\gamma_{1,\max}$ and $\gamma_{2,\max}$. The partition is thus restricted to the brick, *i.e.,* right parallelepiped, $[0, \gamma_{1,\max}] \times [0, \gamma_{2,\max}]$ or more generally $[\gamma_{1,\min}, \gamma_{1,\max}] \times [\gamma_{2,\min}, \gamma_{2,\max}]$ in case of minimal power limitations. If sectors are defined outside this brick, less than eight or nine sectors are relevant.

We aim at computing the minimal power vector $\underline{P}^* = (P_1^*, P_2^*)$ on a centralized fashion. To this end, we assume there is an omniscient NC with full knowledge of system and channel parameters. Consequently, NC can easily compute all equations of $\{\mathscr{B}_i^k\}_k$ and $\{\mathscr{D}_i^k\}_k$ for $i = 1, 2$. By use of the bijection (5.2), NC quickly switches between power P_i and SNR γ_i. Thus, the optimal power P_i^* stands for only one optimal SNR γ_i^*. Computation of vector $\underline{P}^*$ is hence identical to looking for the optimal SNR vector $\underline{\Gamma}^* = (\gamma_1^*, \gamma_2^*)$.

On Figure 5.4 we mark with a yellow star the intersection point between the lower bounds of $\mathscr{R}_1^*$ and $\mathscr{R}_2^*$. This corresponds to the intersection between the piecewise continuous blue and purple curves. This yellow star actually refers to $\underline{\Gamma}^*$. Furthermore, the sector Ω_{k_0,l_0} within which the yellow star is located establishes $O_1^* = k_0$ and $O_2^* = l_0$. The vector $\underline{O}^* = (O_1^*, O_2^*)$ is the optimal pair of strategies to handle in-band interference. NC has then just to derive $\underline{P}^*$ from $\underline{\Gamma}^*$ and notifies sources of P^* and destinations of $\underline{O}^*$. With the knowledge of O_i^*, destination d_i is then able to handle efficiently the in-band interfering signal x_j while meeting a reliable transmission at rate $R_{tg,i}$. Meanwhile, s_i saves power since P_i^* is the minimal transmit power that ensures a reliable transmission.

Even if these results seem obvious, they need to be proved. Hereafter we will first prove the existence of this solution $\underline{\Gamma}^*$ and then prove its optimality. Finally, some remarks and simulation results will conclude the section.

5.4.3 Proof of Existence

To prove the existence of the optimal solution $\underline{P}^*$, *i.e.,* $\underline{\Gamma}^*$, we have to prove that $(\mathscr{D}_1^k)_k$ and $(\mathscr{D}_2^l)_l$ always cross themselves. In other words, we must ensure that the piecewise continuous blue and purple curves are secant for all communication contexts. To this end, we define two piecewise continuous functions φ_1 and φ_2 whose geographical representations are respectively $(\mathscr{D}_1^k)_k$ and $(\mathscr{D}_2^l)_l$.

$$\begin{array}{l} \forall \gamma_j \in [\gamma_{j,\min}, \gamma_{j,\max}], \quad \varphi_i : [\gamma_{j,\min}, \gamma_{j,\max}] \longmapsto [\gamma_{i,\min}, \gamma_{i,\max}] \\ \text{such that} \quad \begin{cases} \varphi_i(\gamma_j) = A_i(1 + f_{j,i} \cdot \gamma_j), & \text{if } (\gamma_j, \varphi_i(\gamma_j)) \in \omega_i^1, \\ \varphi_i(\gamma_j) = A - f_{j,i} \cdot \gamma_j, & \text{if } (\gamma_j, \varphi_i(\gamma_j)) \in \omega_i^2, \\ \varphi_i(\gamma_j) = A_i, & \text{if } (\gamma_j, \varphi_i(\gamma_j)) \in \omega_i^3. \end{cases} \end{array} \tag{5.12}$$

For sake of clarity, existence of $\underline{\Gamma}^* = (\mathscr{D}_1^k)_k \cap (\mathscr{D}_2^l)_l$ will be proved by the following geometrical reasoning (see also Figure 5.5) :

Step 1. By a continuous transformation π of the map applied to φ_2, the function φ_2 is transformed into $\bar{\varphi_2} = \pi \circ \varphi_2$ whose graphic representation is the straight horizontal line $\gamma_2 = A_2$. Here, $f \circ g$ refers to the composition of functions. This continuous transformation π is a kind of homothetic function whose scale ratio depends on φ_2. Figure 5.5a illustrates the principle of this transformation [1].

Step 2. $\bar{\varphi_2}$ is continuous as composition of continuous functions.

Step 3. Two straight and non parallel lines are always secant. It is straightforward to see that red and purple curves are always secant.

Step 4. φ_1 and $\bar{\varphi_2}$ are then secant at a point $\underline{\Gamma}^0$. This step is corroborated by the well-known intermediate value theorem.

Step 5. The image of an intersection under a continuous transformation of the map remains an intersection.

Step 6. By the inverse continuous transformation π^{-1} applied to $\underline{\Gamma}^0$, φ_1 and φ_2 are secant at point $\underline{\Gamma}^* = \pi^{-1}\left(\underline{\Gamma}^0\right)$. Figure 5.5b illustrates the relation between $\underline{\Gamma}^0$ and $\underline{\Gamma}^*$.

This completes the proof of existence of a solution to our power allocation problem. Nevertheless, an analytical reasoning is possible by translating this geometrical reasoning into equations, but it would be tedious. It remains to prove this solution is optimal.

1. With the notations of Figure 5.5a, the transformation π looks like $\pi(x) = y_0(\frac{1}{f(x)} + 1)$. By this transformation the green curve is scaled down as the red curve and becomes a horizontal line.

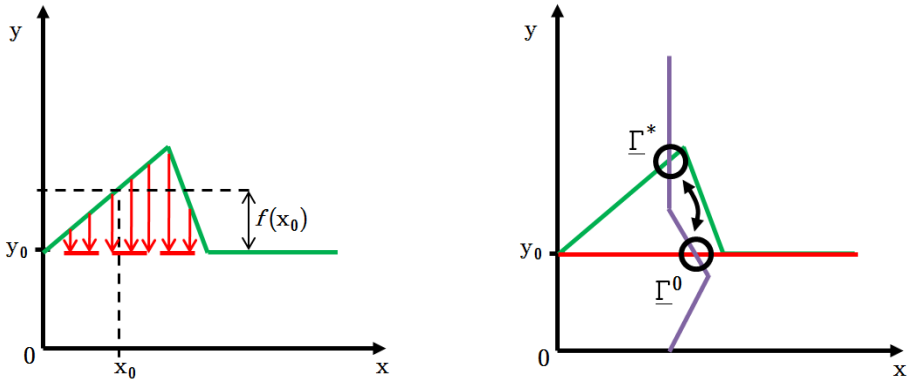

(a) Step 1 (b) Step 5

FIGURE 5.5 – Principle of the continuous transformation of the map. The image of an intersection under a continuous function remains an intersection.

5.4.4 Proof of Optimality

We seek to prove hereafter that the point $\underline{\Gamma}^* = (\gamma_1^*, \gamma_2^*)$ as it was defined on Figure 5.4 is in fact the optimal solution we are looking for.

The region of achievable SNR $\mathscr{R}_i^*$ is the set of all points (γ_j, γ_i) that let meet the constraint in rate $R_{tg,i}$. By superimposing $\mathscr{R}_1^*$ and $\mathscr{R}_2^*$ and by considering their intersection $\mathscr{R}^* = \mathscr{R}_1^* \cap \mathscr{R}_2^*$, we define the set of all points (γ_j, γ_i) that ensures both destinations meet reliable transmissions at rate $R_{tg,1}$ and $R_{tg,2}$. However, we aim also at minimizing power budget. Curve $(\mathscr{D}_i^k)_k$ is the lower boundary of $\mathscr{R}_i^*$. Hence, each point of $(\mathscr{D}_i^k)_k$ ensures first to meet constrained rate $R_{tg,i}$ and second to meet $R_{tg,i}$ with the smallest SNR γ_i. Any other point above $(\mathscr{D}_i^k)_k$ would as well meet target rate but with a higher SNR. Thus, by considering the intersection $\{\mathscr{D}_1^k\}_k \cap \{\mathscr{D}_2^l\}_l$, we define the minimal solution we are looking.

This completes the proof of our algorithm. By deriving $\underline{P}^*$ from $\underline{\Gamma}^*$, we obtain the solution to our problem of minimization of power under constraints of rate.

Now that we have explained how to derive the solution of (5.9), we need to express this solution analytically. To this end, Table 5.2 summarizes coordinates of all possible intersection points $\{\mathscr{D}_1^k\}_k \cap \{\mathscr{D}_2^l\}_l$. We refer to abscissa and ordinate of $\mathrm{CP}_{k,l} = \mathscr{D}_1^k \cap \mathscr{D}_2^l$ respectively by $\mathrm{CP}_1(k,l)$ and $\mathrm{CP}_2(k,l)$ ('CP' means 'crossed point'). These nine points are possible candidates to be the optimal solution we are looking for. Nevertheless, their optimality is driven by the value of momentary channel and system parameters. To determine which $\mathrm{CP}_{k,l}$ is the solution $\underline{\Gamma}^*$ of (5.9), we must check which $\mathrm{CP}_{k,l}$ is relevant. Indeed $\mathscr{D}_1^k$ and $\mathscr{D}_2^l$ always intersect (expect if parallel lines) but their intersection must be located within their region of applicability defined by $\Omega_{k,l}$:

$$\begin{array}{l} \forall (k,l) \in \{1,2,3\}^2, \\ \mathrm{CP}_{k,l} \in \Omega_{k,l} \quad \Leftrightarrow \quad \mathrm{CP}_{k,l} = \underline{\Gamma}^*. \end{array} \tag{5.13}$$

Such a relevant intersection point CP_{k_0,l_0} also establishes which is the optimal pair of schemes $\underline{O}^* = (O_1^*, O_2^*)$ to handle in-band interference at destination, since $\underline{O}^*$ has been defined such that $O_1^* = k_0$ and $O_2^* = l_0$.

$\Omega_{k,l}$	$\mathrm{CP}_1(k,l)$	$\mathrm{CP}_2(k,l)$
$(1,1)$	$\frac{A_1(1+A_2f_{2,1})}{1-A_1A_2f_{1,2}f_{2,1}}$	$\frac{A_2(1+A_1f_{1,2})}{1-A_1A_2f_{1,2}f_{2,1}}$
$(1,2)$	$\frac{A_1(1+Af_{2,1})}{1+A_1f_{1,2}f_{2,1}}$	$\frac{A-A_1f_{1,2}}{1+A_1f_{1,2}f_{2,1}}$
$(1,3)$	$A_1(1+A_2f_{2,1})$	A_2
$(2,1)$	$\frac{A-A_2f_{2,1}}{1+A_2f_{1,2}f_{2,1}}$	$\frac{A_2(1+Af_{1,2})}{1+A_2f_{1,2}f_{2,1}}$
$(2,2)$	$\frac{A(1-f_{2,1})}{1-f_{1,2}f_{2,1}}$	$\frac{A(1-f_{1,2})}{1-f_{1,2}f_{2,1}}$
$(2,3)$	$A-A_2f_{2,1}$	A_2
$(3,1)$	A_1	$A_2(1+A_1f_{1,2})$
$(3,2)$	A_1	$A-A_1f_{1,2}$
$(3,3)$	A_1	A_2

Table 5.2 – Coordinates of all possible intersection points $\{\mathscr{D}_1^k\}_k \cap \{\mathscr{D}_2^l\}_l$.

A conscientious investigation of communication contexts has underlined a surprising situation where there are three intersection points which are simultaneously relevant. This is absolutely not a contradiction with our previous results since we never proved the uniqueness of the solution. Such a configuration is displayed in Section 5.4.5 (Figure 5.10b) and will be investigated more in details in Chapter 6. In that precise case, NC must choose one solution among the three candidates. Here the definition of the function f in (5.9) matters since f may condition the choice. For instance we may seek to minimize the sum $P_1^* + P_2^*$ or just the smallest power $\min\{P_1^*, P_2^*\}$.

Figure 5.6 gives a schematic description of our algorithm. First there is a step of knowledge where NC acquires rate constraints and system limitations in power. Such information can be broadcasted by the sources. This is not a stringent assumption since sources have to send QoS constraints to their destination : no additional transmission is required by our CPA algorithm. Meanwhile NC is also notified of channel parameter values that sources or destinations have estimated with pilot signals for instance. This step could possibly generates additional traffic. Second, NC performs CPA algorithm whose ideas have been developed above but whose process is illustrated on Figure 5.7. Lastly, outputs of CPA algorithm are notified by NC to sources and destinations.

Figure 5.7 is a description of the chronological steps performed by our CPA algorithm. White rectangles refer to computational actions that NC has to perform. All these actions have already been discussed previously. Such coordinates are summarized in Table 5.2. Green rectangles correspond to conditional actions that may prevent CPA algorithm to compute the optimal vector of power. Intersection points must indeed be located within their sector $\Omega_{k,l}$ to be relevant. Blue hexagons monitor the validity and relevance of computation. Green and red arrows respectively mean that condition is true or false. We proved above that there always is at least one solution in theory. Nevertheless, contingent on system limitations $P_{i,\min}$ and $P_{i,\max}$, the theoretic solution may be located outside the region of interest. Consequently no solution is achieved in practice by our CPA algorithm. To counteract this situation, NC can request either to perform a time-sharing based resource allocation or to change system and QoS constraints.

If time-sharing based resource allocation is adopted by the system, both transmissions

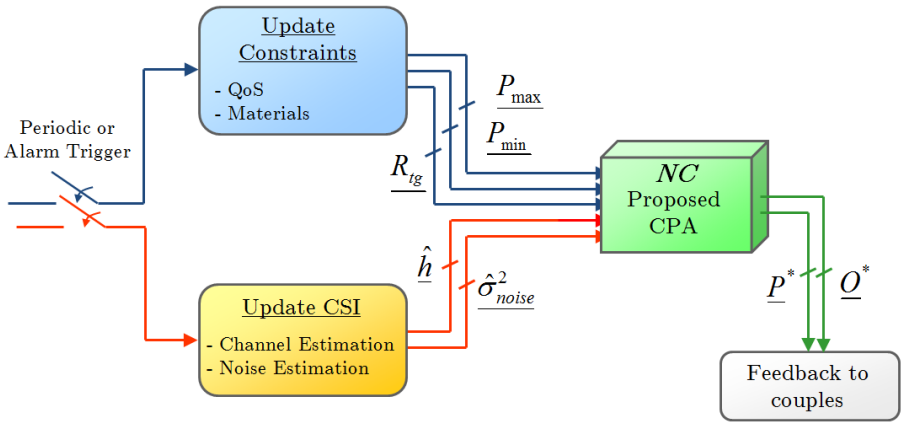

FIGURE 5.6 – Description of our CPA algorithm for minimizing transmission power in rate-constrained networks. Given some inputs, CPA outputs two vectors compliant with inputs : minimal power and advised strategies to efficiently handle in-band interference at each destination.

are then orthogonal and do not interfere any more. Nevertheless they are less spectral efficient since resources are exploited at half. Requested power budget needs then to be higher to meet target rates. We derive below the transmission power that NC would compute if time-sharing was adopted by the system :

$$\begin{aligned} & R_{tg,i} \leq \tfrac{1}{2} \cdot \log_2(1 + \tfrac{|g_{i,i}|^2 \cdot P_{i,\mathrm{TS}}}{N_0}) \\ \Leftrightarrow \quad & P_{i,\mathrm{TS}} \geq (2^{2R_{tg,i}} - 1)\tfrac{N_0}{|g_{i,i}|^2}. \end{aligned} \tag{5.14}$$

5.4.5 Simulation Results and Remarks

In this last subsection we present some simulation results of our CPA algorithm for the case of two 'source-destination' pairs that share a single frequency band for their transmissions. We compare performance of our algorithm to those of two single-strategy based power allocation technique. The first reference technique is a time-sharing based power allocation, *i.e.,* pairs access half time to the frequency band but on an orthogonal way that prevents destinations to encounter in-band interference. The second baseline is a technique where handling of in-band interference is not adapted to the communication context, as we do. The fixed strategy which has been chosen to process in-band interference is the noisy strategy where in-band interference is ignored and added to the noise floor. We will name CPA, NPA and TSPA the algorithms that perform respectively our algorithm, the noisy-based power allocation and the time-sharing-based power allocation. The manner with which NPA and TSPA algorithms compute power to be compliant with target rates is given in (5.15).

Three algorithms are compared in terms of assigned power budget as well as the percentage of successful assignment. In other words, we also investigate the frequency with which each algorithm fails in assigning a power vector that ensures reliable transmissions with rates $R_{tg,1}$ and $R_{tg,2}$. As mentioned on Figure 5.7, CPA algorithm switches to TSPA algorithm when NC does not manage to compute one feasible power vector. We will also present how this additional adaptation affects our algorithm. We cannot use as additional reference a SIC-based power allocation algorithm, since SIC-based strategies are not appli-

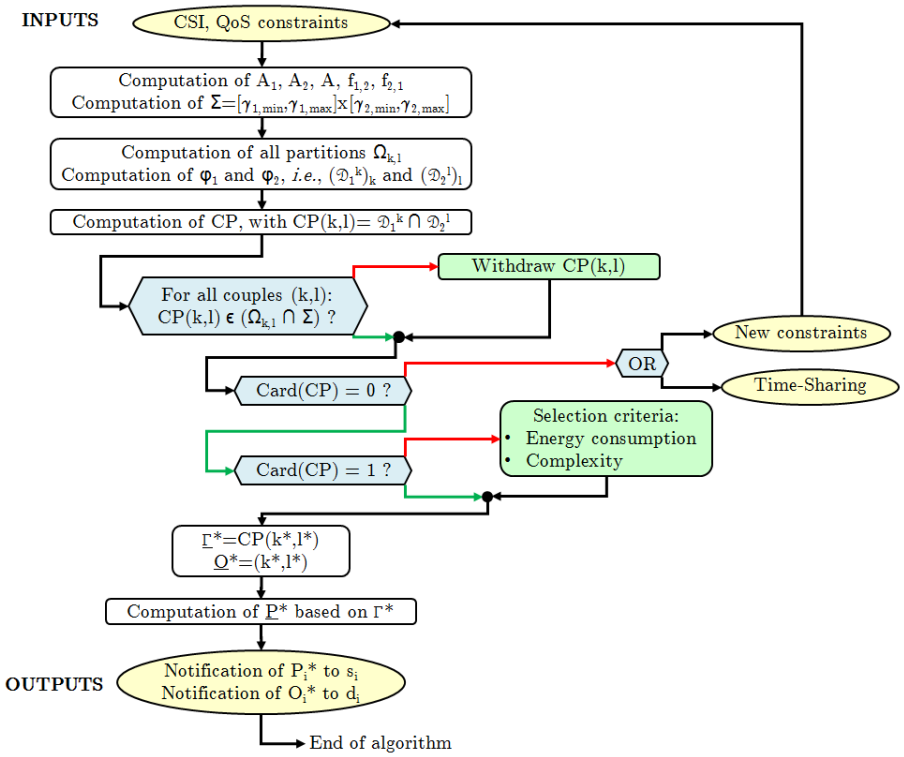

FIGURE 5.7 – Description of the successive computational steps of our CPA algorithm.

cable for any value of δ_i (see Section 4.2). Mostly this algorithm would fail at low in-band interference, so it would be not a reliable baseline.

$$\begin{aligned} P_{i,\mathrm{NPA}} &= \frac{A_i(1+A_j f_{j,i})}{1-A_i A_j f_{i,j} f_{j,i}} \cdot \frac{N_0}{|g_{i,i}|^2} \\ P_{i,\mathrm{TSPA}} &= (2^{2R_{tg,i}}-1)\frac{N_0}{|g_{i,i}|^2}. \end{aligned} \tag{5.15}$$

NPA algorithm is in fact included in our algorithm, since it corresponds to our first regime of interference. However, if NPA algorithm is considered alone, its region of applicability is not restricted to the region ω_i^1 but to all possible values of $\delta_i \in [\delta_{i,\min}, \delta_{i,\max}]$. There are two equivalent ways to explain how NPA computes $\underline{P}_{\mathrm{NPA}}$. First we can note $\underline{P}_{\mathrm{NPA}}$ is nothing else that the power corresponding to the intersection between $\mathscr{D}_1^1$ and $\mathscr{D}_2^1$. In other words, $\underline{P}_{\mathrm{NPA}}$ is determined with $\mathrm{CP}_1(1,1)$ and $\mathrm{CP}_2(1,1)$ expressed in Table 5.2. Second, we can think about $\underline{P}_{\mathrm{NPA}}$ as the solution of the following system of equations that states each destination employs the noisy strategy to cope with in-band interference and meet a reliable transmission at rate $R_{tg,i}$:

$$\begin{cases} R_{tg,i} = \log_2(1+\frac{\gamma_{i,\mathrm{NPA}}}{1+f_{j,i}\cdot\gamma_{j,\mathrm{NPA}}}) \\ R_{tg,j} = \log_2(1+\frac{\gamma_{j,\mathrm{NPA}}}{1+f_{i,j}\cdot\gamma_{i,\mathrm{NPA}}}). \end{cases} \tag{5.16}$$

Solving this system is straightforward and leads to the two expected solutions $\gamma^*_{1,\mathrm{NPA}} = \mathrm{CP}_1(1,1)$ and $\gamma^*_{2,\mathrm{NPA}} = \mathrm{CP}_2(1,1)$.

We present with Figure 5.8 the achievable SNR with NPA algorithm for two different communication contexts. NPA simply considers lines $\mathscr{D}_1^1$ and $\mathscr{D}_2^1$ without any restriction considering their region of applicability. In the first scenario shown on Figure 5.8a, both

lines cross themselves and so define the solution to the problem. On the other hand, Figure 5.8b displays a scenario where both lines never cross themselves in the positive region. In other words, there is no power vector that achieves reliable transmissions, contingent on momentary values of channel and system parameters. Even if sources would transmit with infinite power, there would not be any balance power vector to meet jointly both $R_{tg,1}$ and $R_{tg,2}$. We sense better with this second figure the interest of our CPA algorithm that ensures there is always a theoretical solution.

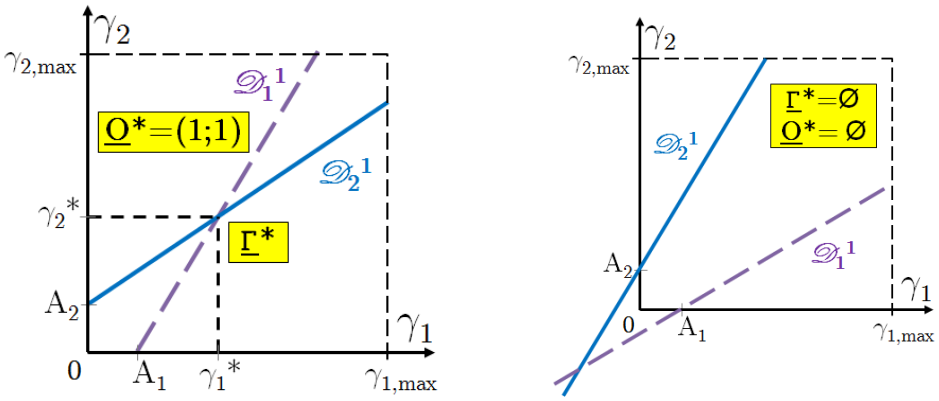

(a) Successful Power Allocation

(b) Failed Power Allocation

FIGURE 5.8 – Behaviour of NPA algorithm for two different communication contexts. On the left there is a compliant allocation of power, while power allocation fails on the right.

Let us try to investigate more in details what means Figure 5.8b. The fact that both lines cross themselves in the negative region means that coordinates of their intersection points are negative, *i.e.*, $1 - A_1 A_2 f_{1,2} f_{2,1} < 0$ (see Table 5.2).

By expressing this condition differently, we obtain :

$$\begin{aligned} & 1 - A_1 A_2 f_{1,2} f_{2,1} < 0 \\ \Leftrightarrow \quad & f_{1,2} f_{2,1} > \tfrac{1}{A_1 A_2} \\ \Leftrightarrow \quad & \left| \tfrac{g_{1,2} \cdot g_{2,1}}{g_{1,1} \cdot g_{2,2}} \right|^2 > \tfrac{1}{A_1 A_2} \\ \Leftrightarrow \quad & \tfrac{\delta_1 \cdot \delta_2}{\gamma_1 \cdot \gamma_2} > \tfrac{1}{A_1 A_2}. \end{aligned} \tag{5.17}$$

which becomes

$$\begin{aligned} & (\tfrac{\delta_i}{\gamma_i})^2 > \tfrac{1}{{A_i}^2} \\ \Leftrightarrow \quad & \delta_i > \tfrac{1}{A_i} \gamma_i \\ \\ \Rightarrow \quad & \log_2 \delta_i > \log_2 \tfrac{1}{A_i} + \log_2 \gamma_i \\ \\ \Rightarrow \quad & \log_2 \mathrm{INR} > \log_2 \mathrm{SNR} \\ \Leftrightarrow \quad & \alpha > 1. \end{aligned} \tag{5.18}$$

by considering first a symmetric system, and then asymptotic infinite transmit power.

Finally, we find again the conclusion illustrated on Figure 4.6 which stated that the noisy strategy collapses for any $\alpha > 1$. For these values of α, there is no need to transmit, even with infinite power since enhancing SNR cannot translate into an increase of data

rate. Indeed there is no degree of freedom available for the transmission ; hence $r_\alpha = 0$, see (4.3).

Likewise, we can compare performance of TSPA algorithm to those of CPA. To this end, we can note that condition (5.14) for TSPA and condition (4.18) for SIC-based strategy look very similar ; there is just a pre-log coefficient $\frac{1}{2}$ that differs. Hence we will express the gap between the SNR achievable with a SIC-based strategy and the one achievable with TSPA algorithm.

$$\begin{array}{lll} \text{SIC-based :} & R_{tg,i} = \log_2(1+\gamma_i) & \text{TSPA :} \quad R_{tg,i} = \frac{1}{2}\cdot\log_2(1+\gamma_i) \\ & 2^{R_{tg,i}} - 1 = \gamma_i & 2^{2=R_{tg,i}} - 1 = \gamma_i. \end{array} \tag{5.19}$$

With use of (5.3) we can reformulate (5.19) differently :

$$\begin{aligned} 2^{2R_{tg,i}} - 1 &= 2^{R_{tg,i}}(2^{R_{tg,i}} - 1) + 2^{R_{tg,i}} - 1 \\ &= (2^{R_{tg,i}} + 1)A_i \\ &= (2^{=R_{tg,i}} - 1 + 2)A_i \\ &= A_i(A_i + 2). \end{aligned} \tag{5.20}$$

Power assigned by TSPA algorithm does not depend on INR level since in-band interference has been avoided by orthogonal resource allocation. Consequently, $P_{i,\text{TSPA}}$ or likewise $\gamma_{i,\text{TSPA}}$ is constant for all values of δ_i. We thus have $\gamma_{i,\text{SIC}} = A_i$ and $\gamma_{i,\text{TSPA}} = A_i(A_i+2)$. Such a result allows us to compare easily performance of TSPA to our CPA algorithm. We represent on Figure 5.9 performance of CPA, NCA and TSPA algorithms, as well as performance of SIC-based strategy assuming an ideal case where SIC would not be restrict to $(\delta_i, \gamma_i) \in \omega_i^3$. This figure is an illustration of one communication context among many possible others. For this context, we sort each algorithm depending on their output value of γ_i^* for the given input δ_i. The dotted brown line on the top illustrates performance of TSPA which is in this case always worse than our CPA. Then, NPA is also outperformed by CPA since $\gamma_{i,\text{NPA}} > \gamma_{i,\text{CPA}}$. Finally, the SIC-based strategy gives the best result ; this is a well-known result since we proved in Chapter 4 that the very strong regime achieved the same performance than a point-to-point transmission without any in-band interference.

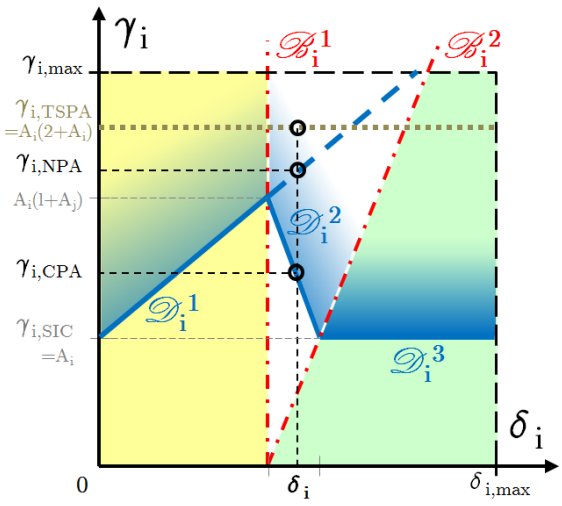

Figure 5.9 – Comparison of CPA, NPA and TSPA for a given communication context.

Figure 5.9 is quite obvious. We easily note that according to values of A_i, A_j and δ_i, NPA algorithm may work as well as CPA algorithm, TSPA algorithm may be better than CPA algorithm and SIC-based performance may be achieved by CPA algorithm. Nevertheless, TSPA will never be better or as good as SIC-based strategy. Likewise, NPA will never be as goog as SIC-based strategy, expect for the single value $\delta_i = 0$.

Simulation Results

The set $\mathscr{P}_S = \{R_{tg,1}, R_{tg,2}, f_{1,2}, f_{2,1}\}$ of system and channel parameters fully characterizes any communication context. Changing one of these values changes optimal solution. $P_{1,\max}$ and $P_{2,\max}$ are also of great importance but they do not influence theoretical performance of algorithm ; they matter during the last step as an an admission control process to check the feasibility in practice of theoretical solutions. Furthermore, they are commonly set one for all and do not vary across time as other parameters do. That is why we choose to not include them in the set $\mathscr{P}_S$. $R_{tg,i}$ is actually the target spectral efficiency in bit per channel use (BPCU), while $f_{i,j}$ emulates simultaneously several communication scenarios. Numerous channel coefficient couples $(g_{i,j}, g_{i,i})$ indeed stand for the same value of parameter $f_{i,j} = \left|\frac{g_{i,j}}{g_{i,i}}\right|^2$. Changing one parameter in $\mathscr{P}_S$ leads to another context of communication with another optimal solution.

$\mathscr{P}_S = (2, 4, 5, 7)$ defines for instance a highly interfered scenario, since both parameters f_i have values greater than one. This implicitly means that crossed-links have a better CQI than direct paths. In this case, optimal solution is given by Figure 5.10a : $\underline{P}^*_{\text{CPA}}$ should be set such that $\underline{\Gamma}^*_{\text{CPA}} = (3.00, 48.00)$. Meanwhile, destinations d_1 and d_2 should process interfering signals with respectively the SIC-based ($O^*_1 = 3$) and the joint-decoding ($O^*_2 = 2$) strategies. The blended shades of yellow refer to the achievable SNR region $\mathscr{R}^* = \mathscr{R}^*_1 \cap \mathscr{R}^*_2$, optimal solutions $\underline{\Gamma}^*_{\text{CPA}}$ are marked with yellow stars.

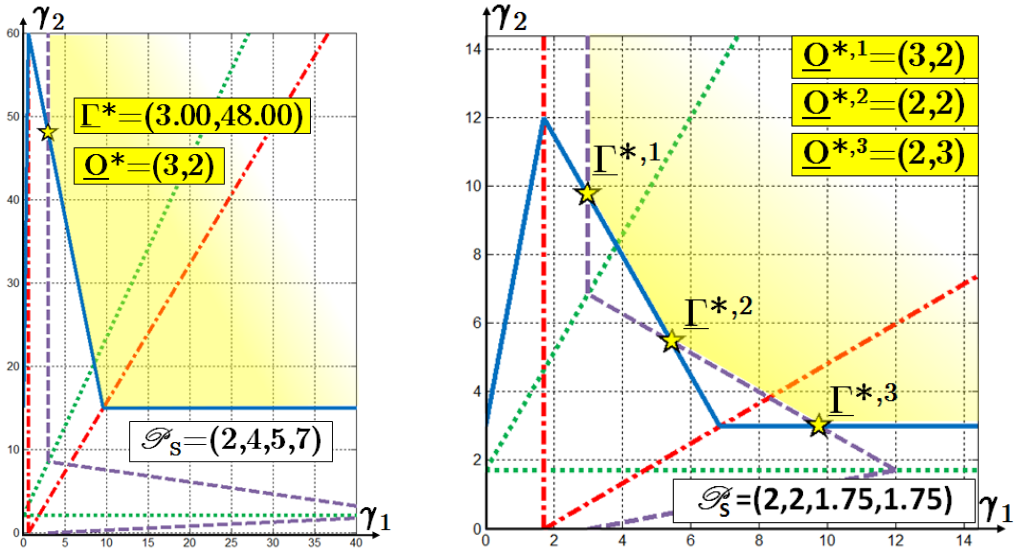

(a) Strong interference

(b) Three optimal solutions

FIGURE 5.10 – Numerical results for two given communication scenarios $\mathscr{P}_S$

To compute the corresponding optimal power vector $\underline{P}^*_{\text{CPA}}$, we assume hereafter a

system of (two) femtocells whose adopted settings are summarized in Table 5.3 [2] [3]. This example has no great illustrative virtue ; it is just a way to show how power can easily be computed by NC. We consequently pay little attention to validity of system model and just consider thermal noise and random fading besides path loss. NC computes transmission power vectors $\underline{P}^*_{\text{CPA}}$, $\underline{P}^*_{\text{NPA}}$ and $\underline{P}^*_{\text{TSPA}}$ with vector $\underline{\Gamma}^*_{\text{CPA}}$, (5.15) and (5.21). Results of each algorithm are also compared to the minimal conceivable power $\underline{P}^*_{\text{SIC}}$, even if it may be not feasible. They are given in Table 5.4. We add two ratios η and η_{lim} which evaluate respectively the gain in comparison to CPA and the merge in comparison to the conventional limitation $P_{\max}$ for femtocells power budget. For this given context $\mathscr{P}_S$, CPA is the single algorithm which successes in being compliant with both $R_{tg,i}$. Indeed, NPA fails in assigning positive powers since the condition $1 - A_1 A_2 f_{1,2} f_{2,1} > 0$ does not hold, while TSPA fails in assigning powers compliant with $P_{\max}$.

Noise variance	$N_0 = -105\text{dBm}$
Fading state	$h_{1,1} = 0.1$ $h_{2,2} = 0.05$
Path loss	$L_{\text{dB},i} = 37 + 30 \cdot \log_{10} d^{(i)}$
Distance	$d^{(1)} = 25\text{m}$ $d^{(2)} = 30\text{m}$
Power limitation	$P_{\max} = 200\text{mW}$

Table 5.3 – System model settings.

$$P_i^* = \frac{N_0}{|g_{i,i}|^2} \cdot \gamma_i^* = \frac{N_0 \cdot 10^{\frac{L_{\text{dB},i}}{10}}}{|h_{i,i}|^2} \cdot \gamma_i^*. \tag{5.21}$$

Algorithm	P_1^* [mW]	P_2^* [mW]	η [%]	η_{lim} [%]
CPA	0.74	82.16	$(100, 100)$	$(0.37, 41.08)$
NPA	NF	NF	$\emptyset$	$\emptyset$
TSPA	3.71	436.48	$(500, 531)$	$(1.86, 218.24)$
SIC	0.74	25.68	$(100, 31.25)$	$(0.37, 12.84)$

Table 5.4 – Comparison of assigned power vectors with CPA, NPA, TSPA and SIC-based strategy for the scenario $\mathscr{P}_S = \{R_{tg,1}, R_{tg,2}, f_{1,2}, f_{2,1}\}$. 'NF' means here 'not feasible'.

A surprising scenario $\mathscr{P}_S = (2, 2, 1.75, 1.75)$ is shown on Figure 5.10b : three solutions are simultaneously feasible with our CPA algorithm. We never proved the uniqueness of our solution, just its existence. Further reasoning would prove it cannot exist more than three solutions with non-zero probability. It would be sufficient to investigate equations of $(\mathscr{B}_i^k)_{i,k}$ restricted to the partition $(\omega_i^k)_{i,k}$ in order to confirm this result. We just precise here that a necessary but not sufficient condition for such a scenario occurring is $(f_{1,2} > 1)$ and $(f_{2,1} > 1)$. Nevertheless, this is not at all a limitation for our algorithm. NC needs just to select among these three solutions which one is the optimal solution for (5.9). Each

2. Coefficient $h_{i,j}$ refers to the fading parameter of channel between source s_i and destination d_j. It was up to now not defined since it was previously included into the global gain $g_{i,j}$.

3. $d^{(i)} = \text{dist}(s_i, d_i)$ $[m]$.

solution lets to meet both target rates with minimal power within their sector $\Omega_{k,l}$ but just one minimizes $f(\underline{P})$. The choice of the objective function f can be animated by objective functions summarized in Table 4.4.

Results of Wide Numerical Simulations

Up to now we considered specific communication contexts for which we compared CPA, NPA and TSPA algorithms. We propose hereafter to compare them with a wide campaign of numerical simulations. Our system model remains the one of two femtocells that share a common frequency band. However, we refine it in addition to Table 5.3 in order to introduce for instance random deployments of devices and thus stimulate the adaptation between our three-level interference classifier. To be fair and as much exhaustive as possible, while being realistic, we consider the deployment of devices illustrated on Figure 5.11. This allows destinations to encounter either highly interfered contexts where transmissions are interference-limited, or weakly interfered contexts where transmissions are rather noise-limited. The first home base station (H-BS, also named FAP for femto access point) s_1 is placed at the centre of the system and has a fixed coverage area characterized by the yellow circle of radius r_{fcell}. A femto user d_1 is randomly placed within this circle by use of a uniform distribution in polar coordinates. The second H-BS s_2 is randomly located within the circle of centre s_1 and radius $r_{\text{system}} + r_0$ where r_0 defines an exclusion area around s_1. This second H-BS has also a coverage radius r_{fcell} and is represented by the blue circle. The random location of the second femto user d_2 follows the same rules as those for location of d_1. Both femtocells may overlap but r_0 avoids they are too close. No exclusion area is defined for a femto user since in femtocell networks a user can be arbitrarily close to its H-BS. Channels are subject to log-normal shadowing [57] and Rayleigh fading.

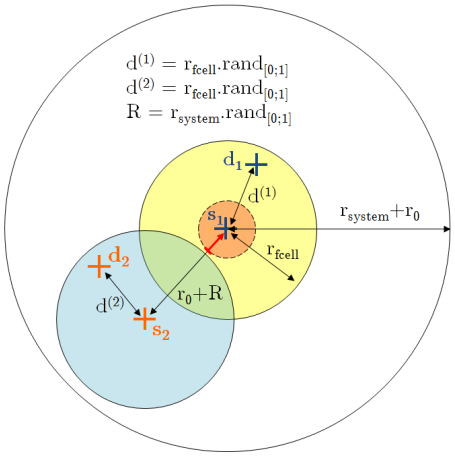

FIGURE 5.11 – Deployment of interfering femtocells.

Simulations consist in N_{simu} random communication contexts $\mathscr{P}_S$ for which channel parameters $f_{1,2}$ and $f_{2,1}$ are defined as previously stated and rate constraints are randomly defined. Adopted settings not previously set in Table 5.3 are summarized in Table 5.5. Coefficients $h_{1,1}$ and $h_{2,2}$, as well as distance $d^{(1)}$ and $d^{(2)}$, already defined are now out-of-date since respectively Rayleigh and uniform distributions are used instead.

We briefly recall main guidelines of each algorithm we compare. We also precise how each algorithm may fail in its power allocation.

– **TSPA :** Powers are assigned as specified in (5.15). If $\underline{P}^*_{\text{TSPA}} \notin [P_{\min}, P_{\max}] \times$

System dimension	$r_{\text{system}} = 50\text{m}$ $r_{\text{fcell}} = 20\text{m}$ $r_0 = 10\text{m}$
Rayleigh parameter	$\sigma_{\text{Rayleigh}} = \sqrt{\frac{2}{\pi}}$
Shadowing [57]	$\sigma_{\text{dev}} = 8\text{dB}$ (standard deviation) $N_{\text{sinus}} = 50\text{m}$ $L_{\text{decor.}} = 50\text{m}$ (decorrelation length)
Target rate	$R_{tg,i} \in \{1, 2, 4, 6, 8\}$ BPCU
Simulation	$N_{\text{simu}} = 10^6$
Power limitation	$P_{\text{min}} = 0\text{mW}$

Table 5.5 – Additional settings of system model.

$[P_{\text{min}}, P_{\text{max}}]$, then $\underline{P}^*_{\text{TSPA}} = 0$. For the momentary communication context both H-BSs are not allowed to transmit, even if just one H-BS does not comply with power limitations.

- **NPA :** Powers are assigned as specified in (5.15). If $\underline{P}^*_{\text{NPA}}$ does not comply with power limitations, then TSPA is used instead.
- **CPA :** Power is computed based on Figure 5.7. We proved there is always at least a theoretical solution. In case of multiple candidates, the solution that minimizes the sum $P_1^* + P_2^*$ is chosen. If $\underline{P}^*_{\text{CPA}}$ does not comply with power limitations, then TSPA is used instead.

Figures 5.12 and 5.13 illustrate performance of CPA algorithm in terms of selection of the optimal sector $\underline{Q}^*$. We first plot the distribution of the optimal selection, *i.e.,* the frequency with which each sector $\Omega_{k,l}$ has been selected (successfully or not) across N_{simu} random communication contexts. This result is displayed with the pie on Figure 5.12 which validates the relevance of our adaptive interference classification. Indeed, if NPA-based power algorithms are widely adopted in literature, the pie proves that it cannot suit to all values of channel and system parameters since just 60% of communication contexts are dealt with NPA-based power algorithms. Then we plot how frequently our CPA algorithm fails in assigning a feasible power vector, *i.e.,* a power vector that does not exceed power limitations. Bar graphs of Figures 5.13a and 5.13b plot the percentage of recourse to TSPA ; with the first bar graph, percentage is computed on all N_{simu} scenarios, while with the second graph, percentage is based on the frequency of selection of each $\Omega_{k,l}$.

Power allocation can fail because of different reasons. Figure 5.14a illustrates why and how much power allocation fails. Thus, we note that NPA mostly fails due to negative power assignment and not due to excessive power assignment. Furthermore, NPA fails thirty times more often than CPA which only appeals to TSPA in 1.1% of scenarios. Nevertheless the recourse to TSPA seems not really help our CPA since there are quite as many failed assignments before and after the call to TSPA (see below to note that this is a false idea !). On the other hand, TSPA greatly improves NPA since 83% of failed assignments are avoided by TSPA. Lastly, TSPA is the worst power allocation algorithm when it is performed alone. To conclude with this figure, we note that our algorithm brings a non neglecting gain. Figure 5.15 goes a little bit further in the cause of failed power allocation : we represent which femtocell is responsible for the failure. As it was expectable, failures of NPA are very correlated in both femtocells since the condition $A_1 A_2 f_{1,2} f_{2,1} \gtrless 1$ holds for both femtocells simultaneously. On the other hand, there is no correlation between failures

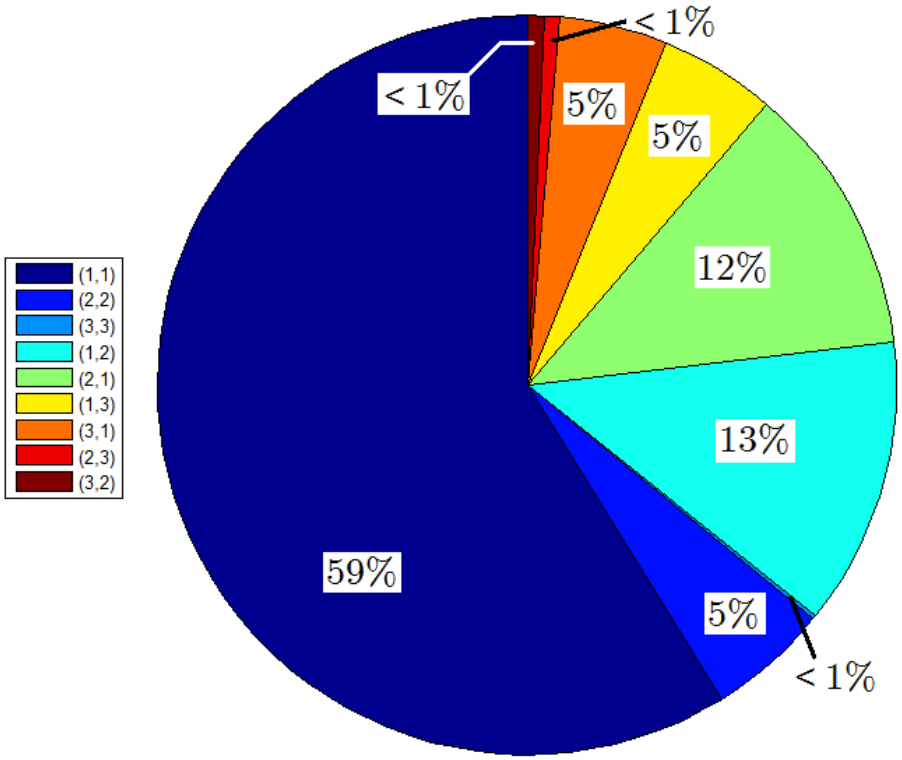

FIGURE 5.12 – CPA Algorithm : Distribution of optimal sector O^* among all $\Omega_{k,l}$.

of two femtocells for CPA and TSPA.

We compare finally with Figure 5.14b performance in terms of power assignment. We plot first the initial power assignment (without any step of admission control) ; we just ignore for NPA the scenarios with negative power assignment, *i.e.,* 30% of scenarios. NPA seems to perform very well but this first result is not relevant at all since 30% of scenarios are not taken into account and these ignored scenarios are precisely the worst ones. Before any admission control process, CPA shows a great gain (93% of reduction) in comparison to TSPA. Once the admission control process and TSPA have been performed, we have a more relevant view of performance. We note that the power budget for NPA is higher after the admission control process than before ; such a result is obvious since the 30% of bad scenarios have now been dealt with TSPA which commonly requires a higher power. This last result must be considered in parallel with results of Figure 5.14a (*Error after TSPA*). Just 1% of scenarios are not taken into account with CPA for the average power budget, against 5% and 7% respectively for NPA and TSPA. The worst scenarios are then ignored with NPA and TSPA ; this reduces their average power budget. However, even with this inequity, CPA remains better than NPA and TSPA by offering a reducing gain of respectively 52% and 71%. Amazing waste of power are then avoided while reliable transmissions are more frequently ensured.

Let us note that any couple $(\gamma_1, \gamma_2) \in \Omega_{O_1^*,O_2^*}$ allows as well to transmit reliably with rate $R_{tg,1}$ and $R_{tg,2}$ but the power requested by these couples is greater than the one requested by $\underline{\Gamma}^*$. Nevertheless, according to the definition of the function f in (5.9), it may be than $\underline{\Gamma}^*$ is not the optimal solution any more.

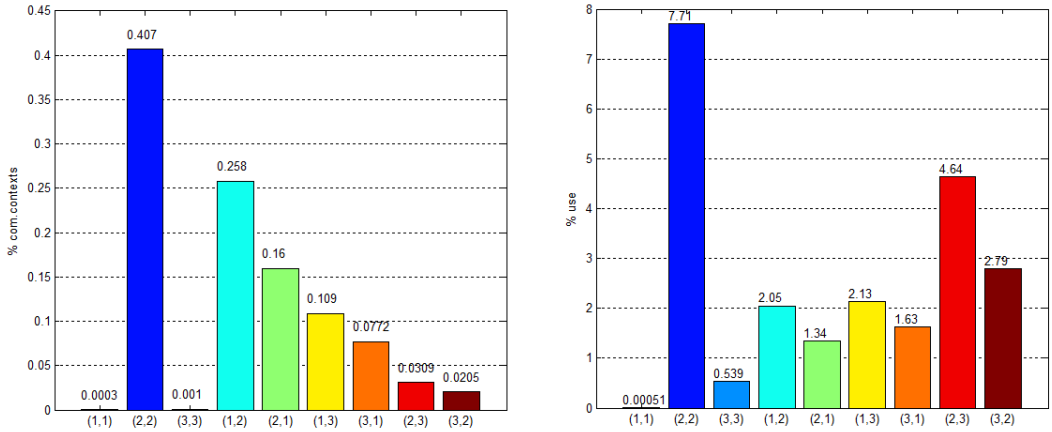

(a) Failed CPA - Total %

(b) Failed CPA - Real %

FIGURE 5.13 – CPA Algorithm : Selection of optimal sector (O_1^*, O_2^*) and percentage of excessive power assignment.

5.5 CPA Generalization to Multi-Source Multi-Destination Cases

In this section we focus on the generalization of our previous results concerning CPA algorithm to a more global system model. Our ultimate goal would be to consider the generic model with n sources, p destinations and N_{SC} frequency bands. This goal will be addressed in Chapter 7 as future work with some propositions to investigate further.We propose hereafter to extend results of the two-user case to the $n-$ user case. In other words, we assume in the remainder of this chapter that $p = n$ and $N_{\mathrm{SC}} = 1$. Consequently, this is the direct continuation of results introduced in Section 4.4, applied to power allocation purposes.

This part of the PhD thesis lacked time to be corroborated by extensive simulations results. We will consequently derive more theoretical results or heuristics without confirming their feasibility and without evaluating their performance in practice.

5.5.1 System Model and Notations

This topic has already been addressed in Section 4.4.1 for the specific case of $n = 3$. The derivation of the model for any value of n is straightforward from what it has been done previously. Figure 4.8 and (4.24) introduce notations which are valid for any n. Concerning (4.25) with the definition of system parameters that state constraints in rate, the framework has been stated with $n = 3$; the extension to any n is a little bit more tedious but it is just a problem of combinatorics. All possible combinations of k 'source-destination' pairs among n pairs ($k \leq n$) should be considered. As it was already said in previous chapters, this is lead by the max-flow min-cut theorem [51, 52] which seeks to maximize the data flows (and hence the throughput) conveyed by all possible combinations of paths. Such a number of combinations is well-known :

$$\binom{n}{k} = C_k^n = \frac{n!}{k!(n-k)!}. \tag{5.22}$$

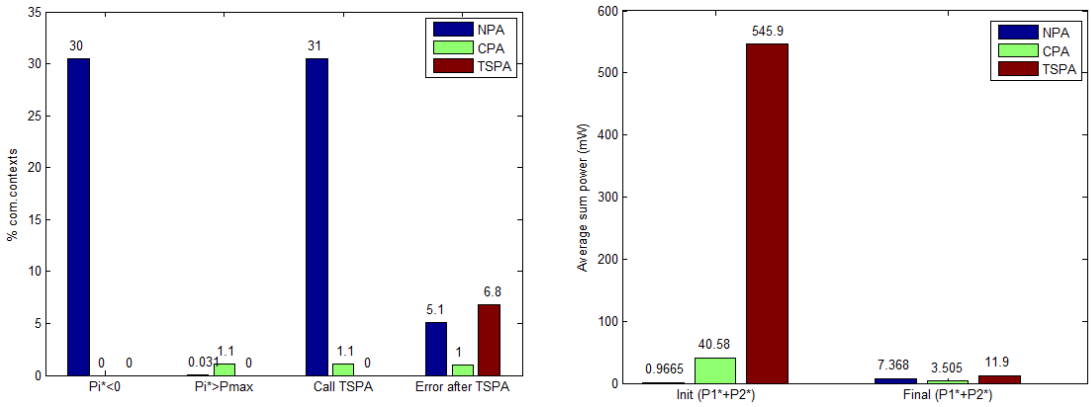

(a) Frequency and causes of failures (b) Assigned power budget

FIGURE 5.14 – Comparison of main results for CPA, NPA and TSPA.

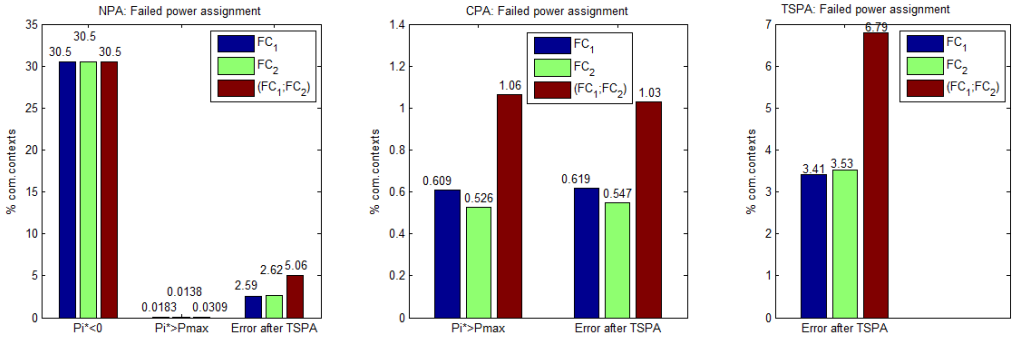

FIGURE 5.15 – Which femtocell is responsible for failed power assignments ?

We will consider in the remainder that rate constraints are characterized by a vector $\underline{R_{tg}} = (R_{tg,1}, \ldots, R_{tg,n})$. Furthermore, we name by $\mathcal{C}_{k,n}$ the set of all combinations of k elements among n and define $\mathbf{N}^{(n)} = \{1, \ldots, n\}$ for more commodity. Hence we have

$$\text{Card}(\mathcal{C}_{k,n}) = \binom{n}{k} \tag{5.23}$$

and besides

$$\forall k \leq n, \quad \forall \Delta \in \mathcal{C}_{k,n}, \quad \Delta \subseteq \mathbf{N}^{(n)} \quad \text{and} \quad \text{Card}(\Delta) = k. \tag{5.24}$$

A convenient way to generalize (4.25) is thus as follows :

$$\forall k \leq n, \quad \forall \Delta \in \mathcal{C}_{k,n}, \quad A_\Delta = 2^{(\sum_{i \in \Delta} R_{tg,i})} - 1. \tag{5.25}$$

Likewise, it is possible to extend to the n-pair system the partition $(\Omega_{k,l})_{k,l} \in \{1,2,3\} \times \{1,2,3\}$ introduced in Section 5.4.2, *i.e.,* the partition into 'sectors' of the region $(\gamma_1; \gamma_2)$. There are always three strategies to classify and handle in-band interference. Nevertheless there are now n-1 (or k-1 if we consider a combination $\Delta \in \mathcal{C}_{k,n}$ of pairs) sources of interference which can be all handled independently by one of the three proposed interference

strategies. For the viewpoint of one given destination d_i, there are then 3^{n-1} different ways to handle all in-band interfering signals $(x_j)_{j\neq i}$; this translates into 3^{n-1} possible and non-overlapping regimes of interference in the region $((\delta_{j,i})_{j\neq i};\gamma_i)$.

We introduce a new operator on sets which specifies that a given index is withdrawn from the original set. Given a set of indexes Δ and an index $i \in \Delta$, we define $\Delta_{\neg i}$ as the set containing all indexes in Δ except i.

$$\forall \Delta \subseteq \mathbf{N}^{(n)}, \quad \forall e_i \in \Delta, \quad \Delta_{\neg_{e_i}} = \{e_1, \ldots, e_{i-1}, e_{i+1}, \ldots, e_{l_\Delta}\} \tag{5.26}$$

where $l_\Delta = \mathrm{Card}(\Delta)$ and e_k refers to the k^{th} index in Δ when they are sorted in ascending order. For sake of clarity, we define the region Λ_i as follows :

$$\Lambda_i = ((\delta_{j,i})_{j\in\mathbf{N}^{(n)}_{\neg_i}};\gamma_i). \tag{5.27}$$

By use of translation variables $\{f_{j,i}\}$ such as those defined in (5.11), we can easily switch between $\delta_{j,i}$ and γ_j. All regions $\{\Lambda_i\}_{i\in\mathbf{N}^{(n)}}$ can thus be superimposed in final region $\Lambda = (\gamma_1;\ldots;\gamma_i;\ldots;\gamma_n)$ to define a total amount of 3^n regimes which are called 'sectors'.

All useful elements have now been defined for introducing the new partition of the region Λ. Let us consider the following partition :

$$\begin{array}{ll} & \underline{\Omega} = \{\Omega_{\underline{O_1},\ldots,\underline{O_n}}\} \\ \text{with} & \underline{O_i} = \{\kappa_{j,i}\}_{j\in\mathbf{N}^{(n)}_{\neg_i}}, \quad \kappa_{j,i} \in \{1,2,3\} \text{ refers to interference strategy,} \\ \text{such that} & \Omega_{\underline{O_1},\ldots,\underline{O_n}} = \bigcap_{k\in\mathbf{N}^{(n)}} \omega_k^{\underline{O_k}}. \\ & \\ & \forall k \in \mathbf{N}^{(n)}, \quad \omega_k^{\underline{O_k}} = \{(\gamma_l)_{l\in\mathbf{N}^{(n)}} \mid \forall l \in \mathbf{N}^{(n)}_{\neg_k},\ \Psi_k(\gamma_l) = \kappa_{l,k}\} \\ \text{where} & \Psi_k(\gamma_l) = \kappa_{l,k} \quad \text{means } x_l \text{ is processed with strategy } \kappa_{l,k} \text{ at } d_k. \end{array} \tag{5.28}$$

Let us note that the condition $\Psi_k(\gamma_l) = s_l$ such it has been defined above is equivalent to say that γ_l verifies the applicability bounds of strategy s_l along the l^{th} direction. This completes the extension to the n-pair case of the partition $\underline{\Omega}$. We precise that this partition fits also to any set $\Delta \in \mathcal{C}_{k,n}$ instead of $\mathbf{N}^{(n)}$. We just have to consider k instead of n and sorted elements $\{e_i\}_{1\leq i\leq k}$ instead of $\mathbf{N}^{(n)}$; this could be useful for future work addressed in Chapter chap :conclusion.

5.5.2 Mathematical Formulation

As it was mentioned in Section 4.4, passing from two to three and then to n adds respectively one and then $n-2$ dimensions to our problem (5.9), in comparison to work introduced in this chapter. The simple problem of lines intersection is thereof substituted by intersection of planes ($n = 3$) or hyperplanes (any n). Graphical representations become tedious for any $n > 2$.

In Section 4.4 where $n = 3$, we derived the explicit expressions of the boundaries for all regions $\{\omega_k^{\underline{O_k}}\}_{k\in\{1,2,3\}}$ as well as the expressions of the objective functions within these regions. The last step would be to compute the intersection of the superposition of all objective functions. However we present hereafter a brief and synthetic way to compute the optimal solution for any value of n. Such a result is met by a matrix representation of the problem.

In previous sections and chapters we referred, sometimes, to max-flow min-cut theorem to characterize optimal regions (rate or SNR achievable regions). We consider here a given cut of our n-pair model that involves n_0 pairs. Nevertheless, to avoid multiplication of variables, we assume $n_0 = n$. To make the reasoning generic, we consider that among the $n-1$ sources interfering with pair '$s_i - d_i$', p interfering signals are classified in the first regime (noisy strategy), q interfering signals are classified in the second regime (joint decoding strategy) while the remainder $t = n-1-p-q$ interfering signals are handled with the third (SIC-based) strategy. We define three sets $\mathscr{P}_i$, $\mathscr{Q}_i$ and $\mathscr{T}_i$ which respectively contain the indexes of the p interfering messages processed as noise by d_i, the indexes of the q interfering messages jointly decoded by d_i and lastly the indexes of the t interfering messages cancelled by s_i. We understand here how combinations may help to consider all possible configurations.

Based on this classification of in-band interference, the objective function for pair '$s_i - d_i$' can be expressed as follows :

$$R_{tg,i} + \sum_{q\in\mathscr{Q}_i} R_{tg,q} = \log_2(1 + \frac{\gamma_i + \sum_{q\in\mathscr{Q}_i} f_{q,i}\cdot\gamma_q}{1+\sum_{p\in\mathscr{P}_i} f_{p,i}\cdot\gamma_p}). \tag{5.29}$$

All messages in $\mathscr{P}_i$ appear at denominator and are thereof seen as noise, while all messages in $\mathscr{Q}_i$ are jointly decoded with x_i and are thus process like x_i. On the other hand, all messages in $\mathscr{T}_i$ are ignored since they have already been decoded and then subtracted (SIC). Equation (5.29) is expressed in terms of rates ; in SNR domain, this translates into :

$$\gamma_i = \sum_{p\in\mathscr{P}} A_0 f_{p,i}\cdot\gamma_p - \sum_{q\in\mathscr{Q}} f_{q,i}\cdot\gamma_q + A_0, \tag{5.30}$$

where $A_0 = A_{\mathscr{Q}_i\cup\{i\}}$, see (5.25).

Let us define some new variables, vectors and matrices. $\underline{\Gamma}$ is the $n\times 1$ vector of SNR, $\underline{C}$ is a $n\times 1$ vector of constants and $\underline{\mathbf{I_n}}$ is the $n\times n$ identity matrix

$$\underline{\mathbf{I_n}} = \begin{pmatrix} 1 & 0 & \cdots & 0 \\ 0 & \ddots & \ddots & \vdots \\ \vdots & \ddots & \ddots & 0 \\ 0 & \cdots & 0 & 1 \end{pmatrix}. \tag{5.31}$$

For sake of clarity, we assume that indexes of $\mathscr{P}_i$, $\mathscr{Q}_i$ and $\mathscr{T}_i$ are sorted as follows :

$$\mathbf{N}_{\neg i}^{(n)} = \{e_1,\ldots,e_p,e_{p+1},\ldots,e_{p+q},e_{p+q+1},\ldots,e_{p+q+t}\} \quad \text{with} \quad p+q+t = n-1. \tag{5.32}$$

Index i is located somewhere between two indexes of this vector, for instance between e_p and e_{p+1}. The $n\times n$ matrix $\underline{\mathbf{F}}$ refers to the matrix of interference handling of the system, *i.e.*, the matrix whose element $\underline{\mathbf{F}}(i,j)$ states how interfering signal x_j is handled by receiver d_i. This is thus a null diagonal matrix ($\underline{\mathbf{F}}(i,i)=0$). Expression (5.30) lets us to fill the i^{th} row of $\underline{\mathbf{F}}$ and $\underline{C}$:

$$\begin{aligned} &\underline{\mathbf{F}}(i,:) = \begin{pmatrix} A_0 f_{e_1,i} & \cdots & A_0 f_{e_p,i} & 0 & -f_{e_{p+1},i} & \cdots & -f_{e_{p+q},i} & 0 & \cdots & 0 \end{pmatrix}, \\ &\underline{C}(i) = A_0. \end{aligned} \tag{5.33}$$

Remaining rows will be defined naturally and obviously once matrix expression will be expressed hereafter.

A matrix form is derived by expressing objective functions for all pairs, as it was done in (5.30) for one pair '$s_i - d_i$'. The global expression becomes :

$$\begin{array}{rl} & \underline{\Gamma} = \underline{\mathbf{F}} \cdot \underline{\Gamma} + \underline{C} \\ \Leftrightarrow & (\underline{\mathbf{I_n}} - \underline{\mathbf{F}}) \cdot \underline{\Gamma} = \underline{C}. \end{array} \tag{5.34}$$

With this expression it is straightforward to express all other rows of $\underline{\mathbf{F}}$ and $\underline{C}$. We just have to know for each pair '$s_k - d_k$' how are processed their $n-1$ interfering signals, *i.e.,* how $\mathscr{P}_k$, $\mathscr{Q}_k$ and $\mathscr{T}_k$ are set. We finally fill $\underline{\mathbf{F}}$ and $\underline{C}$ by properly rearranging all signals according to the order of elements given by (5.32) where index i is assumed to be located between between e_p and e_{p+1}.

Solution to our problem (5.9) for the n-pair scenario may thus be analytically derived iif $n \times n$ matrix $(\underline{\mathbf{I_n}} - \underline{\mathbf{F}})$ is invertible. Thereof we have the following result :

$$\det_n(\underline{\mathbf{I_n}} - \underline{\mathbf{F}}) \neq 0 \quad \Longrightarrow \quad \underline{\Gamma} = (\underline{\mathbf{I_n}} - \underline{\mathbf{F}})^{-1} \cdot \underline{C}. \tag{5.35}$$

Solutions have now been computed for any n and for any sector $\Omega_{\underline{O_1},\ldots,\underline{O_n}} \in \underline{\Omega}$ where $\underline{O_i}$ was introduced in (5.28). Indeed, the set $\underline{O_i}$ refers to one partition regime of region Λ_i, which is in line with the adopted strategies $\{\kappa_{j,i}\}$ to handle all interfering messages $\{x_j\}_{j \in \mathbf{N}_{\neg i}^{(n)}}$. This exactly stands for the definition of sets $\mathscr{P}_i$, $\mathscr{Q}_i$ and $\mathscr{T}_i$, since $\kappa_{j,i} = 1$ means that $j \in \mathscr{P}_i$, $\kappa_{j,i} = 2$ means that $j \in \mathscr{Q}_i$ and $\kappa_{j,i} = 3$ means that $j \in \mathscr{T}_i$. By superimposing all regimes characterized by $\underline{O_i}$ in Λ_i, we obtain the sector $\Omega_{\underline{O_1},\ldots,\underline{O_n}}$ in the wished region Λ.

Nevertheless, this does not mean that computed solutions are the solutions we are looking for. To illustrate the problem, we will refer to the configuration where $n = 2$. Solutions correspond to intersections of lines $\{\mathscr{D}_1^k\}_k$ with lines $\{\mathscr{D}_2^l\}_l$. Two straight lines are always secant if they are not parallel. For any k and any l in $\{1,2,3\}$, there is hence always a solution which is their intersection point $\mathscr{D}_1^k \cap \mathscr{D}_2^l$. Nevertheless, we showed it is not so simple since lines $\{\mathscr{D}_1^k\}_k$ and $\{\mathscr{D}_2^l\}_l$ are not defined on $\mathbb{R}^2$ but within a specific regime of interference. A step of relevance must then be performed to check if the computed intersection point $\mathscr{D}_1^k \cap \mathscr{D}_2^l$ belongs to the sector $\Omega_{k,l}$. This relevance step is also required for $n > 2$.

Once we are sure the solution is relevant, we can derive power vector $\underline{P}$ from SNR vector $\underline{\Gamma}$. An admission control process should lastly validate the feasibility of $\underline{P}$.

Finally, we propose in Table 5.6 a pseudo-code algorithm that aims in computing optimal solution to (5.9) for any value of n. This is mainly a problem of combinatorics, since we need to be exhaustive and consider each of the 3^n sectors whose compose the non-overlapping partition of the region Λ.

Four sets are needed and initially empty. First, $\underline{\mathbf{\Omega}}$ is the set of all partitions of the region Λ, as previously defined. Second, $\underline{\mathbf{\Psi}}$ contains all sectors $\underline{\omega}$ for which the matrix $(\underline{\mathbf{I_n}} - \underline{\mathbf{F}}_{\underline{\omega}})$ is invertible. Then, $\underline{\mathbf{\Gamma}}^*$ contains all SNR vectors computed with (5.35) which are within their sector. Lastly, $\underline{\mathbf{P}}^*$ is the set of all power vectors which pass the power admission step ($P_{\min}$ and $P_{\max}$). Each of these sets defines a main step of the algorithm. First, we compute all possible sectors. Second, we check if solution can be computed for all sectors. Then, we test the relevance of the solution contingent on the boundaries of the sector. Finally, there is a power admission process. At any time during the algorithm, in case of failure, TSPA algorithm is called (see Section 5.4.5 for definition of TSPA).

$\underline{\mathbf{\Omega}} = \emptyset, \quad \underline{\mathbf{\Psi}} = \emptyset, \quad \underline{\mathbf{\Gamma}}^* = \emptyset, \quad \underline{\mathbf{P}}^* = \emptyset.$
$\forall i \in \mathbf{N}^{(n)},$
$\forall (p,q,t) \in \mathbf{N}^{(n)} \times \mathbf{N}^{(n)} \times \mathbf{N}^{(n)} \quad | \quad p+q+t = n-1,$
$\forall \Delta_{p,i} \in \mathcal{C}_{p,n}, \quad \forall \Delta_{q,i} \in \mathcal{C}_{q,n}, \quad \forall \Delta_{t,i} \in \mathcal{C}_{t,n} \quad |$
$\Delta_{p,i} \cup \Delta_{q,i} \cup \Delta_{t,i} = \mathbf{N}_{\neg i}^{(n)},$
$\Delta_{p,i} \cap \Delta_{q,i} = \emptyset,$
$\Delta_{p,i} \cap \Delta_{t,i} = \emptyset,$
$\Delta_{q,i} \cap \Delta_{t,i} = \emptyset,$
$\mathscr{P}_i = \Delta_{p,i}, \quad \mathscr{Q}_i = \Delta_{q,i}, \quad \mathscr{T}_i = \Delta_{t,i}.$
This defines $\underline{O_i}$, with help of strategies $\{\kappa_{j,i}\}_{j \in \mathbf{N}_{\neg i}^{(n)}}$.
$\underline{\omega} = \Omega_{\underline{O_1},\ldots,\underline{O_n}},$
$\underline{\mathbf{\Omega}} = \underline{\mathbf{\Omega}} \cup \{\underline{\omega}\}.$

$\forall \underline{\omega} \in \underline{\mathbf{\Omega}},$
Compute (5.35).
if $\det_n(\underline{\mathbf{I_n}} - \underline{\mathbf{F}}_{\underline{\omega}}) \neq 0$
$\underline{\mathbf{\Psi}} = \underline{\mathbf{\Psi}} \cup \{\underline{\omega}\},$
else $\underline{\mathbf{\Omega}} = \underline{\mathbf{\Omega}} \setminus \{\underline{\omega}\}.$

if $\underline{\mathbf{\Psi}} = \emptyset$
Perform TSPA algorithm,
END OF ALGORITHM.
else $\forall \underline{\omega} \in \underline{\mathbf{\Psi}},$
$\underline{\Gamma} = (\underline{\mathbf{I_n}} - \underline{\mathbf{F}}_{\underline{\omega}})^{-1} \cdot \underline{C}.$
if $\underline{\Gamma} \in \underline{\omega}$
$\underline{\mathbf{\Gamma}}^* = \underline{\mathbf{\Gamma}}^* \cup \{\underline{\Gamma}\},$
else $\underline{\mathbf{\Psi}} = \underline{\mathbf{\Psi}} \setminus \{\underline{\omega}\}.$

if $\underline{\mathbf{\Gamma}}^* = \emptyset$
Perform TSPA algorithm,
END OF ALGORITHM.
else $\forall \underline{\Gamma} \in \underline{\mathbf{\Gamma}}^*,$
Compute $\underline{P}$ with (5.21).
if power_admission$(\underline{P})$ = failed
$\underline{\mathbf{\Gamma}}^* = \underline{\mathbf{\Gamma}}^* \setminus \{\underline{\Gamma}\},$
else $\underline{\mathbf{P}}^* = \underline{\mathbf{P}}^* \cup \{\underline{P}\}.$

if $\underline{\mathbf{P}}^* = \emptyset$
Perform TSPA algorithm,
END OF ALGORITHM.
else
if Card$(\underline{\mathbf{P}}^*) > 1$
Select optimal $\underline{P}^0$ with $f(\underline{P})$,
else $\underline{P}^0 = \underline{\mathbf{P}}^*.$
Notify sources of $\underline{P}^0$,
Notify destinations of $(\underline{O_1}^0, \ldots, \underline{O_n}^0)$,
END OF ALGORITHM.

TABLE 5.6 – Description of CPA algorithm for any n.

To conclude, we note that the algorithm presented in Table 5.6 is exhaustive and may be complex due to the first combinatorics step. It is possible to simplify the n-pair CPA algorithm with some assumptions to reduce complexity. For instance, instead of an exhaustive research of solutions, we can focus only on a subset of interfering pairs, while all other interfering pairs outside the subset are ignored. Typically, the subset could contain the three or four strongest interferers, whereas all other interferers would be processed with the noisy strategy. Such considerations will be addressed in Chapter 7.

5.6 Conclusions

In wireless communication systems, where the same spectrum is shared by some network equipments in the same geographical area, receivers are interfered by concurrent transmissions. In-band interference may seriously reduced reliability and robustness of the transmission and makes the initial message impossible to recover from the received signal. To mitigate detrimental effects of in-band interference and thus to help the receiver in decoding its sensed signal reliably with the targeted satisfaction rate, effective techniques must be performed. The work presented in this chapter is a straightforward application of the three-regime interference classifier developed in Chapter 4. We aim here at allocating power to meet the rates targeted by each pair 'source-destination' while minimizing their transmit power to avoid energy waste.

To this end, a centralized algorithm (CPA) is proposed to perform power allocation in interference-limited and rate-constrained cellular networks. Computation is done by a network controller (NC) which is provided with CSI knowledge and system parameters. NC can thus determine the classification of in-band interference for each destination. Our algorithm exploits all destinations classification of the momentary scenario of communication to meet the goals. The idea of the classifier is that interference is not necessarily a problem, even strong, if efficient schemes deal with it. First, NC computes for each destination d_i the solution of the objective function by defining the SNR achievable region $\mathscr{R}_i^*$. Then, NC superimposes all achievable regions to compute the optimal region $\mathscr{R}^*$ of achievable SNR. Lastly, NC selects the power vector $\underline{P}^*$ that belongs to the lower bounds of $\mathscr{R}^*$ while minimizing all transmit power.

Existence and optimality of this solution $\underline{P}^*$ are proved by a mathematical reasoning. Both theoretical and numerical results illustrate three major achievements for our algorithm. First, QoS constraints of each cell are jointly met. Second, the computed transmit power is minimized for avoiding energy waste. Third, interference processing techniques are adaptively selected, according to the momentary communication context, so that the receiver can efficiently cope with its perceived interference.

We numerically compare our approach to power allocation algorithms where in-band interference is either dealt with a single noisy strategy, or avoided by time-sharing techniques. Numerical results prove that CPA notably outperforms baseline algorithms, both in terms of users rejection and power budget minimization. Chapter 6 focus on the distribution of this algorithm.

Chapter 6

Distributed Power Allocation Algorithm

In the previous chapter we investigated a centralized approach to solve a problem of power minimization under constraints of rate in wireless interference-limited networks. In this chapter, we address the identical problem of power minimization but we now aim at computing the optimal solutions on a non-centralized and fully autonomously way. Commonly centralized approaches require coordination between nodes to achieve a full knowledge of channel and system parameters. Nevertheless, such a coordination may not be feasible or desired in some networks ; it besides suffers from three main drawbacks. First of all, full knowledge seems inconceivable and unachievable in dense networks with high mobility (wireless sensor networks, ad hoc networks), since signalling and control overhead would waste communication resources. Second, effectiveness of centralized approaches depends on the reliability of link quality estimation between each node. Third, all computation complexity is carried out at the network controller.

Therefore we target in this chapter to meet with a distributed and autonomous approach the same performance of those computed by CPA algorithm (see Chapter 5). To this end we derive an iterative process where each node updates in turns its transmit power to react to the power adjustment of its neighbour. The new power is computed based on the interference classifier of Chapter 4. Nevertheless, the convergence of this iterative process, as well as the optimality of the computed solution need to be proved. A rigorous reasoning is hence proposed to prove both optimality and convergence of our distributed power allocation (DPA) algorithm.

The chapter is organized as follows. After introducing our motivations, proposal and the work related to it, the system model and assumptions adopted throughout this chapter are discussed in Section 6.2. Then, Section 6.3 addresses some preliminary knowledge on distributed algorithms. For sake of clarity, DPA algorithm is first introduced in Section 6.4 for the two-user case. Within this section, we investigate and prove the optimality, the convergence and the limits of our algorithm. We lastly tackle the generalization of DPA to the n-user case in Section 6.5 before concluding the chapter with Section 6.6.

6.1 Introduction

Power management techniques become a challenging and trendy issue in the field of wireless communications with the emergence of 'green communications' considerations. Which is targeted here is not just a way for network operators to involve themselves in this universal debate of environment protection ; this is not really a story of self-consciousness. They are more motivated by manufacturing, operating and financial aspects. A lower power budget lets of course operators save money, since a smaller amount of energy is consumed for monitoring the network. However, savings are also met with manufacturing of devices and equipments (antennas, RF circuits, filters, etc.), since transmit features of devices can thus be reduced and so their production cost.

This is also motivated by new wireless communication networks which are designed with numerous short-range transmitters rather than with few long-range base stations. Picocell or even femtocellsnetworks contrast with common macrocell networks. Since the density of data traffic - and hence of interference - goes with the density of transmitters, lowering power may help in mitigating interference.

Lastly, dense and mobile network can hardly be monitored on a centralized way. Network topology is indeed highly variable ; perfect knowledge of system and channel parameters would require huge amount of signalling. This would first waste communication resources (time, frequency) and of course power. This would also force nodes to manifest themselves by updating and broadcasting their own parameters. Such a monitoring traffic may drastically reduce the battery life of nodes which are not power supplied.

6.1.1 Motivations

In-band interference may drastically reduce transmissions performance, especially in highly interference-limited communication scenarios. Such limitations are consider very seriously by network operators which must provide QoS-constrained services for their customers. It becomes hence essential to implement efficient algorithms for limiting and keeping under control in-band interference. A common and effective approach is to solve the interference issue with optimization methods. A utility function taking in-band interference into account is optimized under operating limitations. Two major challenges are usually addressed. First transmission rate can be maximized under constraints of maximal transmit power ; the second problem seek to minimize power budget under constraints of transmission rates. Power allocation algorithms fit well to such optimization problems under QoS constraints. Nevertheless, in agreement with conclusions of Chapter 4, in-band interference should be handled adaptively in line with the momentary regime of interference sensed by each receiver.

Centralized and coordinated power control algorithms have been considered in Chapter 5. However, recourse to a centralized controller responsible for computing optimal power vector may be infeasible or simply not desired in some networks. Distributed and standalone power allocation algorithms must then be considered. Contrary to centralized approaches, complexity and computational tasks are here shared between all nodes. Furthermore, devices are assumed to dispose only of local knowledge of their vicinity.

As a result, this chapter investigates a distributed algorithm for inter-cell power allocation in rate-constrained and interference-limited networks. The optimality of the computed power vector will be discussed, as well as the rate of convergence of this algorithm which consists in an iterative process.

6.1.2 Contributions

In-band interference classifier presented in Chapter 4 acts as a framework for this chapter. The novelty is based on a paper presented at the IEEE Personal, Indoor and Mobile Radio Conference [21] and on a patent published for CEA [22]. A journal paper in preparation for IEEE Transactions on Wireless Communications [140] also relies on some aspects of this chapter. Its innovative contribution is three-fold.

First, we exploit the interference classification introduced in introduced Chapter 4 so as to minimize the power budget assigned for transmission in agreement with all individual constraints in rate. Second, we propose a full-distributed and autonomous algorithm which does not request any additional inter-cell signalling or channel estimation message other than those already requested by base stations to perform link adaptation techniques. Third, we investigate the convergence of this iterative process and propose some solutions to predict non-convergence situations.

6.1.3 Related Works

This chapter comes as an alternative to centralized algorithms addressed in Chapter 5. Many papers dealing with power control and interference mitigation begin with centralized approaches before to restrict their assumptions and address distributed algorithms.

Papers [139, 155] address geometric programming problems of power control and investigate how these problem can be solved on a distributed way. The concept of pricing is commonly adopted. This refers to the idea that each user announces a price reflecting compensation paid by other users for their interference. This illustrates the game theory nature of power control in systems where users are not coordinate. In [156] authors rather consider statistical optimization where each user maximizes the objective function by considering what other users are expected to do.

Femtocell networks deployed within macrocell networks share the same frequency bands than macrocells. If macrocells are usually coordinated, femtocells lack information about macrocells surrounding them. In [64] authors address this problem of cross-tier interference.

Another commonly adopted approach is to combine power control and resource allocation issues, since great improvement can be achieved when sub-carriers are efficiently assigned. Such considerations appear in [9, 71, 150, 151, 157]. For instance, [150] proposes a distributed algorithm for power allocation and considers a first step of sub-carriers allocation, followed afterwards by the power allocation step. A distributed matrix criterion is also derived to investigate convergence of the algorithm. On the other hand, [9] proposes a binary power allocation where sources are either active at full power or remain silent ; it is proved this simple scheme meets quite well performance. [158] deals with energy efficiency topic as well as the trade-off between spectral and energy efficiencies.

Finally, [159] addresses the same problem as us since distributed algorithms for power minimization under rate constraints are proposed ; these algorithms are water-filling-based. We acquaint ourselves with this paper lately to be able to compare our performance with it. But we also use water-filling-based schemes as baselines.

6.2 System Model and Assumptions

To avoid repetitions with Section 5.2, we will just detail how system model and assumptions differ between centralized and distributed algorithms.

The starting system model is always the n-user interference channel illustrated on Figure 5.1 ($n = 2$). Pair '$s_i - d_i$' targets a reliable transmission rate $R_{tg,i}$ while minimizing transmit power P_i. Pair i is conscious that it shares its communication band with neighbour pairs. However, we design an algorithm where each pair acts autonomously ; there is no coordination between pairs, no backhaul network, no NC, no cooperation. Thereof pair i adapts its behaviour to what it senses at the given instant, based only on local knowledge of channel parameters. Pairs are then independently considered.

Such assumptions may be illustrated by Figure 5.2. The whole n-user interference channel IC is subdivided into n isolated n-user multiple access channels $\{\text{MAC}n\}_n$. This subdivision exactly describes what is targeted with decentralized and autonomous approaches : destination d_i can only acquire CSI knowledge of what it can sense (see Figure 6.1). We thereof assume destination d_i has a perfect knowledge of all channel gains $\{g_{j,i}\}_j$. To this end, channel estimation pilots can be for instance periodically broadcasted by all sources. We will see later that this assumption could be reduced since we just need to know the value of INR variables $\{\delta_{j,i}\}_j$.

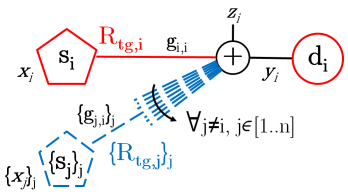

FIGURE 6.1 – A n-user MAC system for decentralized algorithms.

We furthermore assume that d_i is able to decode signal conveyed by any incoming path, even if source s_i is the single source which deliberately sends messages dedicated to d_i. For any $j \neq i$, d_i can recover the message x_j which passed through the channel referred $g_{j,i}$; but this does not mean d_i has access to the content of x_j. This assumption is not critical at all in terms of network security. This just implies that all sources use the same strategy for channel encoding. To guarantee security and integrity of their data, sources may perform their own strategy for source encoding. Nevertheless, rate constraints $\{R_{tg,j}\}_j$ are not necessarily identical between pairs. To be able to decode interfering signals, d_i must have access to $\{R_{tg,j}\}_{j\neq i}$. Full knowledge of system parameters (rate constraints) is then required for each destination. This can be achieve during channel estimation process. Let us recall that periodical monitoring is scheduled between a source and its active destinations to update CSI estimation and perform link adaptation techniques. Such a traffic is required by the network ; we just propose to exploit it instead of adding additional signalling traffic.

Adopted notations are exactly the same as those defined in Chapter 5. With the system model shown on Figure 6.1, working variables for each destination d_i are the SNR γ_i and all INR $\{\delta_{j,i}\}_{j\neq i}$. Nevertheless, coefficients $f_{j,i} = |\frac{g_{j,i}}{g_{j,j}}|^2$ are not available for d_i since channel gain $g_{j,j}$ is unknown at d_i. Thereof in such a n-user MAC it is not possible to switch between $\delta_{j,i}$ and γ_j with help of translation variables $f_{j,i}$. Such a limitation is properly driven by the fundamental difference between centralized and distributed approaches.

6.3 Preliminary on Distributed Approaches

In this chapter, a distributed algorithm is proposed as an alternative to the centralized algorithm in Chapter 5. Both algorithms aim at performing minimal power allocation

subject to rate constraints. Even if their objective function is identical, the way to meet this objective nevertheless radically differs, starting with the existence or not of the network controller (NC) [149]. We derive hereafter some characteristics of non-centralized approaches and oppose them to centralized approaches.

6.3.1 Benefits of Distributed Allocation Algorithms

Distributed approaches have been mainly investigated in the literature for reducing both channel estimation and inter-cell signalling. The main divergence between centralized and non-centralized approach is the absence of coordination between cells or clusters. Whereas with a centralized approach all CSI information is gathered in a single location (NC) to make it be a genie with full knowledge, distributed approaches avoid 'outsourcing' of channel and system knowledge and nodes only deal with their closest neighbours. On the one hand global and full CSI knowledge is required at NC, on the other hand nodes have just to acquire local CSI knowledge. Consequently, distributed approaches are less sensitive to quick variations (network topology, channel states, system constraints) since a local modification has just to be sensed by few nodes without being broadcasted across the system across NC.

As it has already been said, in cellular networks base stations periodically refresh their link quality estimation on locally their active user equipments to perform link adaptation (AMC, power control, channel aware scheduling, etc.). Such estimation messages are required by communication standards ; so there is no extra-signalling, local knowledge is easily met by nodes. On the contrary, centralized algorithms either generate overhead with additional signalling, or use a dedicated (backhaul) network to gather full knowledge at NC. Two fundamental challenges of distribution are thus identified. First, higher reliability and accuracy in channel estimation are met by nodes in comparison to centralized approaches, since estimation is directly made by nodes which need this estimation, when they need it. Second, battery life of nodes is extended and network design is simplified. Nodes have indeed not to periodically awake to broadcast their CQI ; no NC or backhaul network needs to be settle. This last issue is especially important for WSNs and ad hoc networks.

In terms of computation, complexity and tasks are also distributed. Each node is responsible for a part of the computation, based on its own parameters. Overall complexity is then shared between nodes ; this avoids to gather the entire computational burden on a same location (NC) which may become a bottleneck for the network.

6.3.2 Limitations of Distributed Allocation Algorithms

Nevertheless, distributed approaches suffer from some non-neglecting limitations. First, solutions are commonly suboptimal in comparison to centralized approaches. Nodes only dispose of restricted and local knowledge to compute the solution. In the specific case of in-band interference, nodes cannot access to all parameters concerning their neighbour interferers. Consequently, nodes have to make decisions and compute solutions based on conjectures on their neighbours which are not necessarily relevant. Mostly, a worst case solution is derived, *i.e.,* since nodes have no way to know how their interferers will set their transmit power, they assume the worst communication context which impacts them in the worst way.

This lack of knowledge causing performance reduction can be illustrated as follows. Solutions to optimization problems are sometimes achieved with techniques that progressively shrink the region of candidate solutions, so work dichotomy, ellipsoid or gradient

methods for instance [160, 161]. Due to restricted knowledge, these methods may converge to local instead of global optimum. Usually such situations lead to unbalanced and unstable solutions.

Second, distributed processes are commonly iterative and may suffer from excessive convergence rate before to meet a balanced solution. In the precise case of power allocation algorithms aiming at dealing with in-band interference, these iterations describe the game theory nature of setting transmit power. A first transmitter s_i updates its transmit power P_i in line with the momentary communication context it senses. This power adjustment will not just benefit to its receiver d_i but will also affect all neighbour active receivers $\{d_j\}_{j\in\Upsilon_i}$ located in its range of coverage Υ_i. Each receiver d_j will then react to the new communications context it senses by requesting to its own transmitter s_j to adjust its transmit power P_j. All these new power updates affect of course the first receiver d_i, since it probably belongs to region Υ_j for all $j \in \Upsilon_i$. But for any $j \in \Upsilon_i$, new active destinations d_k such that $k \in \Upsilon_j \setminus \Upsilon_i$ also suffer from power adjustments. Such a way the problem may spread over the whole network. Iterations describe the fact that several adjustments are required before a balance situation is met.

A schematic illustration is given with Figure 6.2. First, the red source reduces its transmit power and hence its range coverage Υ_{yellow} to respond to a lower target rate of its destination. Second, this profits to the purple source which extends its range coverage Υ_{purple} to reach the green unsatisfied destination. By this way the purple source affects a blue destination which were not initially affected by the adjustment of the yellow source.

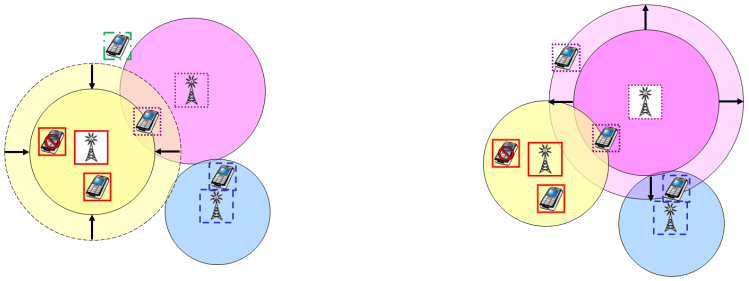

(a) Iteration 1 (b) Iteration 2

FIGURE 6.2 – Iterative process to achieve a balanced solution to power allocation problem.

A major issue is to ensure that convergence will be met. Another challenge is to guarantee that solution will be quickly met in finite time, *i.e.,* with a time much smaller than coherence time of channels and delay requirements of system. Investigation on the rate of convergence can be tedious since there may be besides a high sensitivity to initial conditions. To prevent non-convergence processes to affect system performance, convergence may be monitored. A loop counter can be used as well as metrics that evaluate how much two iterations differ.

6.3.3 A Step Towards Game Theory

Power dependency between pairs in interference-limited networks is a perfect illustration of game theory which attempts to capture how an individual's success in making

choices depends on the choices of others. Huang et al. [155] and Saraydar et al. [162] address such a problem and propose some distributed solutions. The basic idea is that a source will affect neighbour co-channel receivers by adjusting one of its transmit parameters. Sources cannot act selfishly and update their new transmit parameters without considering how their new settings will impact their neighbourhood. Selfishness is not the key of optimization problem. A source should rather behave assuming that all other sources would have acted likewise if they would have been at its place. Hence, sources are conscious that their success depends on others and must try not to penalize them too much. To translate this aspect, a price (or penalty) is added to the objective function. This price is commonly set based on the Lagrangian and its KKT conditions. A negative Lagrange multiplier is linked to this price : the price so evolves oppositely in comparison to what is targeted. To meet their goal, sources are strongly advised to limit their effects on others as much as possible.

Another approach is proposed by [156] where statistical knowledge is exploited. With a distributed and non-coordinated approach, sources cannot access to momentary values of their neighbours parameters. Consequently, they can hardly optimize the global objective function. Assuming that statistical knowledge on neighbours parameters is available, a given source can guess what other users are expected to do. Then this source can access to the expected global objective function and set its own transmit parameters to optimize this expectation.

6.3.4 Distributed Norm and Convergence Criterion

In this subsection we mainly recall some results of [150, 151]. As we said above, distributed algorithms involve mostly an iterative process. We must ensure of the termination of this process to meet a feasible solution. In some cases, the problem of power allocation can be expressed in matrix form (see for instance Section 5.5.2). The generic matrix form is derived as follows :

$$\underline{P} = \underline{\mathbf{DF}} \cdot \underline{P} + \underline{C}, \tag{6.1}$$

where $\underline{P}$ and $\underline{C}$ are respectively $n \times 1$ power and constant vectors, while $\underline{\mathbf{DF}}$ is the $n \times n$ matrix of interference. The explicit derivation of $\underline{\mathbf{DF}}$ is given in [150]. This expression can be turned into

$$(\underline{\mathbf{I_n}} - \underline{\mathbf{DF}}) \cdot \underline{P} = \underline{C}. \tag{6.2}$$

Solution to the problem is easily derived if $(\underline{\mathbf{I_n}} - \underline{\mathbf{DF}})$ can be inverted.

By Perron-Frobenius theorem [163], there exists a positive power allocation

$$\underline{P}^* = (\underline{\mathbf{I_n}} - \underline{\mathbf{DF}})^{-1} \cdot \underline{C} \tag{6.3}$$

iff the maximum eigenvalue of the interference matrix $\underline{\mathbf{DF}}$, *i.e.,* the spectrum radius $\rho(\underline{\mathbf{DF}})$ is inside the unit circle. In other words,

$$\forall i \in \mathbf{N}^{(n)}, \quad \lambda_i(\underline{\mathbf{DF}}) < 1, \tag{6.4}$$

where $\lambda_i(\underline{\mathbf{DF}})$ is the i^{th} eigenvalue of matrix $\underline{\mathbf{DF}}$.

A submultiplicative matrix norm $\| \, . \, \|$ is a matrix norm verifying

$$\forall \underline{\mathbf{A}}, \underline{\mathbf{B}}, \quad \| \, \underline{\mathbf{AB}} \, \| \leq \| \, \underline{\mathbf{A}} \, \| \cdot \| \, \underline{\mathbf{B}} \, \| \, . \tag{6.5}$$

As proved in [163], the spectral radius of matrix $\underline{\mathbf{DF}}$ is lower than any submultiplicative matrix norm $\| \, . \, \|$ of $\underline{\mathbf{DF}}$:

$$\forall \, \| \, . \, \|, \quad \rho(\underline{\mathbf{DF}}) \leq \| \, \underline{\mathbf{DF}} \, \| \, . \tag{6.6}$$

Features	Centralized Algorithm	Distributed Algorithm
Channel and system knowledge	full	local
Computational complexity	high : all tasks performed by a single entity	low : tasks are dispatched between nodes
Coordination, presence of NC	either a NC or coordination between pairs via a backhaul network	pairs are fully autonomous
Optimality of solution	optimal solutions can be met since full knowledge is available	suboptimal solutions can be achieved but not necessarily optimal solutions
Time computation	one-shot process : optimal solution is directly computed based on momentary communication context	iterative process : there are 'ping-pong' iterations between pairs until a balanced and suboptimal solution is met ; this is lead by the rate of convergence
Termination and success	ensured, expect if solution fails in admission control process	convergence is not ensured, process may never meet a balance solution

TABLE 6.1 – Divergences between centralized and distributed algorithms.

Consequently, a suitable matrix norm $\| \ . \ \|$ can be derived for $\underline{\mathbf{DF}}$ to check if the condition $\rho(\underline{\mathbf{DF}}) < 1$ holds. However, $\| \ \underline{\mathbf{DF}} \ \|$ should be computed on a distributed way ; typically, $\| \ \underline{\mathbf{DF}} \ \|$ should involve independent computation $\Upsilon_k(\underline{\mathbf{DF}})$ for each source s_k that only requires knowledge of local parameters. Since the k^{th} row of matrix $\underline{\mathbf{DF}}$ only involves parameters available at source s_k, the distributed criterion $\Upsilon_k(\underline{\mathbf{DF}})$ could consider each row independently. In [150] authors prove that the infinity norm $\| \ . \ \|_\infty$ is the single suitable norm fulfilling this distributed criterion. Infinity norm $\| \ . \ \|_\infty$ considers the max on the sum over each row :

$$\| \ \underline{\mathbf{DF}} \ \|_\infty = \max_{k \in \mathbf{N}^{(n)}} \sum_{l \in \mathbf{N}^{(n)}} |b_{k,l}| = \max_{k \in \mathbf{N}^{(n)}} \Upsilon_k(\underline{\mathbf{DF}}), \tag{6.7}$$

where $b_{k,l}$ is the element of $\underline{\mathbf{DF}}$ located at row k and column l.

In conclusion, each source s_k has to check if $\Upsilon_k(\underline{\mathbf{DF}}) < 1$ holds. This condition holds for all sources $\{s_k\}_{k \in \mathbf{N}^{(n)}}$ iff $\| \ \underline{\mathbf{DF}} \ \|_\infty < 1$ holds. To summarize, we have the following equivalence :

$$\forall k, \quad \Upsilon_k(\underline{\mathbf{DF}}) < 1 \quad \Leftrightarrow \quad \rho(\underline{\mathbf{DF}}) \leq \| \ \underline{\mathbf{DF}} \ \|_\infty < 1. \tag{6.8}$$

The distributed criterion has thus been defined. A given source s_k cannot prove alone the existence of the optimal solution (6.3), but s_k is able to check autonomously if its own settings could cause or not the non-convergence, *i.e.,* the failure, of the iterative process.

6.3.5 Centralized vs. Distributed Algorithms

We summarize in Table 6.1 the main features of centralized and distributed approaches. This description is of course not exhaustive but we only focus on some relevant aspects for comparing CPA with DPA.

Let us note that it is quite conceivable to design halfway algorithms between full-centralization and full-distribution. For instance, some close nodes can be gathered into a cluster ; a cluster then stands for a neighbourhood. The monitoring in each cluster can be performed on a centralized way, while all clusters handle together on a distributed way. Wireless communication networks are commonly designed with such a hierarchical structure. In each cluster at a given layer L_p there is a controller in charge to gather information of the cluster. A super-controller in layer L_{p+1} is in relation with all controllers

of layer L_p located within its coverage range. And so forth till the last layer with the omniscient network operator.

6.4 Proposed Distributed Power Allocation Algorithm

We propose in this section to handle the optimization problem

$$\begin{aligned} &\min_{\{\underline{O_1},\ldots,\underline{O_n}\}} f(P_1^{(\underline{O_1})},\ldots,P_n^{(\underline{O_n})}) = f(\underline{P}), \\ &\text{subject to} \quad R_k^{(\underline{O_k})}(\underline{P}) \geq R_{tg,k}, \quad \forall k \in \{1,\ldots,n\}, \\ &\qquad\qquad 0 \leq P_k^{(\underline{O_k})} \leq P_{k,\max}, \quad \forall k \in \{1,\ldots,n\}, \end{aligned} \tag{6.9}$$

(identical to (5.9)) with a distributed algorithm. We aim at allocating the minimal transmit power vector $\underline{P}^*$ which allows to meet all rate constraints $\underline{R}_{tg} = (R_{g,1},\ldots,R_{tg,n})$. To this end, we exploit the three-regime classification of in-band interference that we developed in Section 4.3. Partition of the region and results concerning rate and SNR achievability of this interference classifier have been summarized in Table 4.1 and illustrated on Figure 4.7. In reference to our centralized power allocation algorithm (CPA) introduced in Chapter 5, we will name our distributed power allocation algorithm with 'DPA' in the remainder.

Since a distributed approach is targeted, each pair should act autonomously, based only on local knowledge. We developed in Section 6.2 the system model and assumptions associated with our DPA proposal. We note that one of the main differences in comparison to our CPA proposal is the absence of a network controller. Hence, computation is not performed any more by NC but by nodes themselves, *i.e.,* sources and/or destinations. In the remainder we will name 'decision-makers' the nodes that perform computation. Note that for each pair $\mathscr{C}_i$ there is at least one decision-maker named by DM_i. Due to the absence of coordination between all nodes, decision-makers dispose now only of partial and local CSI knowledge.

Typically, decision-makers cannot compute variables $f_{j,i} = |\frac{g_{j,i}}{g_{j,j}}|^2$ (see (5.11)) since $f_{j,i}$ involves the channel coefficient $g_{j,j}$ which is unknown to DM_i. See for instance Figure 6.1 to note that $\mathscr{C}_i$ cannot sense channel coefficient $g_{j,j}$. Consequently, DM_i cannot translate the INR variable $\delta_{j,i}$ perceived by d_i into the corresponding SNR variable γ_j. This results in the incapacity for decision-makers to apply a reasoning similar to the one developed in Section 5.4.2 for CPA. Furthermore, the partition of the region $(\gamma_k)_k$ summarized in Table 5.1 cannot be used straightforwardly. Some adjustments are then necessary to be able to exploit our in-band interference classifier in a distributed and autonomous fashion.

6.4.1 Optimal Distributed Power Allocation

We present hereafter how problem (6.9) can be solved on a non-centralized manner. We first develop the principle of DPA algorithm, then prove its validity by investigating the termination of the iterative process, and finally conclude with some remarks on convergence rate and simulation results. For sake of clarity, DPA algorithm will be introduced for $n = 2$. Generalization to any n will be addressed in Section 6.5.

Commonly, distributed approaches cannot perform as well as centralized approaches because decision-makers only dispose of restricted knowledge about the whole system. When distributed algorithms converge, their solutions are mostly suboptimal but sometimes may

O_i	Strategy	Region $\omega_i^{O_i}$	Update function φ_i
1	Noisy	$\omega_i^1 = \{(\delta_i, \gamma_i) \vert 0 \leq \delta_i \leq A_j\}$	$\varphi_i(\delta_i) = A_i(1+\delta_i)$
2	Joint decoding	$\omega_i^2 = \{(\delta_i, \gamma_i) \vert A_j \leq \delta_i \leq A_j(1+\gamma_i)\}$	$\varphi_i(\delta_i) = A - \delta_i$
3	SIC-based	$\omega_i^3 = \{(\delta_i, \gamma_i) \vert \delta_i \geq A_j(1+\gamma_i)\}$	$\varphi_i(\delta_i) = A_i$

TABLE 6.2 – Performance of our three-regime interference classifier applied to the MAC $\{s_i; s_j, d_i\}$: partition of the region $(\gamma_j; \gamma_i)$ and achievable SNR within each region.

be optimal, *i.e.,* equal to those computed by centralized approaches. We target to meet with DPA the same solutions to problem (6.9) as those computed by CPA and presented in Section 5.4.2. Consequently, our iterative DPA algorithm should stop by outputting a SNR vector $\underline{\Gamma}$ - and hence a power vector $\underline{P}$ - that corresponds to the intersection between functions φ_1 and φ_2 (see (5.12) where the piecewise continuous function φ_i is defined as the mapping associated with the graphical representation $(\mathscr{D}_1^k)_k$).

Nevertheless, each pair $\mathscr{C}_i$ is autonomous and its decision-maker DM_i cannot formulate the function φ_j of its neighbour pair $\mathscr{C}_j$. Consequently, decision-makers cannot compute coordinates of all crossed-points $\{\text{CP}_{k,l}\}_{k,l}$ given in Table 5.2. They besides cannot determine which crossed-points are relevant to define $\underline{O}^*$ (see (5.13)).

To tackle these stringent limitations, we propose an iterative process during which each pair alternately updates its transmit power to react to power adjustment of neighbour pair. At each iteration p, DM_i computes γ_i^p by applying function φ_i to the momentary communication context sensed by d_i. This SNR/power adjustment affects concurrent pair $\mathscr{C}_j$, since γ_i^p in $\mathscr{C}_i$ is directly translated into a new δ_j^p in $\mathscr{C}_j$. Hence DM_j reacts by updating γ_j^p into γ_j^{p+1} and so forth, until the stopping criterion is met. We will prove hereafter how the sequences $(\gamma_i^p)_p$ and $(\gamma_j^p)_p$ may converge respectively to $\gamma_i^{O_i^*}$ and $\gamma_j^{O_j^*}$.

To be rigorous, partitions $\{\omega_i^k\}_{i,k}$ and functions $\{\varphi_i\}_i$ should be redefined in line with our assumptions. Indeed we cannot consider region $(\gamma_1; \gamma_2)$ any more because translation variables $\{f_{j,i}\}_{i \neq i}$ are not available at decision-makers. Results for pair $\mathscr{C}_i$ need to be derived in region $(\delta_i; \gamma_i)$. Hence we summarize in Table 6.2 the new partition $\{\omega_i^k\}_k$ and the expression of the piecewise-continuous mapping φ_i within each region of this partition. This table is used in this chapter instead of (5.12) and Table 5.1. We use the same notations $\{\omega_i^k\}_k$ and φ_i since there is no ambiguity between CPA and DPA.

The general operating framework of our DPA algorithm is detailed on Figure 6.3 which can be compared to Figure 5.6 to feel similarities and differences between CPA and DPA.

1. First, there is always the learning step with channel estimation and notification of QoS constraints and system limitations. Nevertheless, all knowledge is not any more entirely intended to NC but partially to each decision-maker. To this end, we show with red dashed arrows that a part of CSI knowledge is provided for the green box describing DM_i while the remainder is supplied to the red box describing DM_j [1].

1. Typically, DM_i needs to know coefficients $g_{i,i}$ and $g_{j,i}$. We will see later that DM_i actually does not need to know the momentary value of channel coefficient $g_{j,i}$ and transmit power P_j^p of its neighbour interferer but just the current INR value $\delta_{j,i}^p$ perceived by d_i.

2. Then, the box illustrating DPA computation is not as simple as the box used for CPA. Indeed, computational tasks are not any more performed by one exclusive device (NC), as CPA does; DPA algorithm requires an iterative process between DMi and DMj, as represented by the grey closed loop between green and red boxes. Each pair updates in turns its power to react to power adjustment of its neighbour interferers.
3. This 'ping-pong' process is repeated until a stopping condition is met. In contradiction with CPA, there is no need to notify the computed optimal solutions to nodes at the end of algorithm, since nodes themselves have computed these solutions.

The principle of this iterative 'ping-pong' process is developed below.

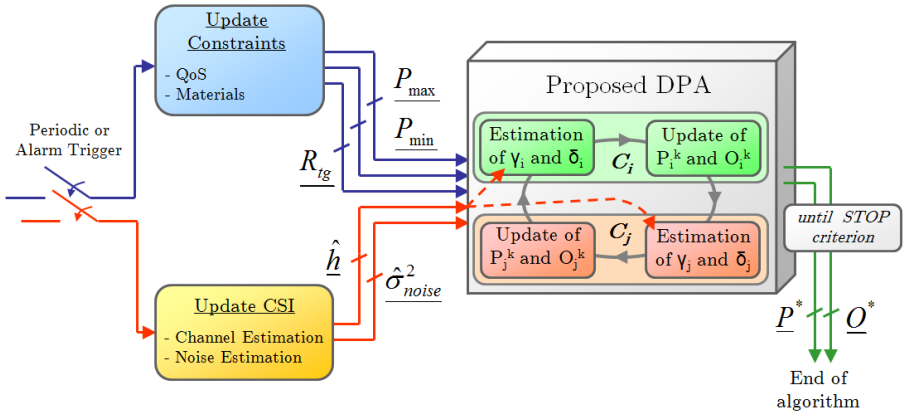

FIGURE 6.3 – Description of our DPA algorithm for power allocation.

6.4.2 The 'Ping-Pong' Iterative Process

First of all, we summarize the main steps of this iterative process :

Step 1. s_1 and s_2 broadcast respectively their target rate $R_{tg,1}$ and $R_{tg,2}$, and their power limitations $P_{1,\min}$, $P_{1,\max}$ and $P_{2,\min}$, $P_{2,\max}$.

Step 2. The power vector is initialized at $p = 0$ with $\underline{P}^0 = (P_{1,\max}; P_{2,\max})$. Pair $\mathscr{C}_i$ starts the process at iteration $p = 1$.

Step 3. d_i estimates δ_i^{p-1} and notifies it to DM$_i$.

Step 4. DM$_i$ classifies δ_i^{p-1} into regime $\omega_i^{O_i^p}$ and computes $\gamma_i^p = \varphi_i(\delta_i^{p-1})$.

Step 5. DMi translates γ_i^p into P_i^p and then notifies s_i of its updated transmit power P_i^p while notifying d_i of the best strategy O_i^p to handle current in-band interference.

Step 6. d_j estimates δ_j^p and notifies it to DM$_j$.

Step 7. DM$_j$ classifies δ_j^p into regime $\omega_j^{O_j^p}$ and computes $\gamma_j^p = \varphi_j(\delta_j^p)$.

Step 8. DMj translates γ_j^p into P_j^p and then notifies s_j of its updated transmit power P_j^p while notifying d_j of the best strategy O_j^p to handle current in-band interference.

Step 9. $\underline{\Gamma}^p \leftarrow (\gamma_1^p, \gamma_2^p)$, $\underline{P}^p \leftarrow (P_1^p, P_2^p)$, $p \leftarrow p+1$. The process restarts at Step 3.

Steps 3–9 are repeated until $\|\underline{\Gamma}^p - \underline{\Gamma}^{p-1}\| < \varepsilon$ *or* $p \leq p_{MAX}$.

Let us note that DM_i has just to know the momentary value of INR δ_i^p, to be able to compute the new value of SNR γ_i^{p+1}. by use of the update function φ_i. The value of δ_i^p is sensed by the destination d_i which feedbacks it to DM_i. We recall that $\delta_i^p = \frac{|g_{j,i}|^2 \cdot P_j^p}{N_0}$. There is however no need to estimate independently the value of channel coefficient $g_{j,i}$ and of transmit power P_j^p. This simplifies the process and reduces signalling.

The iterative process of our DPA algorithm must now be proved to converge to the same solution Γ^* as the one of CPA algorithm. This solution Γ^* has already been proved to exist and to be optimal in Chapter 5 ; we will not do it again. Hereafter we will then just prove that DPA converges to Γ^*.

To be clear, let us precise that decision-makers have not necessarily enough knowledge about the whole system to determine if convergence will be met or not and how fast DPA will converge. What really matters is that at least one decision-maker is able to detect a non-convergence scenario ; hence this decision-maker can inform the neighbour pair of non-convergence to adopt another algorithm for power allocation. To prove the convergence of our DPA algorithm, we consequently assume there is an omniscient genie above the system. This genie does not exist in practice but we need it here just to prove our DPA algorithm mostly converges. In other words, decision-makers are not conscious of the convergence of DPA but the genie can assert DPA will converge.

To feel better how DPA algorithm works, illustrations are given on Figures 6.4 and 6.5. Figure 6.4 is just a way to describe this 'ping-pong' process ; we see that the sequence $(\gamma_1^p, \gamma_2^p)_p$ evolves between lines $\{\mathscr{D}_1^k\}_k$ and $\{\mathscr{D}_2^l\}_l$ until the attractor is met. This is the intuitive approach of convergence for iterated function sequences.

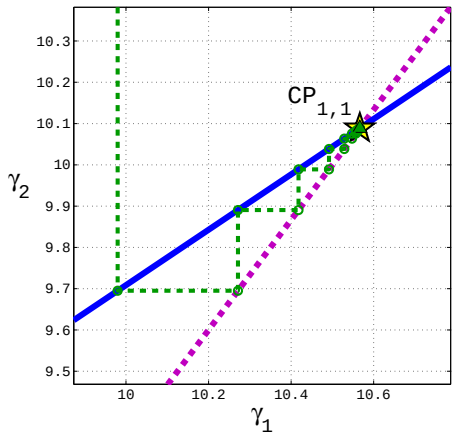

FIGURE 6.4 – Illustration of the 'ping-pong' process for power allocation.

Figure 6.5 presents results for the specific communication context $\mathscr{P}_S = \{1, 1, 2.5, 1.5\}$. First, Figure 6.5a shows the optimal solution $\underline{\Gamma}^*$ computed by CPA, as described in Chapter 5 (see for instance Figure 5.4a). On the other hand, Figure 6.5b illustrates how behaves DPA algorithm for this given context when $\mathscr{C}_1$ starts the process with the initial vector $\underline{\Gamma}^0$ (marked by a yellow downward-pointing triangle). The iterative process manages to meet after three iterations the same solution $\underline{\Gamma}^*$ as the one computed by CPA algorithm.

We develop hereafter the different steps of DPA algorithm illustrated on Figure 6.5b. The final vector $\underline{\Gamma}^*$ is marked by a yellow star. Orange horizontal and green vertical arrows

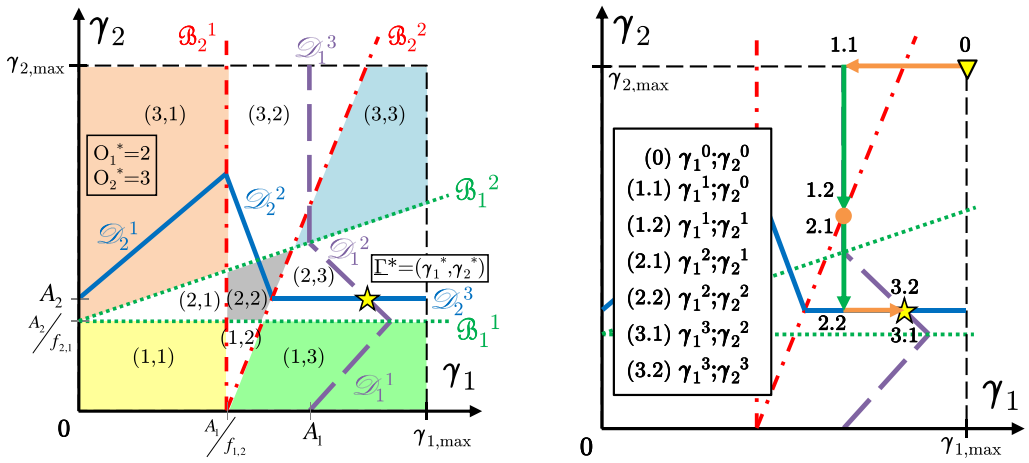

(a) CPA solution

(b) DPA 'ping-pong' process

FIGURE 6.5 – $\mathscr{P}_S = \{1, 1, 2.5, 1.5\}$: optimal solution computed by CPA is shown on the left, while the iterative process of DPA is illustrated on the right.

respectively illustrate the update of $(\gamma_1^p)_p$ and $(\gamma_2^p)_p$. To follow the sequence of events, each step is marked at arrows end : first the iteration counter p, second the active decision-maker.

- At step **1.1**, DM_1 classifies γ_2^0 (actually it is rather δ_1^0) in the third regime since the current point is located above the green diagonal $\mathscr{B}_1^2$. γ_1^1 is simply computed by reaching the purple horizontal line $\mathscr{D}_1^3$.
- At step **1.2**, the second regime is relevant in $\mathscr{C}_2$; the update of γ_2^0 into γ_2^1 would like to join the diagonal blue line $\mathscr{D}_2^2$, but γ_2^1 must remain consistent with the classified regime ; so the diagonal red bound cannot be crossed.
- At step **2.1**, γ_1^1 is already optimal, so $\gamma_1^2 = \gamma_1^1$.
- At step **2.2**, DM_2 classifies γ_1^2 (actually it is rather δ_2^2) in the third regime ; the update γ_2^2 of γ_2^1 joins lastly the horizontal blue line $\mathscr{D}_2^3$.
- At step **3.1**, DM_1 classifies interference in the second regime and use the diagonal purple line $\mathscr{D}_1^2$ to compute γ_1^3.
- At step **3.2** and after, $\underline{\Gamma}^*$ is met and DPA ends.

6.4.3 Proof of Convergence

Convergence of our algorithm can be proved on two different ways. Both of them seem us interesting enough to be developed in the remainder. The first approach is by use of the *fixed point theorem*. A fixed point is also called an *attractor*. The second approach refers to the spectral radius of the interference matrix. This part has already been detailed in Section 6.3.4 where a distributed criterion has been investigated.

6.4.3.1 Fixed Point Theory

We begin this section with introducing some mathematical definitions and theoretical tools which will help us to prove convergence of DPA algorithm [164–166].

Iterated function sequence

Let $u : X \to X$ be a mapping from a set X to itself. An *iterated function sequence* $(u^p)_p$ is defined as

$$\begin{cases} u^0 = id_X \\ u^p = u \circ u^{p-1} \end{cases} \tag{6.10}$$

where id_X is the identity function on X and $u \circ v$ is a composed function, *i.e.*, $u \circ v(x) = u\,[(v(x)]$. Any sequence $(x^p)_p$ is derived from $(u^p)_p$ by its first value x_0 and recurrence

$$x_p = u\,(x_{p-1}) = u^p\,(x_0)\,. \tag{6.11}$$

Contracting mapping

Let $u : E \to E$ be a mapping from a metric space (E, d) to itself, where d is the metric on E. Mapping u is said to be a *κ-Lipschitz* mapping if the following condition holds :

$$\forall (x, y) \in E \times E, \quad d\Big(u(x), u(y)\Big) \leq \kappa \cdot d(x, y) \tag{6.12}$$

where κ is a real number. The smallest value of κ that lets verify (6.12) is called the *Lipschitz constant* of u. If the Lipschitz constant κ is strictly smaller than one ($\kappa < 1$), then mapping u is called a *contraction*.

Banach Fixed Point Theorem

A fixed point, or attractor, for u is a point x^* in E invariant under u, *i.e.*,

$$x^* \in E, \quad u(x^*) = x^*. \tag{6.13}$$

The *Banach fixed point* theorem is the most famous theorem that proves existence and uniqueness of a limit for recurrent sequences $(u^p)_p$ [167].

Theorem. *If (E, d) is a non-empty complete metric space and $u : E \to E$ is a contraction with a Lipschitz constant $\kappa < 1$, then u admits one and only one fixed point x^* in E. Furthermore, the iterated function sequence $(x_0, u(x_0), u^2(x_0), \cdots)$ converges to x^*, whatever the initial value x_0 may be.*

Applicability of these mathematical tools to DPA

We have assumed the existence of an omniscient genie which is especially able to switch between δ_i and γ_j by use of $\{f_{j,i}\}_{i \neq j}$. Consequently, we will use Equation (5.12) and Table 5.1 instead of Table 6.2 when we need to refer to partition $\{\omega_i^k\}_k$ and function φ_i (the argument of φ_i is γ_j instead of δ_i).

DPA algorithm involves a 'ping-pong' process. We show below how this iterative process can be linked to recurrent sequences and fixed points. Section 6.4.2 develops main steps of DPA. We consider now that pair $\mathscr{C}_1$ starts the process by updating P_1^0. This can be translated as follows :

$$\begin{cases} \gamma_1^p = \varphi_1(\gamma_2^{p-1}) \\ \gamma_2^p = \varphi_2(\gamma_1^p) \\ \gamma_1^{p+1} = \varphi_1(\gamma_2^p) \\ \gamma_2^{p+1} = \varphi_2(\gamma_1^{p+1}) \end{cases} \Rightarrow \begin{cases} \gamma_1^{p+1} = \Phi_1(\gamma_1^p) \\ \gamma_2^{p+1} = \Phi_2(\gamma_2^p) \end{cases} \tag{6.14}$$

with the composed mapping $\Phi_i = \varphi_i \circ \varphi_j$.

φ_i is a piecewise-continuous mapping whose expression depends on the partition $\{\omega_i^k\}_k$. The expression of the composed mapping Φ_i is hence linked to the superposition of partitions $\{\omega_i^k\}_k$ and $\{\omega_j^l\}_l$. There are then nine different derivations for Φ_i, according to which sector $\Omega_{k,l}$ we focus on ; they are all detailed in Table 6.3. We furthermore give for each derivation of Φ_i the expression of its attractor γ_i^+, *i.e.,* the solution to $\Phi_i(\gamma_i^+) = \gamma_i^+$.

For sake of clarity and rigour, we introduce $\varphi_i^{(k)} = \varphi_{i|\omega_i^k}$ and $\Phi_i^{(k,l)} = \Phi_{i|\Omega_{k,l}}$ which are the restriction of respectively φ_i and Φ_i to partition ω_i^k and sector $\Omega_{k,l}$. Hence we have $\Phi_i^{(k,l)} = \varphi_i^{(k)} \circ \varphi_j^{(l)}$.

Fixed point and Intersection point

A careful look at Table 6.3 lets to note that the value of the fixed point γ_i^0 in sector $\Omega_{k,l}$ is nothing else that the coordinate $\mathrm{CP}_i(k,l)$ expressed in Table 5.2. Indeed, considering the intersection $\{\mathscr{D}_i^k\}_k \cap \{\mathscr{D}_j^l\}_l$ between function φ_i and φ_j is equivalent to considering the fixed point of their composition $\Phi_i = \varphi_i \circ \varphi_j$.

Démonstration. To be convinced from this result, let us assert that functions $\{\varphi_i^{(k)}\}_{i,k}$ are either constant or bijective. This result is straightforward with Table 5.1 since $\varphi_i^{(k)}$ is either a constant function or a linear function. A constant function cannot be bijective but a linear function is of course bijective.

If $\varphi_i^{(k)}$ is not constant (and then bijective), then we have :

$$\begin{array}{lll} \forall \gamma_j, \quad \gamma_i = \varphi_i^{(k)}(\gamma_j) & \Rightarrow & \gamma_j = \left[\varphi_i^{(k)}\right]^{-1}(\gamma_i) \\ \forall \gamma_i, \quad \gamma_j = \varphi_j^{(l)}(\gamma_i) & & \\ & & \\ & \varphi_j(l)(\gamma_{i_0}) = \left[\varphi_i^{(k)}\right]^{-1}(\gamma_{i_0}) \quad (A) & \\ \Leftrightarrow & \varphi_i^{(k)} \circ \varphi_j^{(l)}(\gamma_{i_0}) = \gamma_{i_0} & \\ \Leftrightarrow & \Phi_i^{(k,l)}(\gamma_{i_0}) = \gamma_{i_0} \quad (B) & \end{array} \tag{6.15}$$

where (A) states that γ_{i_0} is the coordinate $\mathrm{CP}_i(k,l)$ of the point $\mathscr{D}_i^k \cap \mathscr{D}_j^l$ since γ_{i_0} jointly verifies $\left[\varphi_i^{(k)}\right]^{-1}$ and $\varphi_j^{(l)}$, while (B) states that γ_{i_0} is a fixed point for $\Phi_i^{(k,l)}$.

Else $\varphi_i^{(k)}$ is a constant function equal to the value C_0. The point $\mathscr{D}_i^k \cap \mathscr{D}_j^l$ has of course a coordinate $\mathrm{CP}_i(k,l) = C_0$. Besides, $\varphi_i^{(k)} \circ \varphi_j^{(l)}(\gamma_i) = \Phi_i^{(k,l)}(\gamma_i) = C_0$ holds for any value γ_i, and especially for $\gamma_i = C_0$. Hence $\Phi_i^{(k,l)}(C_0) = C_0$.

In conclusion, we prove that the fixed point γ_i^+ of $\Phi_i^{(k,l)}$ is nothing else that the coordinate $\mathrm{CP}_i(k,l)$ of the crossed-point $\mathscr{D}_i^k \cap \mathscr{D}_j^l$. □

To what extent is Φ_i a contraction ?

From Table 6.3 we note $\Phi_i^{(k,l)}$ is either constant or linear. To be a contraction $\Phi_i^{(k,l)}$ must verify the condition (6.12) with $\kappa < 1$. A constant function is of course contracting, since $\kappa = 0$ holds. In case of linear functions, (6.12) is easily proved to be satisfied, since the slope τ_i of $\Phi_i^{(k,l)}$ is the Lipschitz constant. Then $\Phi_i^{(k,l)}$ is a contraction iff its slope τ_i is strictly lower than one ($\tau_i < 1$).

Démonstration. To be exhaustive we detail the nine derivations $\Phi_i^{(k,l)}$.

(O_1, O_2)	$\Phi_1(\gamma_1) = \varphi_1 \circ \varphi_2(\gamma_1)$	$\Phi_2(\gamma_2) = \varphi_2 \circ \varphi_1(\gamma_2)$	γ_1^+	γ_2^+
$(1,1)$	$A_1A_2f_{1,2}f_{2,1} \cdot \gamma_1 + A_1(1 + A_2f_{1,2})$	$A_1A_2f_{1,2}f_{2,1} \cdot \gamma_2 + A_2(1 + A_1f_{2,1})$	$\frac{A_1(1+A_2f_{2,1})}{1-A_1A_2f_{1,2}f_{2,1}}$	$\frac{A_2(1+A_1f_{1,2})}{1-A_1A_2f_{1,2}f_{2,1}}$
$(1,2)$	$-A_1f_{1,2}f_{2,1} \cdot \gamma_1 + A_1(1 + Af_{2,1})$	$-A_1f_{1,2}f_{2,1} \cdot \gamma_2 + A - A_1f_{1,2}$	$\frac{A_1(1+Af_{2,1})}{1+A_1f_{1,2}f_{2,1}}$	$\frac{A-A_1f_{1,2}}{1+A_1f_{1,2}f_{2,1}}$
$(1,3)$	$A_1(1 + A_2f_{2,1})$	A_2	$A_1(1 + A_2f_{2,1})$	A_2
$(2,1)$	$-A_2f_{1,2}f_{2,1} \cdot \gamma_1 + A - A_2f_{2,1}$	$-A_2f_{1,2}f_{2,1} \cdot \gamma_2 + A_2(1 + Af_{1,2})$	$\frac{A-A_2f_{2,1}}{1+A_2f_{1,2}f_{2,1}}$	$\frac{A_2(1+Af_{1,2})}{1+A_2f_{1,2}f_{2,1}}$
$(2,2)$	$f_{1,2}f_{2,1} \cdot \gamma_1 + A(1 - f_{2,1})$	$f_{1,2}f_{2,1} \cdot \gamma_2 + A(1 - f_{1,2})$	$\frac{A(1-f_{2,1})}{1-f_{1,2}f_{2,1}}$	$\frac{A(1-f_{1,2})}{1-f_{1,2}f_{2,1}}$
$(2,3)$	$A - A_2f_{2,1}$	A_2	$A - A_2f_{2,1}$	A_2
$(3,1)$	A_1	$A_2(1 + A_1f_{1,2})$	A_1	$A_2(1 + 1_1f_{1,2})$
$(3,2)$	A_1	$A - A_1f_{1,2}$	A_1	$A - A_1f_{1,2}$
$(3,3)$	A_1	A_2	A_1	A_2

TABLE 6.3 – Updating mapping Φ_i and its attractor γ_i^+

- $\Phi_i^{(1,1)}$: Its slope is $\tau_i = A_1 A_2 f_{1,2} f_{2,1}$. If $\Omega_{1,1}$ is a relevant sector, then $\mathrm{CP}_{1,1} = \underline{\Gamma}^* \in \Omega_{1,1}$ holds (see (5.13)). The positivity of $\underline{\Gamma}^*$ proves that $\Phi_i^{(1,1)}$ is always a contraction if $\Omega_{1,1}$ is relevant.

$$\mathrm{CP}_i(1,1) = \frac{A_i(1 + A_j f_{j,i})}{1 - \tau_i} > 0 \quad \Rightarrow \quad (1 - \tau_i) > 0 \tag{6.16}$$

- $\Phi_i^{(1,2)}$ **and** $\Phi_i^{(2,1)}$: Slopes are $\tau_{i_1} = A_1 f_{1,2} f_{2,1}$ and $\tau_{i_2} = A_2 f_{1,2} f_{2,1}$. However, $(\tau_{i_1} < 1)$ and $(\tau_{i_2} < 1)$ are not always satisfied when sector $\Omega_{1,2}$ or $\Omega_{2,1}$ is relevant. Thus, $\Phi_i^{(1,2)}$ and $\Phi_i^{(2,1)}$ are not always contracting.
- $\Phi_i^{(2,2)}$: Its slope is $\tau_i = f_{i,j} f_{j,i}$. As it was done above for $\Phi_i^{(1,1)}$, the positivity of $\mathrm{CP}_{2,2}$ can be used to compare $\tau_i \lessgtr 1$. This translates as follows :

$$\begin{cases} 1 - f_{i,j} f_{j,i} > 0 \\ 1 - f_{i,j} > 0 \\ 1 - f_{j,i} > 0 \end{cases} \quad \text{or} \quad \begin{cases} 1 - f_{i,j} f_{j,i} < 0 \\ 1 - f_{i,j} < 0 \\ 1 - f_{j,i} < 0 \end{cases} \tag{6.17}$$

  In the first case, $\Phi_i^{(2,2)}$ is a contraction, since $\tau_i < 1$. The second case characterizes a special scenario where sectors $\Omega_{2,2}$, $\Omega_{2,3}$ and $\Omega_{3,2}$ are simultaneously relevant (see for instance Figure 5.10b) : if $\Phi_i^{(2,2)}$ is not contracting within $\Omega_{2,2}$ (since $\tau_i > 1$), $\Phi_i^{(2,3)}$ and $\Phi_i^{(3,2)}$ are ensured to be contractions (see below).
- **Other sectors :** Within sectors $\Omega_{1,3}$, $\Omega_{3,1}$, $\Omega_{2,3}$, $\Omega_{3,2}$, and $\Omega_{3,3}$, Φ_i is constant and so Φ_i is of course contracting.

To sum up, except some (rare) scenarios $\mathscr{P}_S$ for which $\Phi_i^{(1,2)}$ or $\Phi_i^{(2,1)}$ is not necessarily contracting while $O^* = (1,2)$ or $O^* = (2,1)$ (optimal solution), we have established that when the sector Ω_{k_0,l_0} is relevant, then the mapping $\Phi_i^{(k_0,l_0)}$ is always a κ-Lipschitz mapping with a Lipschitz constant strictly smaller than one. □

Proof of convergence - Conclusion

At this point, all required hypotheses have been established to prove the convergence of our DPA algorithm by use of the Banach Theorem :

1. Sequence $(\gamma_i^p)_p$ is built from the iterated function sequence $(\Phi_i^p)_p$ (6.14).
2. Fixed point of $\Phi_i^{(k,l)}$ has been proved to be equal to the coordinate $\mathrm{CP}_i(k,l)$ of the point $\mathscr{D}_i^k \cap \mathscr{D}_j^l$.
3. It has been proved in Chapter 5 that for any communication context $\mathscr{P}_S$, there is always at least one sector Ω_{k_0,l_O} such that $\mathrm{CP}_{k_0,l_0} = \underline{\Gamma}^*$ is the solution to our problem (6.9) (contingent on admission control process).
4. Hence $\Phi_1^{(k_0,l_0)}$ and $\Phi_2^{(k_0,l_0)}$ have at least a relevant fixed point γ_1^* and γ_2^*.
5. We just established that $\Phi_1^{(k_0,l_0)}$ and $\Phi_2^{(k_0,l_0)}$ are quite always[2] contractions.
6. We lastly recall that $\mathbb{R}^2$ is a non-empty complete metric space fitted with the euclidean norm.

The Banach Theorem can now be used to prove that the sequence $(\gamma_i^p)_p$ converges quite always to, and only to, the attractor γ_i^*. Hence DPA admits for quite all communication contexts an optimal solution to our problem (6.9). This solution must just be verified to be feasible, according to power limitations.

2. Except in some scenarios where $O^* = (1,2)$ or $O^* = (2,1)$.

Proof of convergence - Remarks

The Banach Theorem states that convergence of sequences $(\gamma_1^p)_p$ and $(\gamma_1^p)_p$ is ensured, whatever the initial pair (γ_1^0, γ_2^0) may be. Hence, except for some rare communication contexts, convergence of DPA is ensured. Nevertheless, results of the Banach Theorem can only be applied if the whole sequences $(\gamma_1^p)_p$ and $(\gamma_1^p)_p$ remain in the optimal and relevant sector $\Omega_{O_1^*,O_2^*}$. Indeed, if the sector changes between two iterations, then the expression of Φ_1 and Φ_2 change and the Banach Theorem cannot be used any more. However, such limitations do not really matter, as detailed hereafter

Démonstration. Let us consider first the case where the initial value of both sequences is located within the optimal sector :

$$(\gamma_1^0, \gamma_2^0) \in \Omega_{O_1^*,O_2^*}. \tag{6.18}$$

Therefore, what we can assert, based on the Banach Theorem, is that DPA is ensured to converge (for quite all communication contexts) to $\underline{\Gamma}^*$. Indeed, in that given case, we are exactly in the operating framework of the Banach Theorem : whatever (γ_1^0, γ_2^0) may be, $(\gamma_1^p, \gamma_2^p)_p$ is proved to converge to (γ_1^*, γ_2^*). Since first and last values of the sequences are within the same sector and since functions are contracting, we are ensured that at each iteration p the distance between γ_i^p and γ_i^* will shrink. Consequently γ_i^p is forced to remain in $\Omega_{O_1^*,O_2^*}$ for any p.

On the other hand, if DPA starts with a pair

$$(\gamma_1^0, \gamma_2^0) \notin \Omega_{O_1^*,O_2^*}, \tag{6.19}$$

the Banach Theorem cannot be directly applied. Since the sector $\Omega_{O_1^*,O_2^*}$ is by definition the single sector where attractors of Φ_1 and Φ_2 are relevant, $(\gamma_1^p, \gamma_2^p)_p$ cannot remain in any sector other than $\Omega_{O_1^*,O_2^*}$. There are two possibilities for sector $\Omega_{k,l}$ with $(k,l) \neq (O_1^*, O_2^*)$. First, at least $\Phi_1^{(k,l)}$ or $\Phi_2^{(k,l)}$ is not a contraction ($\kappa \geq 1$). Then $\Omega_{k,l}$ is said 'repellent' or 'repulsive', since $(\gamma_1^p, \gamma_2^p)_p$ cannot move close to (γ_1^*, γ_2^*) but move away from it. Second, $\Phi_1^{(k,l)}$ and $\Phi_2^{(k,l)}$ are contracting but their attractor is not located inside the sector $\Omega_{k,l}$. Hence $(\gamma_1^p, \gamma_1^p)_p$ will converge to these attractors until $(\gamma_1^p, \gamma_2^p)_p$ meets the boundaries of $\Omega_{k,l}$. In both cases, it exists a number P_0 of iterations such that $(\gamma_1^{P_0}, \gamma_2^{P_0})$ leaves $\Omega_{k,l}$. Therefore $(\gamma_1^p, \gamma_1^p)_p$ will switch between sectors $\{\Omega_{k,l}\}_{k,l}$ until $\Omega_{O_1^*,O_2^*}$ will be met. We could imagine that $(\gamma_1^p, \gamma_2^p)_p$ may oscillate between two repellent sectors without ever meet $\Omega_{O_1^*,O_2^*}$. However, the transverse and successive updates of $(\gamma_1^p)_p$ and $(\gamma_2^p)_p$, combined with easy rules at regimes boundaries, prevent from such oscillations. □

As a consequence, $\Omega_{O_1^*,O_2^*}$ is always met and Banach Theorem fits well, except if the momentary communication context does not let $\Phi_1^{\underline{O}^*}$ and $\Phi_2^{\underline{O}^*}$ be contracting while $\underline{O}^* = (1,2)$ or $\underline{O}^* = (2,1)$. In quite all communication contexts,

$$\exists P^* \mid \forall p > P^*, \quad (\gamma_1^p, \gamma_2^p) \in \Omega_{O_1^*,O_2^*}. \tag{6.20}$$

Hence there is possibly a transitional period during which some non relevant sectors alternate but finally $\Omega_{O_1^*,O_2^*}$ is met.

Summary

Section 6.4.3.1 is now over but we are conscious the reasoning develop along this section could be tedious. Therefore we propose to sum up main steps of the reasoning.

1. At most nine sectors $\Omega_{k,l}$ with specific mappings $\Phi_1^{(k,l)}$ and $\Phi_2^{(k,l)}$ are defined.
2. Mappings $\Phi_1^{(k,l)}$ and $\Phi_2^{(k,l)}$ have each an attractor which actually corresponds to one coordinate of the point $\mathscr{D}_1^k \cap \mathscr{D}_2^l$. We refer to this crossed-point with $\mathrm{CP}_{k,l}$.
3. However this crossed-point is not necessarily located inside the region defined by $\Omega_{k,l}$. If $\mathrm{CP}_{k,l} \in \Omega_{k,l}$, then sector $\Omega_{k,l}$ is said relevant and is one candidate to problem (6.9). $\mathrm{CP}_{k,l}$ is the optimal solution $\underline{\Gamma}^*$ if admission control process does not reject it (power limitations) and if $\mathrm{CP}_{k,l}$ is the best solution among all possible candidates. Else sector $\Omega_{k,l}$ is repellent and cannot propose a balanced solution.
4. Existence and optimality of such a solution $\underline{\Gamma}^*$ have been addressed in Chapter 5. This solution is located into the sector $\Omega_{O_1^*,O_2^*}$ where $\underline{O}^*$ is the couple of optimal strategies to handle in-band interference.
5. We propose to meet solution $\underline{\Gamma}^*$ by designing a couple of iterative function sequences $(\gamma_1^p, \gamma_1^p)_p$. At each iteration p, in line with the momentary communication context, γ_1^p and γ_2^p are updated respectively with $\Phi_1^{(k_1,l_1)}$ and $\Phi_2^{(k_2,l_2)}$, where Ω_{k_1,l_1} and Ω_{k_2,l_2} are respectively the sectors within which $(\gamma_1^p, \gamma_2^{p-1})$ and (γ_1^p, γ_2^p) are located (if $\mathscr{C}_1$ starts). We would like that $(\gamma_1^p, \gamma_1^p)_p$ converges to $\underline{\Gamma}^*$.
6. To this end, we want to prove the convergence with the Banach Theorem but there are some hypotheses to verify before.
7. Thus we established that it exists a number of iterations P^* from which $(\gamma_1^p, \gamma_1^p)_p$ achieves and remains inside the sector $\Omega_{O_1^*,O_2^*}$.
8. We furthermore established that $\Phi_1^{(O_1^*,O_2^*)}$ and $\Phi_2^{(O_1^*,O_2^*)}$ are contracting mappings.
9. The Banach Theorem can now prove the convergence of our DPA algorithm.
10. **Be careful !** Three last steps are not always verified since there are some rare communication contexts that prevent $\Phi_1^{(O_1^*,O_2^*)}$ and/or $\Phi_2^{(O_1^*,O_2^*)}$ to be contracting. Therefore, even the sector $\Omega_{O_1^*,O_2^*}$ may be repellent and $(\gamma_1^p, \gamma_1^p)_p$ then infinitely switches between repellent sectors without ever meeting a balanced state.

6.4.3.2 Spectral Radius

The distributed criterion introduced in Section 6.3.4 can also be used to prove the convergence of our DPA algorithm. We will not develop again this criterion. We advise the reader to look at [150, 151] for more details. Just to sum up, this consists in a metric that each decision-maker can compute on a distributed way to check if its transmission may cause the non-convergence of the iterative process. This metric is actually applied on the interference matrix of the system. Such a matrix has already been derived for our interference classifier at Section 5.5.2.

This approach needs to prove that the spectral radius of the interference matrix is inside the unit circle. To this end a distributed criterion is derived as an upper-bound of the spectral radius. However, the fact that this distributed criterion is larger than one does not necessarily imply that the spectral radius is outside the unit circle. Furthermore, the classification of in-band interference by decision-makers may change from one iteration to another. Consequently the interference matrix and with it, the distributed criterion,

may also be modified. Besides, as stated in Section 6.4.3.1, a transitional period can occur before the optimal sector is achieved. During this transitional period, the process can be placed into regimes within which convergence is not possible. In those cases, the distributed criterion will notice that convergence of CPA is not possible because there is no possibility for decision-maker to know this is a transitional regime. Therefore, this criterion should be employed carefully because of our adaptive classification of interference that changes the form of the interference matrix from one iteration to another.

6.4.4 Rate of Convergence

In this section some elements, results and heuristics about the rate of convergence of our DPA algorithm will be addressed. Ideally, it would be great if decision-makers could predict the convergence or not of DPA, how fast it will converge. That would let them adopt alternative algorithms if DPA would be not fast enough for instance. Nevertheless such predictions symbolize the trade-off between centralized algorithms with full knowledge and distributed algorithms with partial knowledge. It is indeed inconceivable from decision-makers to foresee such behaviours, since they do not dispose of enough knowledge about the system.

We propose hereafter some heuristics that may help to estimate qualitatively the convergence. We begin however by some preliminaries about convergence of iterated function sequences. To this end, the omniscient genie is again considered. It can access to some variables that decision-makers cannot compute because of their partial knowledge. First of all, the rate of convergence is linked to the value of the Lipschitz constant κ which must be at least strictly smaller than one. The smaller κ, the faster the convergence. This result can be corroborated by :

$$\forall (x,y) \in E \times E, \quad \forall p \in \mathbb{N} \quad d\Big(u^p(x), u^p(y)\Big) \leq \kappa^p \cdot d(x,y) \tag{6.21}$$

which is a straightforward derivation of (6.12).

To investigate more in details this result, let us consider Figure 6.6 which plots the number of iterations before convergence versus the value of κ. The communication context we consider is $\mathscr{P}_S = \{2, 2, f_{1,2}, 0.25\}$, while the initial vector is $\underline{\Gamma}^0 = (40; 20)$. By varying the value of $f_{1,2}$ we want to monitor the value of κ and then to investigate how behaves convergence of DPA for each value. Coefficient $f_{1,2}$ varies between 0 and 0.25 : for this range, $\Omega_{1,1}$ is the single relevant sector of the system. Hence Table 6.3 gives the Lipschitz constant $\kappa = A_1 A_2 f_{1,2} f_{2,1}$ for this sector. By varying $f_{1,2}$ while A_1, A_2 and $f_{2,1}$ are kept constant, we notice that the convergence is faster when $f_{1,2}$ and hence κ are smaller, since $\kappa = 2.25 f_{1,2}$. The convergence is besides met with at most 19 iterations and at least two iterations. Increasing $f_{1,2}$ beyond 0.25 causes $\Omega_{1,1}$ to be not relevant any more.

However, a singular value $f^*_{1,2} = 0.2111$ seems to be optimal and in contradiction with the curve trend. Figure 6.7 zooms in on $\mathrm{CP}_{1,1}$ in region $(\gamma_1; \gamma_2)$ for a value $f_{1,2}$ close to $f^*_{1,2}$. The figure illustrates the different steps of the iterative process which lead to convergence. By changing the value of $f_{1,2}$, directions of $\{\mathscr{D}_i^k\}_{i,k}$ and $\{\mathscr{B}_i^k\}_{i,k}$ as well as location of $\mathrm{CP}_{1,1}$

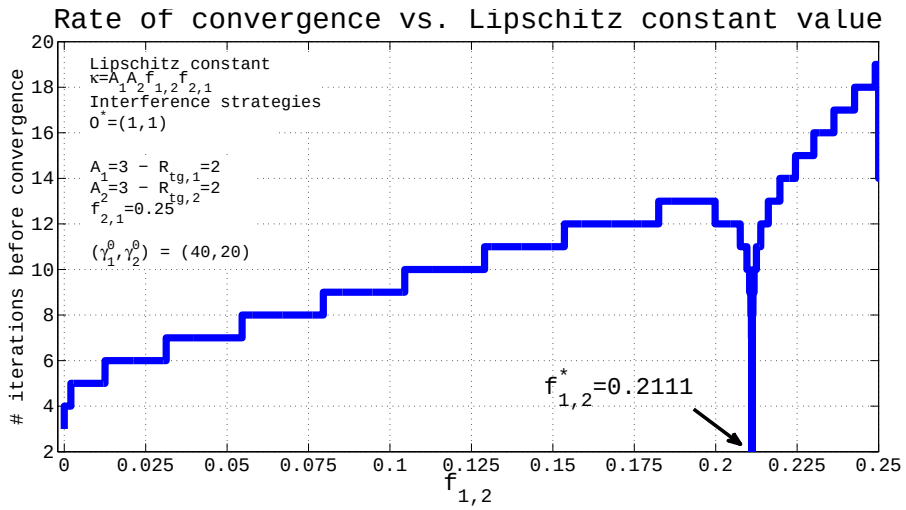

Figure 6.6 – Investigation on convergence rate within sector $\Omega_{1,1}$: Impact of κ value

can be modified. Let Δ be the gap between γ_1^1 and γ_1^*

$$\begin{aligned} & \Delta = |\gamma_1^* - \gamma_1^1| \\ \text{with} \quad & \gamma_1^1 = \varphi_1^{(2)}(\gamma_2^0) = A - f_{2,1} \cdot \gamma_2^0, \\ \text{and} \quad & \gamma_1^* = \tfrac{A_1(1+A_2 f_{2,1})}{1-A_1 A_2 f_{2,1} f_{1,2}}. \end{aligned} \tag{6.22}$$

$$\begin{aligned} & \Delta = 0 \\ \Rightarrow \quad & f_{1,2} = \tfrac{1}{A_1 A_2 f_{2,1}} |1 - \tfrac{A_1(1+A_2 f_{2,1})}{A - f_{2,1} \cdot \gamma_2^0}| \\ & f_{1,2} = \tfrac{19}{90} \approx 0.2111 \end{aligned}$$

We now understand that the value $f_{1,2}^*$ lets γ_1^1 equal the attractor γ_1^* in one iteration, whereas for all other values the process needs several iterations to converge to γ_1^*. But commonly the rate of convergence evolves with κ.

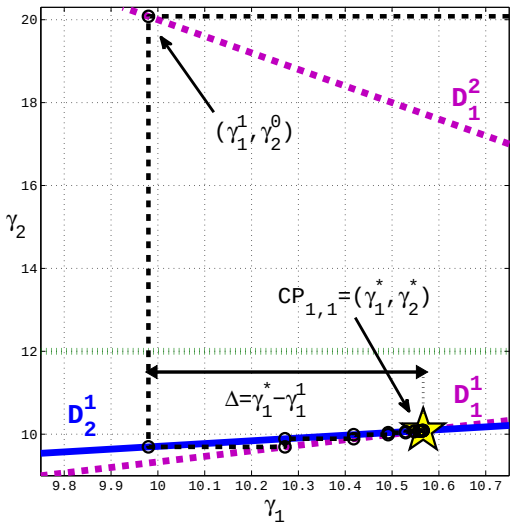

Figure 6.7 – Investigation on convergence rate within sector $\Omega_{1,1}$: Zoom in on $\mathrm{CP}_{1,1}$

One of the main limitations of DPA in terms of convergence prediction is the incapacity of decision-makers to compute κ. DM_i is indeed able to compute φ_i but not φ_j ; hence DM_i cannot access to $\Phi_i = \varphi_i \circ \varphi_j$ to compute its Lipschitz constant. Likewise, DM_i is unable to determine the optimal sector $\Omega_{O_1^*,O_2^*}$; DM_i is even unable to know if the current classified regime is equal or not to O_i^*. Nevertheless, if DM_i can store some data, there are some possibilities to monitor the behaviour of DPA to investigate convergence. Just to be clear, we precise that a non-convergent scenario is not necessarily a divergent scenario. If this precision seems to be anecdotal, it is however of great matter since divergence is easier to detect than non-convergent.

- The simplest solution is to have a loop counter stating a maximal number of iterations. This prevents from infinite loops due to non-convergence but also prevents from very low converging processes.
- Another solution is to measure the gap between two consecutive iterations. We can use for instance the euclidean distance to compute $\|\underline{\Gamma}^p - \underline{\Gamma}^{p-1}\|$. If this distance is below a given threshold ε, then a balanced SNR vector is assumed to be met and DPA stops.
- We define our stopping criterion in DPA with these two conditions.
- However we also investigate some other criteria which perform quite well but which are more sensitive to the systems and heuristics.
- The Banach Theorem claims the fixed point is met whatever the initial point may be. Nevertheless, the fixed point is achieved sooner if the initial point is set close to the fixed point. Such a proposal is an open challenge since there is no way to know when DPA starts where the fixed point is.
- There are at most nine sectors but just one or two are relevant, *i.e.,* just one or two can attract the sequence $\{\gamma_i^p\}_p$ to make it converge. All other sectors are repellent and sequences $\{\gamma_i^p\}_p$ cannot remain endlessly inside these sectors. If it exists a solution to problem (6.9), sequences $\{\gamma_i^p\}_p$ cannot switch endlessly between repellent sectors without ever meeting the relevant sector. Hence a solution is to use at each decision-maker a variable to count the number of switching between regimes. If this counter becomes greater than a given threshold, we can consider that the momentary communication context is a non-converging scenario.
- To deal with the transitional period at the beginning of DPA process, it is possible to use another variable to count how many iterations happen in the same regime. If DM_i switches with another regime, this counter is reinitialized. Until this counter is not greater than a given threshold, we can consider that we are always in the transitional period or that no convergence is possible.
- Lastly, look-up tables can be computed and used to predict the outcome of DPA process. The look-up table $\mathscr{L}_i$ could state for decision-maker DM_i which is the final regime O_i^* for given inputs (target rates $R_{tg,i}$ and $R_{tg,j}$, channel coefficients $g_{i,i}$ and $g_{j,i}$). Channel coefficients $g_{j,j}$ and $g_{i,j}$ are unknown at DM_i but they however affect the computation of O_i^*. Look-up table $\mathscr{L}_i$ can be therefore either computed with numerous random values of $g_{j,j}$ and $g_{i,j}$ and then averaged over all these random values to state how behaves O_i^* in an average context of interference ; or $\mathscr{L}_i$ can be computed with given values for $g_{j,j}$ and $g_{i,j}$, assuming DM_i knows some statistics about its neighbour. Such look-up tables are presented above in Section 6.4.5.

All these ideas can be investigated to try to characterize the convergence of DPA. Ne-

vertheless, the unpredictable behaviour of the neighbour decision-maker makes the problem tedious. Furthermore, if excessively long convergence as well as non-converging scenarios want both to be avoided, it seems not conceivable to adopt the same techniques to recognize these two kinds of scenarios because they behave radically differently.

6.4.5 Additional Remarks

Along this section some remarks will be made concerning the behaviour of our DPA algorithm. We will first illustrate a communication context where convergence is not ensured. Then the particular communication context $\mathscr{P}_S = \{2, 2, 1.75, 1.75\}$ firstly mentioned in Section 5.4.5 and shown on Figure 5.10b (three simultaneous attractors) will be investigated in case of DPA algorithm. Lastly, the influence of coefficients $\{g_{i,j}\}_{i,j}$ on the optimal classification of in-band interference $\underline{O}^* = (O_1^*, O_2^*)$ will conclude this section.

In Section 6.4.3.1 we investigated how the Banach Theorem could be applied to prove the convergence of DPA algorithm. To this end we had to check to what extend mappings $\Phi_1^{(O_1,O_2)}$ and $\Phi_2^{(O_1,O_2)}$ were Lipschitz mappings with a Lipschitz constant κ strictly smaller than one. Here, we consider the communication context $\mathscr{P}_S = \{2, 1, 1.29, 0.262\}$ that states $\Omega_{1,2}$ is the single relevant sector and hence $\underline{O}^* = (1, 2)$. Nevertheless, by referring to Table 6.3 we note that within this sector the Lipschitz constant κ of $\Phi_1^{(O_1,O_2)}$ and $\Phi_2^{(O_1,O_2)}$ is the same and equals $\kappa = A_1 f_{1,2} f_{2,1}$. With the current values of channel and system parameters, we note that $\kappa = 1.014 > 1$ and hence DPA algorithm cannot converge to $\mathrm{CP}_{1,2}$. Figure 6.8 corroborates this result. The iterative process starts with the initial vector $\underline{\Gamma}^0$ marked by a yellow downward-pointing triangle. After hundred iterations of the DPA process, the current position of $\underline{\Gamma}^100$ is marked by a yellow upward-pointing triangle. We show that during these hundred iterations the sequence $(\gamma_1^p, \gamma_2^p)_p$ kept move away from $\mathrm{CP}_{1,2}$. This behaviour is expected : since $\Phi_1^{(O_1,O_2)}$ and $\Phi_2^{(O_1,O_2)}$ have a Lipschitz constant κ greater than one, distance $\|\underline{\Gamma}^p - \underline{\Gamma}^{p-1}\|$ between two consecutive iterations is enhanced instead of being shrunk. To avoid such a non-convergent process, one of the proposals discussed at the end of Section 6.4.4 could be adopted.

We have previously mentioned the existence of particular communication contexts where three attractors are simultaneously relevant and hence candidates to be the optimal solution to problem (6.9). In case of centralized algorithm, the network controller is supplied with full knowledge and can thus elect the best candidate. However, decision-makers of distributed approaches cannot perform such a selection because of lack of knowledge. The final solution is chosen during the process, according to channel ans system parameters values. Actually, we will see that the selection of this final solution is driven first by the initial vector $\underline{\Gamma}^0$ and second by the pair $\mathscr{C}_i$ that launches the process. Up to here we set $\underline{\Gamma}^0$ according to $(P_{1,\max}, P_{2,\max})$ and assumed that $\mathscr{C}_1$ started. But it was one possibility among many ; hereafter we investigate how behaves DPA algorithm when $\underline{\Gamma}^0$ is set to different values and when $\mathscr{C}_1$ or $\mathscr{C}_2$ starts the iterative process.

First of all, Figure 6.9 states the context of our investigation. The communication context is fixed and equal to $\mathscr{P}_S = \{2, 2, 1.75, 1.75\}$. Hence, three attractors exist within the three relevant sectors $\Omega_{2,2}$, $\Omega_{2,3}$ and $\Omega_{3,2}$. Some discussions about such a context have already been done in Section 6.4.3.1, especially with Equation (6.17). We have proved that mappings $\{\Phi_i^{(2,3)}\}_i$ and $\{\Phi_i^{(3,2)}\}_i$ were always contractions since they are constant

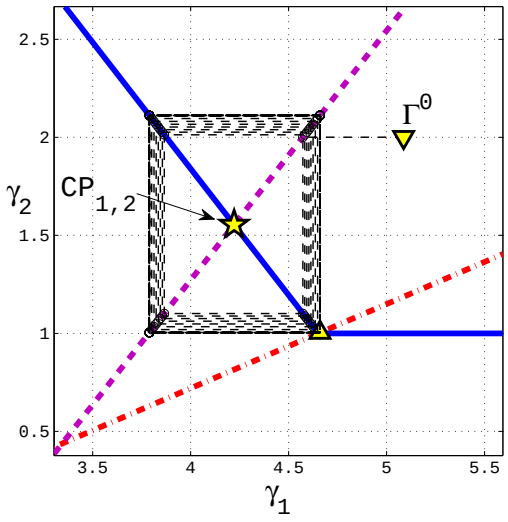

FIGURE 6.8 – $\mathscr{P}_S = \{2, 1, 1.29, 0.262\}$: DPA process does not converge to $\text{CP}_{1,2}$ in spite of the relevance of sector $\Omega_{1,2}$. Mappings $\{\Phi_i^{(1,2)}\}_i$ have a Lipschitz constant $\kappa > 1$ and hence are not contracting.

(see Table 6.3). On the other hand, $\{\Phi_i^{(2,2)}\}_i$ are here not contracting since their Lipschitz constant $\kappa = f_{1,2}f_{2,1} = 3.0625$ is greater than one. Hence DPA process cannot converge to $\text{CP}_{2,2}$. The unique solution for DPA to meet $\text{CP}_{2,2}$ is that $\underline{\Gamma}^0 = \text{CP}_{2,2}$ but this would be a unbalanced solution since any slight change in value of parameters causes $\text{CP}_{2,2}$ would not be achievable any more.

To illustrate the unpredictable nature of this communication context, we have shown on Figure 6.9 the solution computed by DPA for two different starting points : $\underline{\Gamma}^{0,1}$ and $\underline{\Gamma}^{0,2}$ marked respectively by black and magenta downward-pointing triangles. In both cases, $\mathscr{C}_1$ that launches the process. With $\underline{\Gamma}^{0,1}$, DPA converges to $\text{CP}_{3,2}$ after two iterations (see black lines), while $\underline{\Gamma}^{0,2}$ lets DPA meet $\text{CP}_{2,3}$ after four iterations (see magenta lines). A natural idea following from these unpredictable solutions would be to derive the attraction region of the three fixed points, *i.e.,* the set of all vectors $\underline{\Gamma}^0$ that let converge to one given fixed point. Such regions will be referred to by $\Xi_{2,2}$, $\Xi_{2,3}$ and $\Xi_{3,2}$. The fixed point is of course inside its region of attraction. We have already shown that $\Xi_{2,2}$ is a singleton, *i.e.,* $\Xi_{2,2} = \{\text{CP}_{2,3}\}$. Figures 6.10a and 6.10b illustrate these three regions, respectively when $\mathscr{C}_1$ starts and then when $\mathscr{C}_2$ starts. The region $\Xi_{2,3}$ is represented by all cyan points, as attests the cyan star located at $\text{CP}_{2,3}$, while all green points represent $\Xi_{3,2}$. $\Xi_{2,2}$ is indeed a singleton. Figures 6.10a and 6.10b prove these three regions differ when the pair that initiates the DPA iterative process changes. It is not a contradiction with the Banach Theorem that states convergence does not depend on initial values. The adaptive nature of our algorithm with multiple sectors and mappings makes this theorem cannot be straightforwardly applied.

Lastly, influence of coefficients $\{g_{i,j}\}_{i,j}$ on the optimal classification of in-band interference $\underline{O}^* = (O_1^*, O_2^*)$ is investigated. We recall that O_i^* refers to the optimal interference strategy to handle in-band interference at destination d_i ; three strategies are available (noisy, joint decoding, SIC-based) but we add a fourth one to describe the fact that DPA may not converge and hence no strategy can be selected. O_i^* is then a four-state value.

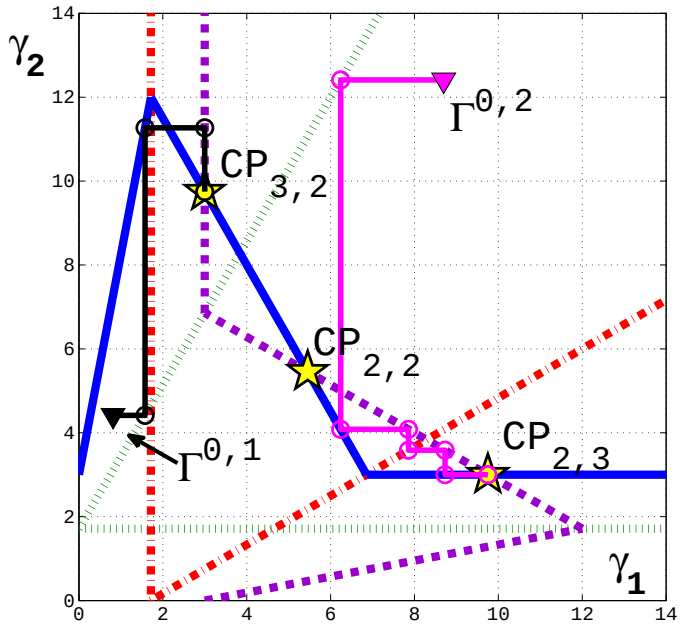

Figure 6.9 – $\mathscr{P}_S = \{2, 2, 1.75, 1.75\}$: Three attractors are simultaneously relevant. The final solution depends on the location of the starting point Γ^0.

In a first time, we consider that parameters $R_{tg,1}$, $R_{tg,2}$, $g_{1,2}$ and $g_{2,2}$ are fixed while parameters $g_{1,1}$ and $g_{2,1}$ vary both between 10^{-3} and 10^3. Channel coefficients are the two parameters that monitor the signals sensed by destination d_1. We further assume that the pair $\mathscr{C}_1$. DPA algorithm is performed for each value of $(g_{1,1}, g_{2,1})$ while solution $\underline{O}^* = (O_1^*, O_2^*)$ is stored for each couple $(g_{1,1}, g_{2,1})$. Then, results are plotted on two figures whose axes represent variations of ($g_{1,1}$ and $g_{2,1}$). The two figures respectively show the value of O_1^* and O_2^* for each couple $(g_{1,1}, g_{2,1})$. In other words, each point $(g_{1,1}, g_{2,1})$ of these two figures corresponds to the value of O_1^* and O_2^* which has been computed and stored by DPA for this couple $(g_{1,1}, g_{2,1})$. For sake of clarity, each value of O_i^* has been associated with a specific colour. $O_i^* = 1$ (noisy), $O_i^* = 2$ (joint decoding), $O_i^* = 3$ (SIC-based) and $O_i^* = \emptyset$ (no convergence) are respectively described by a red point, a green point, a blue point and a yellow point.

Results are summarized in Table 6.4, when $R_{tg,1} = R_{tg,2} = 2$. The first line of this table shows results when coefficients $g_{1,2}$ and $g_{2,2}$ are both equal to 1.0. The figure on the left (**1.1**) illustrates the distribution of O_1^* while the figure on the right (**1.2**) is for O_2^*. As expected, O_1^* is mainly driven by $g_{2,1}$ while O_2^* is mainly driven by $g_{1,1}$. Indeed $g_{2,1}$ characterizes the ability of d_1 to decode or not the interfering message x_2, in line with the target rate $R_{tg,2}$. If $g_{2,1}$ is too low, this crossed-link is in outage and d_1 has then to treat x_2 as noise. If $g_{2,1}$ is quite high, then this crossed-link is good enough to let d_1 decode x_2 first and then subtract it. Intermediate values of $g_{2,1}$ refer to the joint decoding. On the other hand, channel coefficient $g_{1,1}$ implicitly affects the second pair $\mathscr{C}_2$ by way of transmit power P_1 or SNR γ_1. According to the value of $g_{1,1}$ DM_1 sets P_1 to a value more or less high so as to ensure the target rate $R_{tg,1}$. This power is translated into INR δ_2 in the neighbour pair $\mathscr{C}_2$. Identical reasoning can then be made for the selection of O_2^*.

The second line of Table 6.4 shows results for other values for $g_{1,2}$ and $g_{2,2}$. Channel coefficients $g_{1,2}$ and $g_{2,2}$ are now respectively set to 0.316 and 10.0. Since $g_{2,2}$ is enhanced

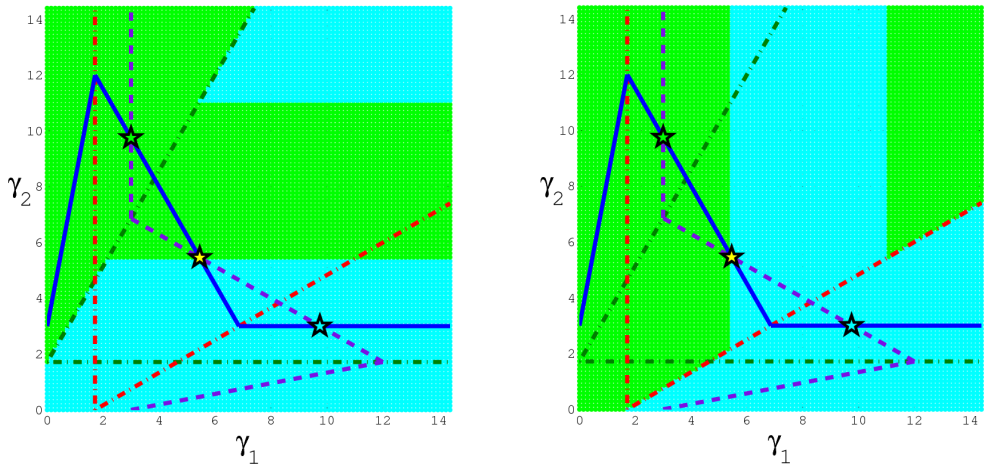

(a) Pair $\mathscr{C}_1$ starts the process

(b) Pair $\mathscr{C}_2$ starts the process

FIGURE 6.10 – $\mathscr{P}_S = \{2, 2, 1.75, 1.75\}$: The final solution depends first on the starting point Γ^0, second on the pair that launches the process.

in comparison to previous simulation, DM_2 in $\mathscr{C}_2$ will set P_2 to a lower value (the target rate is unchanged while the quality of direct path is better : power can be lowered to meet same performance). Consequently INR δ_1 is reduced in $\mathscr{C}_1$ and $g_{2,1}$ must be higher to let d_1 be able to decode interfering signal x_2. In comparison to Figure **1.1**, Figure **2.1** is upwards translated. Likewise, since $g_{1,2}$ is lowered in comparison to previous simulation, destination d_2 experiences a lower INR δ_2 and has more difficulties to decode interfering signal x_1. To be able to decode this signal, δ_2 must be higher. To increase δ_2 whereas $g_{1,2}$ is fixed, the unique solution is to increase P_1 ; this is done by DM_1 when $g_{1,1}$ is too small to meet $R_{tg,1}$. In comparison to Figure **1.2**, Figure **2.2** is translated to the left.

In a second time, we consider that parameters $R_{tg,1}$, $R_{tg,2}$, $g_{1,1}$ and $g_{2,2}$ are fixed while parameters $g_{1,2}$ and $g_{2,1}$ vary both between 10^{-3} and 10^3. By varying $g_{1,2}$ and $g_{2,1}$ while $g_{1,1}$ and $g_{2,2}$ are fixed and both set to 1.0, coefficients $f_{1,2}$ and $f_{2,1}$ likewise vary, since $f_{i,j} = \left|\frac{g_{i,j}}{g_{i,i}}\right|^2$. Now DPA algorithm is launched with each couple $(g_{1,2}, g_{2,1})$ and the optimal pair of strategies $\underline{O}^*$ is stored. As before, specific colours are assigned to each of the ten possible values of $\underline{O}^*$ (nine states coming from the superposition of O_1^* with O_2^* and a tenth for non-convergence). Results are illustrated on the third line of Table 6.4. On the left, Figure **3.1** gives the distribution of $\underline{O}^*$ when $\mathscr{C}_1$ launches the DPA process, while Figure **3.2** on the right shows the distribution of $\underline{O}^*$ when DPA process is initiated by $\mathscr{C}_2$. Both figures seem very similar, which is an expected result, since in most contexts there is only one attractor ; hence whatever the cell may begin, the same attractor will be met. Figures differ when two or three attractors are simultaneously relevant : there is then a sensibility of DPA to the initial condition $\underline{\Gamma}^0$, as shown on Figure 6.10. This is not obvious but both figures differ by their boundary between the white and yellow regions (precisely the two sectors $\Omega_{2,3}$ and $\Omega_{3,2}$).

It can be conceivable to use Figures of Table 6.4 as look-up tables to help decision-makers in predicting the issue of DPA algorithm. For instance, if DM_1 has some information about the statistics of $g_{1,2}$ and $g_{2,2}$, it can then choose which figure is relevant between

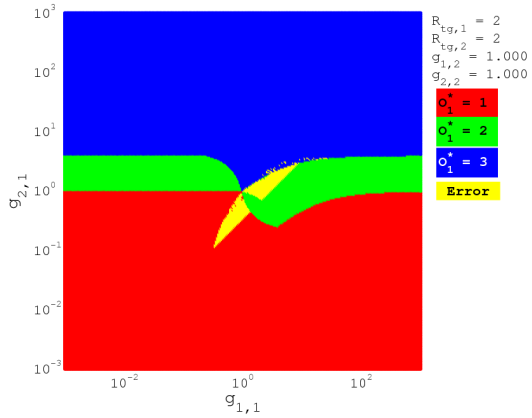

1.1 Selection of O_1^*

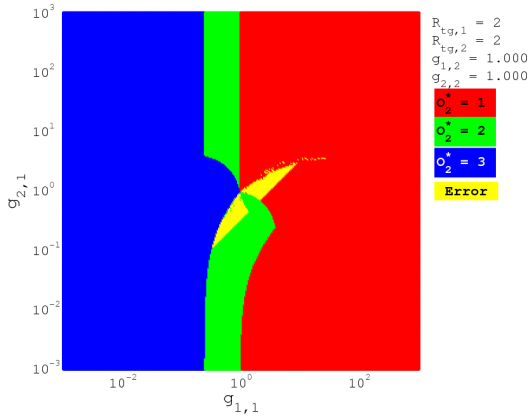

1.2 Selection of O_2^*

Variations of coefficients $g_{1,1}$ and $g_{2,1}$. $\mathscr{C}_1$ starts, $g_{1,2} = g_{2,2} = 1.0$, $R_{tg,1} = R_{tg,2} = 2$.

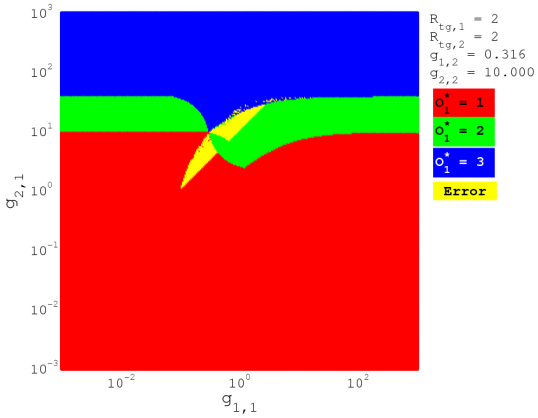

2.1 Selection of O_1^*

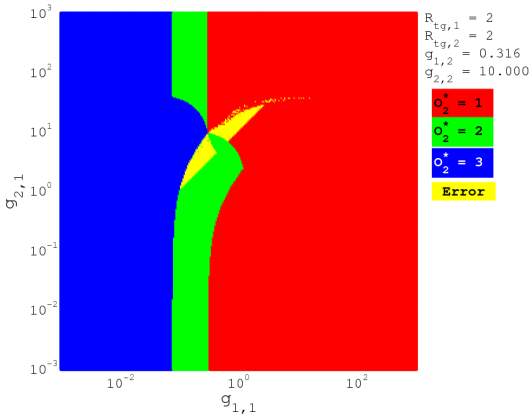

2.2 Selection of O_2^*

Variations of $g_{1,1}$ and $g_{2,1}$. $\mathscr{C}_1$ starts, $g_{1,2} = 0.316$, $g_{2,2} = 10.0$, $R_{tg,1} = R_{tg,2} = 2$.

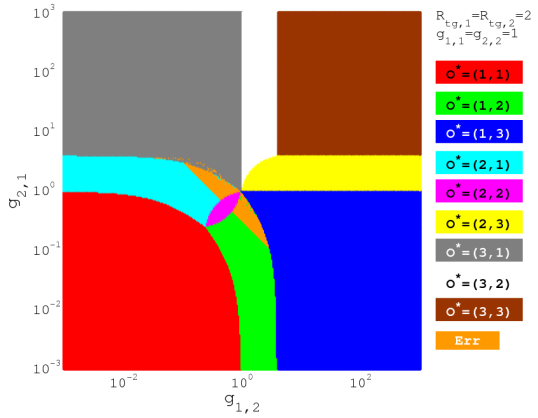

3.1 Selection of (O_1^*, O_2^*) when $\mathscr{C}_1$ starts

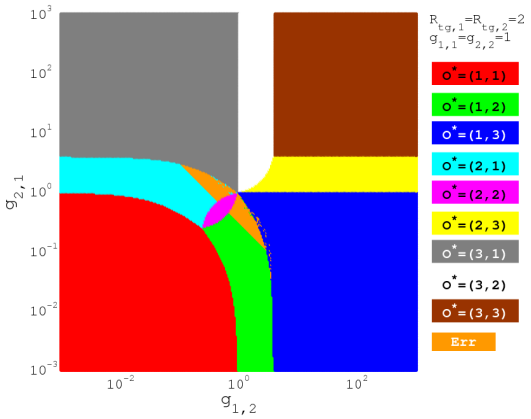

3.2 Selection of (O_1^*, O_2^*) when $\mathscr{C}_2$ starts

Variations of $g_{2,1}$ and $g_{1,2}$. $\mathscr{C}_1$ starts, $g_{1,1} = g_{2,2} = 1.0$, $R_{tg,1} = R_{tg,2} = 2$.

Table 6.4 – How selection of (O_1^*, O_2^*) is affected by variations of channel coefficients ?

Figures **1.1** and **2.1** (or any other figures of its look-up table). Since DM_1 can know value of $g_{1,1}$ and $g_{2,1}$, DM_1 is then able to know in which regime O_1^* it will converge. Hence at each iteration p DM_1 is able to determine if it has reach or not O_1^*. However DM_1 is not necessarily able to determine if the transitional phase is over since O_1^* can be met while O_2 still oscillates between two regimes ! If Figures **3.1** and **3.2** are used to derive look-up tables, then DM_1 can access to rich information (knowledge of $\underline{O}^*$) ; but reliability of this information is linked to the reliability that DM_1 has on the value of $g_{1,2}$.

6.4.6 Simulation Results

This section concludes our investigation of DPA algorithm for the value $n = 2$ with some simulation results. This last section will be quite short since DPA achieves almost always the same results in terms of power allocation as those of CPA which have already been presented. We invite the reader to refer to Section 5.4.5 presenting simulations results for CPA algorithm to find more results of simulation.

Some new results are however proposed to corroborate the fact that CPA and DPA allocate almost always the same power vector $\underline{P}^*$. Furthermore, some results about the rate of convergence are also provided. Our simulations have been performed in the same operating framework as the one described in Section 5.4.5. Thus system deployment is illustrated by Figure 5.11. Tables 5.3 and 5.5 give the channel and system settings. Two new parameters are introduced in comparison to CPA ; they deal with the stopping criterion mentioned on Figure 6.3 and at the beginning of Section 6.4.2. DPA iterative process ends for a given communication context either once the sequence $(\gamma_1^p, \gamma_2^p)_p$ has converged to an optimal solution, or when no convergence has been met after a given number of iterations. The first criterion is described by

$$\|\underline{\Gamma}^p - \underline{\Gamma}^{p-1}\| \leq \epsilon, \tag{6.23}$$

where $\|\cdot\|$ is the euclidean norm on $\mathbb{R}^2$ and ϵ is a constant threshold. In this section, ϵ is set to 10^{-6}. The second criterion is simply a threshold for the number of iterations p which cannot exceed p_{MAX}

$$p > p_{\text{MAX}}, \tag{6.24}$$

p_{MAX} is set to 100 in this section. This value has been chosen arbitrarily, without any consideration of channel and system parameters. In practice, the rate of convergence must be faster than the period with which channel estimation is performed (which is linked to the period of coherence of channel). Indeed our DPA algorithm must be performed with a fixed communication context $\mathscr{P}_S$, *i.e.*, $R_{tg,1}$, $R_{tg,2}$, $f_{1,2}$ and $f_{2,1}$ cannot change during the iterative process. DPA stops when one of these two conditions (6.23) and (6.24) is met.

As it was done in Section 5.4.5, DPA is compared to NPA, TSPA and of course CPA. Two algorithms are considered for DPA : DPA $\mathscr{C}_1\mathscr{C}_2$ and DPA $\mathscr{C}_2\mathscr{C}_1$. With the first algorithm the iterative process is always launches by the pair $\mathscr{C}_1$ while $\mathscr{C}_2$ initiates the 'ping-pong' process in the second algorithm. DPA can fail because of first an excessive power assignment that does not pass the admission control process, second a non-convergent communication context, third a too slow communication context. We precise that the admission control process that check if power assignment is compliant with power limitations is performed at each iteration and not just once at the end of DPA (in case of convergence). If DPA does not converge ($\|\underline{\Gamma}^{p_{\text{MAX}}} - \underline{\Gamma}^{p_{\text{MAX}}-1}\| > \epsilon$), then decision-makers decide

by mutual agreement to adopt the centralized approach TSPA [3]. If DPA fails because of admission control process, then TSPA algorithm is also adopted. If still no feasible solution is computed, then transmission is cancelled until a new communication context is encountered.

We showed on Figure 5.12 how the optimal pairs of strategies $\underline{O}^*$ were distributed among the nine possible pairs when CPA was performed. This distribution was obtained before the admission control process. Such a figure can now be derived with DPA, as illustrated on Figure 6.11a. We do not adopt the pie representation in order to compare simultaneously the distribution of CPA, DPA $\mathscr{C}_1\mathscr{C}_2$ and DPA $\mathscr{C}_2\mathscr{C}_1$. Two new possibilities are added to the nine pairs (O_1, O_2). The first is 'N-CV' (non-convergence) and characterizes the event that DPA algorithm does not manage to converge to a balanced state during the p_{MAX} authorized iterations. The second is 'E-CV' (error-convergence) and characterizes the event that DPA has been stopped by the admission control process before to meet p_{MAX} iterations. The three algorithms have a quite similar distribution, except for $\underline{O}^* = (1,3)$ and $\underline{O}^* = (3,1)$ for which the frequency of selection is higher for CPA. Such a behaviour is for the moment still inexplicable. The events 'N-CV' and 'E-CV' are respectively encountered in 4% and 2% of communication contexts. Consequently, 6% of scenarios require a coordinated call to TSPA algorithm.

On the other hand, Figure 6.11b illustrates the average number of iterations that were required to meet a balanced state for each pair (O_1, O_2). We note that the convergence of DPA is in average quite fast since a balanced state is met with 5.3 iterations. Furthermore, there is a certain homogeneity between all pairs (O_1, O_2) : 3 iterations differ between the fastest and the slowest pairs.

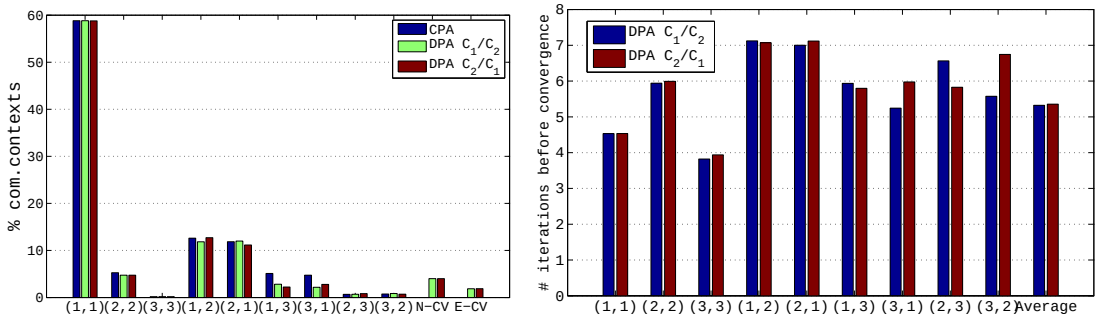

(a) Distribution of O^* among all $\Omega_{k,l}$

(b) Number of iterations before convergence

Figure 6.11 – DPA Algorithm : Selection of optimal sector $(O_1^*; O_2^*)$ and rate of convergence in each sector $\Omega_{k,l}$.

Figure 6.12 represents the extension of Figure 5.14 ; performance of DPA $\mathscr{C}_1\mathscr{C}_2$ and DPA $\mathscr{C}_2\mathscr{C}_1$ have been added to the previous figure. Figure 6.12a shows that both DPA algorithms fail in 5.9% of communication contexts. It is worse than CPA with just 1.1% of failed scenarios but it is much better then NPA with 30% of failed scenarios. Avoiding excessive power assignments during the iterative process seems not too difficult ; we just

3. Since decision-makers are then coordinated to perform TSPA, we could have performed CPA instead of TSPA ; but it would result in almost the same performance as CPA. We preferred to adopt the same protocol as the one adopted for CPA ; hence comparison between CPA and DPA is fairer.

have to add some constraints during the updating step. Nevertheless, we have to be sure that these conditions will not do that DPA is blocked in a suboptimal state. Likewise efficient monitoring of non-convergence (see end of Section 6.4.4) could lower the frequency of non-convergent scenarios. On the other hand, Figure 6.12b illustrates the average power budget computed by each algorithm, first before any call to TSPA and second after the call of TSPA and admission control process. The initial power budget is not really a fair metric to compare all algorithms. Indeed NPA is greatly advantaged since 30% of its worst communication contexts are not taken into account because they lead to negative power assignment. Likewise, DPA does not take into account the 6% of contexts that are not feasible, either because of non-convergence or because of failure at admission control process. These regimes do not comply with our problem (6.9) and hence they have not to be counted. Final power budget is a fairer metric of comparison. Nevertheless, this metric should be considered jointly with the percentage of failed contexts shown on Figure 6.12a (*Error after TSPA*). CPA remains the best algorithm but both DPA algorithms come just after. DPA algorithms require in average a power budget 14% higher than the power budget of CPA. However, gains of 46% and 66% are met with DPA in comparison to respectively NPA and TSPA (52% and 71% with CPA). Hence DPA algorithms perform quite well in comparison to other algorithms.

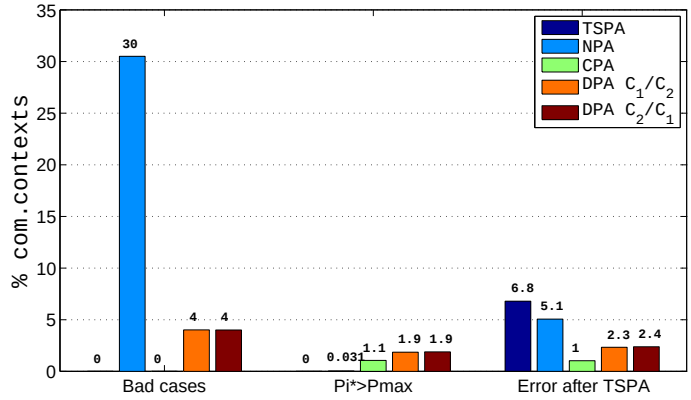

(a) Frequency and causes of failures

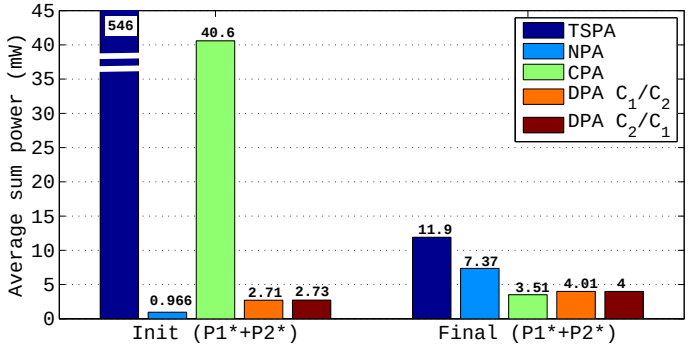

(b) Assigned power budget

FIGURE 6.12 – Comparison of causes of failure and power assignments for CPA, DPA $\mathscr{C}_1/\mathscr{C}_2$, DPA $\mathscr{C}_2/\mathscr{C}_1$, NPA and TSPA.

Finally, we extend the results of Figure 5.15 to DPA algorithms. Figure 6.13 shows which

pair $\mathscr{C}_i$ - or femtocell FC_i since we considered a femtocells network - is responsible for the failure of the algorithm. Two causes of failures are considered ; first the non-convergence and second an excessive power assignment during the iterative process. Obviously the repartition of failed contexts is the same for both pairs, when we consider non-convergent scenarios. The convergence is met when both pairs have reached a balanced state. Admission control process is performed with our simulations once both pairs have updated their transmit power. If at least one pair has assigned an excessive power, then DPA process ends. Hence it is conceivable that both pairs have simultaneously assigned an excessive transmit power. Nevertheless, both pairs seem decorrelated regarding this event.

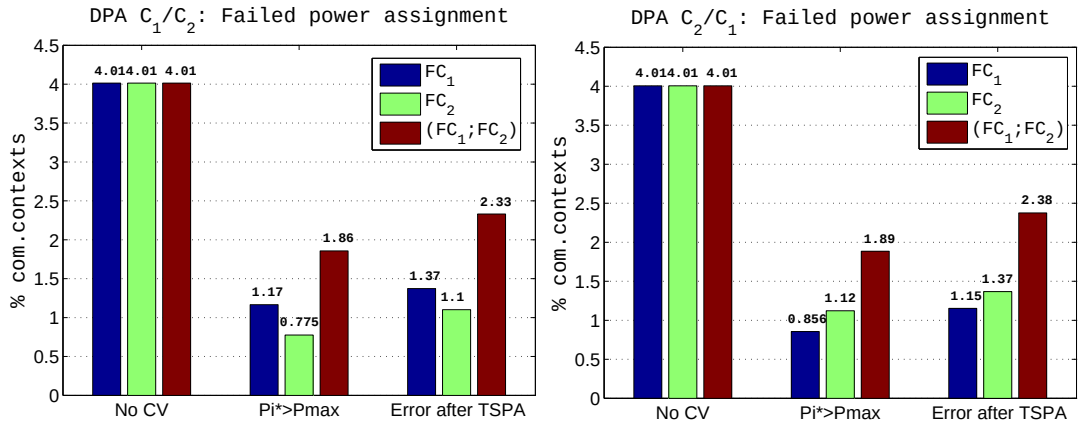

FIGURE 6.13 – Which femtocell is responsible for failed power assignments ?

Just to conclude this section, we add a last remark concerning Figure 6.12b. We showed that DPA algorithm requires in average a power budget 14% higher than the power budget of CPA. We could improve the power budget of DPA by calling CPA instead of TSPA when DPA ends suddenly because of a failure. In this case we would expect to meet exactly the same results since when DPA converges, the solution is exactly the same as the solution computed by CPA. This last remark is not totally accurate. When the network encounters a context which is characterized by three simultaneous attractors, CPA will select among all candidates the optimal solution in line with problem (5.9). However, DPA cannot perform such a selection because decision-makers lack knowledge. The elected solution will then only depend on the initial vector $\underline{\Gamma}^0$; this solution may differ from the one computed by CPA. Therefore, even if DPA would call CPA when it fails, it could exist slight differences at the end between results of CPA and those of DPA.

6.5 DPA Generalization to Multi-Source Multi-Destination Cases

This part has already been addressed in the previous chapter, at Section 5.5. We would like to generalize the two-user case to the generic model with n sources, p destinations and N_{SC} frequency bands. Nevertheless, this problem will be considered later in Chapter 7 as future work.First, it suits to begin with the n-user case ($p = n$), there are hence n concurrent 'source-destination' pairs. The general form of the interference matrix has been introduced in Section 5.5.2. This form can be reused for DPA, provided that decision-maker DM_i can only access to the i^{th} row of the matrix. We have indeed to respect the

assumptions of partial knowledge at DM_i. Hence the distributed criterion of Section 6.3.4 is always applicable.

A new matrix formulation is given for DPA, in line with the distributed criterion. Let us consider the matrix $\underline{\mathbf{F}}$ of interference, as defined in (5.33) at Section 5.5.2. First of all, the reader must be conscious that this matrix $\underline{\mathbf{F}}$ is derived with respect to the classification of in-band interference made by each decision-maker at each iteration. Actually, DM_i computes at each iteration the row i of matrix $\underline{\mathbf{F}}$. Therefore, $\underline{\mathbf{F}}$ is likely to change at each iteration p; thus we should rather consider the matrix sequence $\{\underline{\mathbf{F}}^{(p)}\}_p$, where p is put between brackets so as not to confuse it with matrix power. Based on this slight modification, DPA process at iteration p can be expressed with help of (5.34) as

$$\underline{\Gamma}^{p+1} = \underline{\mathbf{F}}^{(p)} \cdot \underline{\Gamma}^{p} + \underline{C}^{p}. \tag{6.25}$$

Let us note that this matrix formulation does not exactly comply with how our DPA process is carried out. One iteration p of DPA process actually involves n sub-steps (see Section 6.4.2); at sub-step i of iteration p the pair $\mathscr{C}_i$ updates its SNR γ_i^p into γ_i^{p+1}. Consequently, the global SNR vector $\underline{\Gamma}^p$ is modified at each sub-step of iteration p, whereas the matrix formulation (6.25) assumes $\underline{\Gamma}^p$ remains unchanged while the n pairs compute their new SNR value $\{\gamma_i^{p+1}\}_i$. Nevertheless, this last section does not claim to be rigorous; we just seek to provide an alternative overview of distributed power allocation using the matrix formulation. For sake of clarity, we will assume in the remainder that (6.25) correctly describes DPA iterative process.

Before going further in our development, another assumption is made for sake of clarity. As mentioned at the end of Section 6.4.4, DPA iterative process passes through a transitional and unstable period before $\{\underline{\Gamma}^p\}_p$ meets the final and optimal sector $\Omega_{O_1^*,O_2^*}$ where convergence is almost ensured. During this phase of transition, since decision-makers switch from one regime to another between two consecutive iterations, the interference matrix keeps changing. However, once $\Omega_{O_1^*,O_2^*}$ is met, $\{\underline{\Gamma}^p\}_p$ cannot leave $\Omega_{O_1^*,O_2^*}$ any more if convergence is ensured; hence interference matrix remains constant once for all. Thus, we assume in the remainder that the transitional phase is over ($\forall p > P^*$) and that sector $\Omega_{O_1^*,O_2^*}$ has been met. Therefore the interference matrix is not subject to change any more; we then remove its exponent (p). The whole reasoning exposed above also applies to the constant vector $\underline{C}^p$ which does not change any more once the phase of transition is over.

Recursion can be used as follows :

$$\begin{array}{ll} & \forall p > P^*, \\ & \underline{\Gamma}^{p+1} = \underline{\mathbf{F}} \cdot \underline{\Gamma}^{p} + \underline{C} \\ \Leftrightarrow & \underline{\Gamma}^{p+1} = \underline{\mathbf{F}} \cdot (\underline{\mathbf{F}} \cdot \underline{\Gamma}^{p-1} + \underline{C}) + \underline{C} \\ \Leftrightarrow & \underline{\Gamma}^{p+1} = \underline{\mathbf{F}} \cdot (\underline{\mathbf{F}} \cdot (\ldots) + \underline{C}) + \underline{C} \\ \Leftrightarrow & \underline{\Gamma}^{p+1} = \underline{\mathbf{F}}^{p+1-P^*} \cdot \underline{\Gamma}^{P^*} + \left(\sum_{k=O}^{p-P^*} \underline{\mathbf{F}}^k\right) \cdot \underline{C}. \end{array} \tag{6.26}$$

When p tends to infinity, $\underline{\Gamma}^{p+1}$ tends to $\underline{\Gamma}^*$ if the distributed criterion holds (see Section 6.3.4), *i.e.,* if the spectral radius $\rho(\underline{\mathbf{F}})$ is strictly inside the unit circle. In other words,

$$\begin{array}{lll} \rho(\underline{\mathbf{F}}) < 1 & \Rightarrow & \lim_{p\to\infty} \underline{\mathbf{F}}^{p+1-P^*} \cdot \underline{\Gamma}^{P^*} = \underline{0} \\ & \Rightarrow & \lim_{p\to\infty} \underline{\Gamma}^{p+1} = \underline{0} + \left(\sum_{k=O}^{\infty} \underline{\mathbf{F}}^k\right) \cdot \underline{C} \\ & \Rightarrow & \lim_{p\to\infty} \underline{\Gamma}^{p+1} = \underline{\Gamma}^*. \end{array} \tag{6.27}$$

Since $\rho(\underline{\mathbf{F}}) < 1$ holds, the infinite summation on powers of $\underline{\mathbf{F}}$ converges and hence (6.27) can be reformulated as

$$\rho(\underline{\mathbf{F}}) < 1 \quad \Rightarrow \quad \underline{\Gamma}^* = (\underline{\mathbf{I_n}} - \underline{\mathbf{F}})^{-1} \cdot \underline{C}. \tag{6.28}$$

DPA iterative process can then meet the same optimal solution of as the one derived for CPA in (5.35). This last results proves there is no dependency to initial conditions, as claimed by the Banach Theorem. However, this is in contradiction with our remarks of Section 6.4.5. The reason is quite simple : we can have simultaneously more than one feasible solution. We see previously that the Banach Theorem can just be applied once the optimal final sector $\Omega_{O_1^*,O_2^*}$ is achieved. Nevertheless, when there are several optimal sectors, initial SNR vector $\underline{\Gamma}^0$ will set within which optimal sector DPA iterative process will converge.

To conclude, convergence of DPA iterative process seems quite easy to characterize with this new matrix formulation. However we recall that this formulation has been greatly simplified. First by neglecting the transitional phase, which is very hard to characterize. Second by considering a close but inaccurate matrix formulation of our DPA iterative process, which does not exactly translates what really happens during an iteration of the algorithm. An advanced but tedious formulation could be adopted.

6.6 Conclusions

In-band interference can seriously limit performance in wireless communication systems where close devices have to share a same resource block. To guarantee a high satisfaction rate to their customers, even when they are strongly interfered, network operators must perform effective interference mitigation techniques. Chapter 4 addresses a three-regime classifier of in-band interference which can be used by a destination to select the most suited way to handle its perceived interfering signals. The selection of the optimal interference technique is driven by the momentary values of system an channel parameters. Basically, the classifier lets face in-band interference and significantly lower its reductive effects, even when destination is strongly interfered.

In Chapter 5, a centralized power allocation (CPA) algorithm is designed for rate-constrained interference-limited wireless communication networks. CPA exploits our classifier to compute a power vector $\underline{P}^*$ which simultaneously complies with rate constraints of all sources and destinations while minimizing all transmit power. Consequently, CPA succeeds first in avoiding energy waste, and second in ensuring reliable transmissions from any source to its destination, whatever the communication context may be. To this end, the existence of an omniscient network controller (NC) is required. First, NC is provided with CSI knowledge and values of system parameters. Then, NC computes alone the power vector $\underline{P}^*$ and the corresponding optimal interference mitigation techniques. At last, NC notifies sources of their optimal transmit power and destinations of how they should process their in-band interfering signals.

Network operators can be motivated by non-centralized algorithms. Reasons are manyfold. First, in dense systems with highly variable topology, it seems inconceivable to obtain full reliable CSI knowledge in a single location. It would require excessive signalling and overhead which would waste resources and reduce performance. Second, accuracy and

reliability of channel estimation is a crucial element, which can be hard to meet for remote users. Third, NC could become the system bottleneck since it is alone responsible for all computational burden. Lastly, monitoring of network to provide NC with accurate parameters wastes energy. Consequently, the use of a NC may be not possible or not desired.

In this chapter, a distributed and autonomous alternative to CPA is proposed, namely DPA. As CPA, DPA exploits the three-regime classifier of Chapter 4. However, since DPA seeks an autonomous approach, it is not possible to compute to the classification of all destination in order to superimpose them. Indeed, a destination cannot access to values of channel parameters related to its neighbour destinations. Consequently, an iterative process is introduced ; this process aims at converging to the same solution $\underline{P}^*$ as the one computed by CPA.

DPA consists in a 'ping-pong' mechanism where each transmitter updates in turns its transmit power, contingent on the optimal output of the interference classifier. To this end, the interference classifier is supplied in inputs by the receiver with its momentary sensed interference. Each power adjustment of a transmitter affects all neighbour receivers whose transmitter reacts by updating in turns its transmit power. This 'ping-pong' process is repeated until convergence to $\underline{P}^*$ is met.

A tedious mathematical reasoning based on iterated function sequences proves that DPA mostly converges to $\underline{P}^*$. Elements on convergence have been derived to characterize when convergence is ensured and how fast it converges. Specific criteria are thus proposed to identify converging or non-converging scenarios of communication. Nevertheless, these criteria cannot be addressed with restricted CSI knowledge. Therefore, transmitters and receivers cannot forecast if their process will converge or not, and in that event, how fast it will converge.

Numerical simulations are performed to compare DPA to CPA and two other power algorithms which deal interference with respectively a noisy strategy and a time-sharing technique. Results show that the proposed DPA algorithm mostly converges to the same solution as CPA. Hence, target rates are ensured while powers are minimized. Nevertheless, the unpredictable scenarios where DPA does not converge slightly degrade performance of DPA in comparison to this of CPA.

Chapter 7

Conclusions and Future Work

In this dissertation we have focused on the interference issue in wireless communication systems. It occurs when a same spectrum is shared by some concurrent network devices in a close geographical area. Interference may drastically limit transmission performance and make impossible for the destination to decode reliably the received signal. These limitations are even more pronounced when in-band interference is unpredictable. To address to in-band interference mitigation, various radio resource management (RRM) techniques have been proposed, investigated and evaluated. A two-fold gain results from this thesis. First, some of our goals have been met with besides interesting scientific improvements. Second, other issues have remained unsolved or have lead to identify new research hints for future work.

7.1 Conclusions

First of all, some preliminary knowledge about wireless communication, perturbations of radio propagation and interference management has been proposed to introduce the framework of the thesis. In Chapter 3, cooperative transmissions have been considered and investigated as a solution to increase the reliability of transmissions, especially for cell-edge users which are doubly penalized in cellular networks : first, they are farer away from their base stations and therefore experience a higher path loss attenuation ; second, they are closer to neighbour cells and perceive hence a higher inter-cell interference. To this end, efficient resource allocation modes have been specifically designed for half-duplex per chunk relays, as well as an adaptive mechanism which selects among a set of modes the one maximizing an objective function for a cluster of cells. Simulations results have proved that our modes permit to notably increase link reliability without requiring excessive power budget. Moreover, the area in cells where cooperative transmissions improve robustness has been considerably extended. Nevertheless, our modes have not improved as much as hoped transmission performance for cell-edge users.

Then, in Chapter 4, a three-regime interference classifier has been developed to determine in which of the three considered regimes the in-band interference momentarily

perceived by a destination could be classified. The conception of this classifier bas been motivated by several observations. First, interference has a specific structure which can be possibly exploited to mitigate its restrictive effects on receivers. Second, a given interference mitigation technique cannot perform well for all communication contexts. Third, the perceived level of interference is not uniform and varies with time, frequency and space. Consequently, this classifier determines, contingent on the momentarily perceived power of interference, which is the technique the receiver should perform to efficiently deal with its interfering signals. Furthermore, the classifier has been proved to be outperformed by previous techniques of information theory. Nevertheless, these techniques cannot yet be implemented in practice because of drastic assumptions, contrary to our classifier which performs quite well.

Such a classifier has been lastly exploited in Chapters 5 and 6 to propose respectively centralized and distributed power allocation algorithms. Both algorithms aim at minimizing the transmit power vector while ensuring that all rate constraints are jointly met. Even if centralized approaches compute easily and quickly an optimal solution to a given problem of optimization, whereas distributed approaches are sometimes suboptimal and need several iterations to meet a balanced state, centralized approaches can be not desired because of the CSI knowledge they request. With some tedious reasoning, we have managed to prove how the interference classifier could be exploited to solve our objective function and to derive the optimal power vector, whatever the communication context might be. Centralized and distributed approaches have been lastly compared to baseline power allocation algorithms ; numerical results have corroborated that our algorithms notably outperformed baseline algorithms in terms of power assignment and user rejection. However, the distributed approach might not converge in some scenarios which have been identified. Unfortunately, transmitters and receivers cannot forecast if their sensed scenarios will converge or not.

7.2 Future Work and Hints for Future Research

In this section we outline our major proposed axes for future investigation, along with specific open problems. We are especially interested in femtocells contexts, with algorithms for interference mitigation, since such networks are an emergent topic for the scientific community and challenging research can be carried out in the direction of interference management. However, other hints for future research are also addressed.

Further Improvements for Cooperative Communications

Even if simulation results presented in Chapter 3 were conclusive and valuable, it remains that we do not fulfil all the goals we targeted for cooperative wireless communications systems. As attested by Figures 3.17 and 3.18, we indeed do not manage to make effective cooperative transmissions for cell-edge users : cooperation is not planned in sector S_1 when d_1 is located at cell-edge. Consequently, future work could try to fulfil this goal, for instance by considering power allocation in addition to our RRM modes.

Another hints of research has been suggested with Section 3.5 where we proposed to generalize our adaptive resource allocation process (ARAP) to more practical systems. This section brings some conjectures or heuristics for future work but no numerical simulations have been done to corroborate or not our reasoning. We could consider multi-user systems

with several active relays per sector while going into details with our results on relay deployment. Thus we could add a scheduling layer to our work which would be in charge of determining for each active user if cooperative transmissions should be planned or not, and if the need arises, which relay should be used.

At last, a challenging hint of research would be to develop a distributed approach of this work. Indeed we consider up to now that neighbour sectors were coordinated via a backhaul network. But this assumption is possibly made restrictive in some networks such as WSNs or ad-hoc networks.

DPA Algorithm in Realistic Femtocells Networks

Due to time constraints, CPA and DPA algorithms were only evaluated in a system of two femtocells (see Figure 5.11). Nevertheless, even if both cells overlap, they do not represent a realistic interference-limited network. Performance of CPA and DPA for real femtocells deployments [26] is in progress and will be presented in a journal paper in preparation for IEEE Transactions on Wireless Communications [140].

The open issues not addressed in this dissertation are tedious. We considered up to now that all devices are assigned to a same band. In real systems, an algorithm of sub-carriers allocation should be considered. Optimal solution would consist in an algorithm which would jointly allocate power and sub-carrier. Indeed, sub-carriers are commonly assigned according to a SINR-based metric, while SINR is precisely related to the transmit power of all sources which have been scheduled on the given sub-carrier. Nevertheless, this double allocation of power and sub-carriers is complex ; it is an illustration of the hen and egg problem : which should come first, sub-carrier allocation or power allocation ? Therefore, [150] proposes an heuristic where both steps are separated : first sub-carriers are allocated contingent to an expected value of SINR (actually SINR is computed by assuming equal transmit power for all transmitters), then power is allocated based on the previous assignment of sub-carriers.

In [150] the authors treat interference as an additional source of noise. A distributed criterion is derived in this case to determine if algorithm will converge or not. The criterion is based on the interference matrix. With our DPA algorithm, the interference matrix depends on how the momentary communication is classified ; it may change at each iteration. Consequently, it is not possible to derive a fixed criterion as in [150] and we cannot applied these results straightforwardly. However, some hints have been already developed.

To conclude with this research topic, it would be very valuable to characterize more precisely the convergence of our DPA algorithm. Up to now, we can determine if convergence will happen or not, and if the need arises, if DPA will converge quickly or not. To achieve such results, we assume there is an omniscient genie above the system, as it is assumed with CPA. This genie is not involved in the computation of power vector ; it is a silent observer which does not provide any information to sources and destinations.

However, this genie is interesting for theoretical results but is not desired in practice. We have to derive heuristics to be able to forecast if the 'ping-pong' process will converge and how fast it will converge. The main difficulty here is that such information necessarily requires knowledge of some channel parameters which cannot be accessed if cells are autonomous. Nevertheless, some numerical simulations with intuitive reasoning and hard thresholds have shown interesting results.

Maximum Matching for Bipartite Graphs

This section certainly addresses the most promising hint for future research. As the previous section, we aim at allocating optimally power and sub-carriers to many users in a rate-constrained and interference-limited network. Optimality here must be defined by an objective function which can be for instance power minimization or sum-rate maximization. To meet this goal, we propose to assign each sub-carrier to a small cluster of 'source-transmitter' pairs (2 or 3 ?) and then to perform CPA independently on each sub-carrier (*i.e.,* cluster). By this way, resources are orthogonally shared and there is so no interference between clusters since they access disjoint sub-carriers. The problem consists in allocating optimally the sub-carriers to the judicious cluster of pairs.

This can be translated into a problem of matching in a bipartite graph. We indeed seek to optimally match a pool of sub-carriers with a cluster of pairs, subject to individual and system QoS constraints and to the objective function. Elements of graph theory [51, 52] can be used, especially algorithms of maximum matching for (bipartite) graphs [168].

The idea here is near to the famous 'divide and conquer' concept. By making independent each cluster, we consider numerous smaller and easier problems instead of a big and complex one. A pending conference paper on this topic is in pending preparation [169].

Private and Common Messages

This last topic proposed as future work is actually motivated by the paper of Han and Kobayashi [12] where the authors propose an encoding technique which superimposes at a transmitter a common message intended to all receivers and a private message only intended to the corresponding receiver. We saw in Section 4.2.4.1 that superposition coding is a promising technique for theoretical purposes but up to now, no practical encoding scheme manages to meet such a superposition. The authors just introduced the concept without giving any hints on how manage it. Consequently, a certain liberty is given.

We could for instance define a ratio β which characterize how much information is private in the whole message. The ratio β could thus be adapted on the momentary communication context. Moreover, the duality private/common message could also be extended to frequency reuse techniques. For instance, disjoint sets of sub-carriers could be assigned for transmissions of private messages, as done initially for cell-edge users, while the whole spectrum would be allocated to transmissions of common messages, as initially done for cell-centre users.

Power control could be also added by defining specific masks of power, as done in frequency reuse techniques. A binary power control ('On-Off') could set power of private messages while water-filling power allocation would be used for common messages. There are indeed numerous possibilities to deal with this private/common duality. Nevertheless, the original idea of Han and Kobayashi is an open issue for nearly thirty years, so it does not expect to find easily the solution, unless reconsider the problem by keeping slightly away from it, as we have suggested above.

Appendix A

Complements on Chapter 4: Outage Probability

A.1 Preliminary on Outage Probability

A.1.1 Probability Distributions

Throughout this dissertation, the adopted system model assumes Rayleigh fading. The density probability function of Rayleigh distribution is given by

$$f(x,\sigma) = \frac{x}{\sigma^2}\exp(-\frac{x^2}{2\sigma^2}), \quad \forall x \in \mathbb{R}^+, \tag{A.1}$$

with σ the parameter of the distribution and $\sigma\sqrt{\frac{\pi}{2}}$ the mean of such a distribution.

In other words, if the coefficient $f_{i,j}$ states for the fading gain of the link from the source s_i to the destination d_j, then $f_{i,j}$ is a random variable with Rayleigh distribution. Let us recall that in this dissertation the coefficient $g_{i,j}$ denotes the global channel gain between s_i and d_j, including fading, shadowing and path loss attenuation due to distance.

Any transmission with Rayleigh fading can be represented by a complex Gaussian random variable, as follows:

$$F_{i,j} = X_{i,j} + jY_{i,j}, \tag{A.2}$$

where $X_{i,j}$ and $Y_{i,j}$ are real and independent zero-centric Gaussian random variables:

$$X_{i,j} \hookrightarrow \mathcal{N}(0,\sigma^2) \quad \text{and} \quad Y_{i,j} \hookrightarrow \mathcal{N}(0,\sigma^2). \tag{A.3}$$

Their probability density is

$$f(x,\sigma) = \frac{1}{\sqrt{2\pi}\sigma}\exp(-\frac{x^2}{2\sigma^2}), \quad \forall x \in \mathbb{R}. \tag{A.4}$$

The magnitude $|F_{i,j}| = \sqrt{X_{i,j}^2 + Y_{i,j}^2}$ is nothing else that the fading gain $f_{i,j}$. Hence, the Rayleigh fading is the square root of the sum of two squared real and independent Gaussian random variables [2, 49].

However, the squared magnitude $|F_{i,j}|^2 = {f_{i,j}}^2$ is commonly used to compute CQI metrics such as SNR, INR or SINR. We will show below that ${f_{i,j}}^2$ is exponentially distributed, *i.e.*, ${f_{i,j}}^2 \hookrightarrow \mathscr{E}(\lambda)$, with density

$$f(x,\lambda) = \lambda \cdot \exp(-\lambda x), \quad \forall x \in \mathbb{R}^+, \tag{A.5}$$

where λ and $\frac{1}{\lambda}$ are respectively the parameter and the mean of the distribution.

Indeed, ${f_{i,j}}^2 = X_{i,j}^2 + Y_{i,j}^2$ is the sum of two squared real and independent zero-centric Gaussian random variables with the same variance σ^2. Such a random variable is known as following a $\chi - 2$ (Khi-2) distribution with $k = 2$ degrees of freedom and σ as parameter [2, 49].

Let us define the random variable

$$Z = \sum_{i=0}^{k} X_i^2, \tag{A.6}$$

where all $X_i^2 \hookrightarrow \mathscr{N}(0,\sigma^2)$ are independent Gaussian random variables. By definition, Z follows a $\chi - 2$ distribution with k degrees of freedom. Its probability density is given by:

$$f_Z(x,k,\sigma) = \frac{1}{\sigma^k 2^{\frac{k}{2}} \Gamma(\frac{k}{2})} x^{\frac{k}{2}-1} \exp(-\frac{x}{2\sigma^2}), \tag{A.7}$$

where $\Gamma(k)$ is the well-known Gamma function

$$\Gamma \ : \ z \ \mapsto \int_0^{+\infty} t^{z-1} \exp(-t) dt. \tag{A.8}$$

Especially, the Gamma function takes a convenient form with natural inputs:

$$\forall n \in \mathbb{N}, \quad \Gamma(n+1) = n!. \tag{A.9}$$

The mean of the random variable Z is equal to $k\sigma^2$. Consequently, with $k = 2$ degrees of freedom, the density of the distribution becomes

$$f_Z(x,2,\sigma) = \frac{1}{2\sigma^2} \exp(-\frac{x}{2\sigma^2}), \quad \forall x \in \mathbb{R}^+. \tag{A.10}$$

By setting $\lambda = \frac{1}{2\sigma^2}$, the fading squared magnitude ${f_{i,j}}^2$ is indeed exponentially distributed.

A.1.2 Sum of Random Variables

Let us define the random variable Z such as

$$Z = \sum_{i=0}^{k} W_i^2, \tag{A.11}$$

where $W_i^2 \hookrightarrow \mathscr{E}(\lambda)$ are independent and identically distributed exponential random variables. The distribution of the random variable Z is known as being the Erlang distribution [49]. Indeed, Erlang distribution is the distribution of k independent and identically exponentially distributed random variables $\mathscr{E}(\lambda)$. Its density function is given by

$$f_Z(x,k,\lambda) = \frac{\lambda^k}{\Gamma(k)} x^{k-1} \exp(-\lambda x), \quad \forall x \in \mathbb{R}^+. \tag{A.12}$$

Let us also recall the scaled rule on probability density function. If a is a non-null real, then the density f_Y of the random variable $Y = aX$ can be derived from the density f_X as follows:

$$f_Y(x) = \frac{1}{a} f_X(\frac{x}{a}). \tag{A.13}$$

A.1.3 Outage Probability

We recall that the 'outage' event states that the capacity of the channel cannot bear the targeted transmission rate R. Consequently, the source cannot reliably communicate with its destination, whatever the coding scheme may be. For a given rate R [bit/s/Hz], the probability that an outage event occurs is often used as a metric to characterize the performance of transmission:

$$P_{out} = \mathbb{P}\{C(\underline{\mathbf{H}}) \leq R\}, \tag{A.14}$$

where C is the channel capacity and $\underline{\mathbf{H}}$ is the channel matrix. Likewise, the largest rate of reliable communication at a certain outage probability is called the 'outage capacity':

$$C_{out} = f(P_{out}) \quad | \quad \mathbb{P}\{C(\underline{\mathbf{H}}) \leq C_{out}\} = P_{out}. \tag{A.15}$$

All elements have now been introduced to compute the outage probability of interference limited systems: whatever the interference handling strategy may be. To derive the outage probability, we use the generic expression of the channel capacity

$$C(\underline{\mathbf{H}}) = \log_2(1 + \text{SINR}), \tag{A.16}$$

and then we adopt tools recalled in Sections A.1.1 and A.1.2 to compute

$$P_{out} = \mathbb{P}\{\text{SINR} \leq 2^R - 1\}. \tag{A.17}$$

A.2 Interference Classification Based Outage Probability

In this Section we derive the expression of outage probability for each regime of interference. To derive these expressions, we assume that interference is handled with the strategies developed in Section 4.3. Outage expression for the *time sharing* strategy is also computed. All these computations are just materials for a more generic case. A further study should be done to confirm all these results. The reader can give a look at Section 4.4 and more precisely at Table 4.2.

We assume that each fading gain is exponentially distributed: ${f_{i,j}}^2 \hookrightarrow \mathscr{E}(\lambda_{i,j})$.

A.2.1 Noisy Strategy

We consider hereafter a system with n 'source-destination' pairs where the *noisy* strategy is applied to deal with interference.

$$\begin{aligned} P_{out-\text{user}_i} &= \mathbb{P}\{\frac{a_{i,i}{f_{i,i}}^2}{N_0 + \sum\limits_{\substack{1 \leq j \leq n \\ j \neq i}} a_{j,i}{f_{j,i}}^2} \leq A_i\} \\ &= 1 - \exp(-A_i \frac{N_0 \lambda_{i,i}}{a_{i,i}}) \cdot \prod_{\substack{1 \leq j \leq n \\ j \neq i}} \frac{a_{i,i}\lambda_{j,i}}{a_{i,i}\lambda_{j,i} + A_i a_{j,i} \lambda_{i,i}}, \end{aligned} \tag{A.18}$$

where $A_i = 2^{R_i} - 1$ and $a_{j,i} = \frac{P_j}{L_{j,i}}$, with $L_{j,i}$ the path loss attenuation between s_j and d_i.

A.2.2 Joint Decoding Strategy

In this case, n 'source-destination' pairs share the common communication resource and the intended destination adopts the *joint decoding* strategy to decode its wished message.

$$\begin{aligned} P_{out-\text{user}_i} &= \mathbb{P}\{\frac{\sum\limits_{1\leq j\leq n} a_{j,i}{f_{j,i}}^2}{N_0} \leq A\} \\ &= 1 - \sum_{1\leq j\leq n} \left[\exp(-A\frac{N_0\lambda_{j,i}}{a_{j,i}}) \cdot \prod_{\substack{1\leq k\leq n \\ k\neq j}} \frac{a_{j,i}\lambda_{k,i}}{a_{j,i}\lambda_{k,i} - a_{k,i}\lambda_{j,i}} \right], \end{aligned} \tag{A.19}$$

where $A = 2^{(\sum\limits_{j=1}^{n} R_j)} - 1$.

A.2.3 SIC-Based Strategy

With the *SIC-based* approach all interfering signals are cancelled from the received signal; hence the destination has lastly to decode an interference-free signal to recover its wished message. We do not consider here all conditions that must be verified to ensure that destination can decode all interfering signals before recovering

$$\begin{aligned} P_{out-\text{user}_i} &= \mathbb{P}\{\frac{a_{i,i}{f_{i,i}}^2}{N_0} \leq A_i\} \\ &= 1 - \exp(-A_i\frac{N_0\lambda_{i,i}}{a_{i,i}}, \end{aligned} \tag{A.20}$$

where $A_i = 2^{R_i} - 1$.

This is the outage probability of the point-to-point channel which does not suffer from interference.

A.2.4 Time-Sharing Strategy

With the *time sharing* strategy each time slot is divided into $\frac{1}{n}$ parts which are exclusively assigned for orthogonalizing each transmission. Such an approach does not suffer from interference but is poorly spectral efficient. Let us point out the factor n in the rate constraint in expression below.

$$\begin{aligned} P_{out-\text{user}_i} &= \mathbb{P}\{\frac{a_{i,i}{f_{i,i}}^2}{N_0} \leq 2^{n\cdot R_i} - 1\} \\ &= 1 - \exp(-(2^{n\cdot R_i} - 1)\frac{N_0\lambda_{i,i}}{a_{i,i}}). \end{aligned} \tag{A.21}$$

A.2.5 All-in-One Strategy

We conclude this chapter by deriving the generic case where a given destination is affected by n neighbour interferes. Among the n perceived interfering signals, p, q, r and $(n-p-q-r)$ signals are handled respectively with the *noisy*, the *joint decoding*, the *time sharing* and the *SIC-based* approaches ($p+q+r \leq n$, $p \geq 0$, $q \geq 0$, $r \geq 0$). We assume that signals are sorted according to the strategy with which they are handled; the source s_0 and the destination d_0 constitute the pair of interest.

First we derive the outage event:

$$\frac{1}{r}\log(1+\frac{a_{0,0}{f_{0,0}}^2+\sum\limits_{1\leq j\leq q}a_{j,0}{f_{j,0}}^2}{N_0+\sum\limits_{q+1\leq i\leq q+p}a_{i,0}{f_{i,0}}^2})\leq R_0+\sum_{1\leq j\leq q}R_j. \tag{A.22}$$

The probability of this outage event translates into:

$$\begin{aligned} P_{out-\text{user}_0} &= \mathbb{P}\{\frac{\sum\limits_{0\leq j\leq q}a_{j,0}{f_{j,0}}^2}{N_0+\sum\limits_{q+1\leq i\leq q+p}a_{i,0}{f_{i,0}}^2}\leq K\} \\ &= 1-\sum_{j=0}^{q}\left[\exp(-K\tfrac{N_0\lambda_{j,0}}{a_{j,0}})\cdot\prod_{\substack{k=0\\k\neq j}}^{q}\tfrac{a_{j,0}\lambda_{k,0}}{a_{j,0}\lambda_{k,0}-a_{k,0}\lambda_{j,0}}\cdot\prod_{i=q+1}^{q+p}\tfrac{a_{j,0}\lambda_{i,0}}{a_{j,0}\lambda_{i,0}+K\cdot a_{i,0}\lambda_{j,0}}\right], \end{aligned} \tag{A.23}$$

with $K=2^{r\cdot(\sum\limits_{j=0}^{q}R_j)}-1$

Bibliography

[1] Y. Xiang, J. Luo, and C. Hartmann, "Inter-cell interference mitigation through flexible resource reuse in OFDMA based communication networks", in *European Wireless, EW'07*, 2007.

[2] D. Tse and P. Viswanath. *Fundamentals of wireless communication.* Cambridge University Press, 2005.

[3] K. Gomadam, V. Cadambe, and S. Jafar, "Approaching the capacity of wireless networks through distributed interference alignment", *submitted to IEEE Transactions on Information Theory, Preprint arXiv:0803.3816*, 2008.

[4] S. Perlaza, M. Debbah, S. Lasaulce, and J. Chaufray, "Opportunistic interference alignment in MIMO interference channels", in *IEEE International Symposium on Personal, Indoor and Mobile Radio Communications, PIMRC'08*, 2008.

[5] S. Mohajer, S. Diggavi, C. Fragouli, and D. Tse, "Transmission techniques for relay-interference networks", in *Allerton Conference on Communication, Control and Computing, Allerton'08*, pp. 467–474, 2008.

[6] S. Boyd and L. Vandenberghe. *Convex optimization.* Cambridge University Press, 2004.

[7] T. Cover and J. Thomas. *Elements of information theory, 2nd Edition.* Wiley, 2006.

[8] E. Strinati, S. Yang, and J.-C. Belfiore, "Adaptive modulation and coding for hybrid cooperative networks", in *IEEE International Conference on Communications, ICC'07*, pp. 4191–4195, 2007.

[9] D. Gesbert, S. Kiani, and A. Gjendemsjø, "Adaptation, coordination, and distributed resource allocation in interference-limited wireless networks", *Proceedings of the IEEE*, vol. 95, no. 12, pp. 2393–2409, December 2007.

[10] Z. Yong, L. Jun, X. Youyun, and C. Yueming, "An adaptive non-orthogonal cooperation scheme based on channel quality information", in *International Conference on Wireless Communications, Networking and Mobile Computing, WiCom'07*, pp. 988–991, 2007.

[11] ICT-215282 ROCKET project "Reconfigurable OFDMA-based Cooperative networKs Enabled by agile specTrum use", 2008–2009. [Online]. URL: http://www.ict-rocket.eu/.

[12] T. Han and K. Kobayashi, "A new achievable rate region for the interference channel", *IEEE Transactions on Information Theory*, vol. 27, no. 1, pp. 49–60, January 1981.

[13] R. Etkin, D. Tse, and H. Wang, "Gaussian interference channel capacity to within one bit", *IEEE Transactions on Information Theory*, vol. 54, no. 12, pp. 5534–5562, December 2008.

[14] ICT-247733 EARTH project "Energy Aware Radio and neTwork tecHnologies", 2010–2012. [Online]. URL: https://www.ict-earth.eu/.

[15] C. Abgrall, E. Calvanese Strinati, and J.-C. Belfiore, "Inter-cell interference mitigation allocation for half-duplex relays based cooperation", in *IFIP Wireless Days, WD'09*, 2009.

[16] C. Abgrall, E. Calvanese Strinati, and J.-C. Belfiore, "Multi-cell interference aware resource allocation for half-duplex relay based cooperation", in *IEEE Vehicular Technology Conference, VTC'10 Spring*, 2010.

[17] C. Abgrall and E. Calvanese Strinati, "Méthode d'allocation de ressources de transmission dans un réseau cellulaire de type coopératif", Patent, 2009.

[18] C. Abgrall and E. Calvanese Strinati, "Classification d'interférences", Patent, 2010.

[19] C. Abgrall, E. Calvanese Strinati, and J.-C. Belfiore, "Centralized power allocation for interference limited networks", in *IEEE Vehicular Technology Conference, VTC'10 Fall*, 2010.

[20] C. Abgrall and E. Calvanese Strinati, "Allocation de puissance inter-cell centralisée", Patent, 2010.

[21] C. Abgrall, E. Calvanese Strinati, and J.-C. Belfiore, "Distributed power allocation for interference limited networks", in *IEEE International Symposium on Personal, Indoor and Mobile Radio Communications, PIMRC'10*, 2010.

[22] C. Abgrall and E. Calvanese Strinati, "Méthode distribuée pour l'allocation de puissance entre stations de base dans un réseau cellulaire", Patent, 2010.

[23] R. Berry and E. Yeh, "Cross-layer wireless resource allocation: Fundamental performance limits", *IEEE Signal Processing Magazine*, vol. 21, no. 5, pp. 59–68, September 2004.

[24] D. MacKay. *Information theory, inference, and learning algorithms*. Cambridge University Press, 2003.

[25] O. Rioul. *Théorie de l'information et du codage*. Lavoisier, 2007.

[26] ICT-248523 BeFEMTO project "Broadband Evolved FEMTO networks", 2010–2012. [Online]. URL: http://www.ict-befemto.eu/.

[27] Femto Forum: a not-for-profit membership organisation founded to promote femtocell deployment worldwide, since 2007. [Online]. URL: http://www.femtoforum.org/.

[28] ICT-258512 EXALTED project "EXPanding LTE for Devices", 2010–2013. [Online]. URL: https://www.ict-exalted.eu/.

[29] C. Shannon, "A mathematical theory of communication", *Bell System Technical Journal*, vol. 27, pp. 379–423 and 623–656, July and October 1948.

[30] C. Shannon, "Two-way communication channels", in *Berkeley Symposium on Mathematical Statistics and Probability*, vol. 1, pp. 351–384, 1961.

[31] H. Sato, "Two-user communication channels", *IEEE Transactions on Information Theory*, vol. 23, no. 3, pp. 295–304, May 1977.

[32] D. Tse and S. Hanly, "Multiaccess fading channels - Part I: Polymatroid structure, optimal resource allocation and throughput capacities", *IEEE Transactions on Information Theory*, vol. 44, no. 7, pp. 2796–2815, November 1998.

[33] S. Hanly and D. Tse, "Multiaccess fading channels - Part II: Delay-limited capacities", *IEEE Transactions on Information Theory*, vol. 44, no. 7, pp. 2816–2831, November 1998.

[34] T. Cover, "Broadcast channels", *IEEE Transactions on Information Theory*, vol. 18, no. 1, pp. 2–14, January 1972.

[35] R. Gallager, "Capacity and coding for degraded broadcast channels", *Problems in the Transmission of Information*, vol. 10, no. 3, pp. 3–14, July-September 1974.

[36] T. Cover, "An achievable rate region for the broadcast channel", *IEEE Transactions on Information Theory*, vol. 21, no. 4, pp. 399–404, July 1975.

[37] S. Chang and E. Weldon, "Coding for T-user multiple-access channels", *IEEE Transactions on Information Theory*, vol. 25, no. 6, pp. 684–691, November 1979.

[38] T. Cover, A. Gamal, and M. Salehi, "Multiple access channels with arbitrarily correlated sources", *IEEE Transactions on Information Theory*, vol. 26, no. 6, pp. 648–657, November 1980.

[39] J. Thomas, "Feedback can at most double Gaussian multiple access channel capacity (Corresp.)", *IEEE Transactions on Information Theory*, vol. 33, no. 5, pp. 711–716, September 1987.

[40] B. Rimoldi and R. Urbanke, "A rate-splitting approach to the Gaussian multiple-access channel", *IEEE Transactions on Information Theory*, vol. 42, no. 2, pp. 364–375, March 1996.

[41] A. Carleial, "Interference channels", *IEEE Transactions on Information Theory*, vol. 24, no. 1, pp. 60–70, September 1978.

[42] H. Sato, "On degraded Gaussian two-user channels".

[43] H. Sato, "The capacity of the Gaussian interference channel under strong interference (Corresp.)", *IEEE Transactions on Information Theory*, vol. 27, no. 6, pp. 786–788, November 1981.

[44] M. Costa, "On the Gaussian interference channel", *IEEE Transactions on Information Theory*, vol. 31, no. 5, pp. 607–615, November 1985.

[45] V. Cadambe and S. Jafar, "Degrees of freedom of wireless X networks", in *IEEE International Symposium on Information Theory, ISIT'08*, pp. 1268–1272, 2008.

[46] V. Cadambe and S. Jafar, "Interference alignment and the degrees of freedom of wireless X networks", *IEEE Transactions on Information Theory*, vol. 55, no. 9, pp. 3893–3908, September 2009.

[47] S. Golomb, "The limiting behavior of the Z-channel (Corresp.)", *IEEE Transactions on Information Theory*, vol. 26, no. 3, pp. 372–372, May 1980.

[48] I. Moskowitz, S. Greenwald, and M. Kang, "An analysis of the timed Z-channel", *IEEE Transactions on Information Theory*, vol. 44, no. 7, pp. 3162–3168, November 1998.

[49] Wikipedia, The Free Encyclopedia. [Online]. URL: http://en.wikipedia.org/.

[50] M. Badr, "Impact of cooperation for ad-hoc networks", Master's thesis, *TELECOM ParisTech, Paris, France*, 2006.

[51] C. Papadimitriou and K. Steiglitz. *Combinatorial optimization: algorithms and complexity*. Dover Publications, 1998.

[52] R. Diestel. *Graph Theory (Graduate Texts in Mathematics)*. Springer, 1997.

[53] G. Ungerboeck, "Channel coding with multilevel/phase signals", *IEEE Transactions on Information Theory*, vol. 28, no. 1, pp. 55–67, January .

[54] K. Kato, M. Osaki, M. Sasaki, and O. Hirota, "Quantum detection and mutual information for QAM and PSK signals", *IEEE Transactions on Communications*, vol. 47, no. 2, pp. 248–254, February 1999.

[55] S. Jafar and M. Fakhereddin, "Degrees of freedom for the MIMO interference channel", *IEEE Transactions on Information Theory*, vol. 53, no. 7, pp. 2637–2642, July 2007.

[56] R. Etkin, D. Tse, and H. Wang, "Gaussian interference channel capacity to within one bit: The symmetric case", in *IEEE Information Theory Workshop, ITW'06*, pp. 601–605, 2006.

[57] X. Cai and G. Giannakis, "A two-dimensional channel simulation model for shadowing processes", *IEEE Transactions on Vehicular Technology*, vol. 52, no. 6, pp. 1558–1567, November 2003.

[58] ICT-247223 ARTIST4G project "Advanced Radio Interface TechnologIes for 4G SysTems", 2010–2012. [Online]. URL: https://ict-artist4g.eu/.

[59] V. Chandrasekhar, J. Andrews, and A. Gatherer, "Femtocell networks: A survey", *IEEE Communications Magazine*, vol. 46, no. 9, pp. 59–67, September 2008.

[60] D. López-Pérez, A. Valcarce, G. De La Roche, and J. Zhang, "OFDMA femtocells: A roadmap on interference avoidance", *IEEE Communications Magazine*, vol. 47, no. 9, pp. 41–48, September 2009.

[61] H. Claussen, "Performance of macro-and co-channel femtocells in a hierarchical cell structure", in *IEEE International Symposium on Personal, Indoor and Mobile Radio Communications, PIMRC'07*, 2007.

[62] H. Claussen, L. Ho, and L. Samuel, "Self-optimization of coverage for femtocell deployments", in *Wireless Telecommunications Symposium, WTS'08*, pp. 278–285, 2008.

[63] V. Chandrasekhar and J. Andrews, "Uplink capacity and interference avoidance for two-tier femtocell networks", *IEEE Transactions on Wireless Communications*, vol. 8 , no. 7, pp. 3498–3509, July 2009.

[64] V. Chandrasekhar, J. Andrews, T. Muharemovic, Z. Shen, and A. Gatherer, "Power control in two-tier femtocell networks", *IEEE Transactions on Information Theory*, vol. 8, no. 8, pp. 4316–4328, August 2009.

[65] H. Jo, C. Mun, J. Moon, and J. Yook, "Self-optimized coverage coordination and coverage analysis in femtocell networks", *submitted to IEEE Transactions on Wireless Communications, Preprint arXiv:0910.2168*, 2009.

[66] R. Bosisio and U. Spagnolini, "Interference coordination vs. interference randomization in multicell 3GPP LTE system", in *IEEE Wireless Communications and Networking Conference, WCNC'08*, pp. 824–829, 2008.

[67] X. Fan, S. Chen, and Z. Xiaodong, "An inter-cell interference coordination technique based on users' ratio and multi-level frequency allocations", in *International Conference on Wireless Communications, Networking and Mobile Computing, WiCom'07*, pp. 799–802, 2007.

[68] K. Kim and S. Oh, "An Incremental Frequency Reuse Scheme for an OFDMA Cellular System and Its Performance", in *IEEE Vehicular Technology Conference, VTC'08 Spring*, 2008.

[69] Z. Xie and B. Walke, "Enhanced fractional frequency reuse to increase capacity of OFDMA systems", in *International Conference on New Technologies, Mobility and Security, NTMS'09*, 2009.

[70] A. Hernandez, I. Guio, and A. Valdovinos, "Interference management through resource allocation in multi-cell OFDMA networks", in *IEEE Vehicular Technology Conference, VTC'09 Spring*, 2009.

[71] M. Pischella and J.-C. Belfiore, "Weighted sum throughput maximization in multicell OFDMA networks", *IEEE Transactions on Vehicular Technology*, vol. 59, no. 2, pp. 896–905, February 2010.

[72] P. Marsch and G. Fettweis, "A decentralized optimization approach to backhaul-constrained distributed antenna systems", 2007.

[73] A. Carleial, "A case where interference does not reduce capacity (Corresp.)", *IEEE Transactions on Information Theory*, vol. 21, no. 5, pp. 569–570, September 1975.

[74] C. Peel, B. Hochwald, and A. Swindlehurst, "A vector-perturbation technique for near-capacity multiantenna multiuser communicationŮpart I: channel inversion and regularization", *IEEE Transactions on Communications*, vol. 53, no. 1, pp. 195–202, January 2005.

[75] P. Sripathi and J. Lehnert, "Optimizing ZF precoders for MIMO broadcast systems", in *IEEE Wireless Communications and Networking Conference, WCNC'06*, pp. 1874–1880, 2006.

[76] M. Damen, K. Abed-Meraim, and J.-C. Belfiore, "Generalised sphere decoder for asymmetrical space-time communication architecture", *IEEE Electronics Letters*, vol. 36, no. 2, pp. 166–167, January 2000.

[77] J. Boutros, N. Gresset, L. Brunel, and M. Fossorier, "Soft-input soft-output lattice sphere decoder for linear channels", in *IEEE Global Communications Conference, GLOBECOM'03*, vol. 3, 2003.

[78] J. Cioffi, "Generalized decision feedback equalization", EE379C - Advanced Digital Communication, 2007. [Online]. URL: http://www.stanford.edu/class/ee379c/reader.html.

[79] M. Damen, H. El Gamal, and G. Caire, "MMSE-GDFE lattice decoding for solving under-determined linear systems with integer unknowns", in *IEEE International Symposium on Information Theory, ISIT'04*, pp. 538, 2004.

[80] M. Costa, "Writing on dirty paper (Corresp.)", *IEEE Transactions on Information Theory*, vol. 29, no. 3, pp. 439–441, May 1983.

[81] C. Peel, "On dirty-paper coding", *IEEE Signal Processing Magazine*, vol. 20, no. 3, pp. 112–113, May 2003.

[82] Y. Yang, "Half-Duplex Relay-Help Transmission with Dirty Paper Coding", in *IEEE Vehicular Technology Conference, VTC'09 Spring*, 2009.

[83] P. Patel and J. Holtzman, "Analysis of a DS/CDMA successive interference cancellation scheme using correlations", in *IEEE Global Communications Conference, GLOBECOM'93*, pp. 76–80, 1993.

[84] M. Kobayashi, J. Boutros, and G. Caire, "Successive interference cancellation with SISO decoding and EM channel estimation", *IEEE Journal on Selected Areas in Communications*, vol. 19, no. 8, pp. 1450–1460, August 2001.

[85] H. Kim and H. Park, "Efficient successive interference cancellation algorithms for the DSTTD system", in *IEEE International Symposium on Personal, Indoor and Mobile Radio Communications, PIMRC'05*, pp. 524–528, 2005.

[86] R. Böhnke and K. Kammeyer, "Exact outage probability of V-Blast with ordered MMSE-SIC detection", in *Symposium on Communications*, pp. 173–176, 2006.

[87] R. Ramanathan. *Mobile ad hoc networking - Chapter 5 - Antenna beamforming and power control for ad hoc networks.* Wiley, 2005.

[88] R. Mudumbai, D. Brown III, U. Madhow, and H. Poor, "Distributed transmit beamforming: Challenges and recent progress", *IEEE Communications Magazine*, February 2009.

[89] V. Cadambe and S. Jafar, "Interference alignment and degrees of freedom of the K-user interference channel", *IEEE Transactions on Information Theory*, vol. 54, no. 8, pp. 3425–3441, August 2008.

[90] S. Jafar, "Exploiting channel correlations-simple interference alignment schemes with no CSIT", *submitted to IEEE Transactions on Information Theory, Preprint arXiv:0910.0555*, 2009.

[91] A. Gjendemsjø, D. Gesbert, G. Øien, and S. Kiani, "Optimal power allocation and scheduling for two-cell capacity maximization", in *International Symposium on Modeling and Optimization in Mobile, Ad Hoc and Wireless Networks, WiOpt'06*, 2006.

[92] A. Gjendemsjø, D. Gesbert, G. Øien, and S. Kiani, "Binary power control for sum rate maximization over multiple interfering links", *IEEE Transactions on Wireless Communications*, vol. 7, no. 8, pp. 3164–3173, August 2008.

[93] E. Van Der Meulen, "Three-terminal communication channels", *Advances in Applied Probability*, vol. 3, no. 1, pp. 120–154, 1971.

[94] D. Soldani and S. Dixit, "Wireless relays for broadband access", *IEEE Communications Magazine*, vol. 46, no. 3, pp. 58–66, March 2008.

[95] F. Fitzek and M. Katz. *Cooperation in wireless networks: principles and applications*. 2006.

[96] A. Nosratinia, T. Hunter, and A. Hedayat, "Cooperative communication in wireless networks", *IEEE Communications Magazine*, vol. 42, no. 10, pp. 74–80, October 2004.

[97] T. Hunter and A. Nosratinia, "Cooperation diversity through coding", in *IEEE International Symposium on Information Theory, ISIT'02*, 2002.

[98] M. Janani, A. Hedayat, T. Hunter, and A. Nosratinia, "Coded cooperation in wireless communications: space-time transmission and iterative decoding", *IEEE Transactions on Signal Processing*, vol. 52, no. 2, pp. 362–371, February 2004.

[99] A. Sendonaris, E. Erkip, and B. Aazhang, "Increasing uplink capacity via user cooperation diversity", in *IEEE International Symposium on Information Theory, ISIT'98*, 1998.

[100] A. Sendonaris, E. Erkip, and B. Aazhang, "User cooperation diversity - Part I: System description", *IEEE Transactions on Communications*, vol. 51, no. 11, pp. 1927–1938, November 2003.

[101] A. Sendonaris, E. Erkip, and B. Aazhang, "User cooperation diversity - Part II: Implementation aspects and performance analysis", *IEEE Transactions on Communications*, vol. 51, no. 11, pp. 1939–1948, November 2003.

[102] J. Laneman, G. Wornell, and D. Tse, "An efficient protocol for realizing cooperative diversity in wireless networks", in *IEEE International Symposium on Information Theory, ISIT'01*, 2001.

[103] J. Laneman, D. Tse, and G. Wornell, "Cooperative diversity in wireless networks: Efficient protocols and outage behavior", *IEEE Transactions on Information Theory*, vol. 50, pp. 3062–3080, December 2004.

[104] R. Nabar, H. Bölcskei, and F. Kneubühler, "Fading relay channels: Performance limits and space-time signal design", *IEEE Journal on Selected Areas in Communications*, vol. 22, no. 6, pp. 1099–1109, August 2004.

[105] A. Klein and P. Duhamel, "Equalization with part-time help", in *IEEE Conference on Acoustics, Speech, and Signal Processing, ICASSP '07*, vol. 3, pp. 165–168, 2007.

[106] S. Simoens, J. Vidal, and O. Muñoz, "Compress-and-Forward cooperative relaying in MIMO-OFDM systems", in *IEEE Workshop on Signal Processing Advances in Wireless Communications, SPAWC'06*, 2006.

[107] M. Badr, E. Calvanese Strinati, and J.-C. Belfiore, "Optimal power allocation for hybrid amplify-and-forward cooperative networks", in *IEEE Vehicular Technology Conference, VTC'08 Spring*, pp. 2111–2115, 2008.

[108] I. Hammerstrom, A. Wittneben, and Z. ETH, "Power allocation schemes for amplify-and-forward MIMO-OFDM relay links", *IEEE Transactions on Wireless Communications*, vol. 6, no. 8, pp. 2798–2802, August 2007.

[109] M. Chen, S. Serbetli, and A. Yener, "Distributed power allocation strategies for parallel relay networks", *IEEE Transactions on Wireless Communications*, vol. 7, no. 2, pp. 552–561, February 2008.

[110] J. Adeane, M. Rodrigues, and I. Wassell, "Optimum power allocation in cooperative networks", in *Postgraduate Research Conference in Electronics, Photonics, Communications and Networks, and Computing Science*, pp. 23–24, 2005.

[111] S. Vakil and B. Liang, "Balancing cooperation and interference in wireless sensor networks", in *IEEE Communications Society on Sensor and Ad Hoc Communications and Networks, SECON'06*, vol. 1, pp. 198–206, 2006.

[112] M. Pischella and J.-C. Belfiore, "Achieving a frequency reuse factor of 1 in OFDMA cellular networks with cooperative communications", in *IEEE Vehicular Technology Conference, VTC'08 Spring*, pp. 653–657, 2008.

[113] S. Yang and J.-C. Belfiore, "Towards the optimal amplify-and-forward cooperative diversity scheme", *IEEE Transactions on Information Theory*, vol. 53, no. 9, pp. 3114–3126, September 2007.

[114] S. Yang and J.-C. Belfiore, "Optimal space-time codes for the MIMO amplify-and-forward cooperative channel", *IEEE Transactions on Information Theory*, vol. 53, no. 2, pp. 647–663, February 2007.

[115] M. Yuksel and E. Erkip, "Diversity-multiplexing tradeoff in cooperative wireless systems", in *Conference on Information Sciences and Systems, CISS'06*, pp. 1062–1067, 2006.

[116] K. Azarian, H. El Gamal, and P. Schniter, "On the achievable diversity-multiplexing tradeoff in half-duplex cooperative channels", *IEEE Transactions on Information Theory*, vol. 51, no. 12, pp. 4152–4172, December 2005.

[117] K. Sreeram, S. Birenjith, and P. Kumar, "DMT of multi-hop cooperative networks - Part I: Basic results", *submitted to IEEE Transactions on Information Theory, Preprint arXiv:0808.0234*, 2008.

[118] K. Sreeram, S. Birenjith, and P. Kumar, "DMT of multi-hop cooperative networks - Part II: Half-duplex networks with full-duplex performance", *submitted to IEEE Transactions on Information Theory, Preprint arXiv:0808.0235*, 2008.

[119] O. Muñoz, J. Vidal, and A. Agustín, "Non-regenerative MIMO relaying with channel state information", in *IEEE Conference on Acoustics, Speech, and Signal Processing, ICASSP '05*, vol. 3, pp. 361–364, 2005.

[120] Y. Li, B. Vucetic, T. Wong, and M. Dohler, "Distributed turbo coding with soft information relaying in multihop relay networks", *IEEE Journal on Selected Areas in Communications*, vol. 24, no. 11, pp. 2040–2050, November 2006.

[121] C. Abgrall, "Etude des techniques de relais coopératifs en 802.16e/j", Master's thesis, *Grenoble Institut National Polytechnique, Grenoble, France*, 2007.

[122] I. Sason, "On achievable rate regions for the Gaussian interference channel", *IEEE Transactions on Information Theory*, vol. 50, no. 6, pp. 1345–1356, June 2004.

[123] L. Zheng and D. Tse, "Diversity and multiplexing: A fundamental tradeoff in multiple-antenna channels", *IEEE Transactions on Information Theory*, vol. 49, no. 5, pp. 1073–1096, May 2003.

[124] E. Akuiyibo and O. Lévêque, "Diversity-multiplexing tradeoff for the slow fading interference channel", in *IEEE International Zurich Seminar on Communications, IZS'08*, pp. 140–143, 2008.

[125] S. Jafar and S. Vishwanath, "Generalized degrees of freedom of the symmetric Gaussian K-user interference channel", *IEEE Transactions on Information Theory*, vol. 56 , no. 7, pp. 3297–3303, July 2010.

[126] E. Yilmaz and S. Kiani, "Transmit cooperation versus distributed coordination in interference links", in *IEEE Wireless Communications and Networking Conference, WCNC'09*, 2009.

[127] V. Annapureddy and V. Veeravalli, "Gaussian interference networks: Sum capacity in the low interference regime and new outer bounds on the capacity region", *IEEE Transactions on Information Theory*, vol. 55, no. 7, pp. 3032–3050, July 2009.

[128] C. Tan, D. Palomar, and M. Chiang, "Solving nonconvex power control problems in wireless networks: low SIR regime and distributed algorithms", in *IEEE Global Communications Conference, GLOBECOM'05*, vol. 6, pp. 3445–3450, 2005.

[129] S. Sridharan, A. Jafarian, S. Vishwanath, and S. Jafar, "Capacity of symmetric K-user Gaussian very strong interference channels", in *IEEE Global Communications Conference, GLOBECOM'08*, 2008.

[130] R. Tandra and A. Sahai, "Is interference like noise when you know its codebook?", in *IEEE International Symposium on Information Theory, ISIT'06*, pp. 2220–2224, 2006.

[131] A. Motahari and A. Khandani, "To decode the interference or to consider it as noise", *submitted to IEEE Transactions on Information Theory, Preprint arXiv:0711.3176*, 2007.

[132] V. Singh, "On superposition coding for wireless broadcast channels", Master's thesis, *KTH, Stockholm, Sweden*, 2005.

[133] H. Do and S. Chung, "Linear beamforming and superposition coding with common information for the Gaussian MIMO broadcast channel", *IEEE Transactions on Communications*, vol. 57, no. 8, pp. 2484–2494, August 2009.

[134] D. Tse, "Diversity-multiplexing tradeoff in MIMO channels", in *Intel Smart Antenna Workshop*, 2004.

[135] A. Poon, R. Brodersen, and D. Tse, "Degrees of freedom in multiple-antenna channels: A signal space approach", *IEEE Transactions on Information Theory*, vol. 51, no. 2, pp. 523–536, February 2005.

[136] D. Tse, P. Viswanath, and L. Zheng, "Diversity-multiplexing tradeoff in multiple-access channels", *IEEE Transactions on Information Theory*, vol. 50, no. 9, pp. 1859–1874, September 2004.

[137] Z. Fan and L. Scharf, "The approximation of outage probability and the trade-off between capacity and diversity for the frequency-selective channel", in *IEEE International Symposium on Information Theory, ISIT'06*, pp. 1159–1163, 2006.

[138] E. Akuiyibo, O. Lévêque, and C. Vignat, "High SNR analysis of the MIMO interference channel", in *IEEE International Symposium on Information Theory, ISIT'08*, pp. 905–909, 2008.

[139] M. Chiang, C. Tan, D. Palomar, D. O'neill, and D. Julian, "Power control by geometric programming", *IEEE Transactions on Wireless Communications*, vol. 6, no. 7, pp. 2640–2651, July 2007.

[140] C. Abgrall, E. Calvanese Strinati, and J.-C. Belfiore, "Adaptive power allocation for interference limited networks", *in preparation for IEEE Transactions on Wireless Communications*, 2011.

[141] S. Kandukuri and S. Boyd, "Optimal power control in interference-limited fading wireless channels with outage-probability specifications", *IEEE Transactions on Wireless Communications*, vol. 1, no. 1, pp. 46–55, January 2002.

[142] N. Jindal and A. Goldsmith, "Capacity and optimal power allocation for fading broadcast channels with minimum rates", *IEEE Transactions on Information Theory*, vol. 49, no. 11, pp. 2895–2909, November 2003.

[143] J. Cioffi, "Multi-channel modulation", EE379C - Advanced Digital Communication, 2007. [Online]. URL: http://www.stanford.edu/class/ee379c/reader.html.

[144] W. Rhee and J. Cioffi, "Increase in capacity of multiuser OFDM system using dynamic subchannel allocation", in *IEEE Vehicular Technology Conference, VTC'00 Spring*, vol. 2, pp. 1085–1089, 2000.

[145] C. Yih and E. Geranotis, "Centralized power allocation algorithms for OFDM cellular networks", in *IEEE Military Communications Conference, MILCOM 2003*, vol. 2, 2003.

[146] D. Yu and J. Cioffi, "Iterative water-filling for optimal resource allocation in OFDM multiple-access and broadcast channels", in *IEEE Global Communications Conference, GLOBECOM'06*, 2006.

[147] K. Kim, H. Kim, and Y. Han, "Subcarrier and power allocation in OFDMA systems", in *IEEE Vehicular Technology Conference, VTC'04 Fall*, vol. 2, pp. 1058–1062, 2004.

[148] K. Kim, Y. Han, and S. Kim, "Joint subcarrier and power allocation in uplink OFDMA systems", *IEEE Communications Letters*, vol. 9, no. 6, pp. 526–528, June 2005.

[149] J. Adeane, M. Rodrigues, and I. Wassell, "Centralised and distributed power allocation algorithms in cooperative networks", in *IEEE Workshop on Signal Processing Advances in Wireless Communications*, pp. 333–337, 2005.

[150] M. Pischella and J.-C. Belfiore, "Distributed resource allocation for rate-constrained users in multi-cell OFDMA networks", *IEEE Communications Letters*, vol. 12, no. 4, pp. 250–252, April 2008.

[151] M. Pischella, "Distributed resource allocation in multi-cell OFDMA networks", Ph.D. dissertation, *TELECOM ParisTech, Paris, France*, 2009.

[152] D. Tse, "Optimal power allocation over parallel Gaussian broadcast channels", in *IEEE International Symposium on Information Theory, ISIT'97*, 1997.

[153] A. Lozano, A. Tulino, and S. Verdú, "Mercury/waterfilling: optimum power allocation with arbitrary input constellations", in *International Symposium on Information Theory, ISIT'05*, pp. 1773–1777, 2005.

[154] A. Lozano, A. Tulino, and S. Verdu, "Mercury/waterfilling for fixed wireless OFDM systems", in *IEEE Radio and Wireless Symposium*, pp. 211–214, 2006.

[155] J. Huang, R. Berry, and M. Honig, "Distributed interference compensation for wireless networks", *IEEE Journal on Selected Areas in Communications*, vol. 24, no. 5, pp. 1074–1084, May 2006.

[156] S. Kiani and D. Gesbert, "Capacity maximizing power allocation for interfering wireless links: A distributed approach", in *IEEE Global Communications Conference, GLOBECOM'07*, pp. 1405–1409, 2007.

[157] J. Ellenbeck, C. Hartmann, and L. Berlemann, "Decentralized inter-cell interference coordination by autonomous spectral reuse decisions", in *Wireless Conference, EW'08*, 2008.

[158] G. Miao, N. Himayat, G. Li, A. Koc, and S. Talwar, "Interference-aware energy-efficient power optimization", in *IEEE International Conference on Communications, ICC'09*, 2009.

[159] J. Pang, G. Scutari, F. Facchinei, and C. Wang, "Distributed power allocation with rate constraints in Gaussian parallel interference channels", *IEEE Transactions on Information Theory*, vol. 54, no. 8, pp. 3471–3489, August 2008.

[160] M. Grötschel, L. Lovász, and A. Schrijver. *Geometric algorithms and combinatorial optimization.* Springer, 1988.

[161] J. Snyman. *Practical mathematical optimization: an introduction to basic optimization theory and classical and new gradient-based algorithms.* Springer, 2005.

[162] C. Saraydar, N. Mandayam, and D. Goodman, "Efficient power control via pricing in wireless data networks", *IEEE Transactions on Communications*, vol. 50, no. 2, pp. 291–303, February 2002.

[163] C. Meyer. *Matrix analysis and applied linear algebra.* Society for Industrial Mathematics, 2000.

[164] A. Pomellet. *Agrégation de mathématiques, cours d'analyse.* Ellipses, 1994.

[165] X. Gourdon. *Les maths en tête: analyse.* Ellipses, 1994.

[166] J. Demailly. *Analyse numérique et équations différentielles, Manuel pour le Second Cycle de Mathématiques.* Presses Universitaires de Grenoble, 2006.

[167] A. Granas and J. Dugundji. *Fixed point theory.* Springer, 2003.

[168] I. Beichl and F. Sullivan, "Make me a match", *IEEE Computational Science & Engineering*, vol. 4, no. 4, pp. 88–93, October 1997.

[169] C. Abgrall, A. De Domenico, and E. Calvanese Strinati, "Femtocells matching", *in preparation for IEEE Conference*, 2011.